

**BEHAVIOUR OF SIMPLE FRAMING CONNECTIONS
TO PARTIALLY CONCRETE ENCASED H SECTION COLUMNS**

By:

JASON L. MUISE

**A thesis submitted in conformity with the requirements
For the degree of Master of Applied Science
Graduate Department of Civil Engineering
University of Toronto**

© Copyright by Jason L. Muise, 2000



**National Library
of Canada**

**Acquisitions and
Bibliographic Services**

395 Wellington Street
Ottawa ON K1A 0N4
Canada

**Bibliothèque nationale
du Canada**

**Acquisitions et
services bibliographiques**

395, rue Wellington
Ottawa ON K1A 0N4
Canada

Your file Votre référence

Our file Notre référence

The author has granted a non-exclusive licence allowing the National Library of Canada to reproduce, loan, distribute or sell copies of this thesis in microform, paper or electronic formats.

The author retains ownership of the copyright in this thesis. Neither the thesis nor substantial extracts from it may be printed or otherwise reproduced without the author's permission.

L'auteur a accordé une licence non exclusive permettant à la Bibliothèque nationale du Canada de reproduire, prêter, distribuer ou vendre des copies de cette thèse sous la forme de microfiche/film, de reproduction sur papier ou sur format électronique.

L'auteur conserve la propriété du droit d'auteur qui protège cette thèse. Ni la thèse ni des extraits substantiels de celle-ci ne doivent être imprimés ou autrement reproduits sans son autorisation.

0-612-49733-X

Canada

ABSTRACT

Composite columns are increasingly being used as the primary gravity load carrying elements in medium to high-rise construction. In an attempt to optimize the steel weight ratio there has been a new construction detail recently proposed, consisting of partially concrete encased steel WWF sections. The weak axis connection will be made to an end plate connecting the flange tips, and thus providing a terminus at the column face. This research examines the behaviour of simple framing connections to the weak axis of the proposed column.

A total of 14 tests were conducted, with a variety of connection types and beam sizes. The main test variables included the connection type, the beam size and the size of the test column. Out of concerns for the stability of the columns during construction several tests were performed on the bare steel column to evaluate the influence of the locally introduced connection load on the overall column strength.

ACKNOWLEDGEMENTS

I wish to extend my sincere appreciation to Professor P.C. Birkemoe for his suggestions, advice and continual encouragement. Always respectful of my autonomy in the research project, his door was always open when support was required. Many thanks also go out to my office mate Deena Dinno whose advice was always well respected, and often sought.

The author would also like to thank those who supported the research financially, and technically. Specifically, the Natural Sciences and Research Council of Canada (NSERC) for funding in the form of a PGS A scholarship, and the Government of Newfoundland and Labrador for the Atlantic Accord Career Development bursary. Many thanks are expressed to the Canam Manac Group for the supply of test hardware, specimens and most importantly the project. The contributions of Mr. Richard Vincent of Canam, and Professor Robert Tremblay, Professor Bruno Massicotte and Thierry Chicoine of École Polytechnique are hereby recognized.

Many thanks to the technical staff members of the University of Toronto; Mehmet Citak, Peter Heliopoulos, John Macdonald, Renzo Basset, John Buzzeo, Alan McClenaghan, and Joel Babbín. Although terribly understaffed, the civil engineering laboratories at the University of Toronto continue to function because of the dedication and work ethic of its employees. The assistance of summer student Mr. Richard Yee is also appreciated. My thanks is also extended to Roman Yaworsky in taking the final specimen photographs.

Personally, I would like to thank the many friends that I came to know here at the University of Toronto. I would like to thank my loving parents and my sisters, Dawn and Wanda for their patience, love and support. Most importantly, I would like to thank my new wife Stephanie, who can now breath a sigh of relief.... It is over!

TABLE OF CONTENTS

1	INTRODUCTION	1
1.1	BACKGROUND ON COMPOSITE GRAVITY FRAME SYSTEMS	1
1.2	OBJECTIVE AND SCOPE	3
1.3	ORGANIZATION AND PRESENTATION	5
2	LITERATURE REVIEW	7
2.1	SIMPLE SHEAR CONNECTIONS	7
2.1.1	EXPERIMENTAL WORK ON SHEAR CONNECTIONS	8
2.1.2	INFLUENCE OF CONCRETE SLAB ON CONNECTION BEHAVIOUR.....	13
2.2	COMPOSITE COLUMNS	15
2.2.1	NON-COMPOSITE COLUMN STRENGTH	15
2.2.2	COMPOSITE COLUMN STRENGTH.....	18
2.3	CONNECTIONS TO COMPOSITE COLUMNS.....	20
2.3.1	SIMPLE SHEAR CONNECTIONS TO CONCRETE FILLED HSS	21
2.4	FORCE TRANSFER MECHANISM	23
3	EXPERIMENTAL PROGRAM	24
3.1	DESIGN PARAMETERS	24
3.2	TEST SET-UP - LOADING MECHANISM	25
3.3	DESIGN OF TEST SPECIMENS	27
3.3.1	TEST COLUMNS	27
3.3.2	TEST (FRAMING) BEAMS	32
3.3.3	CONNECTION TYPES	35
3.3.4	MECHANICAL SHEAR CONNECTION.....	37
3.3.5	FINAL TEST MATRIX	38
3.4	SPECIMEN FABRICATION	38
3.5	TESTING PROCEDURE.....	40
3.5.1	NON-COMPOSITE CONNECTION LOADING.....	41
3.5.2	COMPOSITE CONNECTION LOADING	42
3.6	INSTRUMENTATION.....	42
3.7	BRACING CONSIDERATIONS	44
3.7.1	LATERAL BEAM BRACING	44
3.7.2	LONGITUDINAL BRACING OF BEAM.....	45
3.7.3	COLUMN BRACING	47
4	TEST RESULTS AND OBSERVATIONS	48
4.1	MATERIAL PROPERTY RESULTS	48
4.1.1	STEEL PROPERTIES	48

4.1.2	CONCRETE PROPERTIES	49
4.2	PRELIMINARY MEASUREMENTS.....	49
4.3	PROTOTYPE SPECIMEN TESTS.....	52
4.3.1	PROTOTYPE COMPOSITE TEST RESULTS	52
4.3.2	RECOMMENDATIONS FOR SUBSEQUENT TESTING	56
4.4	COMPOSITE CONNECTION TEST RESULTS	57
4.4.1	GENERAL OBSERVATIONS AND FAILURE MODES	57
4.4.2	LOAD-DISPLACEMENT RESPONSE OF COMPOSITE CONNECTIONS.....	68
4.4.3	MOMENT-ROTATION RESPONSE OF THE COMPOSITE CONNECTIONS	75
4.4.4	FORCE TRANSFER BETWEEN STEEL AND CONCRETE	83
4.4.5	REVIEW OF COMPOSITE TESTS	83
4.5	NON-COMPOSITE TESTS	89
4.5.1	GENERAL OBSERVATIONS.....	89
4.5.2	NON-COMPOSITE RESULTS	91
4.5.3	NON-COMPOSITE TEST SUMMARY	93
4.6	EFFECTS OF INCREASING COLUMN LOADS	95
5	DISCUSSION OF RESULTS.....	97
5.1	CONNECTION STATICS – INFLUENCE OF BEAM RESTRAINT	97
5.2	EVALUATION OF ORIGINAL TEST VARIABLES	100
5.2.1	CONNECTION TYPE.....	100
5.2.2	DEPTH OF EXTERIOR END PLATE	101
5.2.3	COLUMN SIZE	102
5.2.4	PRESENCE OF SHEAR STUDS.....	102
5.3	TENSION STIRRUPS	104
5.4	USE OF EXTERIOR COLUMNS.....	106
6	CONCLUSIONS AND RECOMMENDATIONS.....	109
6.1	REVIEW OF SCOPE OF WORK.....	109
6.2	MAJOR CONCLUSIONS	110
6.3	RECOMMENDATIONS FOR FURTHER STUDY.....	111
7	REFERENCES.....	113

List of Figures

Figure 1.1: Typical Composite Columns in North America.....	1
Figure 1.2: Proposed Column System.....	2
Figure 1.3 : Proposed Loading.....	5
Figure 2.1: Typical Beam Line Model.....	8
Figure 2.2: Shear Force Vs. Beam End Rotation (Astaneh, 1989).....	9
Figure 2.3: Typical Slab Detail for Partially Restrained Composite Connection.....	14
Figure 2.4: Typical Force Transfer Mechanism.....	14
Figure 2.5: General Plate Buckling Solution.....	15
Figure 2.6: General Buckled Shape of Test Column.....	16
Figure 2.7: Results From École Polytechnique: Bare Column Results ¹	18
Figure 2.8: Results From École Polytechnique: Composite Results ¹	19
Figure 2.9: Types of Composite Moment Connections.....	20
Figure 3.1: Test Set-up.....	26
Figure 3.2: Test Apparatus with Specimen C600-W410-SDA-C June 8, 1999. Mark Huggins Laboratory, The University of Toronto.....	27
Figure 3.3: Drawing of Column C450-W410.....	29
Figure 3.4: Drawing of Column C450-W530.....	30
Figure 3.5: Drawing of Column C600-W410.....	31
Figure 3.6: Load Beams W410 x 67 and W530 x 92.....	33
Figure 3.7 : Shear Stud Layout in Specimen C18-Seat-Anchorage.....	37
Figure 3.8 : Overview of Fabrication Process.....	39
Figure 3.9: Typical Instrumentation.....	42
Figure 3.10: Free Body Diagram of Test Set-up.....	44
Figure 3.11: Lateral Bracing of Beam.....	45
Figure 3.12: Overall View of Bracing a) Lateral Beam Bracing, b) Slab Restraint.....	46
Figure 3.13: Column Bracing: Horizontal Forces Taken into Test Frame.....	47
Figure 4.1: Typical Residual Stress Pattern ¹	50
Figure 4.2: Oblique View of Failed Specimen C450-W410-SDA-C.....	53
Figure 4.3: Oblique View of Failed Specimen C450-W410-LDA-C.....	53
Figure 4.4: Prototype Composite Specimen: Connection Load vs. Vertical Beam Displacement.....	54
Figure 4.5: Prototype Composite Specimen: Connection Load vs. Displacement of Flange.....	54
Figure 4.6: Prototype Composite Specimen: Connection Load vs. Average Steel Strain 685 mm Below Connection Plate.....	56
Figure 4.7: Typical Deformation of Connection and End Plate.....	57

Figure 4.8: Connection Forces at the Bolt Line a) Stiff Column Face, b) Flexible Column Face	58
Figure 4.9: Typical Bolthole Deformation Pattern Observed in Test Beam.....	59
Figure 4.10: Typical Bolthole Deformation Pattern Observed in Connection Header.....	59
Figure 4.11: View of Failed Specimen C450-W410-TAB-C: Side View	62
Figure 4.12: View of Failed Specimen C450-TAB-C- Front View	62
Figure 4.13: Specimen C450-W530-LDA-C Following Loading.....	64
Figure 4.14: Specimen C450-W530-TAB-C Following Loading.....	64
Figure 4.15: View of Failed Specimen C450-W530-SDA-C	65
Figure 4.16: View of Failed Specimen C600-W410-SDA-C	65
Figure 4.17: View of Failed Specimen C600-410-LDA-C.....	67
Figure 4.18: Typical Seat Connection Following Loading.....	67
Figure 4.19: C450-W410: Applied Connection Load vs. Vertical Beam End Displacement.....	69
Figure 4.20: C450-W410: Applied Connection Load vs. Displacement of Beam Flanges	69
Figure 4.21: C450-W530: Applied Connection Load vs. Vertical Beam End Displacement.....	72
Figure 4.22: C450-W530: Applied Connection Load vs. Beam Flange Displacement.....	72
Figure 4.23: C600-W410: Applied Connection Load vs. Vertical Beam End Displacement.....	73
Figure 4.24: C600-W410: Applied Connection Load vs. Flange Movement From Column Face	73
Figure 4.25: C450-Seat: Applied Connection Load vs. Vertical Beam End Displacement	74
Figure 4.26: C450-Seat: Applied Connection Load vs. Flange Displacement From Column Face....	74
Figure 4.27: Bending Moment Diagram of Varying End Restraint	75
Figure 4.28: Free Body Diagram of Beam - With Restraint.....	76
Figure 4.29: C450-W410: Total Moment Developed at the Beam End, M_{Face} vs. Connection Load ..	78
Figure 4.30: C450-W410: Applied Connection Load vs. Beam End Rotation.....	78
Figure 4.31: C450-W530: Total Moment Developed at the Beam End, M_{face} vs. Connection Load ..	80
Figure 4.32: C450-W530: Applied Connection Load vs. Beam End Rotation.....	80
Figure 4.33: C600-W410: Total Developed Moment at Beam End, M_{Face} vs. Connection Load	81
Figure 4.34: C600-W410: Applied Connection Load vs. Rotation of Beam End.....	81
Figure 4.35: C450-Seat: Total Moment Developed at Beam End M_{Face} vs. Connection Load.....	82
Figure 4.36: C450-W410: Strain Distribution Over Depth vs. Connection Load of 500 kN	84
Figure 4.37: C450-W530: Strain Distribution Over Depth vs. Connection Load of 500 kN	85
Figure 4.38: C450-Seat: Strain Distribution Over Depth vs. Connection Load of 500 kN	86
Figure 4.39: C600-W410: Strain Distribution Over Depth vs. Connection Load of 500 kN	87
Figure 4.40: Typical Buckling Pattern of Non-Composite Specimen	90
Figure 4.41: Typical Buckling Pattern of Non-Composite Specimen - East View.....	90
Figure 4.42: Non-Composite: Connection Load vs. Beam Flange Movement from Column Face	92
Figure 4.43: Non-Composite: Nominal Stress in Column Cross Section vs. Strain at Flange Tips ...	92

Figure 4.44 : Summary of Non-Composite Test Results	95
Figure 4.45: Failure Initiated in Specimen C450-W530-LDA-C	96
Figure 5.1: Restraint Moment, S_j, vs. Applied Connection Load for W410 Test Series	99
Figure 5.2: Restraint Moment, S_j, vs. Applied Connection Load for W530 Test Series	99
Figure 5.3: Applied Connection Load vs. Change in Steel Strain in Column flanges (-50 mm) for Various End Plate Depths	105
Figure 5.4: Total Column Load vs. Tensile Strain in Stirrups 0.5D Below Connection Plate	105
Figure 5.5 : Exterior Column Layout	107

List of Tables

Table 1-1 : Proposed Test Matrix	4
Table 3-1 : Summary of Uniformly Distributed Design Loads	24
Table 3-2: Range of Factored Design Loads for Beam to Column Connections	25
Table 3-3: Column Test Loads	28
Table 3-4 : Summary of Connection Details	36
Table 3-5: Calculated Capacities for the Connections Included in This Study	36
Table 3-6: Final Test Matrix.....	38
Table 4-1 : Tensile Coupons; Tested in Accordance with ASTM E8/E8M-99	51
Table 4-2: Concrete Properties; Tested in Accordance with ASTM C39/C39M-99	51
Table 4-3: Summary of Composite Results	88
Table 4-4: Summary of Column Parameters	94
Table 4-5: Summary of Design Variables - S136	94
Table 5-1: Summary of Connection Eccentricities	98
Table 5-2: Summary of Column Eccentricity: Exterior Column	108

General Nomenclature

A	Cross sectional area (mm²)
A_e	Effective area reduced for buckling (mm²)
A_c	Area of concrete (mm²)
A_s	Area of steel (mm²)
B	Maximum column dimension (mm)
D	Nominal Size of Encased Column (mm) (See Fig. 1.2)
E, E_s	Young's Modulus, Steel (200 GPa)
E_c	Young's Modulus, Concrete
EI	Beam stiffness
F_{brace}	Force in column bracing (kN)
F_{cr}	Critical Buckling Stress (MPa)
F_c	Euler's buckling stress (N/mm²)
F_p	Reduced Stress (MPa)
F_y	Yield stress of steel (N/mm²)
F_u	Ultimate stress of steel (N/mm²)
H	Nominal Dimension of HSS (mm)
L, L_b	Length of Load Beam (mm)
L_c	Column length (mm)
M	Moment in beam (kN.m)
M_{bolt}	Moment developed at bolt line (kN.m)
M_{connect}	Moment at weld line (kN.m)
M_{face}	Moment Developed at column face (kN.m)
P_{applied}	Load applied by the Fox Jack (kN)
P_{MTS}	Load Applied by the MTS Universal Testing Machine (kN)
P₁	Force at roller 1 (kN)
P₂	Force at roller 2 (kN)
R	Support Reaction (kN)
S	Tension stirrup (Tie) spacing (mm) (See Fig. 1.2)
S_r	Restraint Force (kN)
V	Shear Force at connection (kN)
W	Unsupported Plate Width (mm)
W_s	Weight of Spreader Beam (kN)
W_{lb}	Weight of Load Beam (kN)
a	Distance from connection top to the top of the beam flange (mm)

a_1	Distance from connection plate to near (East) roller (mm)
a_2	Distance from connection plate to far (West) roller (mm)
b_e	Effective width, reduced for local buckling (mm)
d_{p1}	Depth of connection element (mm)
e	Connection eccentricity (Distance from inflection point to weld line) (mm)
e_w	Shear eccentricity from weld line (mm)
e_b	Distance from bolt line to column face (mm)
h	Unsupported length of web element (mm)
k	Buckling Coefficient
m, n	Number of Bolts
q	Uniform loading (kN/m)
t	Thickness of plate element (mm)
t_w, w	Web thickness (mm)
t_f	Flange thickness (mm)
α	Aspect ratio of plate in compression (b/a)
ϕ	Beam End Rotation (Rad)
τ	E_s/E
ν	Poisson's ratio

1 Introduction

1.1 Background on Composite Gravity Frame Systems

Increasingly, composite steel-concrete columns are being used as the primary gravity load carrying elements in medium to high-rise building applications. Their enhanced structural capabilities, combined with inherent advantages in areas of fire protection, construction techniques and decrease in footprint area, have proven to be an economical route for designers. In North America composite columns have been limited to two main alternatives: concrete filled hollow structural shapes (HSS) or fully encased steel profiles.

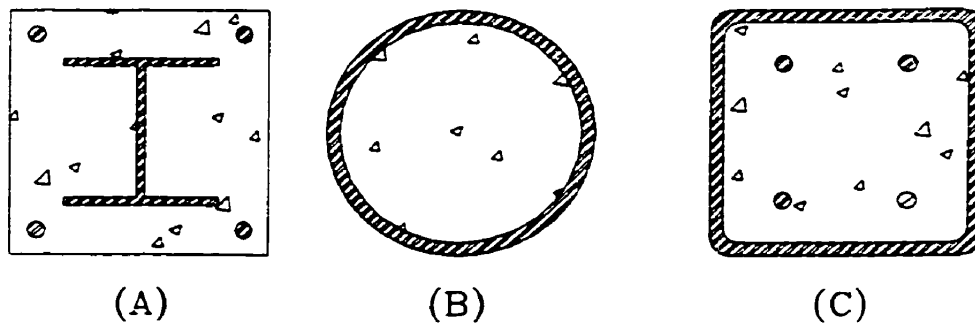


Figure 1.1: Typical Composite Columns in North America

Although there are numerous advantages to these two composite techniques, there are limitations. The size of commonly available hollow structural sections is limited to about 305 mm in largest dimension, and HSS are generally more expensive than other structural steel products. Although size limitations are not as great a concern for encased W sections, additional concrete reinforcement and formwork are required, as with reinforced concrete columns. Also, limitations placed on the available sizes of HSS and rolled W profiles do not generally lead to economical steel weight percentages.

Recently, there has been a perceived need for a new type of composite column that incorporates the attributes of the two systems given above. The Canam Manac Group has proposed a new composite column system combining the positive features of the two conventional methods¹, as illustrated in Figure 1.2. The column consists of a WWF steel profile that is partially encased in concrete. European designers have been using a similar technique with compact W sections, but have been limited to smaller sections that do not optimize the steel/concrete weight ratio. With the welded H

shape the designer has full freedom to optimize steel weight by selecting from a range of flat plate products. The column has been specifically developed for a gravity frame only, and as the standard practice, composite beam action will be assumed, with all beam column connections consisting of simple framing connections. Generally, the columns will be square, with a steel area proportioned to support the construction loads. To inhibit local buckling a tension stirrup between the flange tips, would be provided at regular spacing, S .

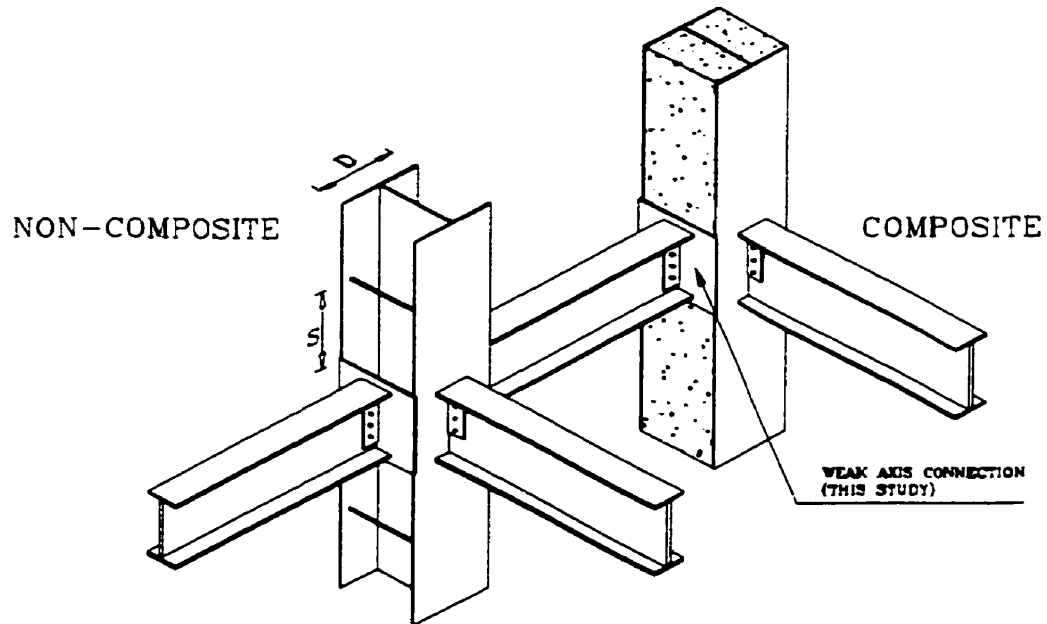


Figure 1.2: Proposed Column System

A preliminary investigation into the proposed framing system was initiated by the Canam Group and École Polytechnique in the Fall of 1996. This included a literature review, numerical analysis and testing of several prototype column specimens. The effectiveness of the system was realized when the stirrups prohibited local buckling of the steel flange, prior to yielding, for composite columns with b/t ratios of up to 30^1 . As a result of this preliminary examination several technical issues were noted for further examination.

- Effectiveness of stirrups in concrete confinement.
- Long-term effects of creep and shrinkage on column behaviour
- Role of stirrup spacing on the behaviour of composite and non-composite columns, in prohibiting local buckling of the column flanges.
- The effects of the sequence of loading on overall column behaviour.
- Nature of the connection into the weak axis of column.
- Force transfer mechanism at point of load introduction

The University of Toronto became involved in the collaborative effort in May, 1998, agreeing to investigate the nature of the simple framing connection to the weak column axis. In conjunction with Canam and École Polytechnique, a complete experimental program was developed to investigate the suitability of several connection types, and the influence of a connection load on column behaviour.

1.2 Objective and Scope

As with most composite construction, the beam column connection is of special concern. Not only the performance of the connection itself, but also the issue of strain compatibility between the steel and concrete at the point of load introduction. To ensure strain compatibility, older versions of design codes (CAN/CSA S16.1 – M89) specified that composite action could only be assumed when both the concrete and steel were loaded simultaneously, often requiring a complex construction detail. For connections to concrete filled tubes, strain compatibility was achieved by using a through beam, or a complicated means of mechanical shear anchorage. For encased W sections, which are often part of moment frames, the beam generally runs through the concrete and frames directly onto the steel column, resulting in dual loading. This too results in an expensive formwork detail, and further complicates the placement of concrete.

From conception this new gravity frame concept was driven by economy and ease of construction. Thus, it was intended that the beams not be imbedded in the concrete, but terminate at the column face. This was not a problem along the strong axis of the column, as the framing connection would be shop welded to the column flange. For the weak axis, a connection was envisioned where the connection would be made to an exterior endplate. This plate would be the same depth as the beam, and would be welded to the tips of the column flanges (as seen in Figure 1.2). As to not prohibit concrete placement there will not be any additional mechanical anchorage, in the form of shear studs or other embedded elements, unless initial tests indicate their required presence. It was anticipated that the natural bond between the steel and the concrete would be adequate for transfer of the loads from the steel into the concrete.

The major objectives of the experimental program were to 1) determine the effect of the connection load on the local buckling behaviour of a bare steel column subjected to a axial load, 2) assess the performance of several types of simple connections to the weak axis through the end plate, and 3) to investigate the force transfer mechanism. Initially, all major types of shear connections were considered for the testing program but this was narrowed to two types, a single plate shear tab, and a double angle web framing connection. Both short double angle and long double angle connections (different bolt spacing) were tested to determine the effects of connection length on overall

performance. As the testing progressed, two unstiffened seat connections also were added to the test matrix.

To ascertain whether additional mechanical shear transfer devices were required a single prototype specimen was cast and tested prior to casting the remainder of the specimens. This initial test indicated that the shear transfer from the steel into the concrete occurred over a depth $2D$ without the use of additional anchorage. With one exception, the remainder of the specimens were cast without shear studs. In addition to these main parameters, the influence of column size and connection plate depth (beam size) were also investigated. The following test matrix resulted, and was agreed upon by all involved parties.

Column Size	Beam Depth	Composite	Connection Type
450 x 450	W410	Non	Short Double Angle Shear Plate
		Comp	Short Double Angle Long Double Angle Shear Plate
	W530	Non	Long Double Angle
		Comp	Short Double Angle Long Double Angle Shear Plate
		Comp	Seat – No Anchorage Seat – With Anchorage
	600 x 600	W410	Non
Comp			Short Double Angle Long Double Angle

Table 1-1 : Proposed Test Matrix

A schematic of the proposed loading arrangement is given in Figure 1.3. To assess the performance of the beam column connection it was important that in addition to being full size, the column and the connection must be loaded to appropriate and realistic levels. Thus all loads were based on typical design loads, and floor layouts provided by Canam.

For the composite state, an axial load corresponding to 1.0 Dead load + 0.5 Live Load was considered to be an adequate nominal axial column load. This corresponded to approximately 50% of the calculated ultimate resistance of the column. Under this axial load, the connection would be tested to failure. In the non-composite state the connection was loaded to a typical construction load, and the axial load gradually increased until local buckling occurred in the column.

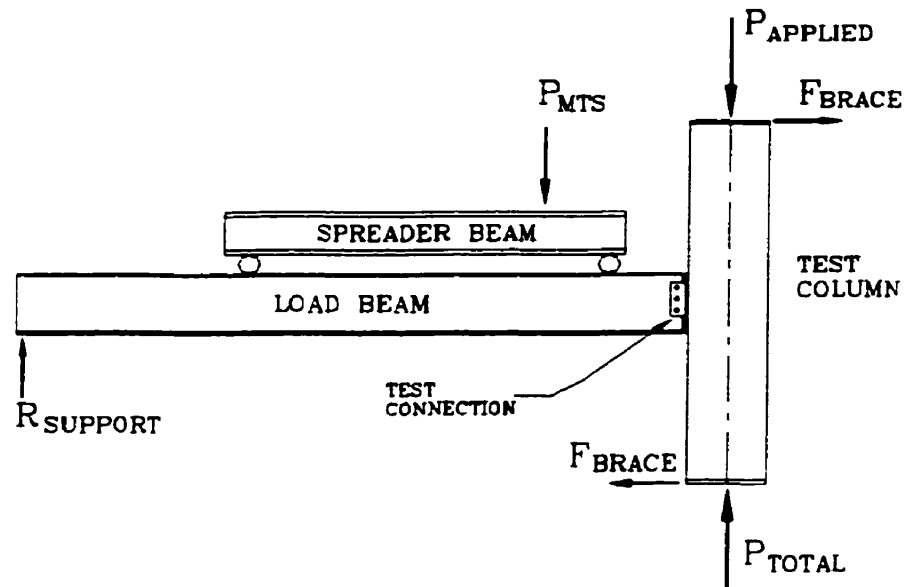


Figure 1.3 : Proposed Loading

1.3 Organization and Presentation

This report summarises the University of Toronto's contribution to the ongoing collaborative effort into the investigation of the proposed gravity framing method, and eventual development of design provisions. The first chapter of this report has provided a history of the research, and described the University of Toronto's role in the investigation of the behaviour of the beam column connection. Chapter 2 presents a review of issues related to structural joints in composite construction. This includes the basic theory of shear connectors, with a summary of the basic design provisions for the three connection types included in this study. Issues related to composite construction will then be discussed with the major studies on composite shear connections reviewed. To better understand the influence of the connection on column behaviour a summary of the major findings of the research conducted by École Polytechnique will be provided.

Chapter 3 of this report summarises the experimental program, including the formulation of the test matrix, design of the test specimens, and documentation of other laboratory related issues. These include a description of the loading mechanism, instrumentation, and bracing considerations.

The results and observations are presented in Chapter 4 of this report. The results have been divided into four main groups; the material properties, the results of the initial prototype tests, the major composite test results (10 tests) and the non-composite test results (four tests). Only the primary results have been included in the main body, with full details, observations and results of each individual test provided in Appendix D.

Preliminary analysis and discussion of the test results have been provided in Chapter 5. In addition to the influence of each of the major test variables, other technical issues which emerged during the course of the test will be addressed. A complete summary of the testing program has been included in Chapter 6, with recommendations for further research.

2 Literature Review

For any structure, whether traditional steel, concrete or a hybrid system the beam column connection region is generally the most uncertain area, in terms of behaviour, of the entire framing system. The complex behaviour resulting from combined loading and tedious geometry will often result in an inelastic response while the structure is still well within the realm of service loading. The overall uncertainty in connection design is respected by the Limit States Design (LSD) and by the Load and Resistance Factor Design (LFRD) methodology with a more conservative reduction factor for connections, compared to other building elements.

Although the benefits of composite construction are long recognised, and behaviour of the composite beams and columns well studied, the structural connections are less understood^{4,5,6}. The design of composite connections has been largely based on the knowledge of steel and concrete connections and sound engineering judgement. The designer must have a good knowledge of the mechanics of the connection, the flow of forces between the steel and concrete and the ability to visualise all potential failure modes. Economic and construction issues are even of a greater concern than they are in conventional construction involving a single material.

To understand the full scope of the problem it is not only important to understand the mechanics of the connection itself, but also the behaviour of the composite beam and column. Although a detailed description of composite construction is beyond the scope of this review there are many texts that provide an in-depth analysis of composite construction^{4,6}. Since partially encased columns are not used extensively in the North American construction industry, a basic review of these columns will be included. The results from the adjunct testing at École Polytechnique will be presented for both the steel and composite columns.

2.1 Simple Shear Connections

The main role of the structural joint is to transfer forces between members while maintaining structural integrity. Most design codes (AISC, CAN/CSA-S16.1) have traditionally defined beam column connections as rigid, simple or partially restrained (Type 1, 2, and 3 respectively). A rigid connection is defined as permitting less than 10% of the ideal "pin" rotation while developing a minimum of 90% of the fixed end moment. A simple connection will allow over 80 % of the ideal "perfect pin" end rotation while developing less than 20 % of the fixed end moment. A partial restraint will lie between these two classifications.

A common tool aiding designers in connection classification is the beam line model. Fig. 2.1 contains a typical beam line model for a beam of flexural stiffness, EI , and exposed to a uniform loading of, q . This is a $M-\phi$ plot, where each axis represents an ideal end restraint. Lines A and B define the classification zones based on the above limits. The beam line connects the 2 axis intercepts for a given beam.

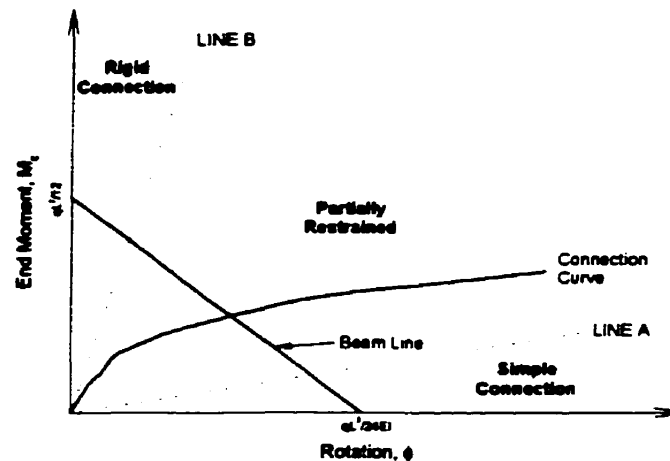


Figure 2.1: Typical Beam Line Model

When a connection $M-\phi$ relationship has been determined from either experimental or analytical methods the classification is based on where the connection curve intersects the beam line. In the above example, the connection would be a partially restrained. The rotational stiffness of the connection is the slope of the $M-\phi$ curve.

2.1.1 Experimental Work on Shear Connections

A simple shear connection must meet the dual criteria of strength and flexibility. The inability of the connection to accommodate the rotation (degree of restraint) will cause a moment to develop at the beam end. Thus a simple connection must be detailed to accommodate the rotation and minimise the developed moment. For simple connections attached at the web, the rotational flexibility will result from bolthole deformation, connection element deformation, and bolt distortion. The stiffness of the connected face will also significantly contribute to the rotational flexibility of the system. Thick column webs, and reinforced concrete columns will have a negligible contribution, whereas, supports such as thin walled HSS will contribute significantly to the overall flexibility.

As a result of this rotational demand most shear connections experience an inelastic response while still well within service loads. This inelastic response is recognised and permitted in Clause 21.2 of

CAN/CSA-S16.1. Thus, for most simple framing connections the $M-\phi$ response remains linear only in the initial stages of loading. As the connection yields the shear to moment ratio does not remain constant with the decrease in the rotational stiffness of the connection. The effective connection eccentricity changes throughout the loading. Early research into shear connections generally involved a cantilever set-up, where the shear-to-moment ratio was constant through out the test. As a result the shear rotation response was properly represented in the elastic region, but not after initial yielding of the connection.

Thus, in examining the experimental behaviour of simple framing connections the $M-\phi-V$ relationship is of particular importance. Figure 2.2 contains the shear - rotation curves used by earlier researchers who tested shear connections. The actual shear rotation response shown in Figure 2.2 is that proposed by Astaneh⁷. It is based on a finite element examination performed on common W sections, with various L/d ratios, that monitored beam end rotations under an increasing uniform loading until full plastic collapse of the beam occurred. The shown curve is based on a L/d ratio of 23, and accounts for strain hardening of the beam.

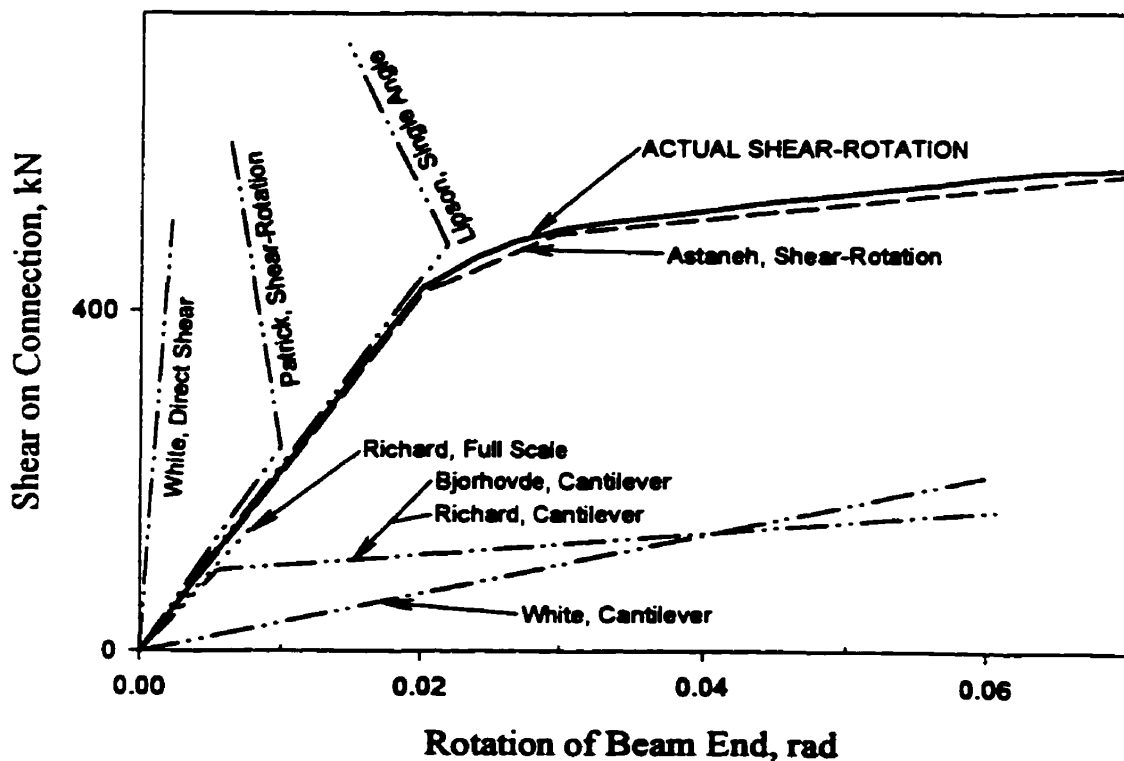


Figure 2.2: Shear Force Vs. Beam End Rotation (Astaneh, 1989)

2.1.1.1 Single Plate Shear Tabs

Single plate shear connections, commonly referred to as “shear tabs”, have become increasingly popular. Their relative simplicity and overall economy⁸ have lead to general usage and well developed design provisions. Using the shear-rotation response discussed in the previous section Astaneh et al. participated in a three part study to investigate the behaviour of (1) shear tabs, (2) shear tabs with short slotted holes, and (3) beam girder connections^{7,9}. The recommended design procedures⁹ form the basis of the design tables in the Canadian Institute of Steel Construction Design Handbook¹⁰.

In order to achieve the realistic $V-\phi$ relationship explained in the previous section a system of two jacks were used with a cantilever type set-up⁹. A load controlled actuator was placed adjacent to the connection to provide a shear force and a second, displacement controlled actuator was placed at the end of the test beam to control the rotation. A total of six shear tabs were tested, with 3, 5, 7 and 9 bolts. All were standard connections, consisting of 300W Grade Steel, ¾ inch diameter bolts (A325 and A490), with a bolt spacing of 75 mm. All connections were to a stiff column flange, which can be classified as a relatively rigid support. All test specimens failed in single shear through the bolts, and were accompanied with considerable shear deformation of the plate and hole bearing deformation.

Based on the test results the following empirical relationship was proposed for the shear force eccentricity from the weld line and bolt line respectively⁹.

$$\begin{aligned} e_w &= 25(n-1) \\ e_b &= 25(n-1) - a \end{aligned} \quad \text{(in millimetres)} \quad \text{(Eqn. 2.1)}$$

where n is the number of bolts in the connection, and a is the distance from the bolt line to the column face. Using these values for the eccentricity the ultimate capacity of the connection could be calculated. Potential failure modes that must be considered include; gross yielding of the plate, bearing failure of the boltholes, net fracture of plate, weld and bolt failure. The bolts and weld groups are to be designed for the combined effect of moment and shear. There are also limitations on maximum plate thickness to ensure rotational flexibility from bolthole deformation.

This testing was performed on a beam column connection to an essentially rigid support. Although Astaneh presented provisions for the design of shear tabs to flexible supports⁹ it was not a parameter, in the testing program. Other researchers^{8,11,12} have tested a variety of simple shear connections to

HSS columns of various width to thickness ratios, which would classify as a flexible support. To investigate potential limit states arising from HSS tube wall flexibility, Sherman and Ales⁸ conducted a total of 13 tests on standard shear tab connections to HSS using two V-φ beam relationships. There were five separate H/t ratios tested ranging from 5 to 45. In tests with H/t < 10 the shear tabs yielded along their length. For more flexible HSS column faces (H/t > 16) yielding of the shear tab appeared to be limited to the area between the top and bottom boltholes.

It was also observed that the connection eccentricity was influenced by both the width to thickness ratio of the tube wall and the span to depth ratio of the test beam. The results demonstrated that the connection eccentricity decreased with both the higher H/t ratio and the lower beam end rotation. An empirical relationship was proposed on the basis of finite element analysis.

$$e = 0.08 \left[\frac{\sqrt{t}}{H} \right] \left(\frac{L}{d} \right)^{1.35} (d_{pl})^{1.35} \quad (\text{in inches}) \quad (\text{Eqn. 2.2})$$

In the proposed design method if the calculated value of e, based on Equation 2.2, is in excess of 75 mm (3 inches) Astaneh's method is suggested. If Equation 2.2 gives an e less than 75 mm it is recommended to design the weld and bolt group for the shear load, at an eccentricity of 62 mm. It is also recommended to reduce the effective length of the shear plate in gross yield calculations.

There was little distortion observed in the tube wall other than a yield line failure, which was limited by beam rotation. Localized punching failure was an initial concern and although no punching failures were observed strain gauges located 25 mm below the shear tab registered a longitudinal strain of 3900 microstrain.

In these test only the connection was loaded, and the HSS column was not loaded axially. In a series of subsequent tests¹² on shear tab connections to axially loaded HSS, the column strength could be developed only when the HSS was classified as being stiff (H/t < 16). A shear tab connection to thin walled HSS was shown to have a considerable effect on column capacity.

2.1.1.2 Double Angle Web Cleats

The double angle web connection is the most common type of simple framing connection in use. Because the bolts are in double shear the connections are usually shorter than for a tab connection. The shorter connection results in a lower rotational stiffness, and less developed moment than the shear tab. Since the resulting connection eccentricity is smaller it is often neglected in design. This

assumption of eccentricity having little effect on connection capacity has been validated with experimental studies¹⁵ for some connections.

The Canadian Institute of Steel Construction Design Handbook¹⁰ has design tables for double angle connections for both cases of the cleats being bolted or welded to the column face. Potential failure modes include, gross section yield, net section rupture, bolt deformation, weld/bolt failure (shear only), and block shear rupture. The CISC Design Handbook¹⁰ also gives minimum thickness requirements for both the webs and angles, at 6 mm. It also recommends that the angles not be much thicker than required to ensure connection flexibility.

Sherman¹¹ reported two tests on double angle connections to HSS columns. These were standard 3 and five bolt connections, with width to thickness ratio of the HSS of 36 and 16. Although both tests were terminated early, because of yielding of the load beam, there was no evidence of failure below the predicted ultimate load.

2.1.1.3 Unstiffened Seat Connections

Seat connections are commonly used for lighter connection loads, and for applications such as open web steel joists. The seat connection is a very economical connection because it is relatively easy to shop weld and field erect. The seat is usually used with a small clip angle placed at the top of the beam flange for stability reasons. The clip must be light enough to accommodate beam rotations without the introduction of a significant moment into the column.

The seat can either be shop welded or field bolted to the column and may be stiffened for higher loads. When the vertical leg of the seat is welded to the column face, as in this experimental program, the designer must check the following limit states in the seat; bending capacity of the horizontal leg, and the bending capacity of the angle between the two vertical weld lines. The beam web must be checked for the bearing strength of the web, web shear strength and the web crippling capacity. The vertical weld group must also be checked for combined moment and shear force, for a given connection eccentricity.

The Canadian Institute of Steel Construction Design Handbook¹⁰ provides design tables for the weld capacity and beam web capacities for various seat connections. The area used in the web bearing calculation is equal to the bearing area causing moment capacity of the horizontal leg to be met, when the vertical force is assumed to act through the centroid of the bearing area. The weld capacity given in the table is based on an assumed value of e .

2.1.2 Influence of Concrete Slab on Connection Behaviour

Composite floor systems, encompassing composite joists, trusses, beams and decks are widely used gravity frame systems¹⁶. The presence of the slab has two immediate effects on connection behaviour. First, the increased beam stiffness influences the shear-rotation relationship of post construction loads. Even if the slab is terminated prior to the column, and has no effect in resisting the moment, the rotation of the simply supported composite beam is less than that of a the same steel beam subjected to similar loads. Thus the $M-\phi$ response suggested in Figure 2.2 is not entirely valid for connections in composite beam gravity systems.

Secondly, the presence of the concrete slab around the column has been shown to make an otherwise simple connection become rather rotationally stiff¹⁷⁻²¹. Although the slab has negligible effect on the transfer of vertical shear forces, there is a considerable restraining force provided by the slab. A typical reinforcing pattern shown in Figure 2.3 will restrict movement of the beam from the column face. As the beam is loaded a compressive force will be developed in the connection, as indicated in Figure 2.4. The resulting is a negative moment couple, which will cause a simple “steel” connection to become a “composite” partial moment connection. Depending upon the construction detail the partial moment may exceed 70% of the fixed end moment¹⁸.

To be able to design with these partially restrained connections the designer must be aware and confident of the connection’s beam line model. In the early years of composite construction designers were not fully aware of this response and justifiably designed connections as either a simple or a rigid connection²¹. It was also thought that the $M-\phi$ response was not linear and therefore difficult to approximate for lateral drift calculations. As a result of connection tests, the relationship within service loads is now known to be relatively linear. Research has been performed on seat connections, web cleats, and single shear angles in order to determine a relationship suitable for use in design. The result culminated in a design guide for partially restrained composite connections¹⁶.

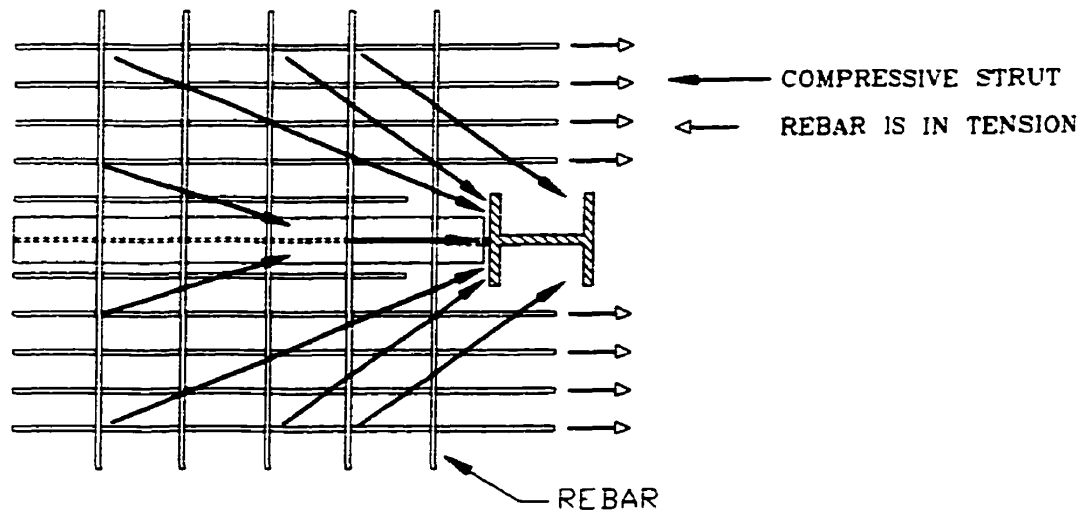


Figure 2.3: Typical Slab Detail for Partially Restrained Composite Connection

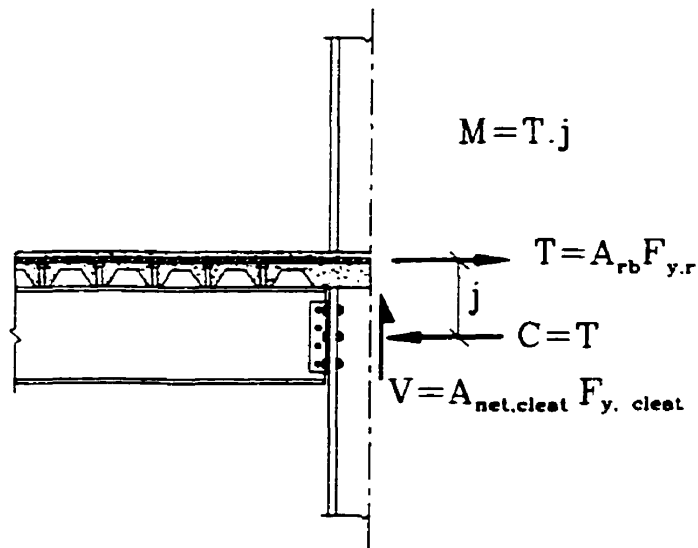


Figure 2.4: Typical Force Transfer Mechanism

For this study the connections are intended to be simple only. Thus any moment developed at the face will be neglected in beam design. Taking advantage of the partially restrained characteristics could very well be a future research path. This could potentially reduce the size of steel beam required in the gravity frame. For the floor layout and design loads for which this framing system is proposed, construction considerations would not allow for significant reductions in steel beam size, unless falsework is used prior to the slab hardening.

2.2 Composite Columns

There has been considerable work during the last 30 years into the performance and behaviour of composite columns using concrete filled hollow structural sections or encased W sections. A full description of these results is beyond the scope of this study, but this review will provide a summary of the major findings of the concentric column tests at École Polytechnique. These include concentric tests on both the bare steel profile, and the fully composite column, for a variety of column characteristics.

2.2.1 Non-Composite Column Strength

In CAN/CSA S16.1-M94 Limit States Design of Steel Structures², a general equation is given for the design of columns consisting of W sections, HSS, and WWF cross sections. This design equation is based on the assumption that the column will undergo global buckling, or reach the squash load prior to any local instability of the cross-section. To ensure that a section will not buckle locally the maximum width to thickness ratio, as defined in Table 1 of S16.1-M94 is given as²:

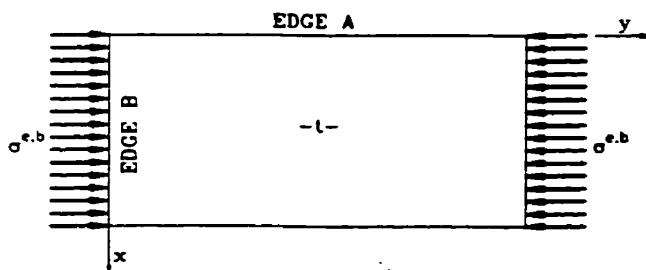
For Flanges of Columns:

$$\frac{b}{t} \leq \frac{200}{\sqrt{F_y}} \quad (\text{Eqn. 2.3})$$

Webs in Axial Compression:

$$\frac{h}{w} \leq \frac{670}{\sqrt{F_y}} \quad (\text{Eqn. 2.4})$$

For Grade 350W steel the maximum b/t ratio for this Class 3, non-compact classification is 10.6 and the maximum h/w is 35. Since the objective of using partially encased H columns is to optimize the steel to weight ratios, the b/t ratio is much larger than the above limit. The columns tested to date have b/t ratios of the range of 24 to 35, and h/w of up to 60¹. The steel column section can therefore be classified as Class 4, and the web or the flange will generally experience local buckling prior to yield stress being attained.



$$F_{\sigma} = k \frac{\pi^2 E_s}{12(1-\nu_s^2) \left(\frac{b}{t}\right)^2} \quad (\text{Eqn. 2.5})$$

Figure 2.5: General Plate Buckling Solution

The problem of determining the capacity of the bare steel column is directly related to the buckling strength of an axially loaded, restrained plate. The general solution²² for this problem is given in Figure 2.5.

The term, k , is referred to as the plate stability coefficient, and accounts for the edge constraints, nature of the loading and the aspect ratio of the plate. The k value depends also on the buckled shape, that is the number of wave half-lengths in both the transverse, m , and longitudinal, n , directions. For each n , the k value varies with the plate's aspect ratio. As the aspect ratio increases, k will decrease until it reaches a minimum. It will then increase, with an increasing aspect ratio. The minimum buckling coefficient will correspond to the critical buckling value for a plate. If n varies, $k_{critical}$ remains constant but the associated aspect ratio increases on the same order as n . Thus, for sufficiently long plates, where the aspect ratio is greater than the critical value, the critical stress is defined by the minimum k value. The buckling stress for long plates is therefore dependent upon the edge constraints only.

The capacity of the column shown in Figure 2.6 could be considered as the sum of the buckling loads of each of its comprising elements. In this case it can be taken as the sum of the column web and the buckling capacity of each flange half. The column web can be considered as a plate of length equal to the column height, L_c , and a width, W . Following the notation of Figure 2.5 the plate is loaded along edge "B", and is constrained along edge "A" by the web.

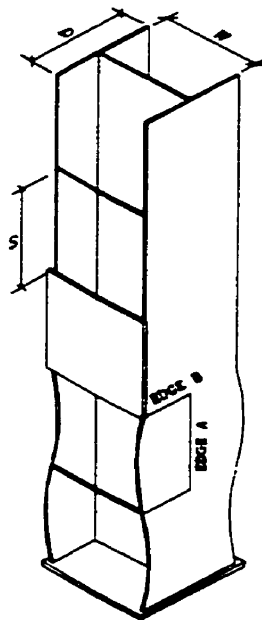


Figure 2.6: General Buckled Shape of Test Column

This plate buckling theory is the basis for the design provisions in CAN/CSA-S136 Cold Formed Metal Structures²³, which includes the design of Class 4 compression members. In the design process the area effective in resisting compression loads is reduced to account for local buckling. This effective area is multiplied by an effective stress, which is reduced to account for global buckling, to calculate the axial load capacity. The general equation for the resistance of a Class 4 column is (Clause 6.6.1, CAN/CSA S136-Cold Formed Steel Structural Members):

$$C_r = \phi A_e F_e \quad (\text{Eqn. 2.6})$$

where:

$$F_e = F_y - \frac{(F_y)^2}{4F_p} \quad (\text{Eqn. 2.7})$$

$$F_p = 0.833 \frac{\pi^2 E}{\left(k_1 L / r\right)^2} \quad (\text{Eqn. 2.8})$$

The $k_1 L / r$ ratio is based on the properties of the original column cross section.

The effective area will be the sum of the effective areas of the individual elements of the column. Clause 5.6.2 outlines the effective design width for each element type in compression. The effective width is defined in general form as²³:

$$\frac{b_e}{t} = 0.95 \sqrt{\frac{k_2 E}{F}} \left[1 - \frac{0.208}{b/t} \sqrt{\frac{k_2 E}{F}} \right] \quad (\text{Eqn. 2.9})$$

Where:

- b_e effective width (mm)
- t plate thickness (mm)
- k_2 buckling constant
- b original width (mm)
- F Nominal stress from Clause 13.3, CAN/CSA-S16.1 $\left(\frac{C_r}{A_g}\right)$

The value of k_2 is given in S136 – Design of Cold Formed Metal Structures for a variety of element types. For a web of an I-shape both sides are constrained, thus the corresponding k_2 value is 4. For the column flange of width b , one edge is assumed free and the other is assumed rigid, thus the k is taken as 0.43. Even if the tie spacing will lead to an aspect ratio that is less than the critical value, the final result assuming a k_{min} is conservative.

As part of École Polytechnique's research into column behaviour there were 11 tests conducted on bare steel stub columns, with a total length of 5D. Column sizes included 300 x 300, 450 x 450 and 600 x 600 mm specimens with tension stirrup spacing of either 0.5D or 1.0D. The b/t ratios of the column flanges were 24, 32, or 35. Results of the concentric tests are presented in Figure 2.7 and are compared to S136 predictions. The tested values for strength were generally greater than those calculated using S136.

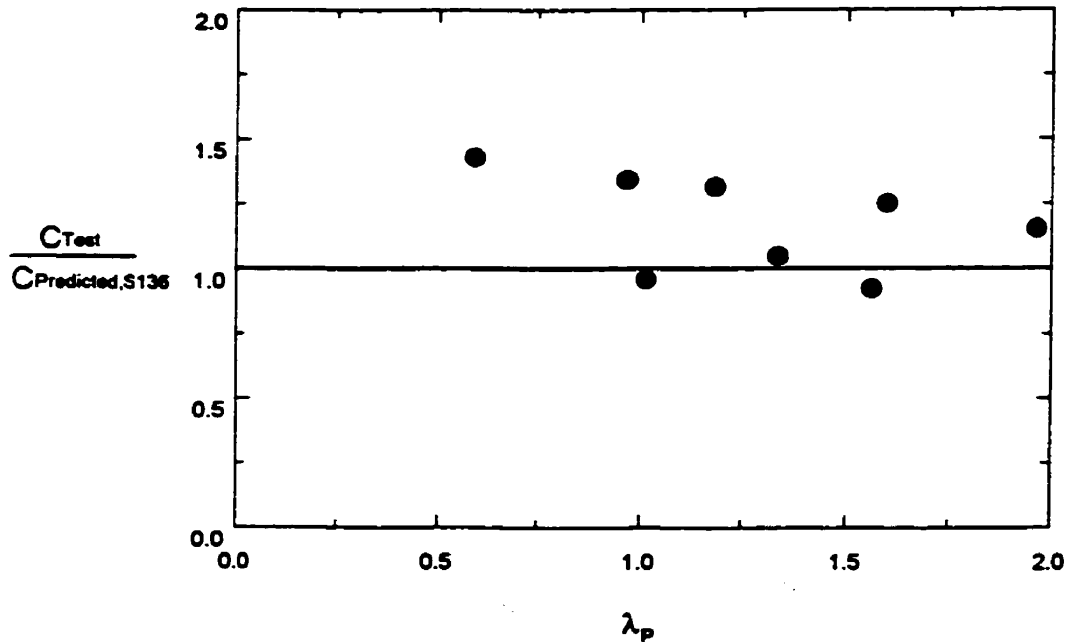


Figure 2.7: Results From École Polytechnique: Bare Column Results¹

2.2.2 Composite Column Strength

The overall strength of composite stub columns can be generally taken as:

$$P_R = \phi_s A_s F_y + 0.85 \phi_c A_c f'_c \quad (\text{Eqn. 2.10})$$

This is generally for concrete filled tubes and encased sections where the steel section is at least Class 3 designation. For a composite column composed of a partially encased Class 4 steel profile, allowances must be made for the probable buckling of the steel elements prior to the attainment of yield stress. This can be calculated as¹:

$$C_U = A_m F_y + 0.85 A_c F'_c \quad (\text{Eqn. 2.11})$$

where: $A_m = t(d - 2t + 4b_e)$ (Eqn. 2.12)

For the column web the steel is continually supported on both faces by the concrete. Thus the web will be able to attain yield stress. The flanges, although supported on one side by concrete, will be prone to outward buckling. A k value has been determined for a steel plate supported on one side by concrete¹.

$$k = \left[\frac{4}{(s/b)^2} + \frac{15}{\pi^4} (s/b)^2 + \frac{20}{3\pi^2} (2-3\nu) \right] \quad (\text{Eqn. 2.13})$$

Similar to the non-composite specimens, the effective flange width can be calculated as:

$$b_e = 0.6 \left(\frac{b}{\lambda_p} \right) \leq 1.0 \quad (\text{Eqn. 2.14})$$

where:
$$\lambda_p = \frac{b}{t} \sqrt{\frac{12(1-\nu^2)F_y}{\pi^2 E k}} \quad (\text{Eqn. 2.15})$$

In investigating the behaviour of the composite columns, the École Polytechnique group concentrically tested 10 specimens¹ with the following variables; tie spacing of 0.5 D and 1.0 D, and column sizes of 300, 450 and 600 mm with various b/t ratios. From the test results shown in Figure 2.8 there was good correlation between the experimental and calculated values of ultimate strength.

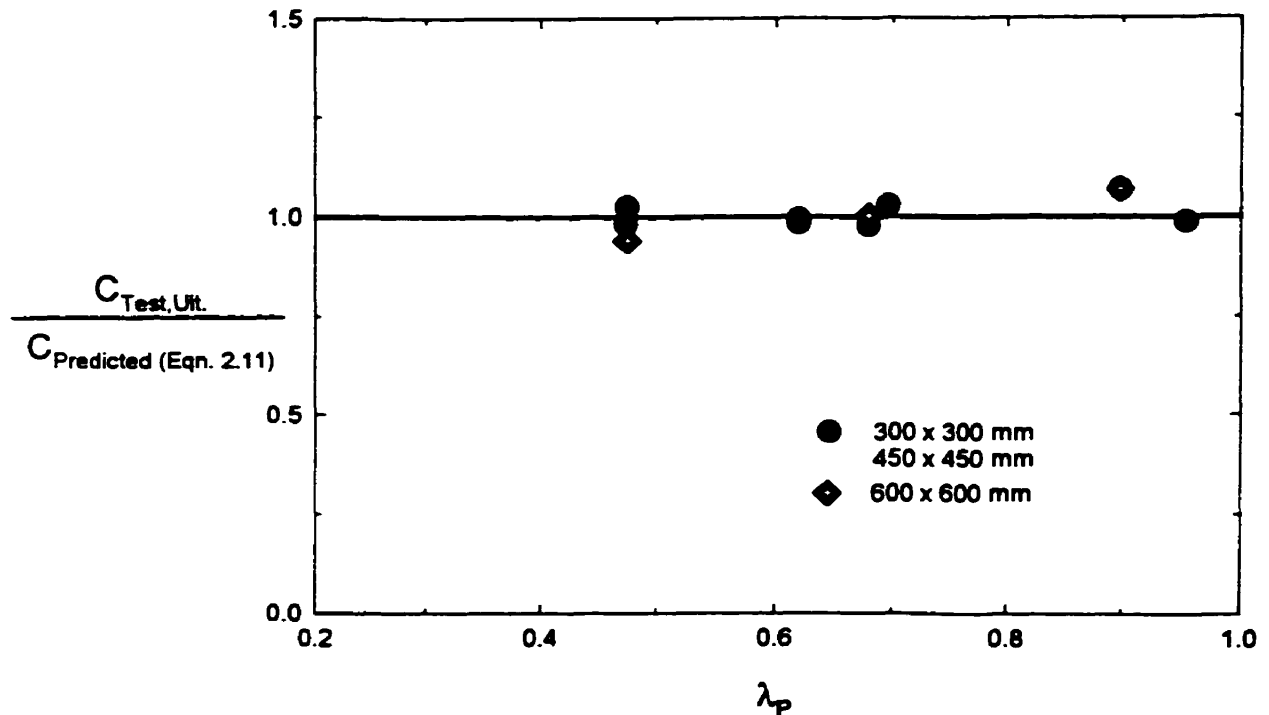


Figure 2.8: Results From École Polytechnique: Composite Results¹

2.3 Connections to Composite Columns

For the two major types of composite columns used in general practice in North America; concrete encased steel profiles, and concrete filled tubes, the connection design is both varied and the subject of continued research. For fully encased composite columns, the connection is usually made directly to the steel column, with the beam passing through the concrete. For the purpose of this study connections made to concrete filled tubes share many similarities and subsequent comparisons will be addressed.

There have been numerous connections suggested for concrete filled tubes, as illustrated in Figure 2.9. Most of the details presented have been suggested for full, or partial moment connections, intended for lateral resisting frames. There has been testing on moment connections to concrete filled tubes where the beam has been welded directly to the HSS²⁴, however the behaviour was limited by local failure of the tube wall. To help distribute the forces introduced at the flange locations several researchers have studied the possibility of an exterior diaphragm plate, as is often used in bare steel HSS truss connections^{24,25}. Connections of this sort have performed well under monotonic loading, and the results from cyclic tests indicated that they would be satisfactory in low to medium seismic applications.

There are also various suggested connections where the beam passes through the larger tube section^{26,27}. The through beams are effective in transferring the loads into the column, but the detail is expensive, and construction is more difficult because the beam impedes concrete placement. Other connection types with anchoring or stiffening hardware located on the inside of the tube are extremely difficult to fabricate. Shear studs must be welded on the inside to improve load transfer into the concrete and reduce connection flexibility. The problem with cheap and efficient connections to concrete filled tubes has been one of the main factors limiting their usage in moment frames.

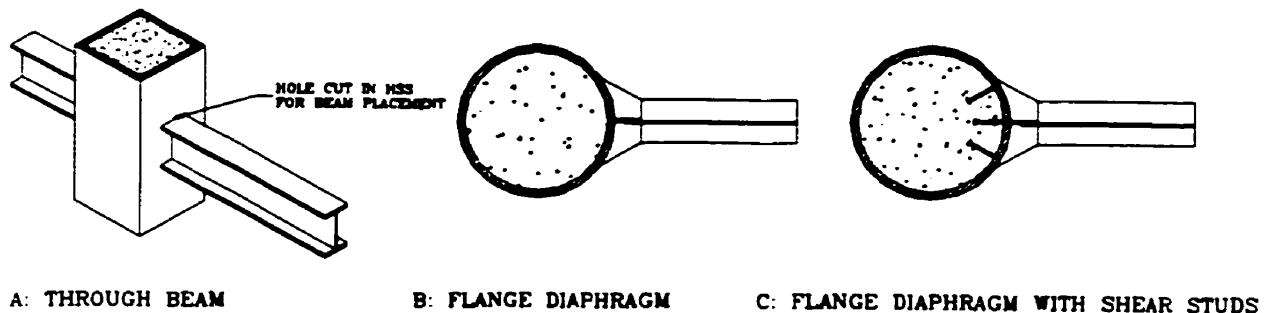


Figure 2.9: Types of Composite Moment Connections

2.3.1 Simple Shear Connections to Concrete Filled HSS

Unlike moment connections where the moment causes excessive separation between the steel and concrete, it is conceivable that simple framing connections can be connected to the steel only, and allow the forces to transfer from the steel into the concrete along the depth of the column. As long as there is strain compatibility existing at a distance below the connection, the use of anchorage may not be a prerequisite for an effective simple framing connections.

There have been several experimental investigations on the performance of simple shear connections to concrete filled hollow structural sections. Many of the connections are similar to those presented in this report and thus the studies were useful for the conception of the test set-up, instrumentation and better understanding of the behaviour. These studies dealt not only with the performance of the connection itself, but also provided a description of the force transfer mechanism from the steel into the concrete.

2.3.1.1 Dunberry, Leblanc, and Redwood³⁰

A series of 24 tests³⁰ were performed on concrete filled rectangular hollow structural sections, loaded axially and at a connection over the column height. The purpose was to evaluate the force transfer mechanism from simple shear connections into the concrete core without the aid of additional mechanical anchorage or shear transfer devices. Identical connections were loaded on both sides of the column, with the ratio of the connection load to the column load varied to assess the influence of the connection load on the overall column behaviour. Other test variables included the type of simple connection, the B/t ratio for the square HSS, and whether the column was capped or uncapped at the end points.

A series of steel strain gauges and concrete surface targets were placed over the column height to provide a strain gradient in both materials. This indicated the nature of the load transfer mechanism from the steel into the concrete. Generally, under the combined loading there was a zone of strain compatibility above and below the connection. In the vicinity of the connection there was a net slip on the order of 0.08 to 0.16 mm. For most specimens strain compatibility was achieved at a distance of three times the nominal HSS width below the connection, and twice the width above the connection. The transition was gradual, but the influence of the connection “pinching” against the concrete was obvious with a higher degree of concrete loading near the bottom of the connection. The pinching was caused by moments introduced from beam end rotation.

The predominant failure mechanism was that of local buckling, generally (but not exclusively) below the connection region. Of the 24 tests, covering a variety of column sizes (the largest being a HSS 203 x 203 x 6.25), connection types and loading patterns, the axial strength of the column was never less than 92 % of the calculated squash load of the concrete filled tube while under concentric loading. Local buckling was the general failure pattern, but none occurred prior to the steel yielding. The longer connections also allowed for a more gradual introduction of loads into the concrete.

2.3.1.2 Shakir-Khalil³¹

Full scale specimens of composite connections to concrete filled circular tubes were tested³¹ where both the column and the connection were loaded to represent the typical building application. Connections were installed on both sides of the column and consisted of single plate shear tabs welded to the tube only. For four of the eight tests Hilti nails were used near the connection as shear connectors in an effort to determine their effectiveness in allowing for a more efficient force transfer mechanism from the steel into the concrete.

All column specimens consisted of HSS 168.3 x 5.0 (British Standards) and were 2.8 m long. Connections consisted of 100 x 10 mm single shear tabs, with 3 or 4, 20 mm bolts. Part of the test variables was that there were two types of applied loading; first the connection eccentricity varied as either 204 or 334 mm from the column face, and secondly, the ratio of column load to connection load was either 8 or 5 to 1. The shear connectors consisted of 3.7 mm diameter, 62 mm long Hilti nails. There were four nails provided at the top, middle and bottom of the shear tabs. A rather extensive network of strain gauges, and LVDTs was used to monitor both the column response, but also to understand the force transfer mechanism from the steel into the concrete.

It was observed that yielding generally commenced not below the connection but rather in the middle of the shear tab. Shakir-Khalil attributed this to the residual strains resulting from the welding of the plate onto the steel tube. Heat generated by the welding process would cause tensile stresses in the connection region, and to ensure self-equilibrium the remainder of the column would be in compression. These residual compression stresses were the reason given for the yielding at the connection mid-height.

The longitudinal strains over the column height showed the disturbance was restricted to a length equal to the HSS diameter above and below the connection. Only steel strains were measured so the actual slip between the concrete and steel was uncertain. The strains recorded in the steel profile were compared to the theoretical strains based on strain compatibility and values for E_c and E_s .

calculated from material tests. The steel strain values were within 5% of the predicted values, suggesting little slip, even in the area of the connection.

It was shown that the failure load of the connection assembly increases with the presence of the shear connectors (7% improvement), use of a deeper shear tab (11% improvement with an increase of four from three bolts), and decreasing the lever arm of the beam load (8% increase).

2.4 Force Transfer Mechanism

In composite column design strain compatibility between the steel and concrete is generally assumed. Early research into column behaviour ensured strain compatibility by loading both the steel and concrete simultaneously. Early design codes (CAN/CSA S16.1-M89) ensured this condition, even for simple framing conditions, by stating that the concrete contribution can be used only when there was direct bearing. Due to the expense associated with the resulting construction detail there was limited research into the behaviour of connections made only to the steel section. The results of the research, which are summarised in the previous section, indicated that natural bond could be depended upon for load transfer in simple framing applications.

The natural bond between the loaded steel and concrete is due to adhesion from chemical reactions and/or suction forces from hydration, the mechanical interlocking between the concrete and the steel surface, and the binding of the two materials³². For the purpose of this report the term bond will refer to the surface bonding and friction agents collectively. At points of load introduction the quick transferral of forces is important for the overall performance of concentric tests³³. Natural bond is therefore of critical importance for the success of this connection type.

The bond stress is affected by a number of different parameters, especially the age of the concrete. Creep and shrinkage, could potentially have a major effect on the bond stress between steel and concrete, and thus the performance of the connection itself. This is a pilot study into the behaviour of the connection to the weak column axis, and the assessment of long-term effects is beyond the scope of this effort. Although not a part of this report the long term effect on the column behaviour was one of the technical issues to be addressed by the Canam Group.

In addition to the natural bond between the steel and concrete there may also be a load transfer directly at the connection itself. As the beam is loaded the beam end rotates, causing the connection to deform, and the connection plate to move away from the concrete face under the developed moment. This will cause the base of the connection to bear directly on the concrete, and direct shear transfer through friction.

3 Experimental Program

3.1 Design Parameters

The composite system proposed by the Canam Manac Group is intended for gravity frames, with all connections consisting of simple framing elements. Columns are to be spaced 12↔15 m (40↔50 ft) in one direction and 7.5↔9 m (25↔30 ft) in the other direction. Beams will be running along the longer dimension, with a spacing of approximately 3 m (10 ft). It is possible that either the beam or the girder could be framed into the proposed connection, along the weak axis of the column. Composite action can be assumed with a 75 mm deep slab, used in conjunction with a 75 mm metal deck, for a total floor depth of 150 mm. The metal deck can be considered as an effective lateral beam brace.

The design loads considered in discussions with Canam to develop a realistic experimental program for this study at the University of Toronto are given in Table 3.1.

DEAD			LIVE		
DL stl.frame	0.38	KPa	Construction		
DL columns	0.3	KPa	LL concrete&form	0.6	KPa
DL concrete	2.77	KPa	LL apron	0.3	KPa
DL mech+elec	0.24	KPa	LL finishing	0.3	KPa
DL ceiling	0.24	KPa	LL erection	1	KPa
DL flooring	0.15	KPa	Service		
DL walls int	1	KPa	LL occupation	3.83	KPa
DL walls ext	1	KPa			
$\alpha_{DL} =$	1.25		$\alpha_{LL} =$	1.5	

Table 3-1 : Summary of Uniformly Distributed Design Loads

This testing program investigated the effectiveness of the connection not only under full loading conditions but also during the construction stages. Thus it was important to determine a realistic range of loads that the beam column connection will have to endure in both the non-composite and composite phases of construction. These realistic load ranges will also have to be determined for either cases of the girder or the beam framing into the weak axis.

Although the connections tested in this experimental program were designed for this loading, they also met the 50% $V_{r,beam}$ requirement, as contained in Clause 21.4 of S16.1. This simply states that a bearing beam column connection must be designed for 50 % of the factored shear resistance of the supported beam, even if it exceeds the factored design loads.

Appendix A contains a complete summary of the design of the experimental program. For a range of column spacing the connection loads in both the construction and full service state were determined. Based on the above design parameters a typical beam size was selected to determine the 50% V_r requirements. The summary of the connection design loads is contained in Table 3.2.

Type	Construction Load (kN)	Full Design Load (kN)	50 % V_r Requirements (kN)
Beam Framing (Type I)	130 ↔ 180 kN	211 ↔ 293 kN	300 ↔ 352 kN
Girder Framing (Type II)	261 ↔ 360 kN	422 ↔ 586 kN	470 ↔ 574 kN

Table 3-2: Range of Factored Design Loads for Beam to Column Connections

3.2 Test Set-up - Loading Mechanism

The proposed test set-up, as shown in Figure 3.1, was intended to provide both an axial load on the test column and a connection load on the load beam. For the composite connection test the column was to be axially loaded to a nominal load of 1.0 Dead Load + 0.5 Live Load, then the connection loaded to failure. The bare steel tests were intended to evaluate the strength of the column while subjected to a typical construction load. Thus, the connection was loaded to typical construction load, and the axial load increased until buckling failure occurred in the test column.

To provide the axial load, the 8895 kN (2 million lbs.) capacity Fox Jack was used. The jack was mounted to a stiff cross-head that was connected to four columns, which were anchored to the reaction floor. Although the jack has a 8895 kN rating, the capacity of the system is limited by the strength of the floor bolts. The system, based on the floor bolts, is conservatively rated at 7250 kN. This was the upper bound used in the design of the column specimens.

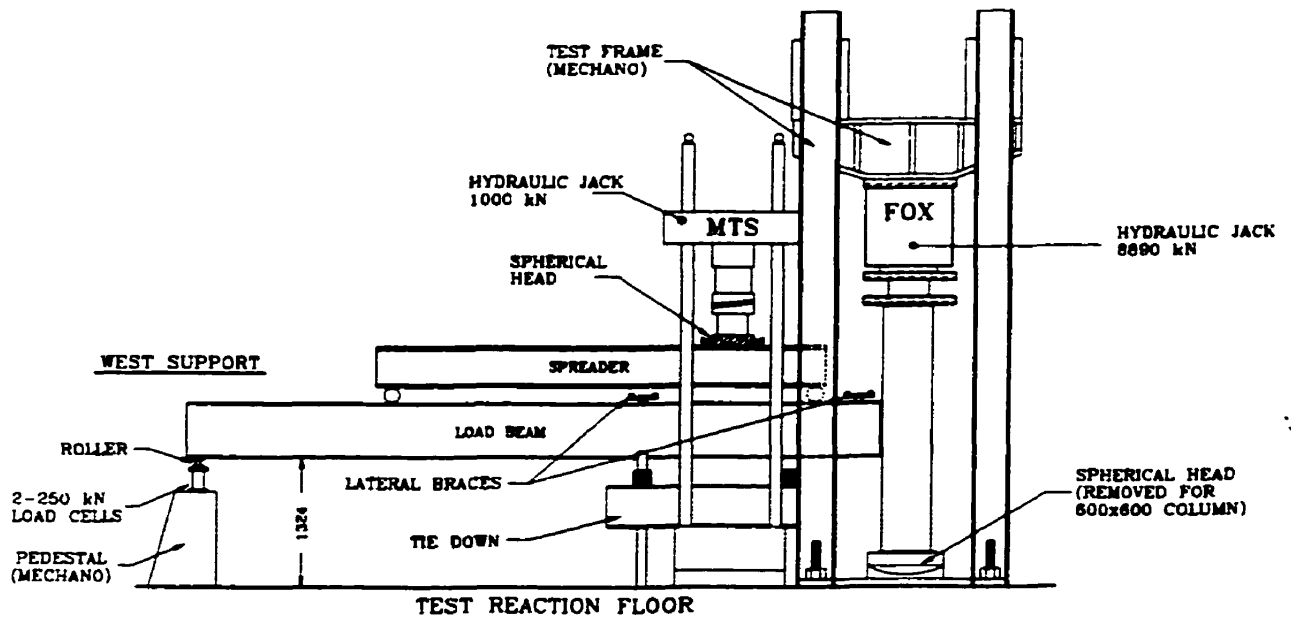


Figure 3.1: Test Set-up

The connection load was provided by the 1000 kN MTS universal testing machine. There were no provisions to anchor the MTS frame directly to the reaction floor. Thus a restraint system was designed to tie the MTS to four floor bolts. The east side of the MTS anchor system framed into the west set of Fox Jack frame columns. At the maximum MTS load approximately 500 kN was introduced into the columns, and the floor bolts. In determining the maximum permissible axial load on the column the anticipated connection load was considered. Based on these restrictions the maximum axial load that was available to test the specimen was conservatively taken as 6500 kN.

The geometry of the Fox Jack frame restricted the final placement of the MTS jack. The resulting distance between the actuator centrelines was 1575 mm, thus a long test beam was required to achieve higher beam shears at the column face. To limit the bending moment in the test beam a spreader beam was also used to distribute the applied load, without reducing the end beam shear. A very stiff beam, with a total length of 3900 mm, from the apparatus inventory at the University of Toronto was used. This was a very stiff section that experienced very little deformation during testing.

To react the beam on the far (West) end a support of stiffened structural steel, bolted to the strong floor, was used. There were rollers located at the far end and under both supports between the spreader and load beams. A photograph of the entire set-up is given in Figure 3.2.



Figure 3.2: Test Apparatus with Specimen C600-W410-SDA-C June 8, 1999. Mark Huggins Laboratory, The University of Toronto.

3.3 Design of Test Specimens

3.3.1 Test Columns

The main objective of the research conducted at the University of Toronto was to determine whether a connection to the weak axis of a partially encased, WWF composite column was possible through an exterior plate. It was not primary objective of the testing to fail the composite column, but rather to test the connection to failure while the column was loaded to an appreciable load level. The composite test condition governed the specimen design since the nominal load applied to the composite column is in excess of that anticipated to fail the non-composite section.

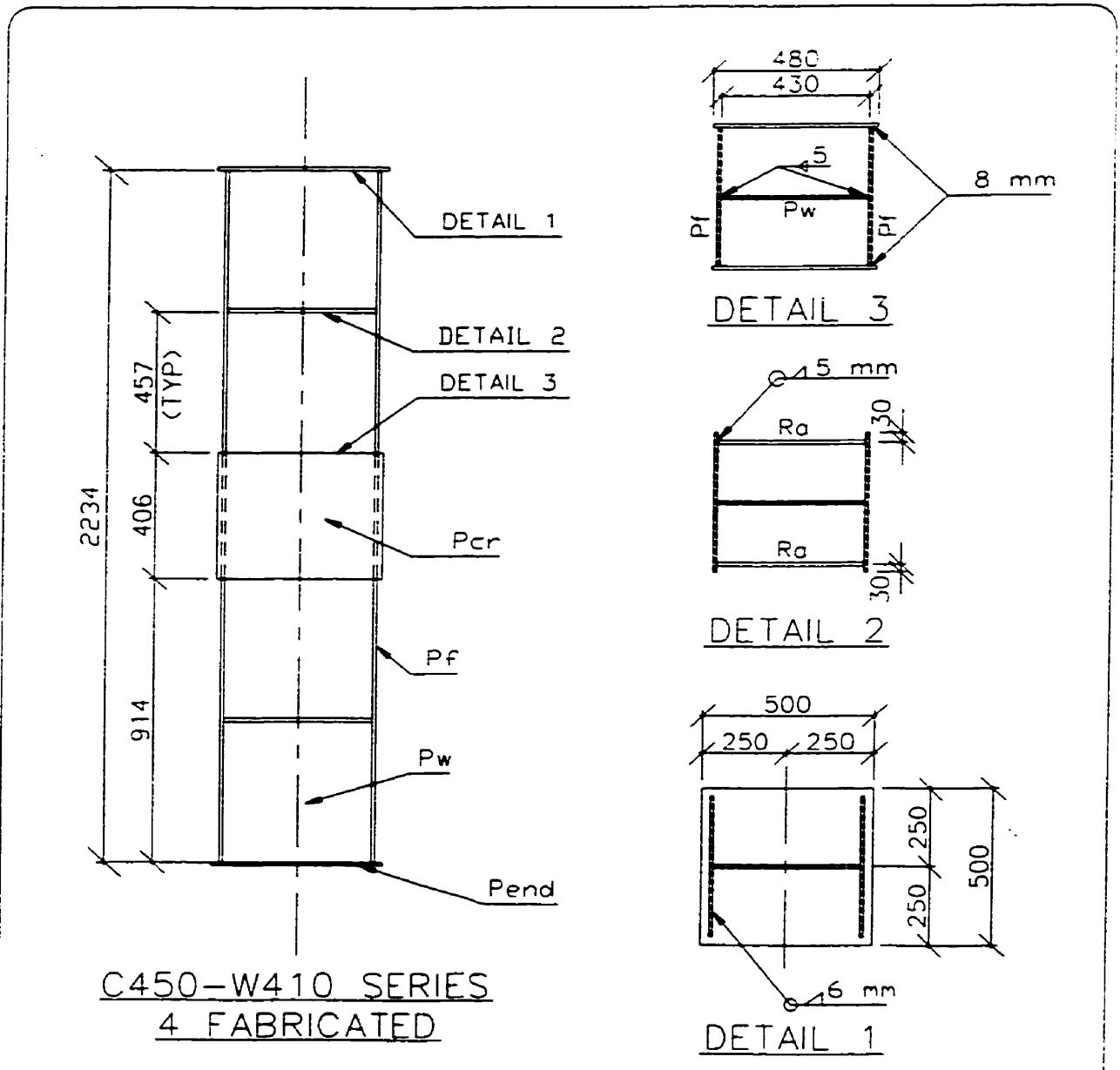
This research was meant to compliment the research conducted at École Polytechnique, thus the column sizes were originally limited to those within the parallel test program; namely, 300 x 300, 450 x 450 and 600 x 600 mm nominal square sections. Based on the design loads and floor layout provided in Section 3.1, the nominal load of 1.0 DL + 0.5 LL corresponds to about 67% of the factored resistance of the column. This is assuming a concrete compressive strength of 25 MPa and 350 W grade steel. In the initial specimen design the steel thickness was taken as 9.53 mm (3/8"). The axial test loads, for each of the three column sizes, are given in Table 3.3.

Column	b/t	w/t	P_r (kN) Eqn. 2.10	P_u (kN) Eqn. 2.10 ($\phi=1.0$)	P_{Test} (67% P_r)
300 x 300	24	46	2821 kN	3732 kN	1890 kN
450 x 450	22.5	43	6602 kN	8676 kN	4423 kN
600 x 600	30	58	9970 kN	9970 kN	6679 kN

Table 3-3: Column Test Loads

Based on the 6500 kN axial load limit it was decided that 450 x 450 mm would be the primary column size. Seven 450 x 450 mm columns were provided, all with a 9.53 mm steel web and flange thickness. Three columns were intended for bare non-composite tests, and four columns were cast for the composite tests (eight connection tests in total). To investigate the role of column size in connection performance an additional two 600 x 600 column specimens were provided for a single non-composite test and two composite connection tests. For the larger column size the column load was the 6500 kN capacity.

In order to examine the force transfer the column length was taken as the connection plate depth, with 2 x (Column Width) both above and below the connection plate. As will be discussed, there were two test beams corresponding to the different sized connection plates for the 450 x 450 mm column size. Complete fabrication drawings are given in Figures 3.3 to 3.5.



MATERIALS LIST					CANAM CONNECTION: C450-W410 TEST COLUMN	
MARK	QTY	DESCRIPTION	L(mm)	GRADE		
Pf	8	PL 450 X 9.53	2234	350W	DRAWN BY	J.L. MUISE
Pw	4	PL 430 X 9.53	2234	350W	CHECKED BY:	
Pend	8	PL 500 X 9.53	500	350W	DATE:	APRIL 20, 1999
Pcr	8	PL 406 X 9.53	480	350W	SCALE:	N.T.S.
Ra	16	BAR 12.7 dia.	430	350W		

Figure 3.3: Drawing of Column C450-W410

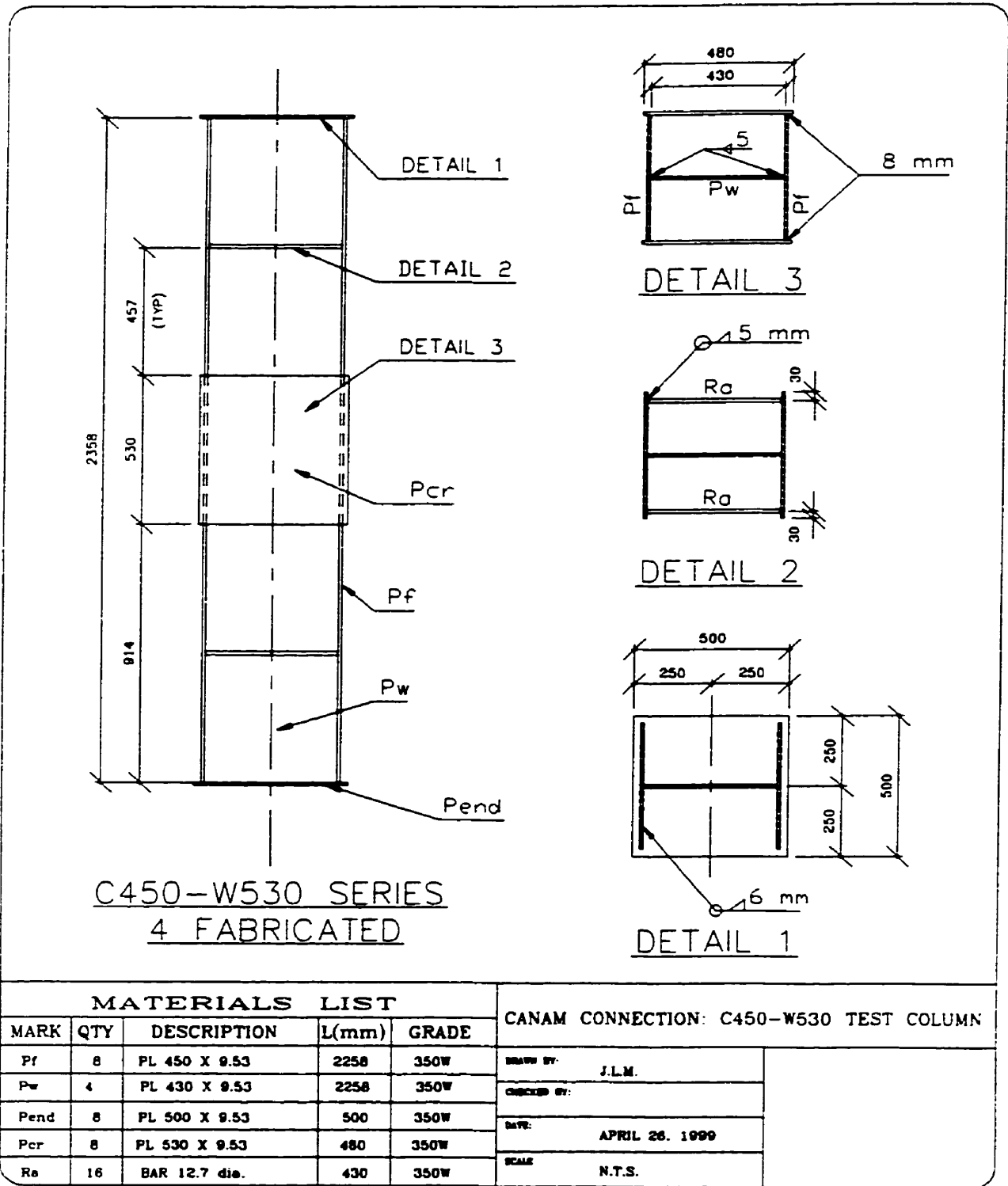
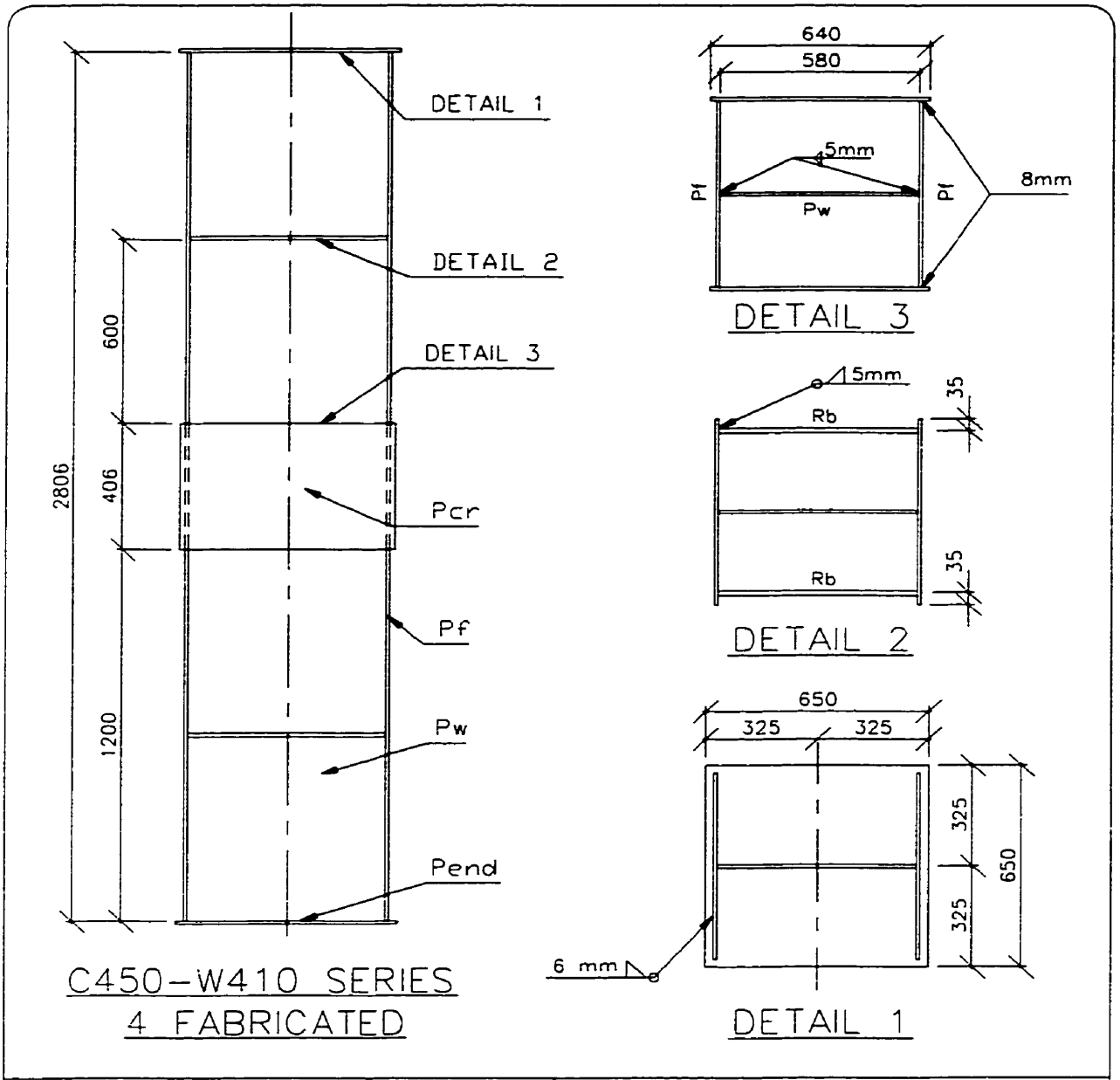


Figure 3.4: Drawing of Column C450-W530



MATERIALS LIST					CANAM CONNECTION: C600-W410 TEST COLUMN	
MARK	QTY	DESCRIPTION	L(mm)	GRADE		
Pf	4	PL 600 X 9.53	2806	350W	DRAWN BY:	J.L.M.
Pw	2	PL 580 X 9.53	2806	350W	NOTE:	ALL DIMENSIONS IN mm
Pend	8	PL 850 X 9.53	650	350W	DATE:	APRIL 30, 1999
Per	4	PL 406 X 9.53	640	350W	SCALE	N.T.S.
Rb	16	BAR 16 dia.	430	350W		

Figure 3.5: Drawing of Column C600-W410

3.3.2 Test (Framing) Beams

In the design process detailed in Appendix A, a range of realistic framing beams were designed to evaluate the 50% $V_{r,beam}$ restriction on the connection detail. The actual test beams did not necessarily have to be within this range, but they had to meet certain criteria. Since the MTS universal testing machine was located 1350 mm away from the column face, the beams had to be of sufficient length to get the required beam shear to fail the connection. Because of the 1000 kN limit on the MTS jack, the test beam had to be in excess of 5 m to get adequate shear force at the column face.

After the non-composite tests there was little observed distortion in the test beam, and the same end could be used for the corresponding composite test. After the composite tests there were shear and bolthole deformation at the beam end. Since the test beams were intended for multiple use, the beam end was cut (200 mm length) and the next connection detail prepared. Although local shear related deformation of the beam end was acceptable during the test, the general yielding of the test beam due to bending was not. Most important was a realistic beam web thickness to produce bolthole deformation typical of practical applications.

As outlined in Appendix A the minimum lengths required to get the percentage of applied MTS load at the column face were 5 m and 7.2 m for the cases of the beam and girder framing into the column. There was also an upper limit of approximately 7.5 m on the beam length imposed by available laboratory space. Therefore the beams were ultimately selected as a W410x67 and W530x92, which matched the range of realistic beam sizes outlined in Appendix A. The final shop detail prepared for the beams are shown in Figure 3.6. Additional length was provided to allow for the cutting of the shear deformed area following the composite test. As evident in the shop drawings both ends of the test beams were also used.

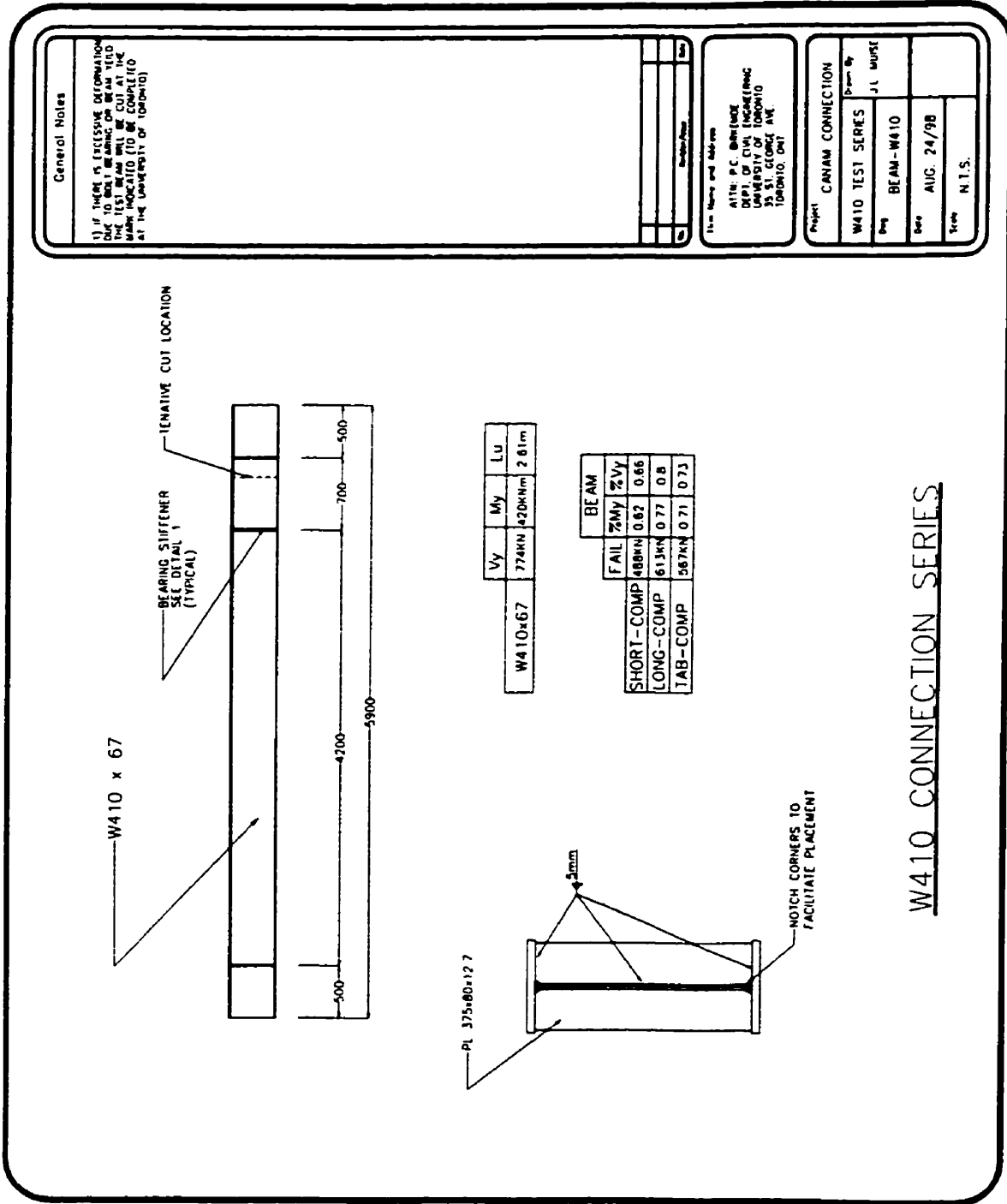


Figure 3.6: Load Beams W410 x 67 and W530 x 92

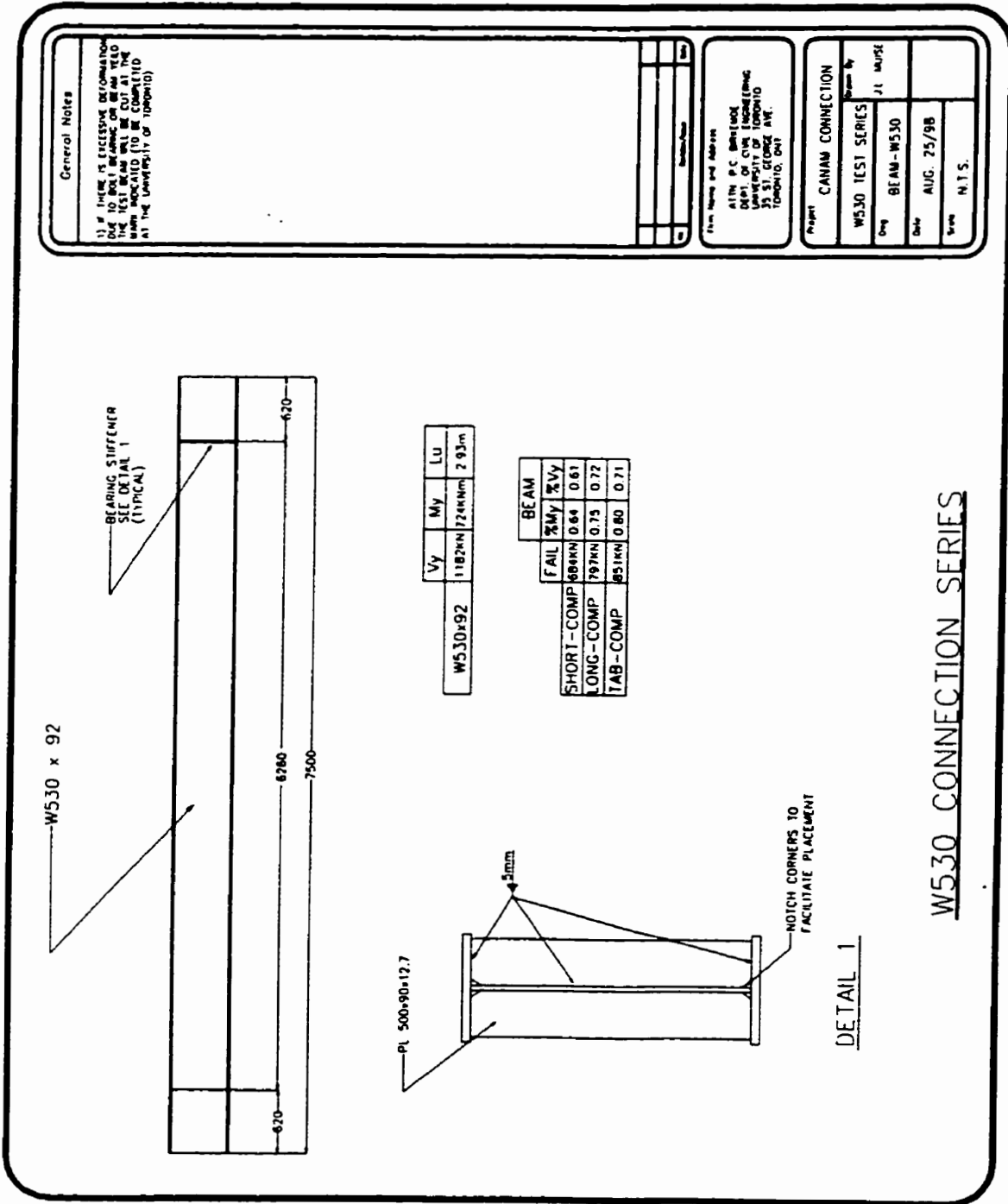


Figure 3.6b: Load Beam W530x92

3.3.3 Connection Types

Initially all major types of shear connectors identified by the Canadian Handbook of Steel Construction¹⁰ were considered for the experimental program. This initial list included the following:

- Shear Tab
- Single Angle Shear Connection
- Double Angle Shear Connection
- Endplate Connection
- Seat Connection (stiffened and unstiffened)
- Web End Plates
- Tee Connection

Canam technical staff indicated that in gravity frame systems double angle framing connections are the most common connection in use and should be included in the final test matrix. Due to the general economy associated with shear tabs¹¹ they too were included in the test matrix. To investigate the influence of the connection length on the overall performance, a short and long double angle connection was included for each beam and column size. For each beam size the number of bolts remained constant, but the bolt spacing varied. Thus for each beam and column configuration there were three connection tests to be performed in the composite state, the short double angle (SDA), long double angle (LDA), and the shear tab (TAB). After the initial prototype tests (as will be discussed subsequently) two additional seat connections were included. Canam did not intend to use a seat connection for a beam column connection, but it was recognised as a potential method of attaching open web steel joists.

All connections were designed to resist the shear loads given in Table 3.2 with the 50 % V_{beam} generally governing. The connections were designed for the basic shear load only and taken as being “in-line”. When considering each potential failure mode (i.e.; bolt group failure) the effect of any moment was ignored, and the capacity based on the shear load only. Tables 3-4 and 3-5 summarise both the connection details, and the connection resistance for all the connections included in this experimental program. These values are based on Grade 300 W steel for the connection angles. The factored connection resistances are based on a yield and ultimate stress of 300 and 450 MPa respectively. The calculated failure loads are based on the actual material properties (Appendix C) and a resistance factor taken as unity. All potential failure modes are listed in the table.

Table 3-4 : Summary of Connection Details

Test	Test Identifier	No. of Bolts	Bolt Spacing (mm)	Connecting Element	Total Length (mm)	Factored Resistance (kN)	Calculated Ult. ($\phi=1.0$) (kN)
1	C450-W410-SDA-N	3	60	L76x76x6.4	190	-	-
2	C450-W410-SDA-C	3	60	L76x76x6.4	190	336	488
3	C450-W410-LDA-C	3	90	L76x76x6.4	250	455	613
4	C450-W530-LDA-N	4	85	L76x76x6.4	325	-	-
5	C450-W530-SDA-C	4	65	L76x76x6.4	265	484	684
6	C450-W530-LDA-C	4	85	L76x76x6.4	325	593	797
7	C450-W410-TAB-N	4	80	PL 110 x 10	310	-	-
8	C600-W410-SDA-N	3	60	L76x76x6.4	190	-	-
9	C450-W410-TAB-C	4	80	PL 110 x 10	310	380	567
10	C450-W530-TAB-C	6	80	PL 110 x 10	445	570	851
11	C450-SEAT-NoAnch	2	N/A	L203x102x20	225	-	-
12	C450-SEAT-Anchor	2	N/A	L203x102x20	225	-	-
13	C600-W410-SDA-C	3	60	L76x76x6.4	190	336	488
14	C600-W410-LDA-C	3	90	L76x76x6.4	250	455	613

Table 3-5: Calculated Capacities for the Connections Included in This Study

300 W	Yield (MPa)	Ultim. (MPa)	Connection Angle			Web	Web	Bolt	Weld
			Yield (kN)	Net Sect. (kN)	Tear (kN)	Bearing (kN)	Tearout (kN)	Failure (kN)	Failure (kN)
Angle:	322	514							
Plate:	370	523							
W410x67	SDA	Factored	390	336	380	455	400	571	347 (w)
		Ultimate	466	502	560	-	-	852	489 (b)
	LDA	Factored	514	494	554	455	509	571	457 (w)
		Ultimate	613	737	801	-	-	852	647 (b)
TAB	Factored	558	448	494	606	581	380	567 (w)	
	Ultimate	655	680	712	-	-	567	845 (w)	
W530x92	SDA	Factored	574	478	540	703	582	760	484 (w)
		Ultimate	684	715	779	-	-	-	686 (b)
	LDA	Factored	668	686	698	703	764	760	593 (w)
		Ultimate	797	950	1014	-	-	-	841 (b)
	TAB	Factored	801	632	694	909	928	570	814 (w)
		Ultimate	941	961	1010	-	-	851	1213 (w)

Note:

- 1) The capacities are based on "shear load" only unless otherwise noted.
- 2) The actual yield and ultimate stresses were used for the calculated ultimate. Specified strengths were used for the factored resistances. The specified strengths were 300W for the angles, 350W for the shear plate, and 350 W for the test beam.

3.3.4 Mechanical Shear Connection

It was originally thought that the use of mechanical anchorage would be a prerequisite to ensure acceptable behaviour of the connection endplate in the fully composite state. This anchorage could either be placed over the interior depth of the connection end plate, or on the column flanges adjacent to the plate. This mechanical anchorage would have likely consisted of conventional welded shear studs. The role of the anchorage would have been two fold; namely, to prevent excessive distortion of the connection plate and to allow for a means of force transfer from the steel into the concrete other than by bond strength and friction.

The perceived need for mechanical anchorage resulted in an initial prototype test of a 450 x 450 mm column specimen, cast with no anchorage. If column failure did not occur during testing of the connection, the prototype column specimen could potentially be successfully tested on both sides. Thus the prototype specimen was prepared for both a SDA and LDA connection test. The results indicated that mechanical anchorage was not as great of a concern as was first thought. Following discussions with Canam engineers and researchers from École Polytechnique it was decided that only one test with anchorage would be done. A seat connection with four shear studs welded to the back of the connection end plate was included in the test matrix. The shear stud layout is shown in Figure 3.7. For direct comparison an additional test with the same seat detail was included without the anchorage.

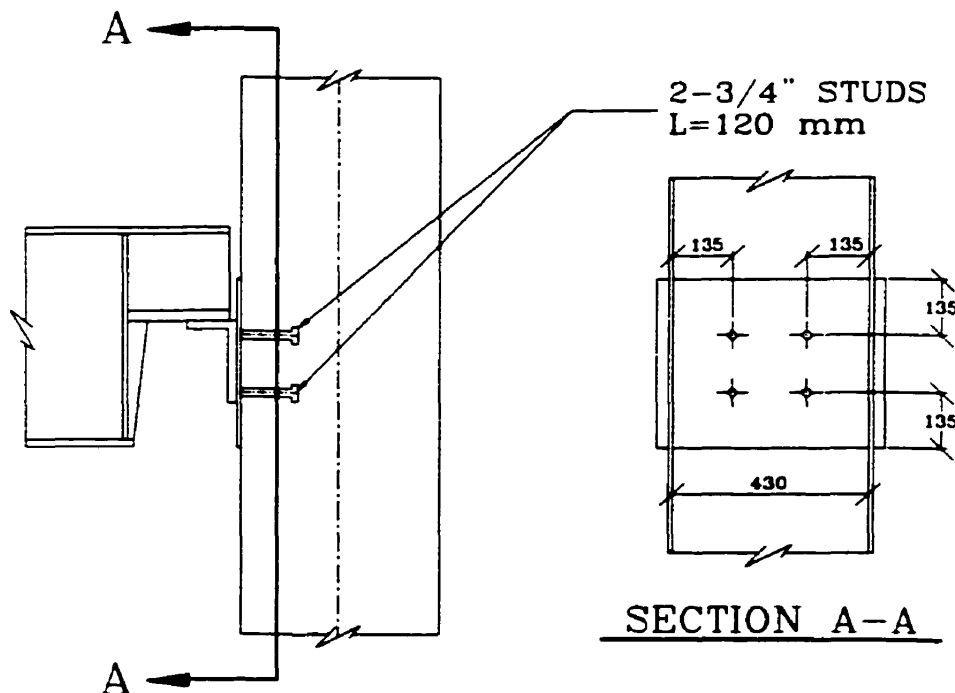


Figure 3.7 : Shear Stud Layout in Specimen C18-Seat-Anchorage

3.3.5 Final Test Matrix

The final test variables include the column size, the beam depth, connection type and composite/non-composite status. There were two tests performed on seated connections to cover the possibility of open web steel joist being used in the framing system. Shear stud anchorage was included for one of the seat connection tests. Table 3.6 provides a summary of the resulting test matrix, with the specimen identification used throughout the remainder of this report.

Column Size	Beam Depth	Construction State	Connection Type	Specimen Identification
450 x 450	W410	Non-Composite	Short Double Angle Shear Plate	C450-W410-SDA-N C450-W410-TAB-N
		Composite	Short Double Angle Long Double Angle Shear Plate	C450-W410-SDA-C C450-W410-LDA-C C450-W410-TAB-C
	W530	Non-Composite	Long Double Angle	C450-W530-LDA-C
		Composite	Short Double Angle Long Double Angle Shear Plate	C450-W530-SDA-C C450-W530-LDA-C C450-W530-TAB-C
600 x 600	W410	Non-Composite	Short Double Angle	C600-W410-SDA-N
		Composite	Short Double Angle Long Double Angle	C600-W410-SDA-C C600-W410-LDA-C

Table 3-6: Final Test Matrix

3.4 Specimen Fabrication

All material for the test specimens was supplied by Canam, and delivered in three separate shipments. The first shipment consisted of the test columns, as shown in Figures 3.3 to 3.5. Rods were provided if additional stirrups were deemed necessary after the prototype test. The load beams, and the connections were supplied in the second shipment. The connection angles were specified as 6.25 mm (1/4") thick. Upon delivery it was noticed that the actual thickness was 9.53 mm (3/8"). Thus a third shipment was required containing the correct connection angles, two channel lengths

used for the MTS universal testing machine tie down and the structural bolts. The first two deliveries were from the Canam plant located in Laval, Quebec, and the third delivery was from the Canam joist plant in Brampton, Ontario.

The columns consisted of 9.53 mm (3/8"), 350 W plate. During fabrication a piece of plate section was put aside for material testing, the results of which are contained in Chapter 4. A general summary of the fabrication is given in Figure 3.8. Following the flame cutting of the plate to the required dimensions, the flange-web-flange assembly was first tacked then fully welded with 8 mm fillet weld. After the main welding the tension stirrups (12.7 mm and 16 mm rods for D= 450mm and 600 mm respectively) were welded in place. For the University of Toronto specimens there were four stirrups included on each column. The last stage was the welding of the column cap-plates at the column ends, and then the welding of the connection plate at the column mid-height.

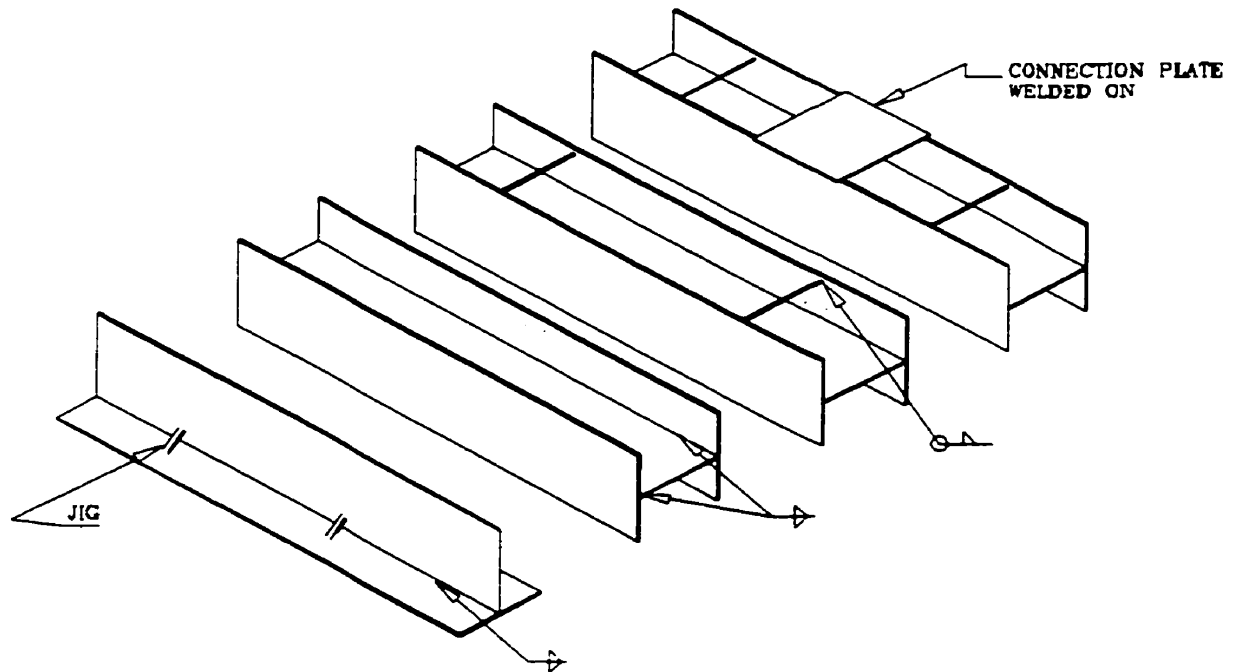


Figure 3.8 : Overview of Fabrication Process

The connections themselves were not welded to the plate in the Canam shop. To allow flexibility during the testing it was decided to weld the connections using the University of Toronto facilities. The connections for the first four test were welded by university staff. The welding for the second phase of testing was also conducted at the University of Toronto, but performed by a welder from the Canam Brampton joist plant.

The two load beams (W530 x 92, and W410x 67) were cut to length, the bottom flange coped, and the holes punched at the Canam plant. After each composite test the beam underwent an expected amount of shear deformation. To remove the damaged length the beam end was cut and the holes drilled for the subsequent test at the University of Toronto, Mark Huggin's Laboratory. The University of Toronto staff also performed the modifications made to the W530 test beam to accommodate the seat connection.

The five composite columns (ten tests) were cast using ready mix concrete from a local supplier. All columns were cast vertically, with the top end plate removed to facilitate concrete placement. There were two concrete casts; the first for the initial prototype specimen (Oct. 7, 1998), and a second cast for the remainder of the specimens (March 25, 1999). Each column was filled in two lifts, with approximately 20 minutes between lifts. The concrete was cast to about 10-25 mm below the edge of the steel profile, with the gap later capped with a high performance grout. For the prototype specimen top column endplate was welded back on the column after the concrete cast. The connections were also welded after the cast. For the remainder of the composite columns the connections was welded prior to the concrete placement and the endplate was not returned.

3.5 Testing Procedure

Initially, the spherical head was levelled, locked and centred with respect to the Fox Jack. The column was then positioned on the spherical head, and the specimen referenced to the four columns of the loading frame. Once the geometric centering was ensured the column levelling was again checked.

Following placement of the column the loading beam was installed. After the bolts came into bearing under the beam self weight the bolts were pretensioned. For the first two tests the bolts were pretensioned with a Torque Wrench, to 300 ft-lb. The remainder were tightened in the recommended turn-of-nut method. Each bolt was brought 1/3 turn past snug, as defined for a 3/4" A325 bolt of 2 1/4 inch length, by the AISC³.

Following beam fit-up the various bracing systems were installed. The articulated bracing rod ends used in the lateral beam and column bracing were tightened so they just slipped over the pin. The slab restraint was also tightened to a snug state. To accommodate the unevenness of the beam flange, the rollers placed between the load beam and the spreader beam were grouted and levelled.

Prior to testing, high performance Hydrostone cement grout was used between the top of the column at the Fox Jack loading plate. This was a fixed end, not a spherical head, and had a relatively smooth contact surface prior to placing the grout. Although Hydrostone was ready to be loaded ½ hour after casting, it was generally placed two hours before commencement of the test.

Just prior to the test the spreader beam was placed on top of the load beam, and all measurements (i.e.; a_1 , a_2 , L , d_{MFS}) were recorded. The crane was left connected to the spreader beam during the test as a precautionary measure against collapse caused by sudden failure of the connection; as the spreader beam was not braced.

The test started by first applying a small (100-200 kN) preload on the column and unlocking the spherical head. The axial load would then be increased to the desired level. After a small preload was placed on the connection the rollers under the spreader beam (2) and the west support (1) were unlocked. The connection would then be loaded to a construction story load for the non-composite tests, or to failure in the composite tests.

3.5.1 Non-Composite Connection Loading

The purpose of the non-composite testing was to evaluate the influence of the connection on the overall behaviour of the column, and was intended to complement previous and ongoing research¹. There were three options in testing the non-composite beam column connection. The first, to apply a nominal load on the column then load the connection until failure. Secondly, to load the connection to a typical construction load then load the column to failure, and finally load the column and connection simultaneously in realistic proportions.

There is an upper limit to the possible connection load during construction, and it is less than the post-construction factored connection load. The real interest in the construction stages is the number of floors of steel frame that can be supported prior to placement of the concrete. It was therefore decided that the second option would reveal the more important information. That is, to determine the load that a typical column can withstand, while loaded along the weak axis.

The testing procedure involved three separate load stages. The column was first loaded to 700 kN, which represented a typical one story construction load. The connection was then loaded to 1.5 x (Floor Load). This corresponds to 300 and 375 kN for the two cases of the beam (W410 load beam) and girder (W530 load beam) framing into the column. The column was loaded first to minimise the lateral movement of the column in the test frame during the connection loading. In the third load stage the axial load on the test column was increased until buckling occurred.

3.5.2 Composite Connection Loading

The primary objectives of the composite testing were to investigate the behaviour of the connection, specifically the integrity of the exterior connection plate under loading and secondly, investigate the force transfer from the steel into the concrete. Thus, it was necessary to load the column axially while the connection was loaded to failure. As previously discussed the nominal load was taken as 1.0 Dead Load and 0.5 Live Load. This corresponded to approximately 50% of the ultimate squash load. The calculated values are given in Table 3.3, but for testing the axial loads were 4500 kN and 6500 kN for the 450 and 600 mm test columns respectively.

3.6 Instrumentation

The instrumentation had to meet two main objectives. First, it must monitor the general load deformation response of the connection and column in both the bare steel state and fully composite state. Secondly, it had to help determine the force path from steel into concrete. A general schematic of a typical instrumentation pattern is shown in Figure 3.9.

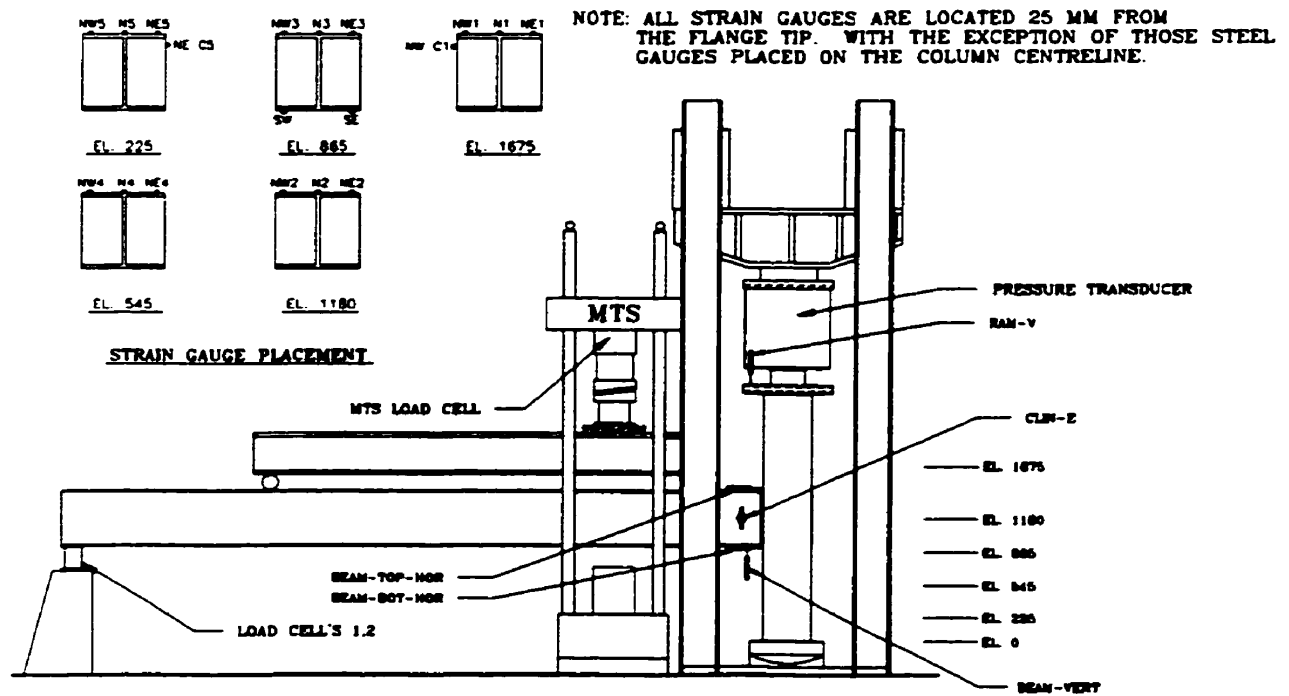


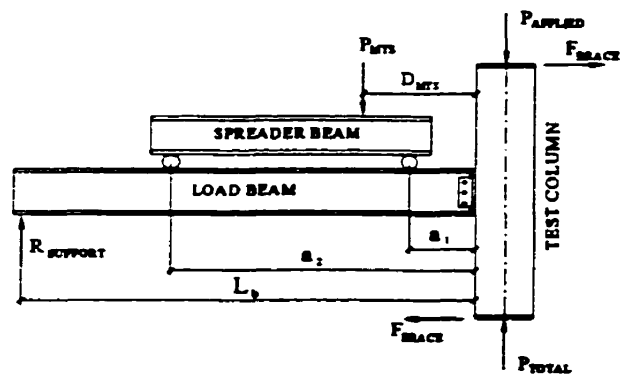
Figure 3.9: Typical Instrumentation

There were four primary reactions which had to be recorded during testing. Two 250 kN load cells were placed under the load beam on the west side to record the far end reaction. The load applied by the 1000 kN MTS was recorded with the load cell built in the testing machine. The applied column load was measured by two separate means. For tests with the shorter C450-W410 column a 6300 kN capacity load cell was sandwiched between the Fox Jack and a loading plate. Otherwise, a pressure transducer was connected to the hydraulic hose. From the pressure in the hose the force applied by the Fox jack could be determined. Prior to general testing the pressure transducer was calibrated with the before-mentioned load cell. The total column load under the beam could be simply taken as the algebraic sum of the applied loads, with the west reaction subtracted. The only other external reactions were from the braces, which were horizontal and self-equating.

Since the total beam length, the distance to the MTS, and the distance from each of the rollers to the column face are known, the beam shear and the moment at the column face can be calculated. On the following free body diagram shown in Figure 3.10 the moment developed at the bolt line or the column face can be readily calculated. For the purpose of this illustration the load transfer through the spreader beam has been explicitly included, but in the subsequent discussions the beam shear, V_{applied} , will be directly equated as a function of P_{MTS} .

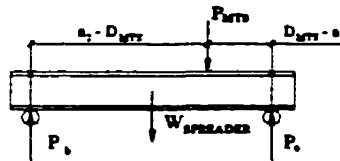
In addition to the forces and reactions instrumentation was also in place to record the deformation response. A clinometer was placed on the beam web beam and at the column centreline to measure the respective rotations. To measure the separation between the beam flange and the column face a LVDT was mounted on the top and bottom flanges of the load beam and referenced to the column face. For the composite specimens the plunger rested directly on the concrete. For the non-composite tests the plunger was referenced to a 15 mm plate that was installed from flange tip to tip. This plate could accommodate some flange movement, but as the buckling in the column progressed the plate used for the datum also buckled. The deformation recorded by these two LVDTs not only included the separation of the beam from the exterior connection plate, but also the separation of the cross plate from the concrete.

In several non-composite specimens, strain gauges were placed at the same location in both the inside and outside of the column flange, directly below the loaded connection. The strain gauges were vertically at an equidistant location from the connection plate and the tension stirrup. This is where buckling would likely initiate, and the gauges were installed to monitor it's progression. For the composite tests a network of strain gauges were installed on the steel flanges and at key locations on the concrete face. A typical gauge pattern used in the composite testing is shown in Figure 3.9.



$$P_{\text{Total}} = P_{\text{MTS}} + P_{\text{Applied}} + R_{\text{Support}} \quad (\text{Eqn. 31.})$$

$$P_o + P_b = P_{\text{MTS}} + W_s \quad (\text{Eqn. 3.2})$$



$$V_{\text{Connect}} = P_b + P_o + W_{\text{LB}} - R_{\text{Support}} \quad (\text{Eqn. 3.3})$$

$$\sum M = 0;$$

$$M_{\text{Bolt}} = P_b(a_2 - c_{\text{bolt}}) + P_o(a_1 - c_b) + W_{\text{LB}}(L/2) - R_{\text{Support}}(L - c_b) \quad (\text{Eqn. 3.4})$$

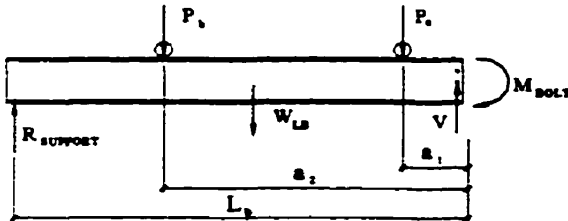


Figure 3.10: Free Body Diagram of Test Set-up

3.7 Bracing Considerations

3.7.1 Lateral Beam Bracing

The load beams, being of realistic size and length, were subjected to a bending moment nearing yield for the higher connection loads. With the addition of the spreader beam to distribute the applied load a high bending moment was constant over the length of the spreader beam. Since the test beams would be reused for subsequent tests it was important to ensure that no plastic deformation occurred and to limit out of plane displacement of the top flange, which could lead to lateral buckling.

From the lateral bracing calculations in Appendix B the minimum brace length was 2150 and 2490 mm for the W410 and W530 load beams respectively. This is based on a constant moment over the beam length, but a near constant moment does exist in the test beam between the spreader beam

supports. From existing components of the test frame, brace points were most easily positioned 500 mm and 1850 mm from the column face (See Figure 3.1). Although the second brace point would be 5 m from the end on the longer load beam, it would just be just 2.2 m from the west spreader beam roller. The majority of the unbraced length of the load beam would not be under a constant bending moment.

The articulated lateral brace system used for the test beam is shown in Figure 3.11. A 1-1/4" threaded rod, with swivel rod ends, was attached to a "three pin" bar attached to the test beam. The system allowed the test beam to move both vertically and longitudinally, but lateral movement was prohibited. The strength and stiffness of the system was checked in accordance with Winter's Method for bracing design³⁴.

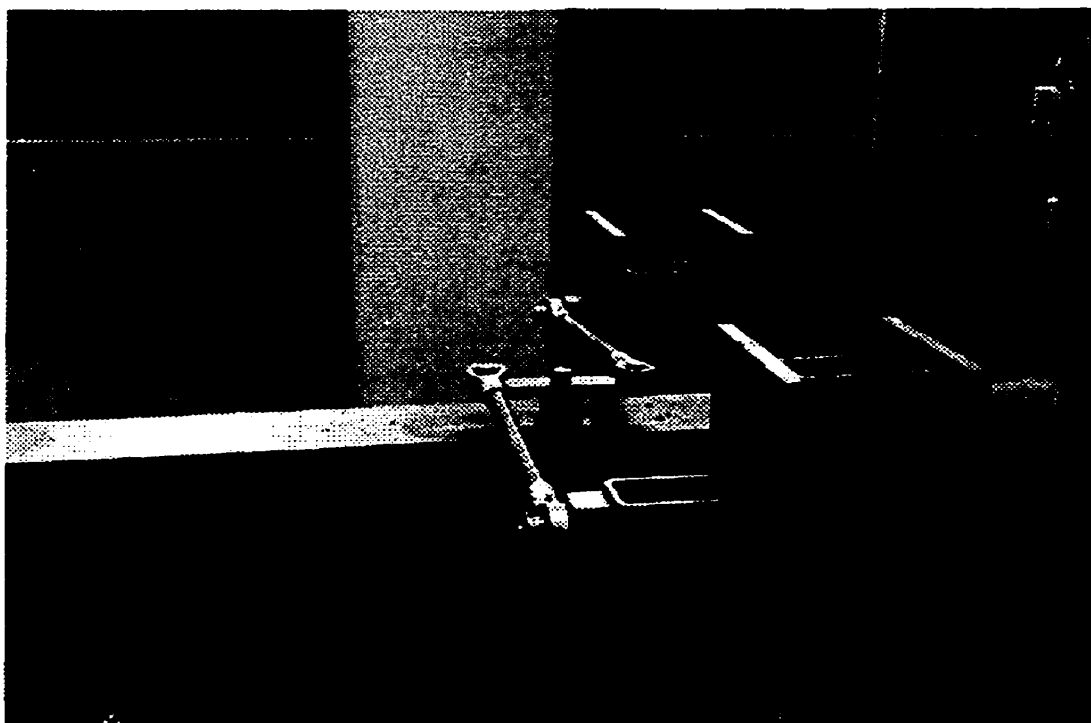


Figure 3.11: Lateral Bracing of Beam

3.7.2 Longitudinal Bracing of Beam

During construction and prior to placement of the concrete slab, longitudinal bracing (in line of beam) is limited to the restraint provided by the connection plate, at both beam ends. This can essentially be viewed as a free state, with no extra considerations provided for in this research. Following hardening of the concrete in the composite floor system, the beam is restrained against

longitudinal movement by the slab. The restrained movement of the top beam flange from the column face has been shown to enhance connection performance.

The beam restraint was an initial concern in the composite connection tests, but there were no provisions for a bracing system in designing the experimental set-up. Following the prototype tests it was decided to provide a longitudinal beam restraint system. Although it is difficult to quantify the restraint provided by a slab in an actual building application, the bracing system was included to illustrate the role of the concrete slab. The system would not be as stiff as the slab, but would better reflect the reality of the restraint.

To make the forces equilibrating the top flange restraint was tied to the column and not the test frame. It consisted of an HSS 126 x 75 x 9.5 connected to the load beam with two 3/4" diameter A325 bolts. A smaller HSS 75 x 75 x 6.25 straddled the east side of the column. Threaded rod (3/4" diameter) tied the HSS sections together. Since the threaded rod was delivered in shorter 914 mm lengths a threaded coupler was used to attach two rods on each of the North and South sides of the test column. Strain gauges were installed on the sleeved couplers to monitor the forces developed in the restraint system.

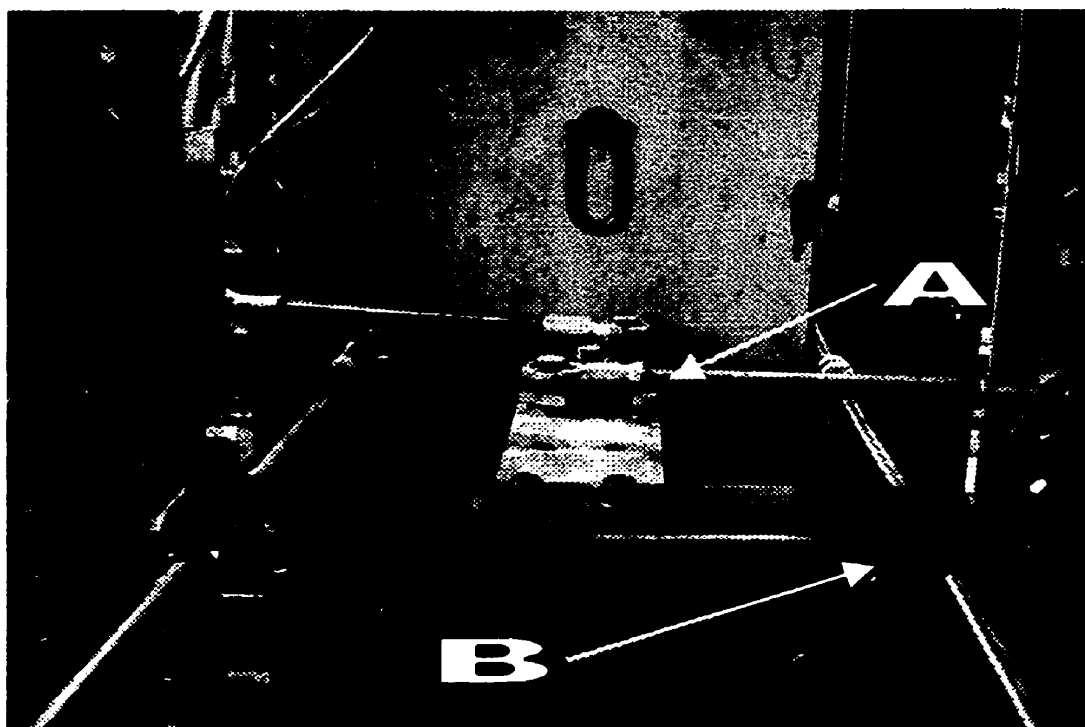


Figure 3.12: Overall View of Bracing a) Lateral Beam Bracing, b) Slab Restraint

3.7.3 Column Bracing

Due to the eccentricity of the connection load there will be a horizontal force at the ends of the test column. Due to the ratio of the axial load to the connection load, friction could be depended upon to transfer the horizontal force into the Fox Jack. The existing test frame for the Fox Jack can only accommodate small shear forces thus there could potentially be slip, or even damage to the Fox Jack resulting from the horizontal loads. A separate bracing system was therefore provided to transfer the horizontal shear into the test frame.

The column ends were prevented from movement by a “stop” placed adjacent to the test specimen and bolted to the loading plate. The loading plate was then braced to the frame columns with a 1-1/4” diameter threaded rod, with a swivel rod end as used in the lateral beam bracing. This provided horizontal restraint but allowed rotation, changing the spherical head to a pin condition.

The small vertical displacements of the loading plate under the Fox Jack, during the loading of the composite columns were easily accommodated by the bracing. For the non-composite tests the top braces were replaced by a single roller reacting against the test frame. This roller provided horizontal restraint while still allowing free vertical displacement of the column.

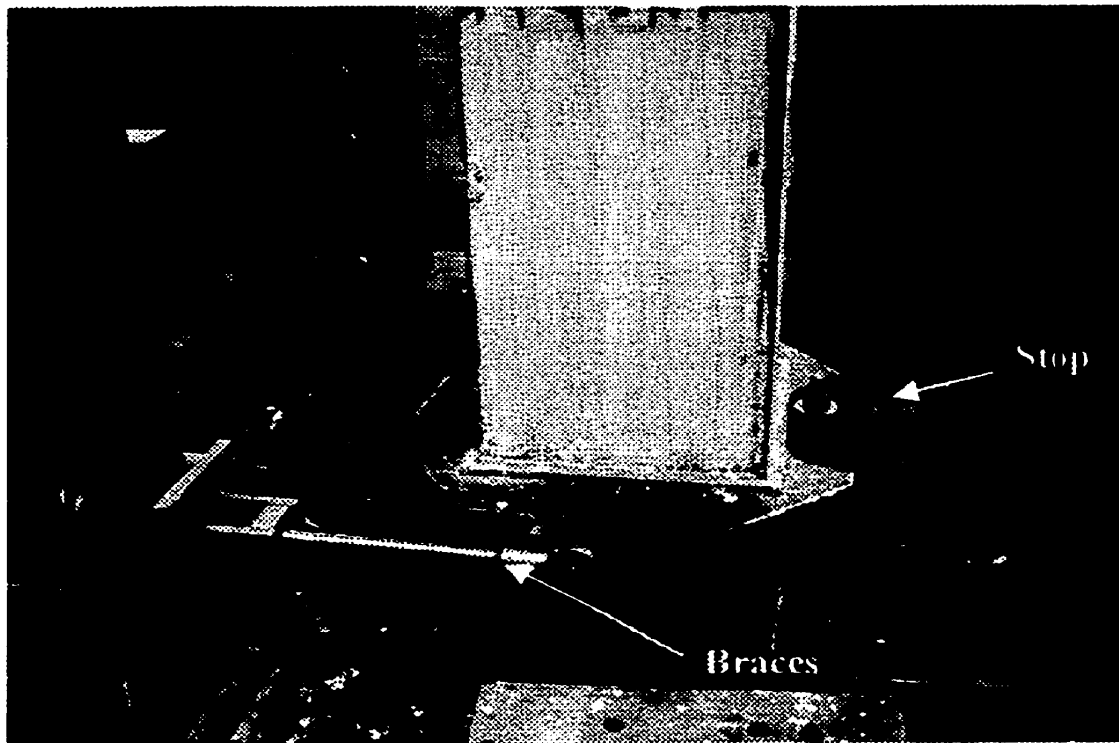


Figure 3.13: Column Bracing: Horizontal Forces Taken into Test Frame

4 Test Results and Observations

4.1 Material Property Results

4.1.1 Steel Properties

All plate material used in the fabrication of the column specimens was from the same rolling of a 9.53 mm (3/8") nominal thickness. Six coupons were cut from a sample of the plate material accompanying the specimens. Coupons P1, P2 and P3 were cut perpendicular to the rolling direction, at 100, 125, and 150 mm from a flame cut respectively. Coupons P4, P5 and P6 were cut parallel to the rolling direction, at distances of 75, 100, and 125 mm from a flame cut edge. In fabrication the column length was in the direction of rolling.

The connection shear tabs were 9.53 mm (3/8") thick and cut from the same plate as the columns. All double angle connections consisted of 75 x 75 x 6.35 angles. Two coupons were cut from each leg of a 1.2 m length of angle from the same material lot. Coupons CA1 and CA4 were cut from one leg, and CA2, CA3 from the other leg. The double angle connections and the shear tabs were delivered, cut and punched.

Additional coupons were taken from the webs of the two test beams (W410x67 and W530x93). The coupons were cut from a free end, with the coupon length running perpendicular to the beam. The coupon information was taken for the evaluation of the web strength at the connection.

All tensile coupons were tested in the 1000 kN MTS universal testing machine that was also used to provide the connection load in the "full size" test set-up described in Section 3.2. All tensile coupons were initially loaded at a strain rate of 0.002/min, then as the 0.002 strain offset was intercepted the MTS actuator was held at zero displacement rate until the load stabilized; during this period zero strain change was observed. The stress reading refers to the 1st static yield load. After this was recorded, the displacement was again continued until an absolute strain of 0.005 at which point the process was repeated. The reading refers to the second static yield load. The displacement rate was then maintained at 0.002 strain/min until well into the strain hardening, at which point the head displacement rate was increased to 2 mm/min until rupture. A summary of all tensile coupons is given in Table 4.1, while the complete load deformation responses are presented in Appendix C.

4.1.2 Concrete Properties

The composite columns were cast at two times; the prototype column specimen (Tests C450-W410-SDA-C and C450-W410-LDA-C) was the first, and all remaining specimens were later cast in the second. For the purpose of material testing, concrete cylinders were cast from each of the two concrete batches. Cylinders were tested at seven day, 14 day and 28 day intervals to monitor the strength development of the first cast. For the second batch the time intervals were the same, with the exception of the 28 day strength. Because of building renovations it was not possible to test the cylinders until 40 days after casting.

All concrete cylinders were tested in accordance with ASTM testing procedures and were loaded at 4.5 kN/s until failure. Cylinders beyond 28 days were tested in the 5000 kN MTS Stiff Frame to get the complete load deformation response of the concrete. A complete summary of concrete properties is given in Table 4.2. The load deformation response of the cylinders tested in the Stiff Frame are found in Appendix C.

4.2 Preliminary Measurements

Following the fabrication of the test columns there was an initial distortion in the column flanges resulting from the welding. This consisted of an inward bow of the column flange between the connection plate and the tension stirrup. A similar deformation pattern existed between the tension stirrup and the column end plate. In both cases the flange tips were brought closer together by an amount ranging from 0.5 to 1.5 mm. This deformation was observed in all column specimens, with the magnitudes and deformation pattern remaining consistent. This was not a concern for the composite tests, because during the casting of concrete the column flanges returned to a near flat state.

The residual stress pattern in the steel column resulting from the fabrication was also examined. As part of the parallel study on the column behaviour¹ the residual stress pattern was estimated by measuring the strain release in selected areas of the cross section. The typical stress distribution is given in Figure 4.1.

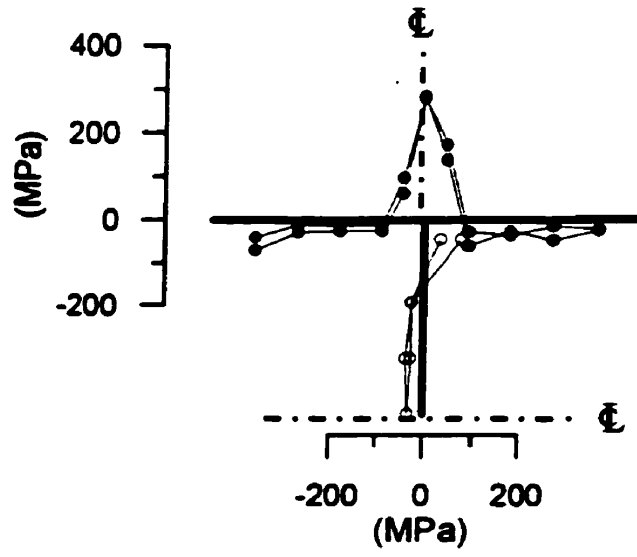


Figure 4.1: Typical Residual Stress Pattern¹

Table 4-1 : Tensile Coupons; Tested in Accordance with ASTM E8/E8M-99

Coupon	Yield Stress (MPa)	1st Static (MPa)	2nd Static (MPa)	Ultimate (MPa)	Max Strain	Young's Modulus (GPa)	Sim. Hard. Mod. (GPa)	Comments
P1	376.9	336.9	327.1	526.8	0.313	210	3.3	Subset 1
P2	375.6	359.3	355.2	530.7	0.310	214	3.4	Subset 1
P3	369.4	353.2	-	528.5	0.304	205	3.4	Subset 1
P4	366.0	347.2	351.3	522.9	0.347	205	3.9	Subset 2
P5	367.0	345.0	341.8	515.5	0.366	212	3.7	Subset 2
P6	367.9	343.4	344.2	519.2	0.345	213	3.4	Subset 2
CA1	338	313	320	508.0	0.337	205	3.3	Leg 1
CA2	355	325	329	517.3	0.333	209	3.6	Leg 2
CA3	358	330	327	515.6	0.337	208	3.3	Leg 2
CA4	341	320	328	516.0	0.332	206	3.5	Leg 1
W16-1	411	385	384	509.1	-	219	2.5	W16-Web
W16-2	416	390	386	516.0	0.194	230	2.4	W16-Web
W21-1	476	457	461	583.9	-	223	2.4	W21-Web
W21-2	496	467	475	591.0	-	230	2.7	W21-Web

Note: Subset 1 and 2 represent coupons cut in orthogonal directions in the plate.

Table 4-2: Concrete Properties; Tested in Accordance with ASTM C39/C39M-99

Batch No.	Specimens	Cast Date	Test Date	Age	Slump	%air	7d	14d	28d	141d	Ec
1	C18-W16-SDA C18-W16-LDA	Oct. 7/98	Feb. 9/99	125 d	125 mm	7.2%	24.8 MPa (3 cyl's)	29.2 MPa (3 cyl's)	30.8 MPa (3 cyl's)	36 MPa (2 cyl's) (Feb. 23/99)	30.3 GPa
			Feb. 13/99	131 d			7d	14d	40d	90d	Ec
2	C18-W21-SDA C18-W21-LDA C18-W16-TAB C18-W21-TAB C18-SEAT-NO C18-SEAT-ANC	March 23/99	April 29/99	35 d	150 mm		18.0 MPa (2 cyl's)	21.9 MPa (2 cyl's)	33.0 MPa (2 cyl's) (May 6/99)	33.8 MPa (2 cyl's) (June 23/99)	
			May 4/99	40 d							
			May 18/99	54 d							
			May 26/99	62 d							
			June 1/99	68 d							
			June 3/99	70 d							
June 8/99	75 d										
	C24-W16-SDA C24-W16-LDA		June 10/99	77 d							

4.3 Prototype Specimen Tests

As discussed, a single prototype composite column was cast and tested to determine if additional mechanical anchorage was required to ensure satisfactory connection performance and examine the assumptions made about the anticipated behaviour. There were two immediate issues to be addressed in the prototype tests; 1) was direct anchorage required to limit the deformation of the connection end plate under load, and 2) were additional mechanical devices required for direct transfer of forces from the steel directly into the concrete?

Although the separation of the connection plate from the concrete column and the yielding of the connection angles were expected, the amount of yielding in the column flanges and possible crushing of the concrete was difficult to estimate. Therefore, the prototype tests would also indicate if two connection tests could be done on each column specimen, and thus complete the proposed test matrix with the available column specimens.

4.3.1 Prototype Composite Test Results

The potential for the connection detail was realised when aside from the gross yielding of the connection angles, and minimal deformation of the connection end plate, there was little to no unusual local distress in the column. This is illustrated in Figures 4.2 and 4.3. Although the connection plate moved away from the concrete because of the negative moment at the column face, there was little vertical displacement of the connection plate. The vertical displacement of the beam end, as shown in Figure 4.4, was the result of extensive yielding of the connection angles, and the bolthole deformation. The abrupt drop in the plotted data was caused by the slippage of the bolted connection. This occurred in both tests, at approximately the same applied load per bolt.

Test C450-W410-SDA-C was terminated at a connection load of 478 kN when the load could not be maintained under displacement control, although there was not a complete rupture. Test C450-W410-LDA-C was terminated at 650 kN following excessive yielding of the connection angles. There was still considerable reserve strength remaining in the connection, so the load was reduced and the applied column load increased in an attempt to introduce failure in the column.

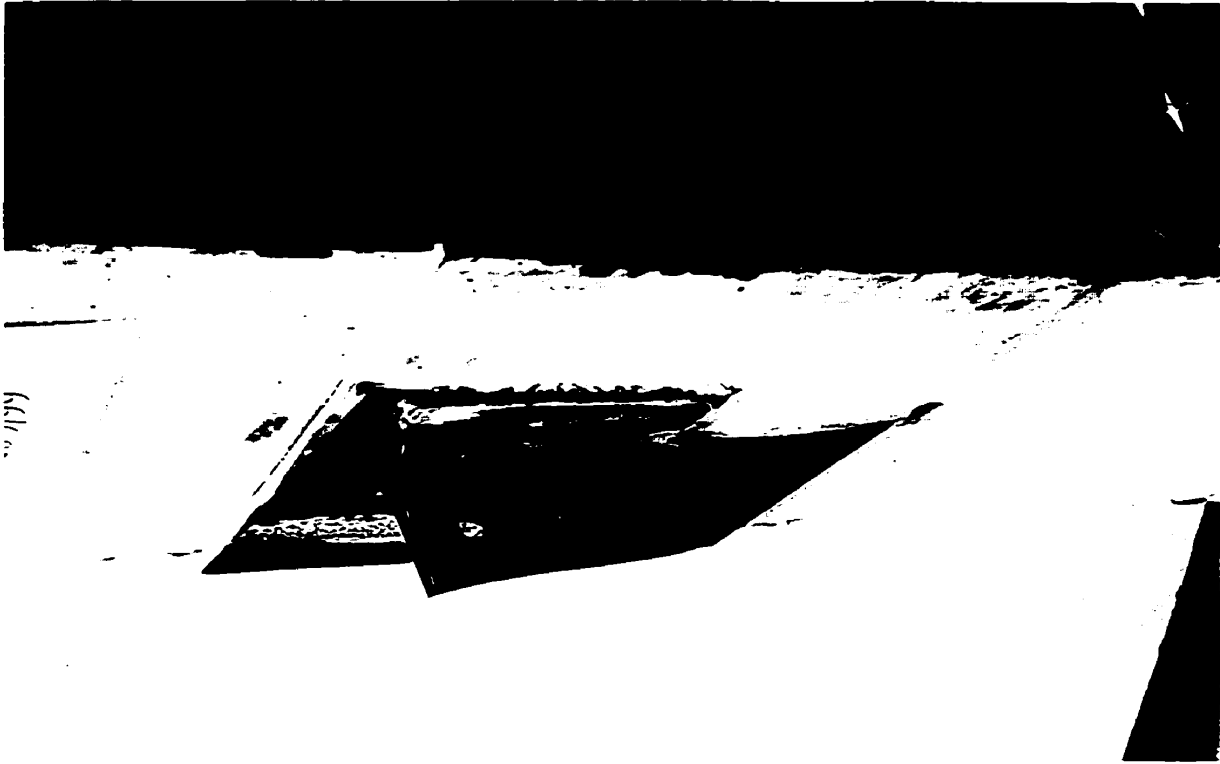


Figure 4.2: Oblique View of Failed Specimen C450-W410-SDA-C

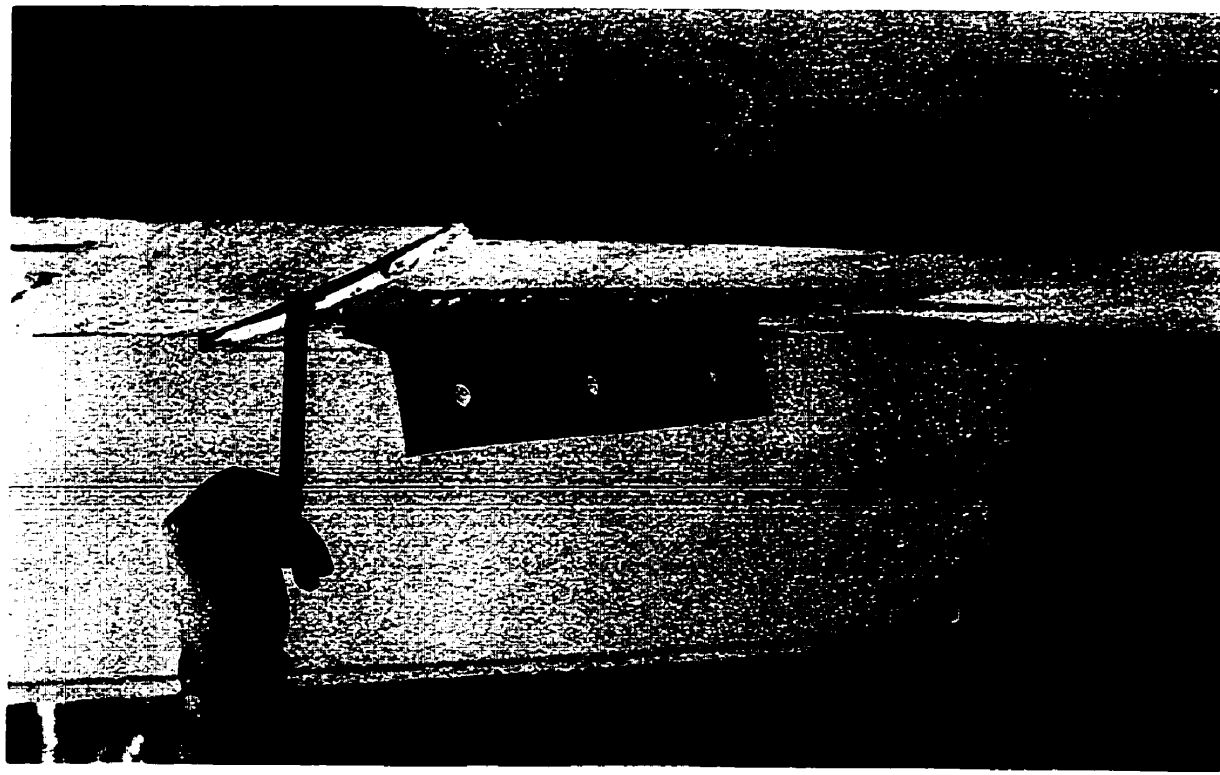


Figure 4.3: Oblique View of Failed Specimen C450-W410-LDA-C

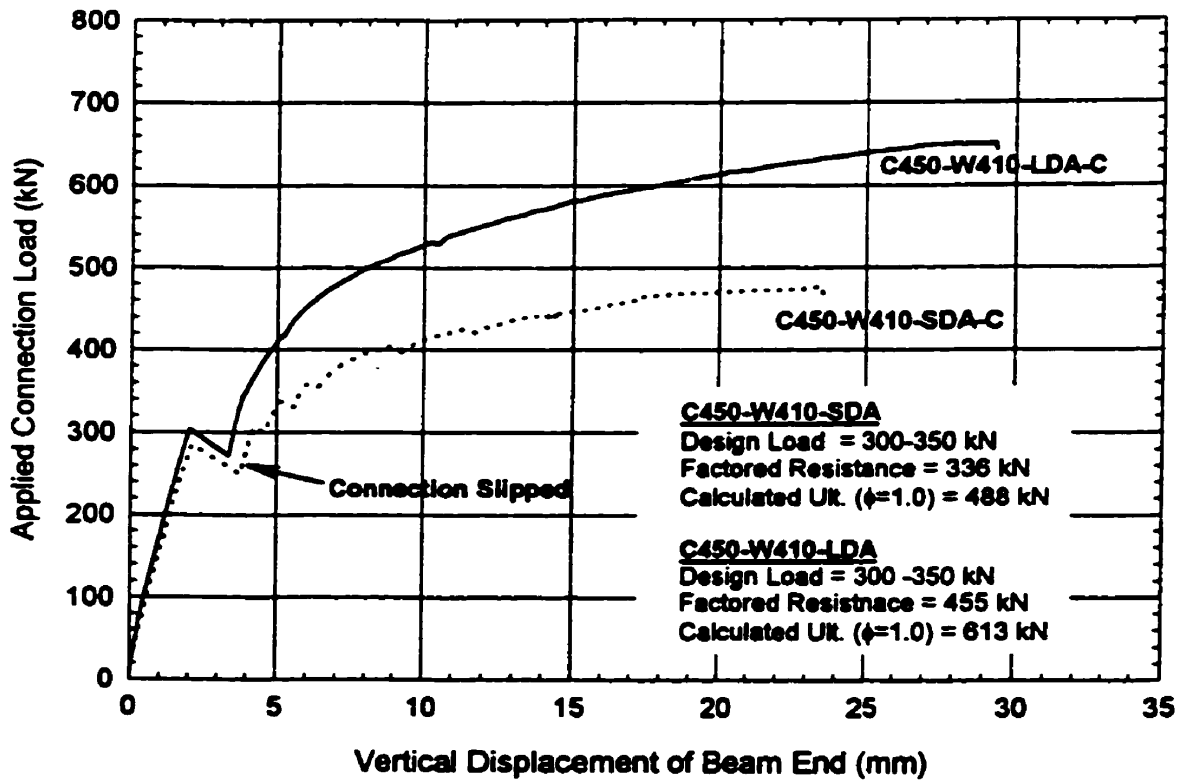


Fig. 4.4: Prototype Composite Specimen: Connection Load vs. Vertical Beam Displacement

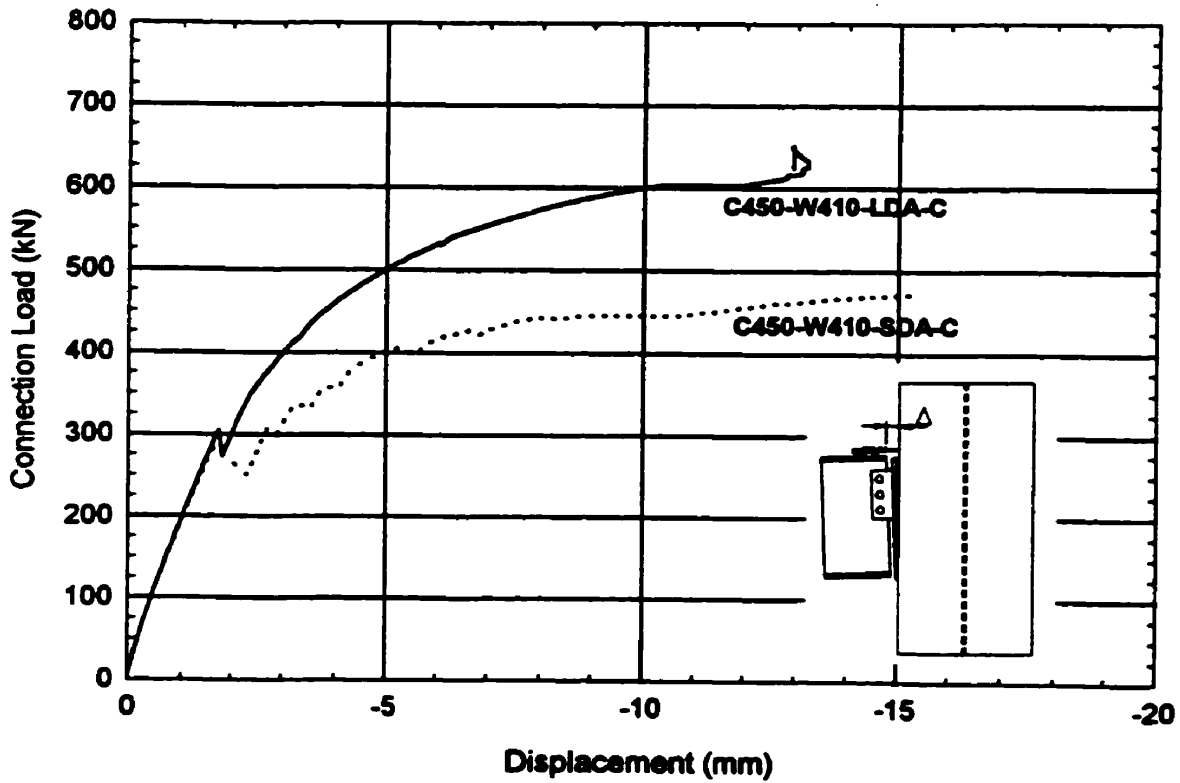


Fig. 4.5: Prototype Composite Specimen: Connection Load vs. Displacement of Top Flange From Column Face

The separation of the top flange from the concrete column face was measured with an LVDT mounted on the top flange and referenced to the concrete column face. The results are shown in Figure 4.5. At loads corresponding to the factored design load range (300-350 kN) the separation of the beam flange from the column face was on the order of 2-3 mm. The final separation measured after the termination of the test and removal of the load beam was 6 and 7.5 mm, for the SDA and LDA test respectively.

It is obvious from the test data and the photos that both connections performed well. Loads in excess of the calculated ultimate were reached for the LDA, and the SDA test was terminated due to excessive deformation just prior to reaching the calculated ultimate. Both tests indicated that overall connection stiffness was not the concern it was first thought to be. At the factored loads the separation between the flange and column was less than 3 mm and the vertical displacement of the beam end was less than 4 mm for both connection types. There was also no permanent distortion in either the steel or concrete in the column as a result of the combined connection and axial load.

Although the load deformation response of the connection system did not indicate the need for direct anchorage, the lack of strain compatibility between the steel and concrete at a reasonable distance below the connection could suggest the need for additional local shear connection between the concrete and steel. Thus a series of steel strain gauges were installed over the cross section of the column to determine the stress distribution. Figure 4.6 shows the plot of the connection load versus the average steel strain for both connection types. This is the average steel strain at a distance of 685 mm (1.5 x D) below the bottom of the connection end plate. Unfortunately, there was no instrumentation in-place to record concrete strain and the average steel strains could only be compared to the ideal strain values. The ideal strain is that which would result in the column for full composite behaviour and uniform distribution of stress, and is calculated as:

$$\epsilon_{Ideal} = \frac{P_{Connect}}{A_s E_s + A_c E_c} \quad (\text{Eqn. 4.1})$$

The slopes for each plot show that the steel strains reasonably match the expected strains, assuming the concrete is fully effective in resisting the load. Thus it appeared possible that at a reasonable distance (i.e.; 1.5 x D) below the connection there existed a state of strain compatibility, or near strain compatibility, in the column cross section.

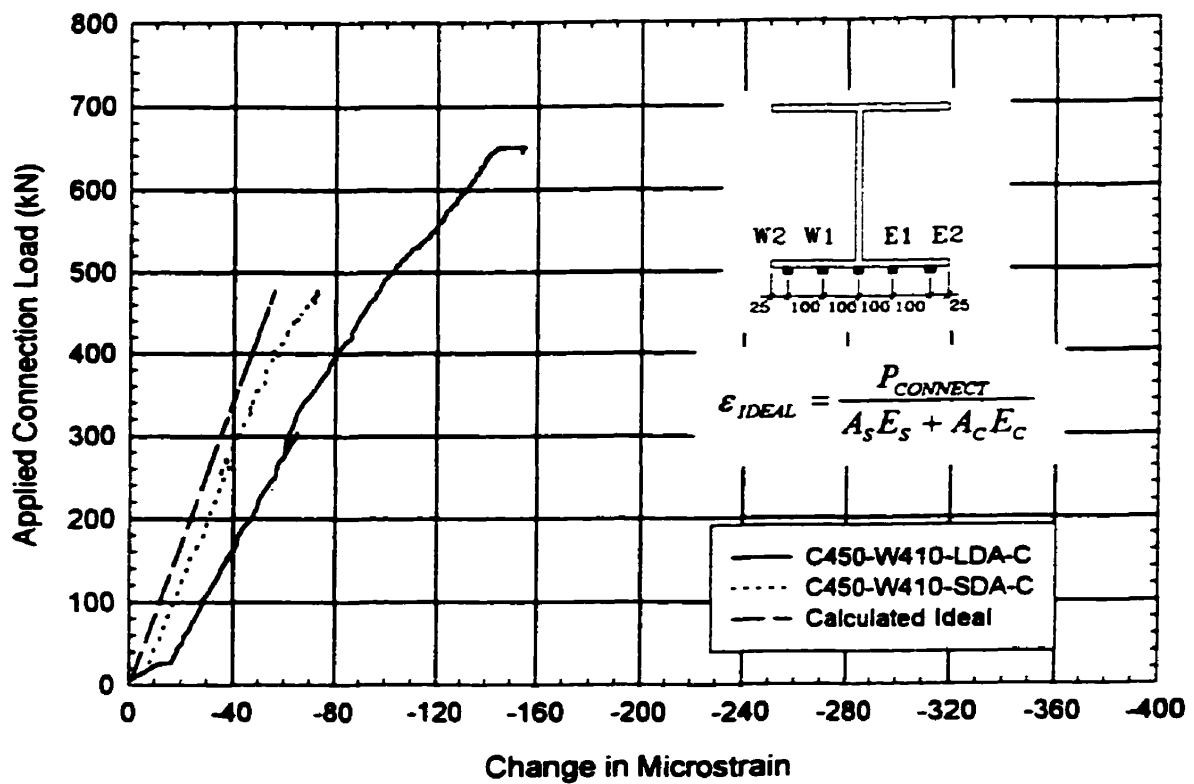


Figure 4.6: Prototype Composite Specimen: Connection Load vs. Average Steel Strain 685 mm Below Connection Plate

4.3.2 Recommendations for Subsequent Testing

Following the initial testing, discussions were held with Canam engineers and researchers from École Polytechnique regarding the nature of the remaining experimental work. It was decided that the test results indicated that the connection system would work without provisions for direct anchorage or mechanical shear transfer devices. Thus the test matrix, as shown in Table 3.6, was finalised. Although not a primary test variable, it was decided to test a single seat connection with shear studs to investigate possible concrete failure modes that may be initiated by the stud. A similar seat detail was also cast without shear studs for the purpose of direct comparison.

It was also recommended to install a restraint to limit the longitudinal movement of the test beam. In the prototype tests the beam was not longitudinally restrained, and it pulled away from the column face as the connection was loaded. The result was that both the top and bottom flange moved away from the column face as the connection yielded. There was approximately 20 mm of permanent movement of the beam. To limit the movement a restraint system shown in Figure 3.12 was agreed to in concept.

In preparing the two prototype tests the beam web was cleaned free of mill scale but there was no additional surface preparation prior to the installing the beam and bolt pretensioning. In each test

there was slippage of the bolted connections, at about 100 kN per bolt; the slip was sudden, accompanied by an audible report, and is clearly indicated by a disruption in the test data. In an attempt to eliminate the sudden slip all additional composite tests had the web of the test beam painted prior to installation.

4.4 Composite Connection Test Results

There were two major issues to be addressed in the composite connection testing; the general behaviour of the connection under load, and the force transfer mechanism between the steel and the concrete. For the purpose of presentation of the test results the discussion will be subdivided into the load deformation response and the moment rotation response of the various simple framing connections, grouped according to the major design parameters that were being addressed.

4.4.1 General Observations and Failure Modes

All composite connections exhibited similar response under the applied connection load. As the load was increased the moment developed at the connection caused the end plate to deform outward as shown in Figure 4.7. This was a typical yield line failure for a plate subjected to out-of-plane loading. This was accompanied with shear deformation of the connection, bolthole deformation, and rotation of the connection. Since the base of the plate and connection were prevented from moving inward by the concrete, the connection only rotated away from the column, with a centre of rotation near the bottom of the connection.

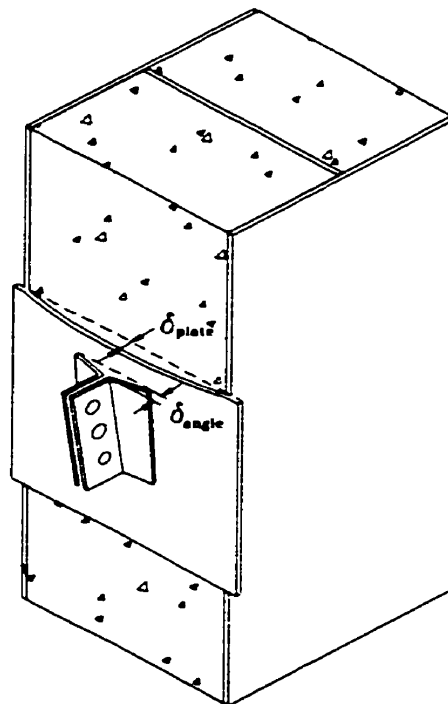


Figure 4.7: Typical Deformation of Connection and End Plate

Of the 10 composite connections tested in the experimental program, four had capacities in excess of the test frame capacity. Of the six remaining connections, three failed through a net section rupture, and three tests were terminated after excessive deformation of the end plate and connection. A complete summary of the failure modes, and explanation to why the connections were not brought to rupture are included in the following sections.

A common observation made of all composite connection tests was the bolthole deformation pattern. For simple framing connection tests a bolthole deformation pattern similar to that shown in Figure 4.8(a) is generally expected. This is indicative of a hogging moment at the bolt line, with an inflection point lying outside the bolt line. Although this is what is expected, it was not the deformation pattern observed in the connection tests reported herein. For the TAB and double angle connections the deformation pattern in the connection was similar to that shown in Figure 4.8(b). This was indicative of a positive, sagging moment at the bolt line. This was the result of the flexibility at the column face, and will be discussed in more detail in Section 4.4.3. The typical deformation pattern in both the connection and the beam web is shown photographically in Figures 4.9 and 4.10.

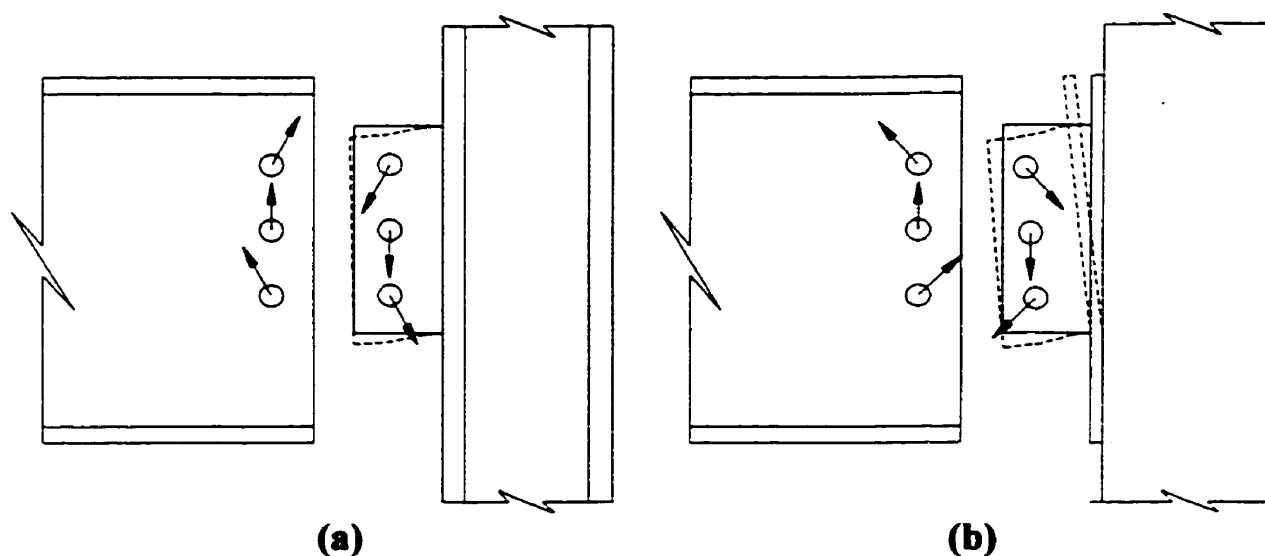
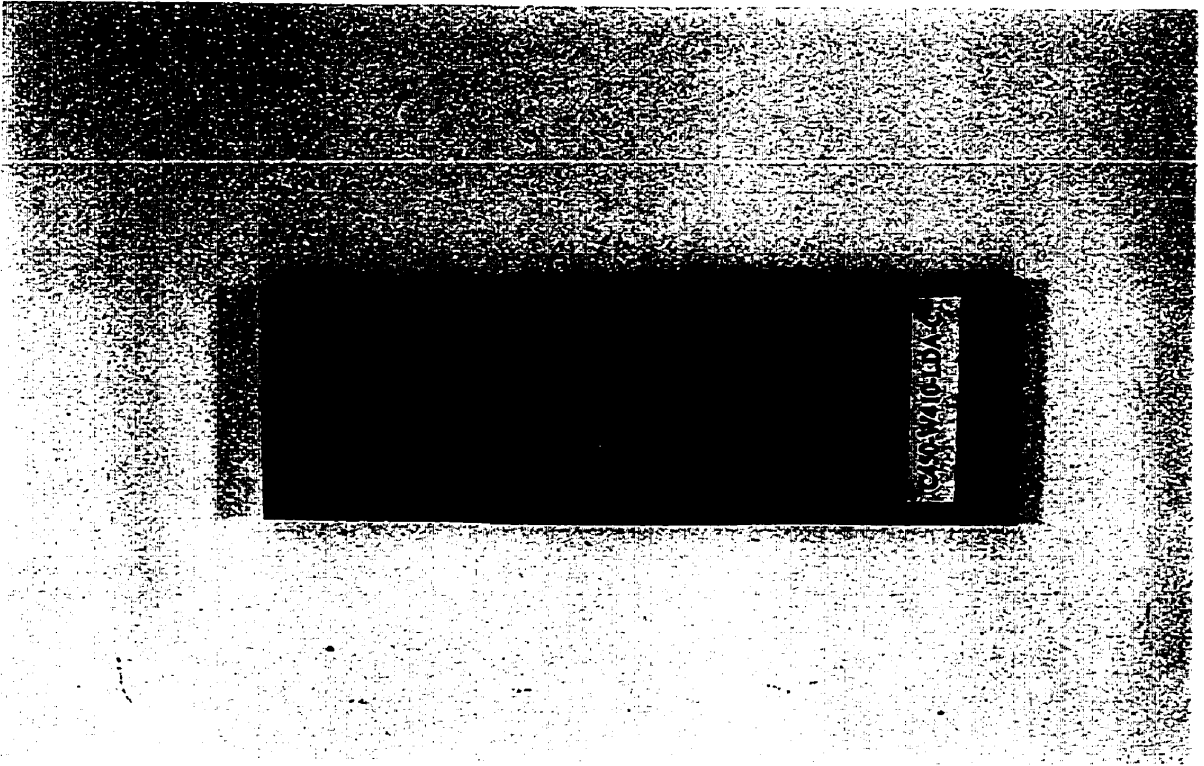
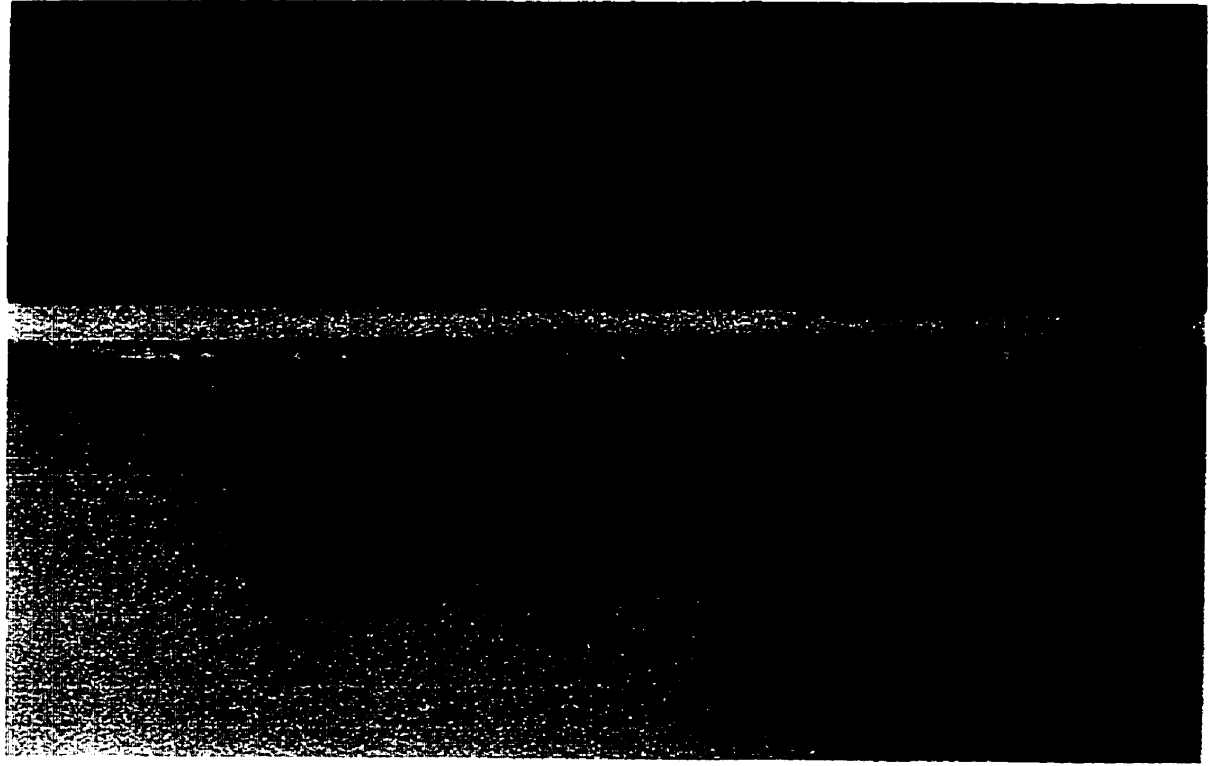


Figure 4.8: Connection Forces at the Bolt Line a) Stiff Column Face, b) Flexible Column Face

As the connection load was first applied the column tended to shift slightly in the test frame until the column bracing system mobilized. The rotation of the column was an order of magnitude less than the rotation of the beam, thus was ignored in the analysis. In tests C450-W530-LDA-C, C450-W410-SDA-C, and C450-Seat 2 where the column load was increased, the column returned to its original alignment under the increased axial load.



**Figure 4.9: Typical Bolthole Deformation Pattern
Observed in Web of Test Beam**



**Figure 4.10: Typical Bolthole Deformation Pattern
Observed in Connection Header**

There was no unusual distress observed in the columns while subject to the applied connection load, and axial load corresponding to 1.0 Dead Load + 0.5 Live Load. The maximum stress recorded was 67% σ_y , at the steel strain gauges located just below the connection. In the second test performed on each composite column, the axial load would be further increased in an attempt to fail the column. There were four tests where the column load was increased (C450-W410-LDA-C, C450-W530-LDA-C, C450-Seat2, C450-W530-TAB-C) after the original connection test was completed. There was observed concrete failure and yielding of the steel in several of these tests. A complete summary of the results of the increased axial load is given in Section 4.6.

4.4.1.1 C450-W410 Connection Series

There were three connection types included in this test series, the short double angle (SDA), long double angle (LDA) and the single plate shear tab (TAB). Both the SDA and LDA were three, ¾" diameter A325 bolted connections, consisting of 76 x 76 x 6.35 mm angles. The beam was bolted and the header was welded to the column face. The variable was the bolt spacing, with the SDA having a 60 mm and the LDA a 90 mm centre to centre bolthole spacing. They were the prototype tests discussed in the previous section and their inclusion in this and subsequent sections is to provide a complete presentation of the results. The TAB connection was a standard four bolt, ¾" diameter A325 bolted connection detail, taken from the CISC Design Handbook¹⁰. The only difference was that the plate grade was 350W, as opposed to the recommended 300 W.

The prototype composite connection tests both failed in a similar fashion. As the load was increased on the beam, the plate and connections rotated and the test beam moved away from the column face. The bolted connections slipped at approximately 300 kN, in both tests, which was accompanied by a very loud report and disruption in the test data. The maximum applied connection load applied on the SDA connection was just less than the calculated ultimate of 488 kN. There was no rupture of the connection, but the test was stopped because of the excessive deformation of the angles and the plate. Bolthole deformation was on the order of 1/2 a bolt diameter (10 mm). After removal of the test beam the permanent separation of the cross plate from the column face was 5.5 mm. The framing legs of the connection, had also separated 20 mm from the connection end plate. There were also tears obvious at both the bolt line and weld lines of the double angle. The tearing at the bolt line was indicative of a net section failure, which was the calculated critical failure mode. The location of the tearing is shown photographically in Figure 4.2.

The maximum applied load on the LDA connection was 650 kN. This was in excess of the calculated ultimate of the connection (613 kN) but the test was stopped because of excessive deformation. The final bolthole deformation was on the order of 1.5 times the bolt diameter. The

permanent separation of the cross plate from the concrete, measured after the removal of the load beam, was 6.5 mm. The framing leg of the connection angle was also 15 mm removed from the connection cross plate. Again there was slight tearing at the top of the outstanding leg, originating at the weld return. Unlike the SDA test there was some minor yielding of the test beam, observed at the connection. The maximum connection load was 96% of the calculated resistance using the actual beam strength, thus localized deformation was not unexpected. This disturbed region was limited to 200 mm at the beam end, and was removed when the beam end was prepared for the subsequent test.

The C450-W410-TAB-C test was the only test in the entire matrix to fail through the bolts. The bolts were 1¼ inch long, and failed in single shear at a lower than expected load of 441 kN (110.3 kN/bolt). Upon further investigation it was found that the shear plane had just intercepted the threads. The original bolts were replaced with two inch long bolts, and the connection reloaded. The failure load was again through the bolts, but this time through the shank, at a load of 576 kN. This was not unexpected since the calculated ultimate was 567 kN (Table 3.5) with the governing failure mode being shear failure of the bolts. Although the MTS was loaded with displacement control, the four bolts failed simultaneously in both tests.

At failure there was considerable out-of-plane distortion of the shear tab, caused by the bolts being in single shear with the small eccentricity of the connection load. This caused a moment at the bolt line, perpendicular to the beam web, resulting in the top of the TAB to be laterally 20 mm out of line, at the termination of the test. Photographic front and side views of the failed TAB specimen are shown in Figures 4.11 and 4.12.

4.4.1.2 C450-W530 Connection Series

Test specimens C450-W530-LDA-C and C450-W530-TAB-C represent the highest capacity connections in the test matrix, and could not be brought to rupture. In the initial design process it was assumed that the entire 1000 kN MTS load was available, but the actual maximum load available was 960 kN. For the 7.1 m W530 test beam length the maximum load that could be developed at the connection was:

$$V_{\max} = \frac{L_B - d_{MTS}}{L_B} P_{MTS} \approx 780 \text{ kN} \quad (\text{Eqn. 4.2})$$

The calculated ultimate capacity ($\phi=1.0$) for the LDA and TAB connections was 797 kN and 851 kN respectively. Although it was impossible to bring these connections to failure, there was a slight loss of proportionality indicated in the test data. Upon termination of test and removal of the test beam, there was permanent separation between the plate and the concrete for both tests. For the LDA

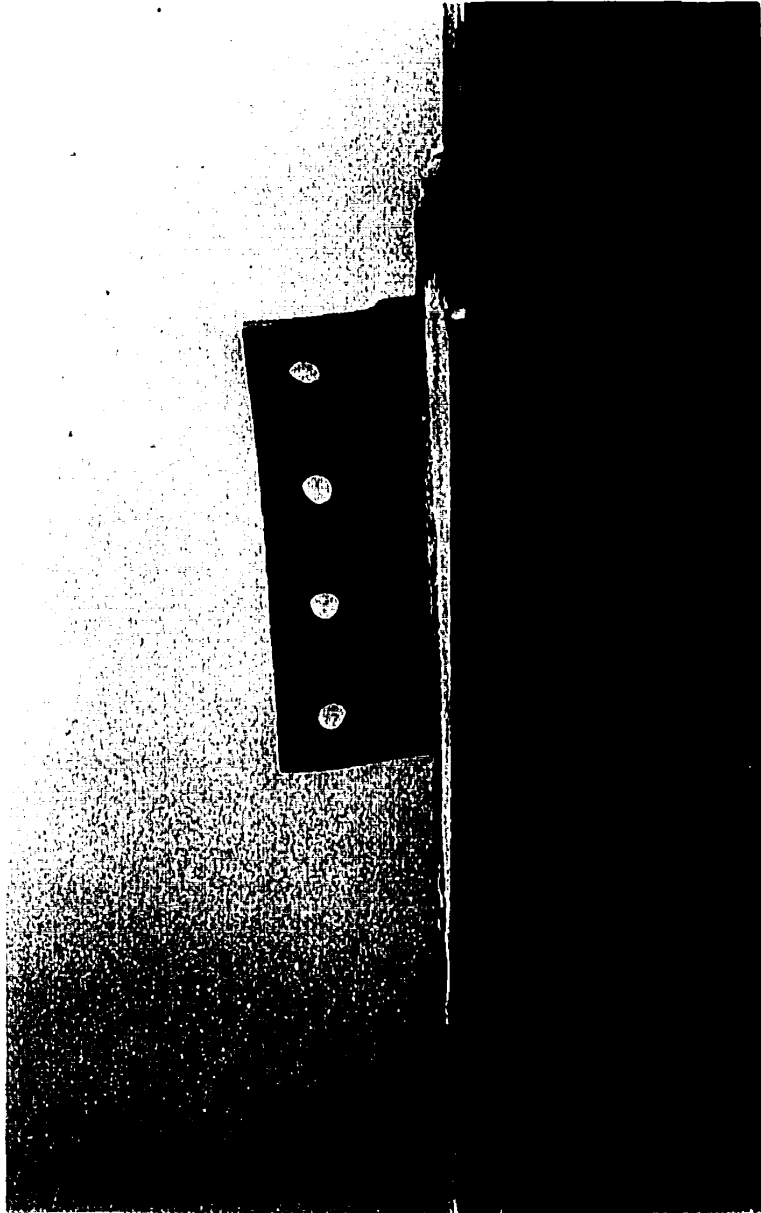


**Figure 4.11: View of Failed Specimen C450-W410-TAB-C:
Side Profile**

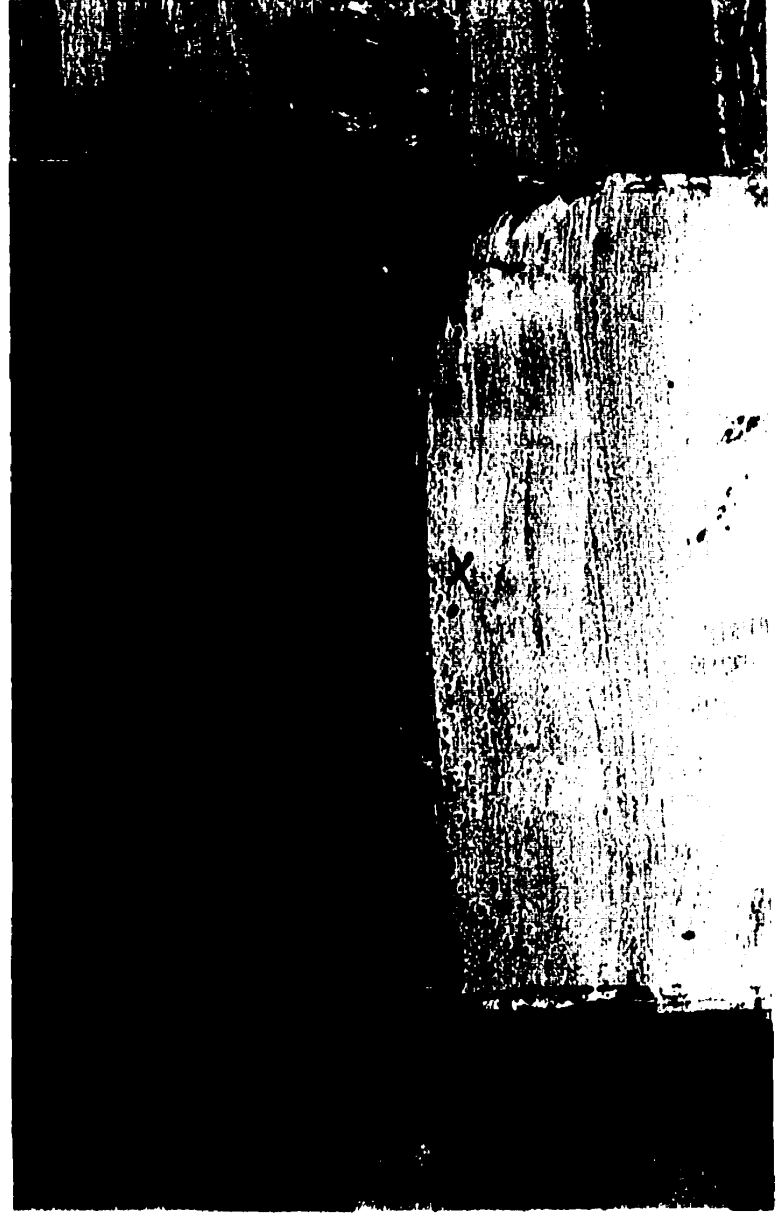


**Figure 4.12: View of Failed Specimen C450-TAB-C:
Front Profile**

connection there was 3 mm of permanent separation and 4 mm for the TAB. The framing leg of the LDA connection also separated 1 mm from the connection end plate. Unlike earlier reported tests there was no visible tearing at the weld or bolt lines for either of the tests.

Bolthole deformation was obvious in both the beam web and the connection for the LDA test, but was limited to 5 mm. There was negligible hole deformation in the 6-bolt TAB connection. Photographs of the failed specimens are shown in Figures 4.13 and 4.14, with additional photographs included in Appendix D of this report.

The only connection that could be brought to failure in the C450-W530 connection series was the short double angle. The ultimate failure was a net section at the bolt line, at an applied connection load of 678 kN. There was a clear tear through the bottom three bolts holes as can be seen in Figure 4.15. The rupture did not continue through the entire section, but ended about halfway between the 1st and 2nd boltholes (from the top). There was also a tear formed at the weld line.

The permanent separation between the steel plate and the concrete surface, measured after the test, was comparable to the other connection types in the series, at 3 mm. As anticipated there was considerably more shear deformation of the connection angle, as evident in the photos.

4.4.1.3 C600-W410 Connection Series

The two connection tests for the C600 composite column, C600-W410-SDA-C and C600-W410-LDA-C, were the same detail as those in the C450-W410 series, with the exception of the connection plate width, W . Other differences included the fact that the longitudinal beam restraint was used in the C600 composite tests, and that the column end conditions varied slightly. The spherical head used with the 450 x 450 mm column specimens was removed to accommodate the longer length of the C600 column. As a result the column did not shift in the test frame when the connection load was applied, as was observed in the other composite tests.

Although the connections were painted, prior to “fit up” of the test beam, to reduced slip reports, the SDA bolted connection began to slip at an applied connection load of 183 kN; and was followed by an audible “ping” that occurred every 2-3 seconds for the duration of the test. Yielding was first observed in the connection angles at an applied load of 366 kN. The maximum load was 508 kN, after which the jack could not maintain the load. A net section rupture occurred at 471 kN. The oblique view of the failed specimen is shown in Figure 4.16. After removal of the test beam the final separation between the connection plate and concrete column face was measured at 5 mm.



**Figure 4.13: Specimen C450-W530-LDA-C:
Following Loading**

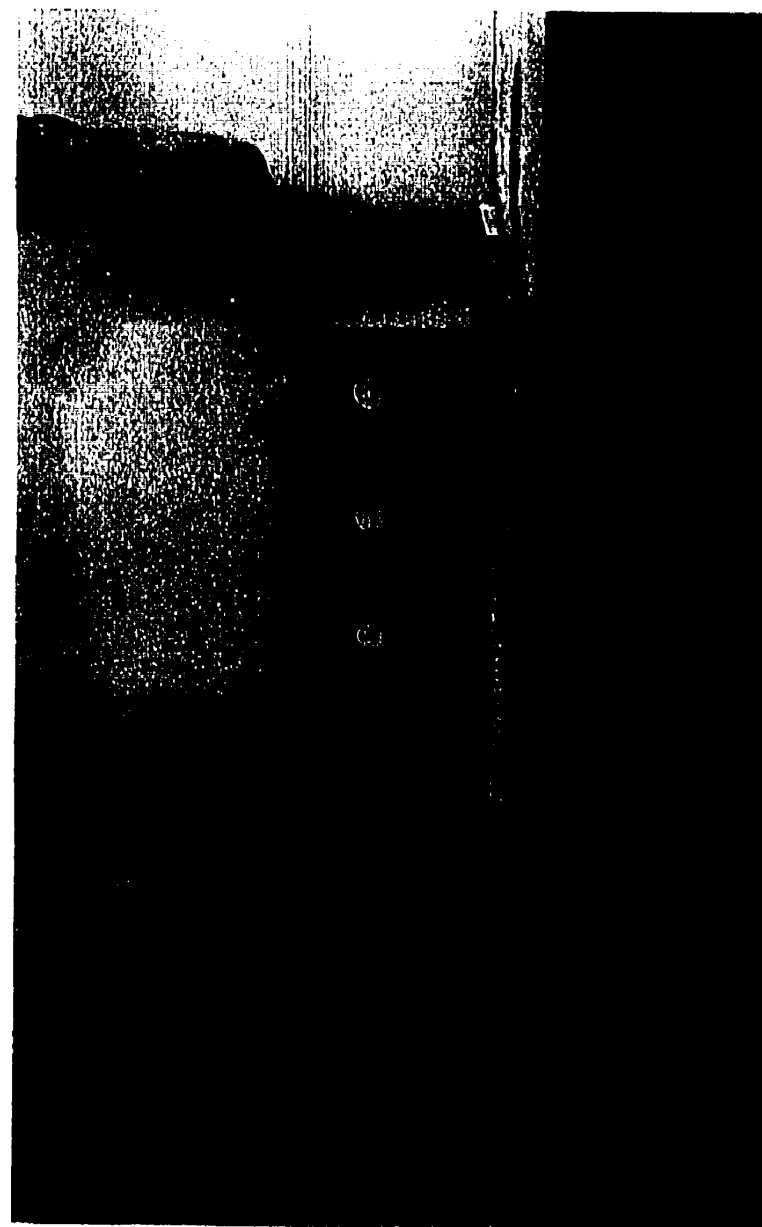


**Figure 4.14: Specimen C450-W530-TAB-C:
Following Loading**



Figure 4.15: View of Failed Specimen C450-W530-SDA-C



Figure 4.16: View of Failed Specimen C600-W410-SDA-C

The LDA connection also slipped at 313 kN and the original slip was again followed by “pings” at regular intervals. The LDA connection was loaded until the test beam flange came to rest directly on the double angle connection. At the start of the test there was 30 mm between the top of the connection and the bottom of the top flange. The majority of the deformation was the result of the bolthole deformation in both the beam web and the connection itself. The final separation between the connection plate and the concrete column face was 9 mm. As with C450-W410-LDA-C, there was some shear deformation observed in the test beam.

4.4.1.4 Unstiffened Seats

The seat connection consisted of a 203 x 104 x 19 (L 8x4x3/4”) angle with the longer leg welded to the end plate. The W530 load beam was modified to accommodate the seat connection, such that the middle of the bearing area was 60 mm from the column face. Based on bending, the predicted connection failure load is:

$$P_{Connect} = \frac{\sigma_y I}{ye} = \frac{350 \left(\frac{230}{12} (19.05)^3 \right)}{\frac{19.05}{2} 60} 0.001 = 81 kN \quad (\text{Eqn. 4.3})$$

This of course does not account for the inward movement of the bearing centre as the unstiffened seat deforms. When the outstanding leg deforms the bearing centre moves towards the column face changing the failure mode from bending to a simple shear situation. The predicted shear strength of the seat angle would be:

$$V_{fail} = 0.6 \sigma_y A_s = 0.6(350)(19.05)(230)(10^{-3}) = 920 kN \quad (\text{Eqn. 4.4})$$

This load was in excess of the maximum load available at the connection. Generally the seat deformed in accordance with the rotation of the beam end at the test connection. The single 3/4” A325 bolt placed on either side of the web, connecting the bottom flange to the seat connection, also ensured that the bending deformation of the seat was limited by the rotation of the beam end.



Figure 4.17: View of Failed Specimen C600-W410-LDA-C

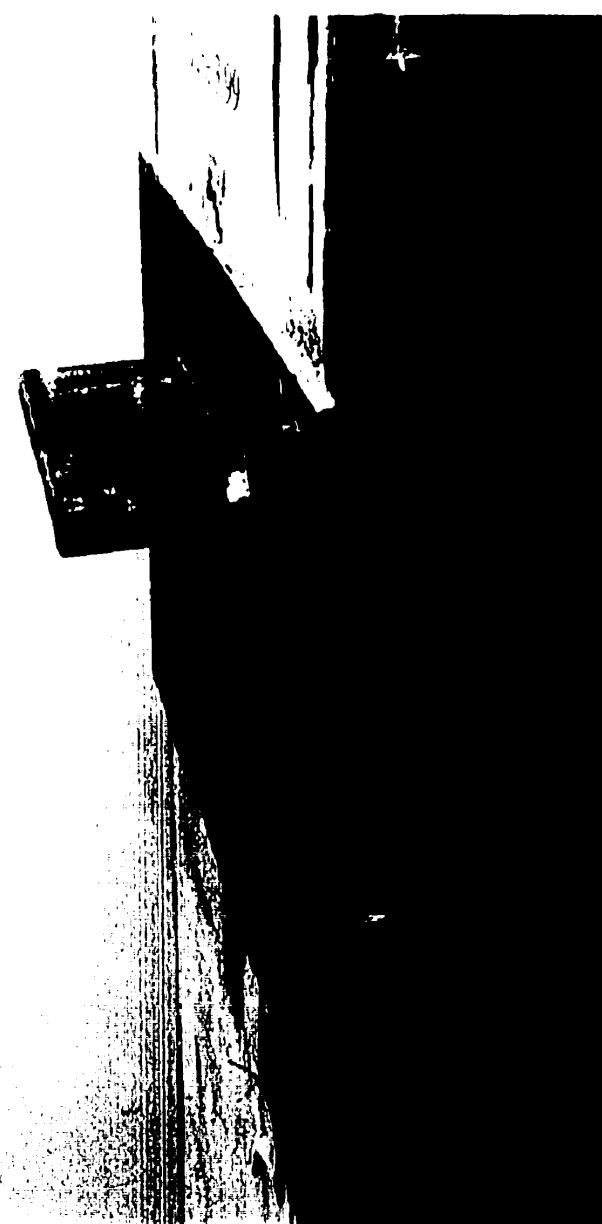


Figure 4.18: Typical Seat Connection Following Loading

4.4.2 Load-Displacement Response of Composite Connections

The load deformation response of the connection and connection end plate was of primary interest in the evaluation of the connection types. Each beam column connection was therefore instrumented to record both the vertical deformation of the beam end, and the separation of the beam flanges from the column face. For the latter, LVDTs were placed on both the top and bottom flange to monitor the beam movement. The reading from the top flange included both the displacement between the steel end plate and the concrete face, and the relative displacement between the beam flange and the connection plate. The bottom LVDT measured the connection deformation only, as the end plate did not move horizontally relative to the concrete, below the connection.

4.4.2.1 C450-W410 Connection Series

The plot of the connection load versus the vertical displacement of the beam end is shown in Figure 4.19 for the three connection types. Of interest is the difference in the initial stiffness between the TAB and the double angle framing connections. Both the SDA and LDA had comparable stiffness in the initial stages of loading, and are considerably stiffer than the TAB connection. This is true despite the fact that the cross sectional area of the TAB connection is comparable to the LDA, and larger than that of the SDA. This appears as if there was gradual slippage of the connection, but there was no audible evidence of slippage of the bolted connection.

The movement of the beam flange from the column face, while under an increasing connection load, is shown in Figure 4.20. Both the displacement of the top and bottom flanges are included, along with the final measurement of the separation between the steel and concrete. The top flange data for the C450-W410-TAB-C data is only included up to an applied load of 350 kN. The LVDT plunger was referenced to a small aluminium plate that was cemented to the concrete face. As the connection end plate deformed it hooked the aluminium plate and corrupted the subsequent readings.

Although there is a greater permanent separation between the concrete and steel for the TAB connection the test beam did not move away from the column face, as with the SDA and LDA tests. This is indicated by the bottom flange readings, where the flange has negligible movement until the applied connection load reaches 500 kN. This is when the bottom bolt started to deform under the shear load and sagging moment. With the deformation the bottom flange started to move away from the column face.

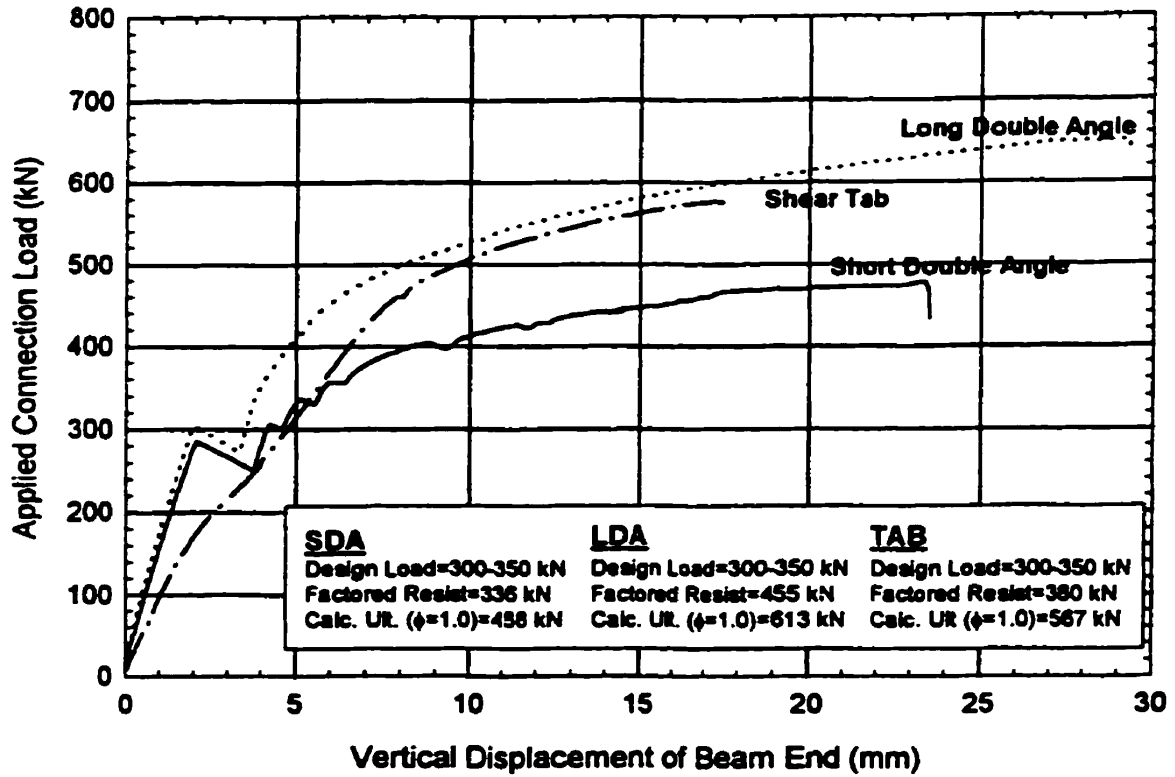


Fig 4.19: C450-W410: Applied Connection Load vs. Vertical Beam End Displacement

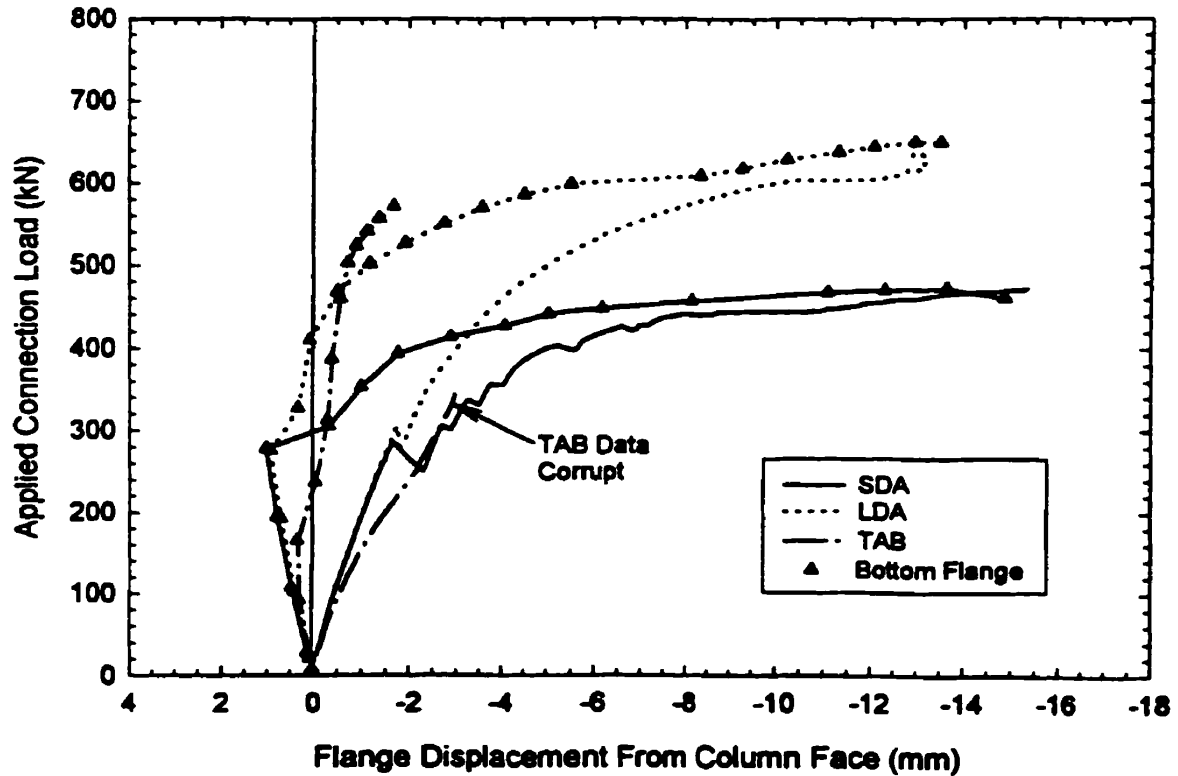


Fig. 4.20: C450-W410: Applied Connection Load vs. Displacement of Beam flange From Column Face

4.4.2.2 C450-W530 Connection Series

The W530 connection series was designed to represent the range of girder loads for the gravity frame system. The deeper connections required higher loads to cause failure. The SDA connection was the only specimen that experienced complete rupture, with a net section failure through the bolt line in the angles. There was permanent deformation observed in the LDA and TAB connections even though they could not be loaded to failure. The lack of proportionality can be observed in the test data.

The plot of the vertical displacement of the beam end is shown in Figure 4.21. There were some differences in the stiffness of each of the connection types, but the order corresponded to the cross-sectional areas. The order of stiffness in ascending order was short double angle, long double angle and the shear tab. At the commencement of loading all 3 connections had similar stiffness in the vertical direction. At just below 200 kN the deformation plot slightly deviates for the SDA and the LDA. For the Tab connection there is a deviation in the curve at 340 kN. These slight deviations occur well below loads associated with general yielding of the connection, and represent only a slight change in the slope. It is likely due to the yielding of the cross plate. Development of the yield line pattern is not dependent upon the shear load, but the moment developed at the connection weld line.

This slight deviation in the general load deformation curve is again observed for the SDA and LDA connections in the flange displacement plot shown in Figure 4.22. Although the connection end plate is yielded there is no apparent loss of stiffness. The separation is dependent upon the rotation of the beam end.

4.4.2.3 C600 Connection Results

The connection details for the tests C600-W410-SDA-C and C600-W410-LDA-C were nearly identical to those in the C450-W410 series. The major differences were the width, W , of the connection end plate, and that the longitudinal beam restraint to simulate the constructed condition was used for the C600 composite tests. Figure 4.23 displays the plots of connection load versus the vertical beam end displacement for the tests C600-W410-SDA-C and C600-W410-LDA-C. The results from the equivalent C450-W410 connection series have also been plotted on the same graph for comparison. There is good correlation between the tests, with the exception of the initial loading of C600-W410-SDA-C. At an applied connection load of 140 kN the load deformation curve changes abruptly. The stiffness is lower, but remains linear until a connection load of 380 kN, when

there was yielding observed in the connection angles. The apparent loss of stiffness was likely due to the gradual slipping of the bolted connection as observed during the test.

Of note is also the increase in the stiffness near the end of the test ($V_{app} > 675$ kN). This localized increase was caused by the beam flange coming into direct bearing on the connection from excessive deformation. The test was terminated when this was observed.

The influence of the longitudinal beam restraint is obvious when comparing the C600 and C450 tests results. When the connection yielded in the C450 tests, the beam had clearly moved away from the column face. There was excessive bolthole deformation, and both the top and bottom flange moved away from the column face. For the C600 series the flange movement was restricted by the restraint. Although the vertical beam deflection is similar, the plot of the beam flange displacement from the column face (Fig. 4.24) shows a clear distinction.

Only results from the LDA connections have been included in Figure 4.24 because the data from the top flange LVDT for the test C600-W410-SDA-C was corrupt for the same reason as that given for test C450-W410-TAB-C.

4.4.2.4 Unstiffened Seat Results

For previously explained reasons it was impossible to load the seat connections to failure, and at point of maximum load there was little deformation observed in either the end plate or the connection. Thus there was little difference between the load deformation response of the two connections, but Seat2 with the four – ¾” shear studs, was slightly stiffer than Seat1. This is obvious in both the plot of vertical deformation of the beam end, shown in Figure 4.25 and the displacement of the beam flanges from the column face, shown in Figure 4.26. Although there was some permanent deformation of the outstanding leg, there was little to no permanent separation of the end plate and the concrete column.

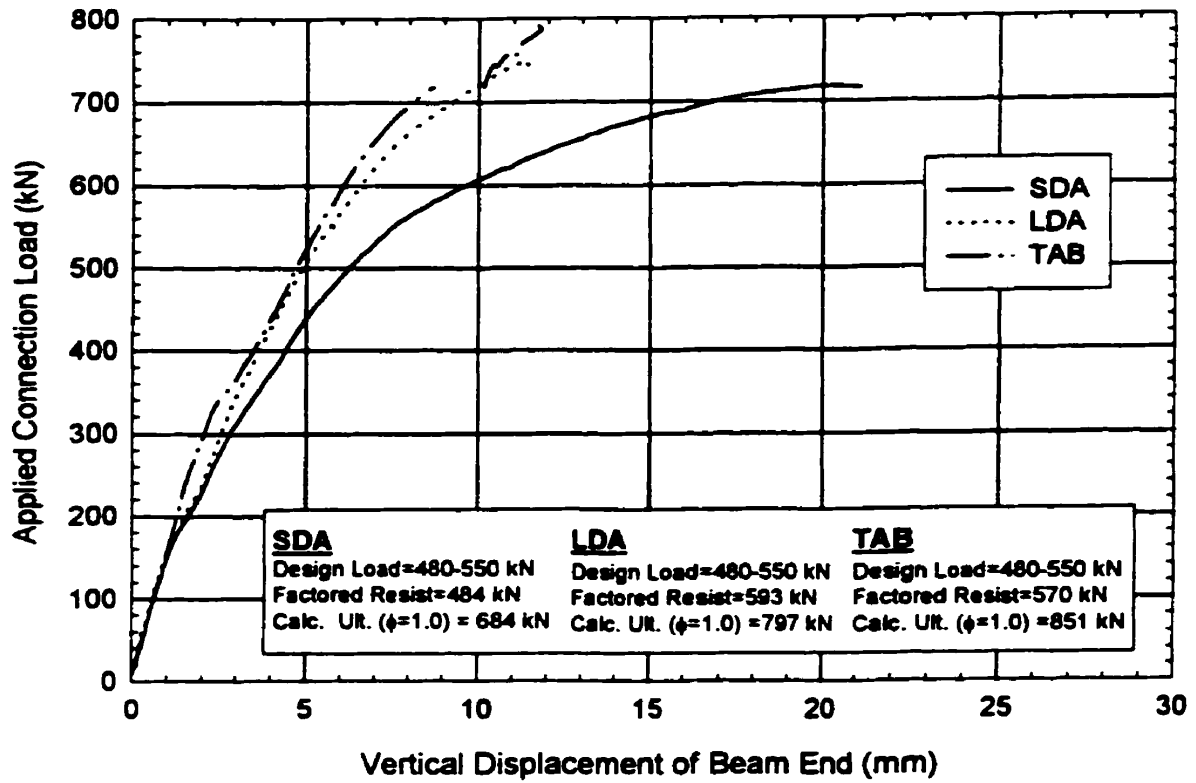


Fig 4.21: C450-W530: Applied Connection Load vs. Vertical Beam End Displacement

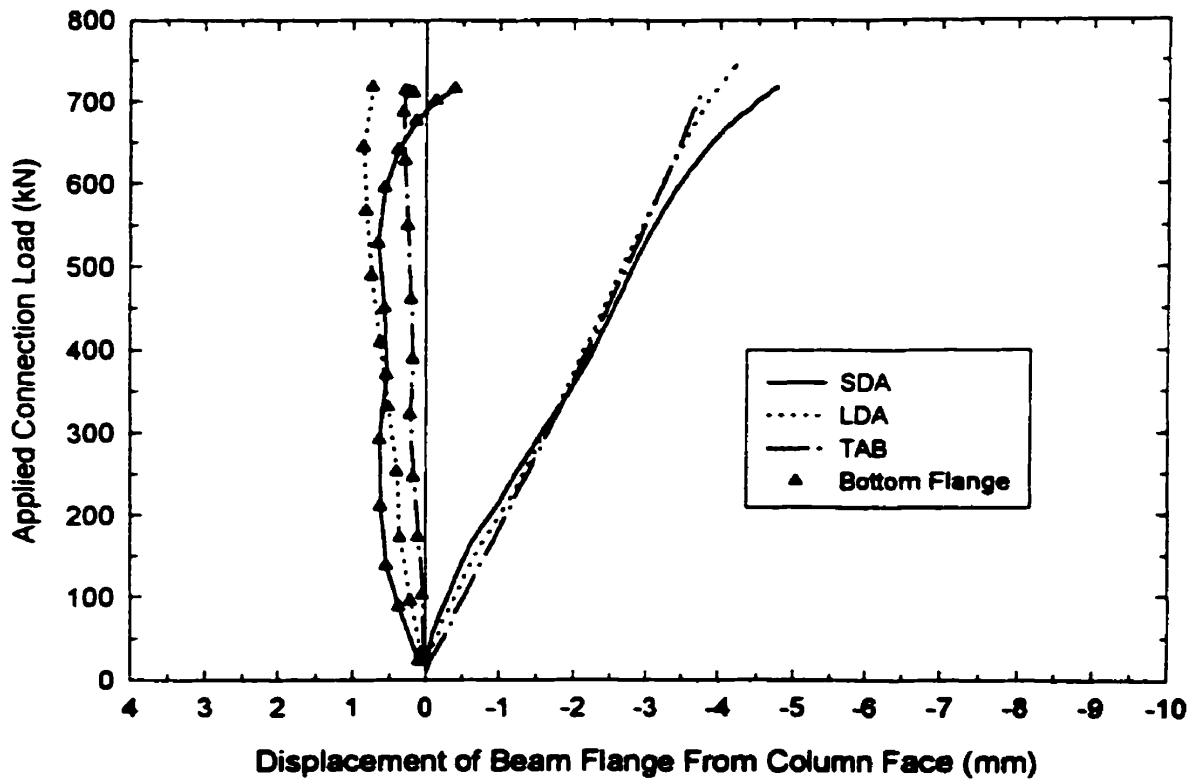


Fig. 4.22: C450-W530: Applied Connection Load vs. Beam Flange Displacement

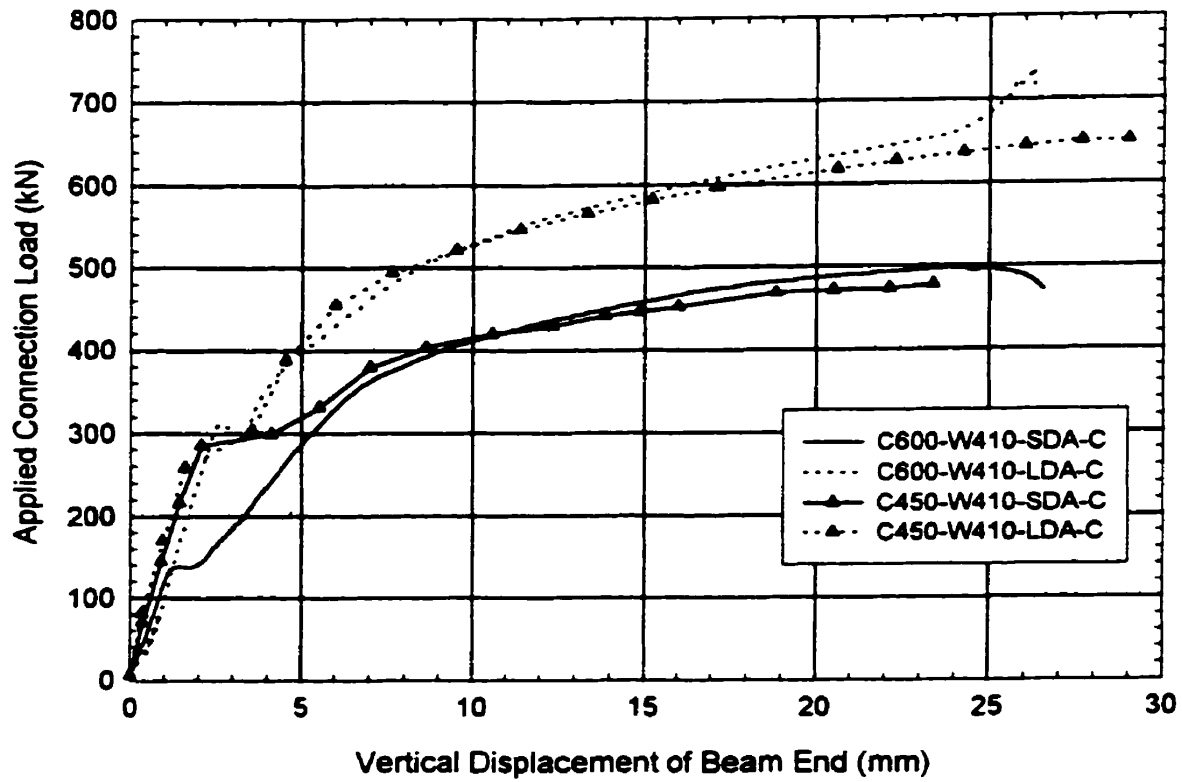


Fig. 4.23: C600-W410: Applied Connection Load vs. Vertical Beam End Displacement

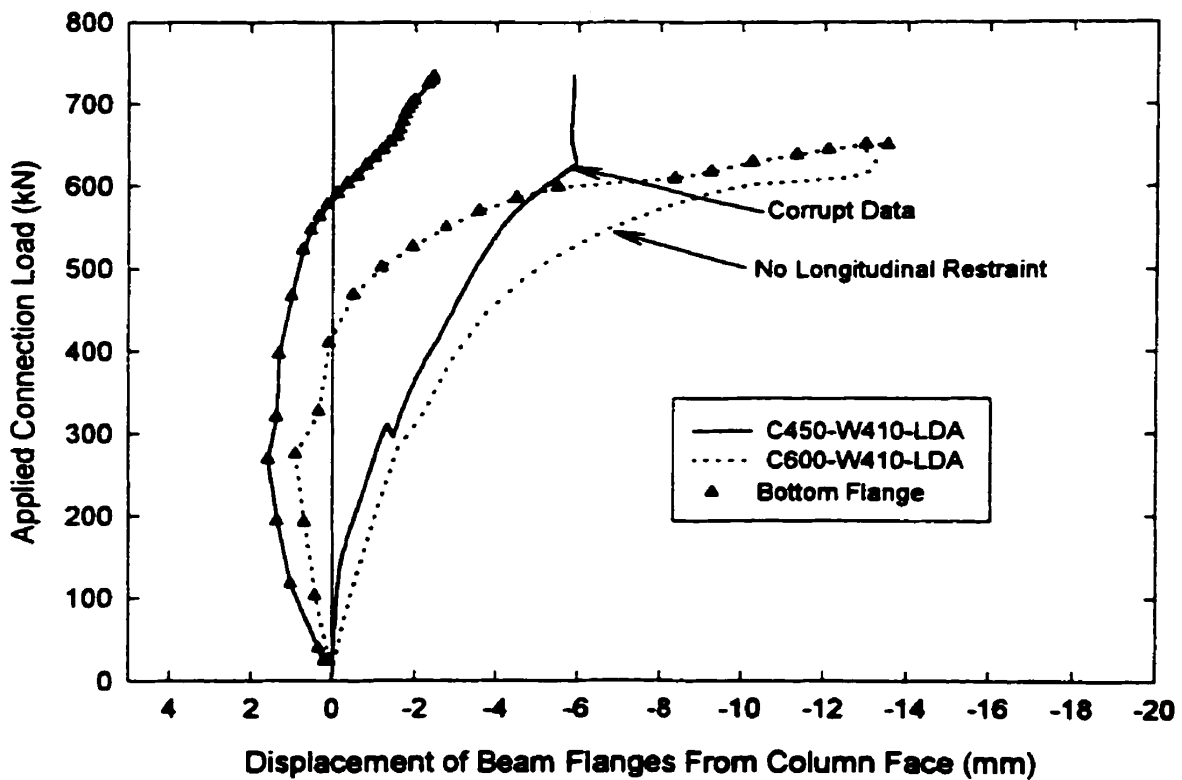


Fig. 4.24: C600-W410: Applied Connection Load vs. Flange Movement From Column Face

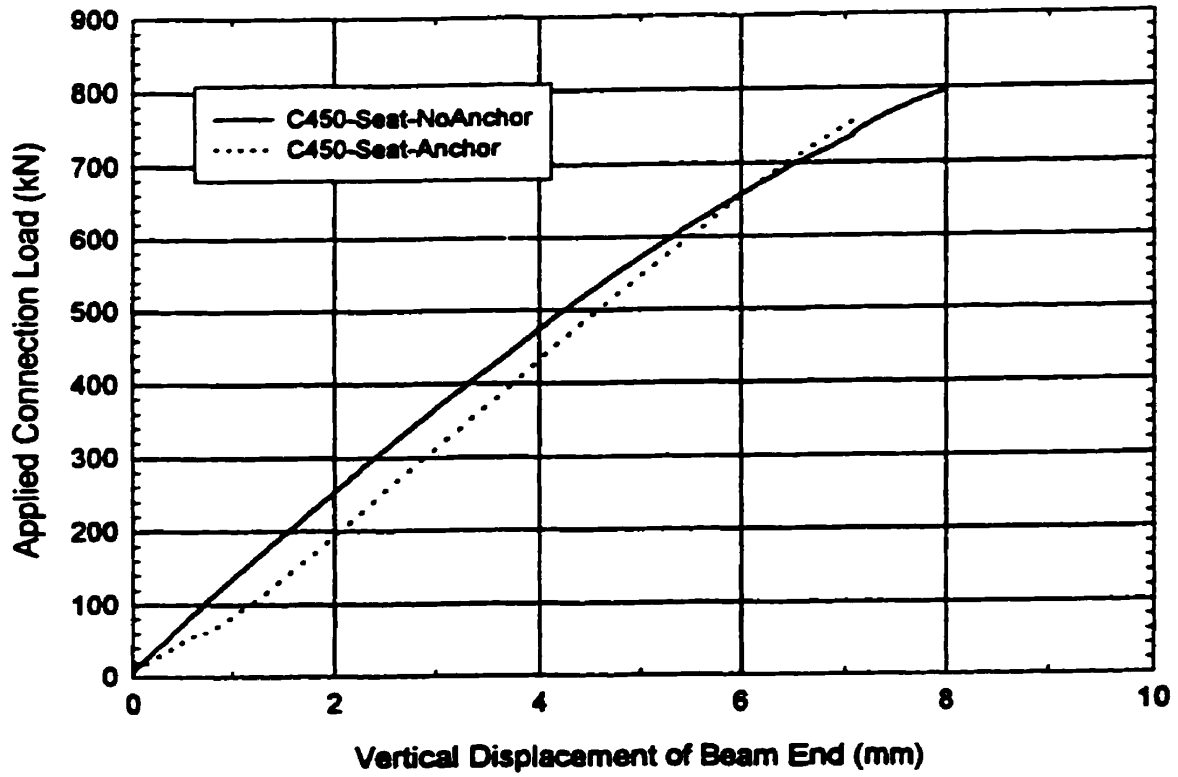


Fig. 4.25: C450-Seat: Applied Connection Load vs. Vertical Beam End Displacement

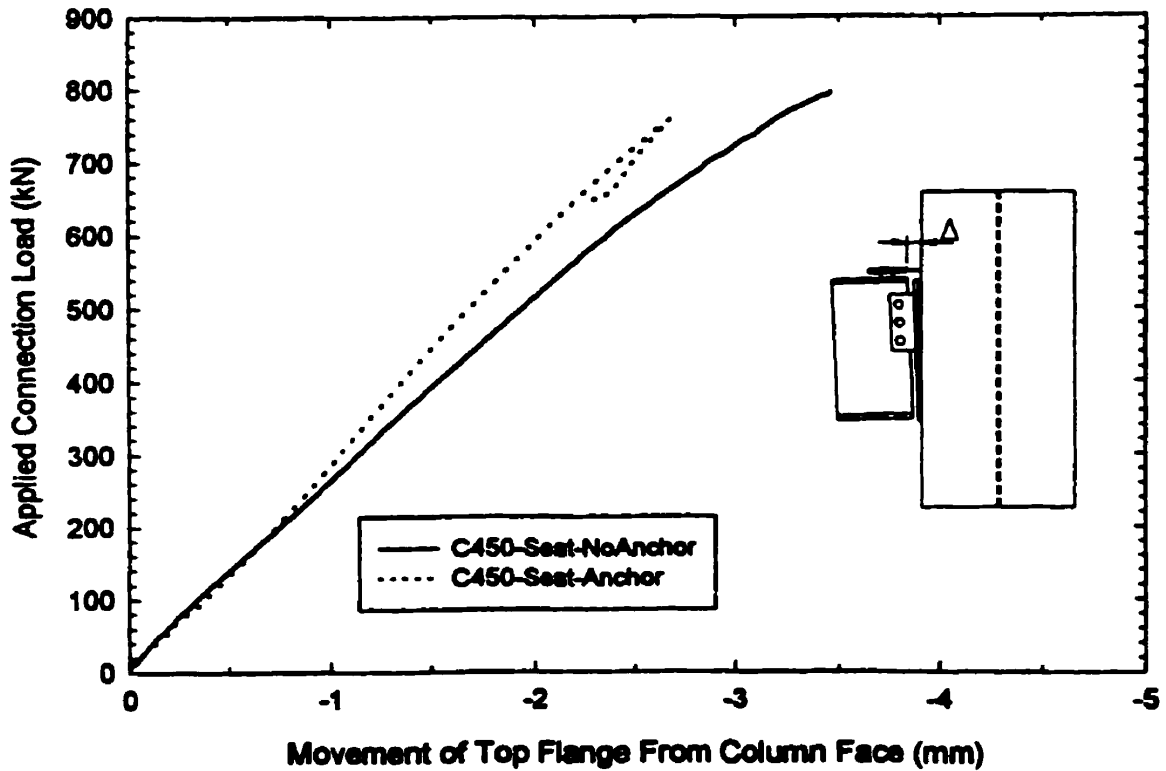


Fig. 4.26: C450-Seat: Applied Connection Load vs. Top Beam Flange Displacement From Column Face

4.4.3 Moment-Rotation Response of the Composite Connections

A simple framing connection has been defined³ as allowing 80% of the perfect pin rotation, while developing less than 20% of the fixed end moment. For a conventional simple connection, attached to a rigid column face, a considerable moment may develop. Even though it may be less than the 20% of the fixed end moment, it cannot necessarily be neglected in the connection design. A typical bending moment diagram for a simple framing connection, to a rigid column face is shown in Figure 4.27(b). The inflection point may lie outside of the bolt line (left of the bolt line in Figure 4.27), resulting in a hogging moment that must be transferred across the bolt line.

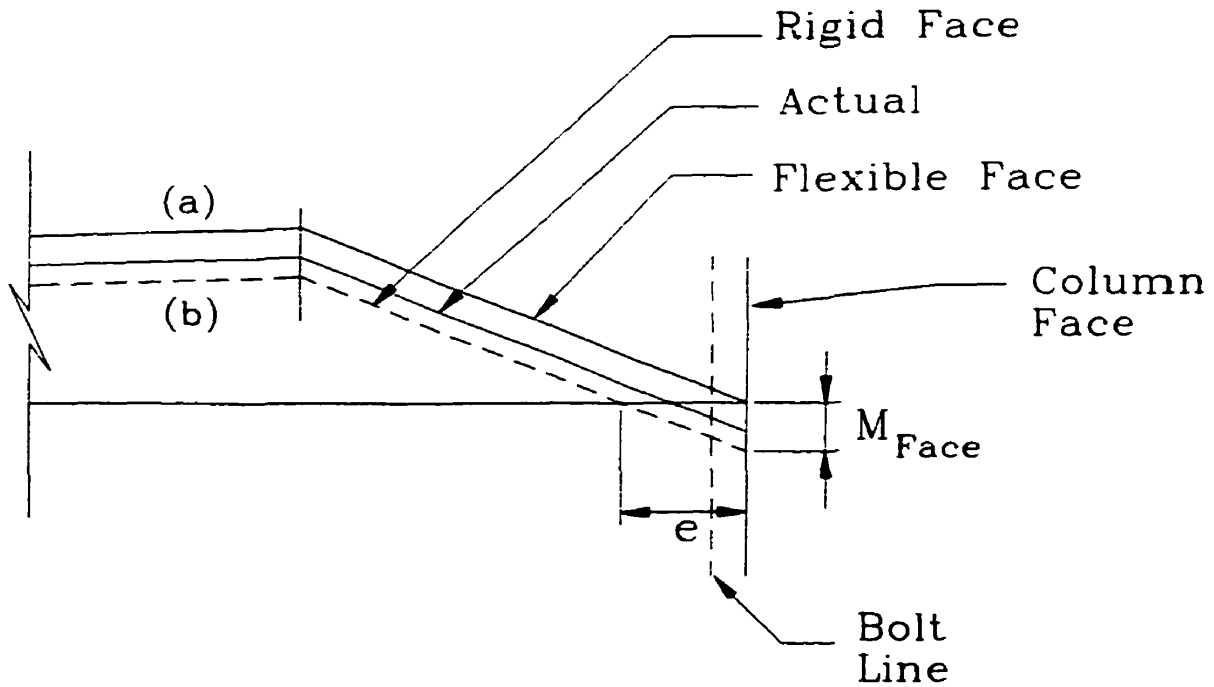


Figure 4.27: Bending Moment Diagram of Varying End Restraint

For the composite connection detail proposed in this study, the column face can not be classified as rigid. The actual restraint provided at the column face is somewhere between the rigid case (Fig. 4.27b) and the zero restraint case when the face is considered as an ideal pin (Fig. 4.28a). Although the partial restraint provided at the beam end will generally not be recognised in beam design, it is still important to quantify the size of the moment that could be expected at the column face.

By recording the test geometry; L , a_1 , a_2 and d_{MTS} it is possible to calculate the moment at the column face.

$$M_{Face} = P_{MTS}d_{MTS} + W_{Spreader} \left(\frac{a_1 + a_2}{2} \right) + W_{TestBeam} \frac{L}{2} - R_{Support}L \quad (\text{Eqn. 4.5})$$

For tests where the longitudinal beam restraint was in place the value M_{Face} is equal to sum of the moment at the connection weld line, $M_{Connect}$, and the restraint moment couple.

$$M_{face} = M_{Connect} + Sj \quad (\text{Eqn. 4.6})$$

Where the variables $M_{Connect}$, S and j are defined in the free body diagram in Figure 4.28. For the two prototype specimens where the slab restraint was not used $M_{Face} = M_{Connect}$. With the slab restraint being used the rotation of the beam end was restricted and the total moment at the face, which includes the restraint couple, was higher. A full discussion of the influence of the slab restraint on the connection behaviour is included in Chapter 5 of this report.

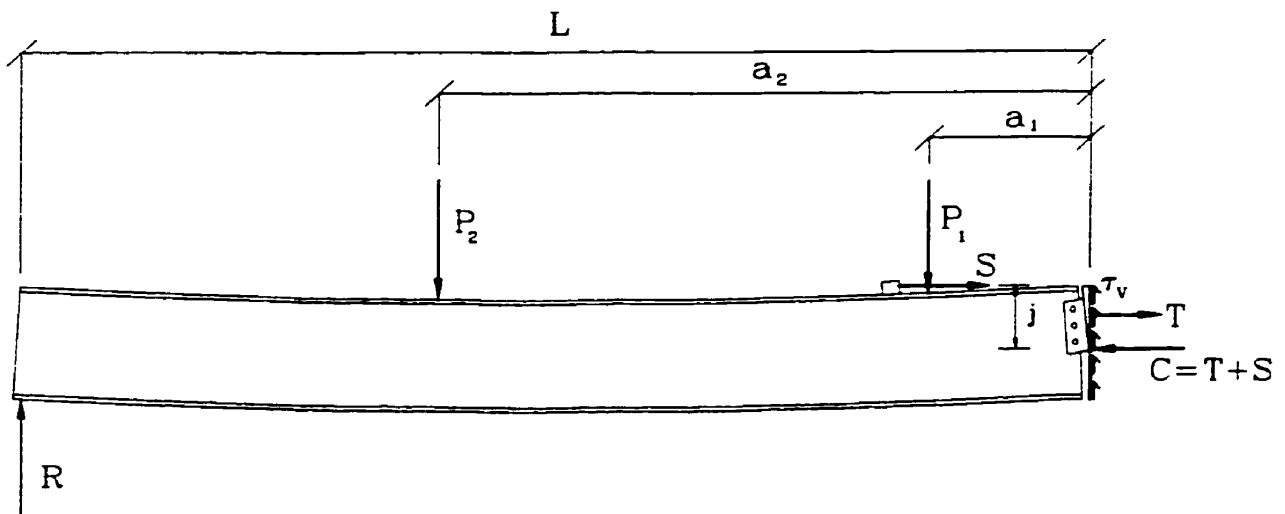


Figure 4.28: Free Body Diagram of Beam - With Restraint

4.4.3.1 C450-W410 Connection Series

The TAB connection was the only specimen in the C450-W410 series to be tested with the longitudinal beam restraint in place. The result was that M_{Face} for the TAB was much higher than for the SDA and LDA specimens, as shown in Figure 4.29. Another common characteristic of all restrained tests is that a sagging moment is registered as the connections were initially loaded. As the applied connection load reaches 100 kN the shape of the M-V plot changes to the expected shape with a negative moment at the face.

It is intuitive to have a positive moment at the face, and the initial negative moment is likely a result of initial zeroing of the test data, and seating of the entire test specimen. Prior to analysis, the far end load cell reading was adjusted to equal the weight of the load and spreader beams, proportioned by the test geometry. Thus, there was a calculated zero moment at the face, when there was actually a slight negative moment caused by the slab restraint being in a snug state. Because of the large size

of the moment arm a slight difference in the load cell reading would have had a great effect on the calculated moment at the face.

The initial irregularities could have also been caused by the seating of the entire test set-up. In the composite tests, where the restraint was used, a small preload was placed on the connection before the various roller supports were unlocked. The preload was not constant for all tests, but the change in the moment diagram generally corresponds to the rollers being unlocked. Other seating related issues include an initial out-of-straightness of the test beam flange. The beam was not grouted at the end support thus a small load was likely required before proper seating occurred. These slight changes in the load distribution would have had produced an appreciable difference in the calculated value of M_{Face} . Once the test specimens were properly seated, the M-V plot remained linear until the connection yielded.

For the unrestrained tests the SDA connection develops the higher moment at the connection face. This may appear counterintuitive since longer connections generally develop higher moments at the bolt line and at the weld line. The longer connection length does increase moment transfer at the bolt line, but due to the relatively flexibility of the connection at the column face, it is an increasing sagging moment at the bolt line. The entire moment diagram is being shifted up, effectively reducing the moment at the weld line. This is better illustrated by an upward shift of the “actual” line in Figure 4.27. For the composite connection, without the beam restraint in place, the point of zero moment in the beam (i.e.; inflection point) is between the bolt and weld lines, causing the observed sagging moment at the bolt lines.

4.4.3.2 C450-W530 Connection Series

All three connections in the W530 connection series were tested with the longitudinal beam restraint in place. The calculated value for M_{Face} remained linear with respect to the applied connection load until yielding of the connection. The linear relationship is indicative of a linear elastic response of the connection, with a relatively constant location of zero moment in the test beam. The rotational stiffness of the connections, with the restraint in place, can be compared by comparison of the slope of the M-V curve. From the M-V plot shown in Figure 4.31, the slopes are 121, 69, and 86 mm for the SDA, LDA and TAB connections respectively. It must be remembered that the calculated value of M_{face} includes the restraint moment couple (i.e.; $S \times j$). From the observed bolthole deformation the actual inflection point should be located between the weld and the bolt lines. This will be further discussed in Chapter 5 of this report.

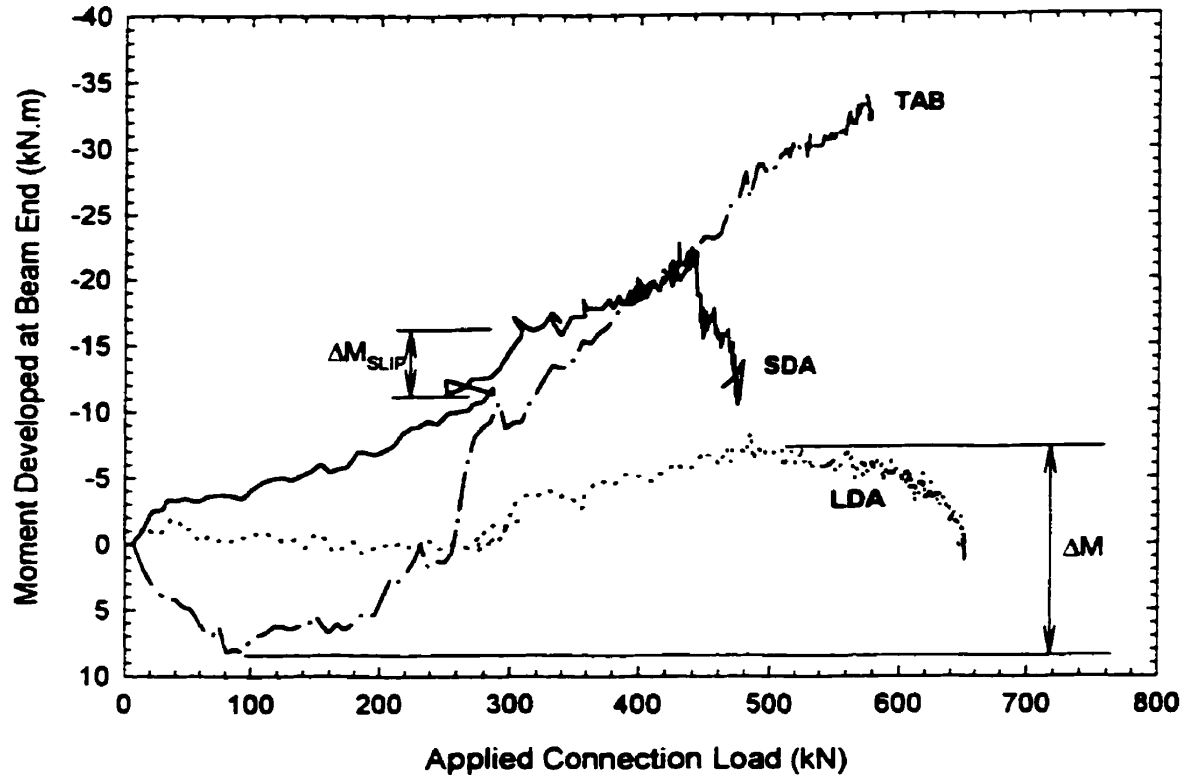


Fig. 4.29: C450-W410: Moment Developed at Beam End, M_{face} vs. Connection Load

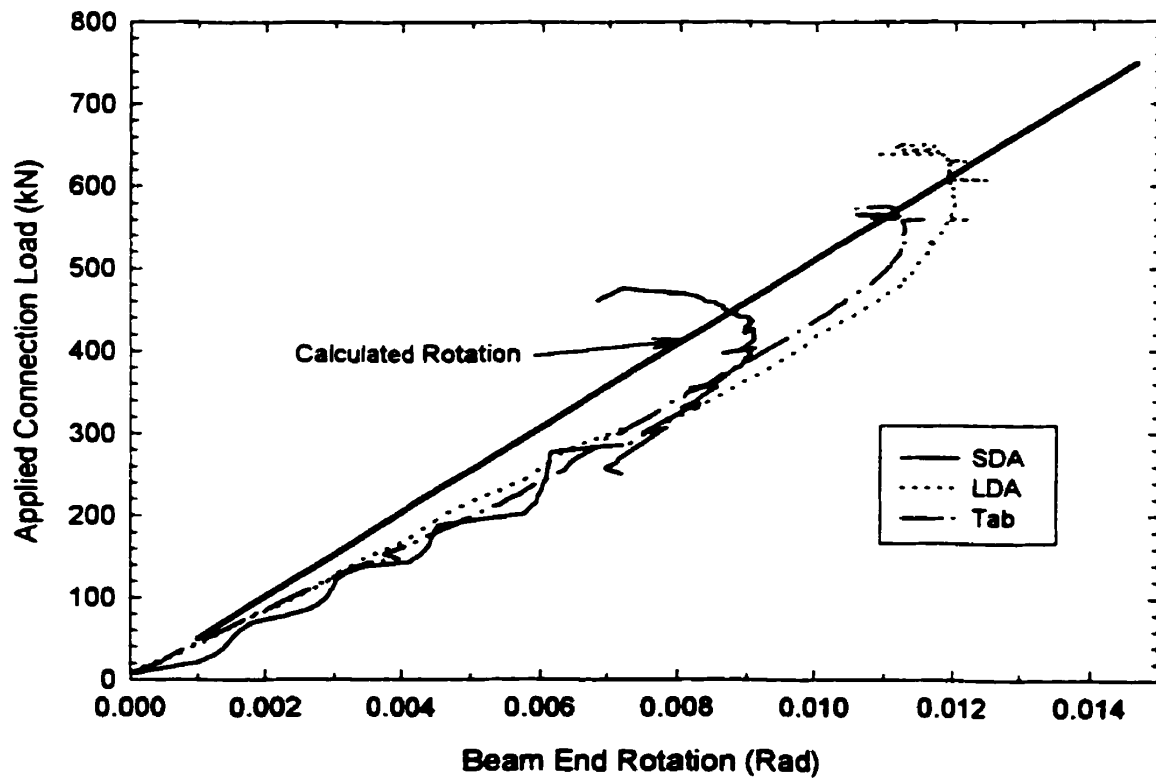


Fig. 4.30: C450-W410: Applied Connection Load vs. Beam End Rotation

There is a significant difference in the $V - \theta$ relationship for the three connection types, as can be seen in Figure 4.32. Although there were slight differences in the test geometry, the differences should only have minor effects on the beam end rotation. The most influential factor is the variability in the restraint provided at the column face. The order of the rotation from the highest to lowest is LDA, TAB, and SDA. This corresponds with the order of the end moment, with the SDA having the highest connection eccentricity.

4.4.3.3 C600-W410 Series

Aside from the initial seating effects, the $M-V$ response of the two C600 connections were similar. Again the relationship remained relatively linear until advanced yielding of the connection. From the $M-V$ plot of Figure 4.33 the slopes for the SDA and LDA connections can be calculated as 106 and 120 mm respectively. This was the first test series where the longer double angle connection developed a higher moment at the beam end than the short double angle.

Of interest are the differences in the measured rotations shown in Figure 4.34. The longitudinal restraint is effective in reducing the rotation of the beam end for the C600 test series. The SDA connection appears to be restrained to a greater extent than the LDA connection. This does not reflect the moment information, as the LDA develops the higher moment at the face.

4.4.3.4 Unstiffened Seat Results

The $M-V$ relationship for the tests C450-Seat1-NoAnch and C450-Seat2-Anch are shown in Figure 4.35. Taking a line of best fit, the eccentricities can be estimated as 58 and 94 mm respectively. Although these are based on a linear fit, there is actually a slight increase in the tangential slope as the connection load increases.

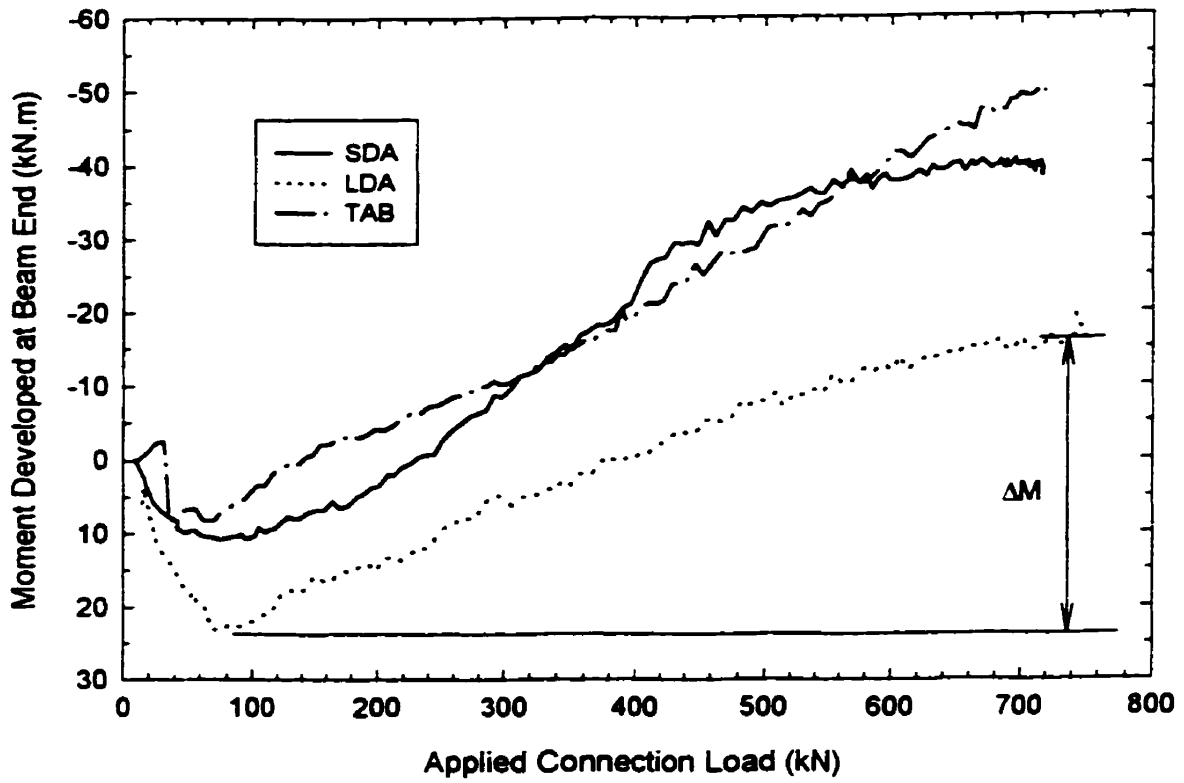


Fig. 4.31: C450-W530: Moment Developed at Beam End vs. Connection Load

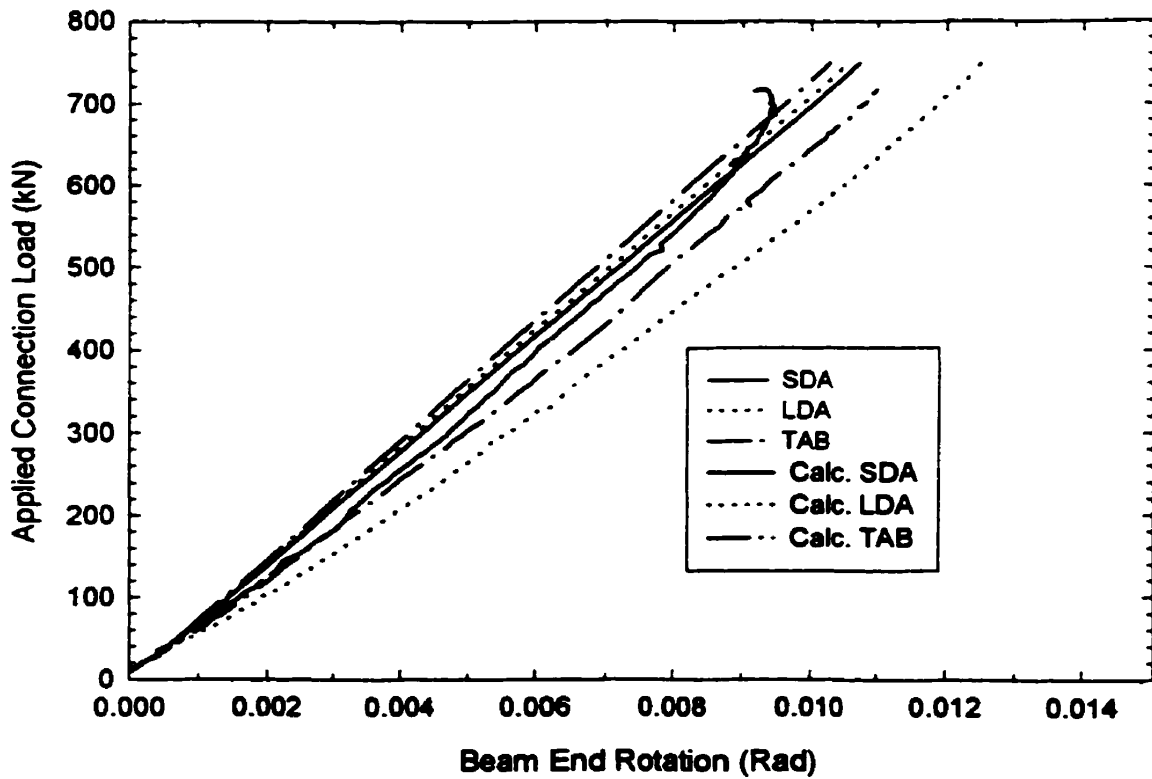


Fig. 4.32: C450-W530: Applied Connection Load vs. Beam End Rotation

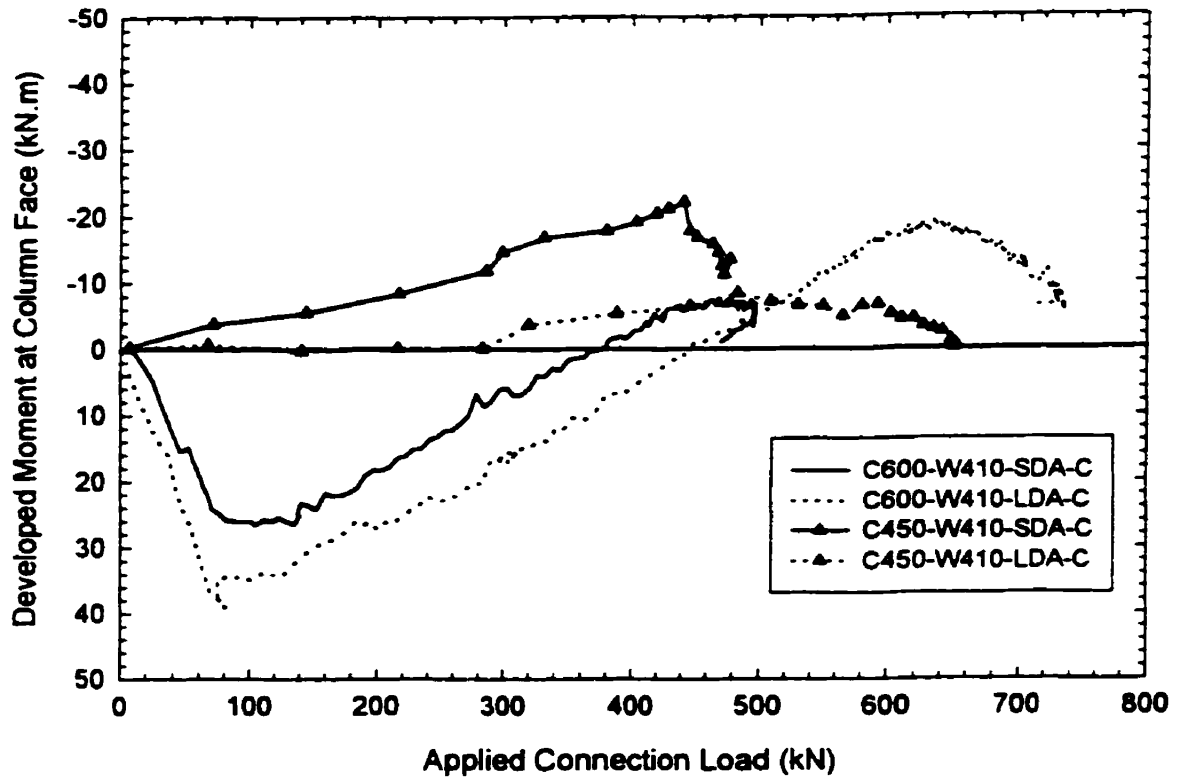


Fig. 4.33: C600-W410: Developed Moment at Beam End M_{facc} vs. Applied Connection Load

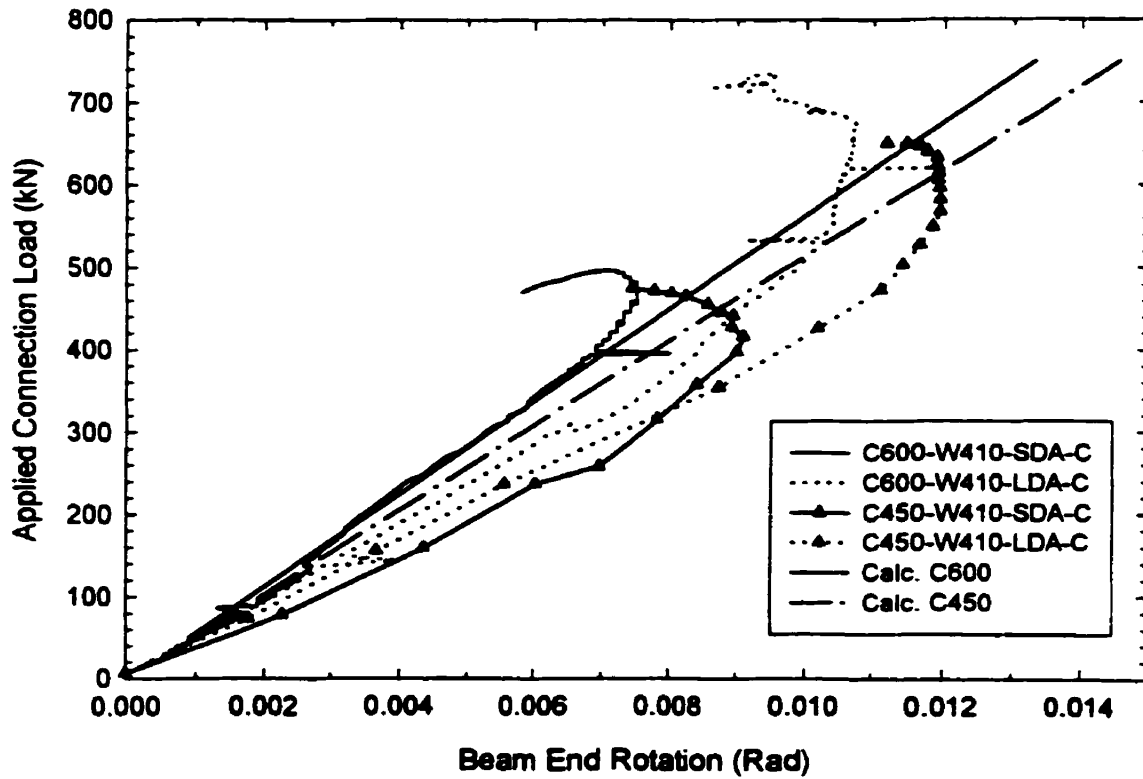


Fig. 4.34: C600-W410: Applied Connection Load vs. Rotation of Beam End

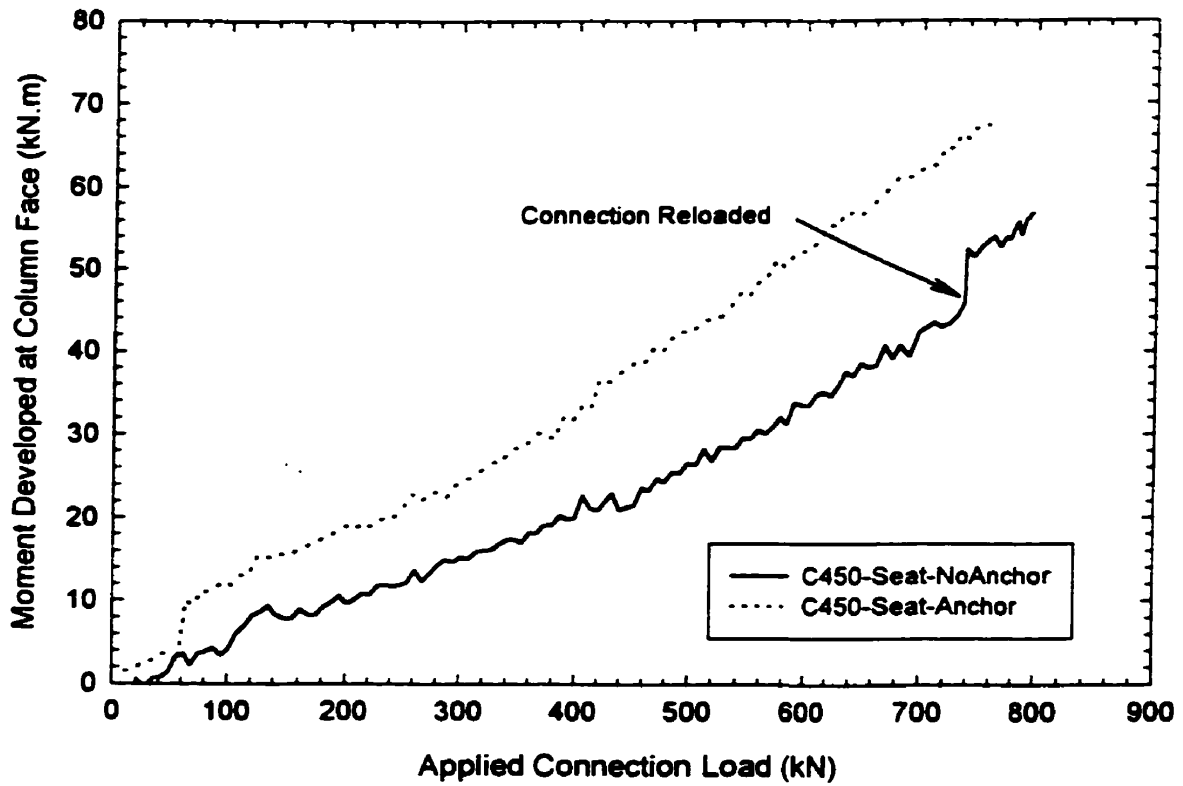


Fig. 4.35: C450-Seat: Moment Developed at Beam End, M_{face} vs. Connection Load

4.4.4 Force Transfer Between Steel and Concrete

Following the prototype tests it became obvious that the primary concern would not be the performance of the connection itself, but rather the issue of force transfer from the steel into the concrete. Thus a complete network of strain gauges were installed on the remaining test columns. Gauges were placed on the column flange, on a single side of the column with intermediate concrete surface gauges placed at key locations over the column height. Complete drawings showing the strain gauge locations for each specimen are given in Appendix D.

As previously mentioned the columns were geometrically aligned only, and not adjusted in the test frame for perfect concentric loading. The result was that after the application of the axial load there was generally a strain gradient existing over the cross section. To analyse the stress flow in the column resulting from the connection load the strains must first be normalized for the axial load. The strain distribution for each of the composite test specimens are shown in Figures 4.36 to 4.39. The values are the change in strain at a connection load of 500 kN (when $V_{\text{applied}} = 0$ then strain = 0), and are given as microstrain.

At a depth of 1.5 D below the connection plate, plane strain generally existed. There were several tests where a seating problem at the bottom of the load column, which resulted in localized strain increases, was apparent. In Test C450-W530-SDA-C the average steel strain 685 mm below the connection plate was 140 microstrain. This was approximately 60% higher than the typical average strain in the 450 x 450 mm column, under those applied loads. This was accompanied by small readings in associated concrete surface gauges. Further evidence of a seating problem, rather than a lack of force transfer, was in instances where the concrete surface gauges located just below the connection were registering higher strain readings than those 685 mm below the connection (Test C450-Seat1).

The force transfer varies with the connection length and the column size as will further discussed in Chapter 5. Although there were differences in the strain distribution over the range of test variables the actual difference are very small, generally less than 150 microstrain.

4.4.5 Review of Composite Tests

A summary of all composite connection tests is provided in Table 4.3. The tests have been presented according to their sub-groupings as they have been presented in the preceding chapters.

C450-W410 CONNECTION SERIES V=500 kN
Microstrain

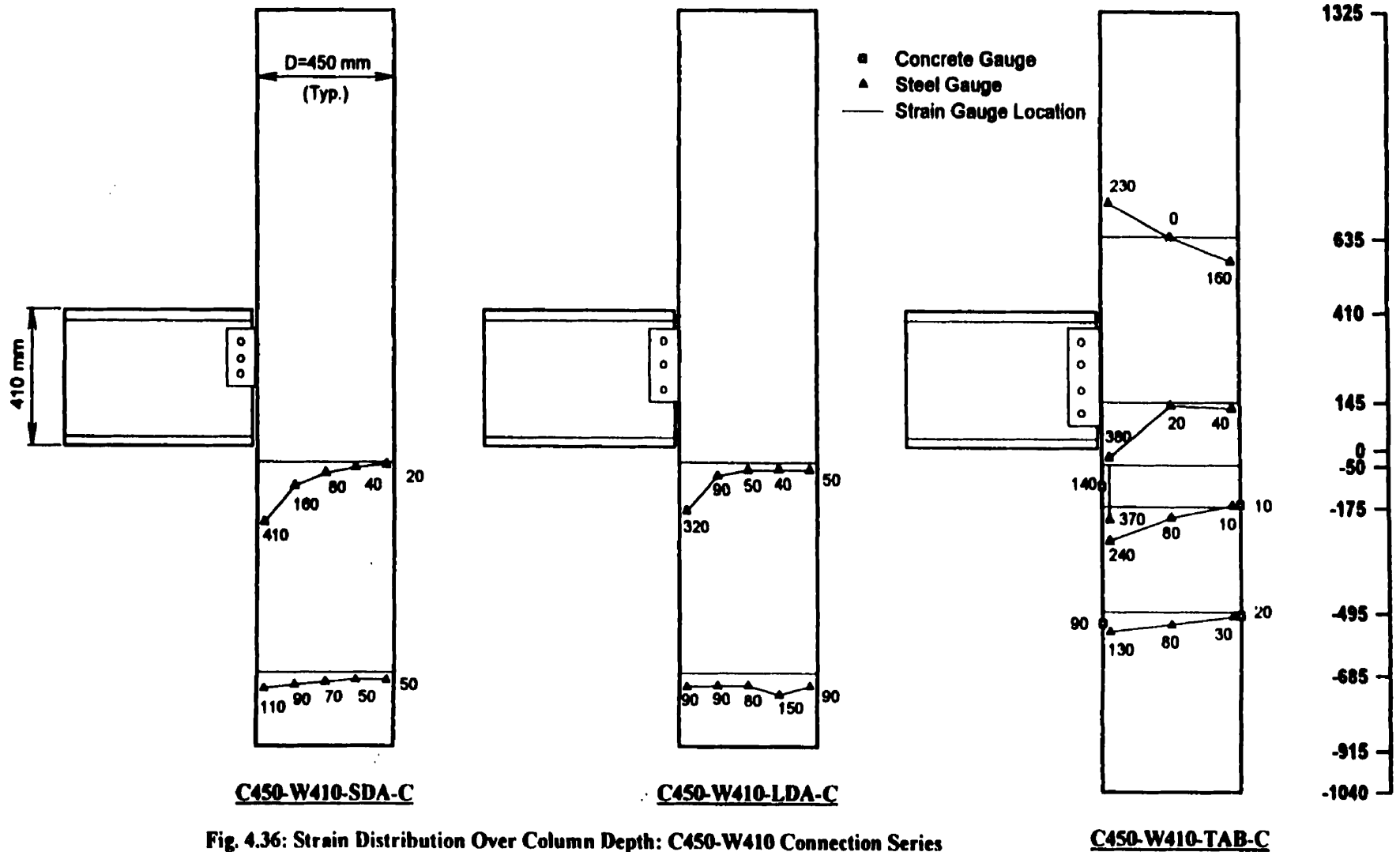


Fig. 4.36: Strain Distribution Over Column Depth: C450-W410 Connection Series With an Applied Connection Load of 500 kN.

C450-W530 CONNECTION SERIES V=500 kN

Microstrain

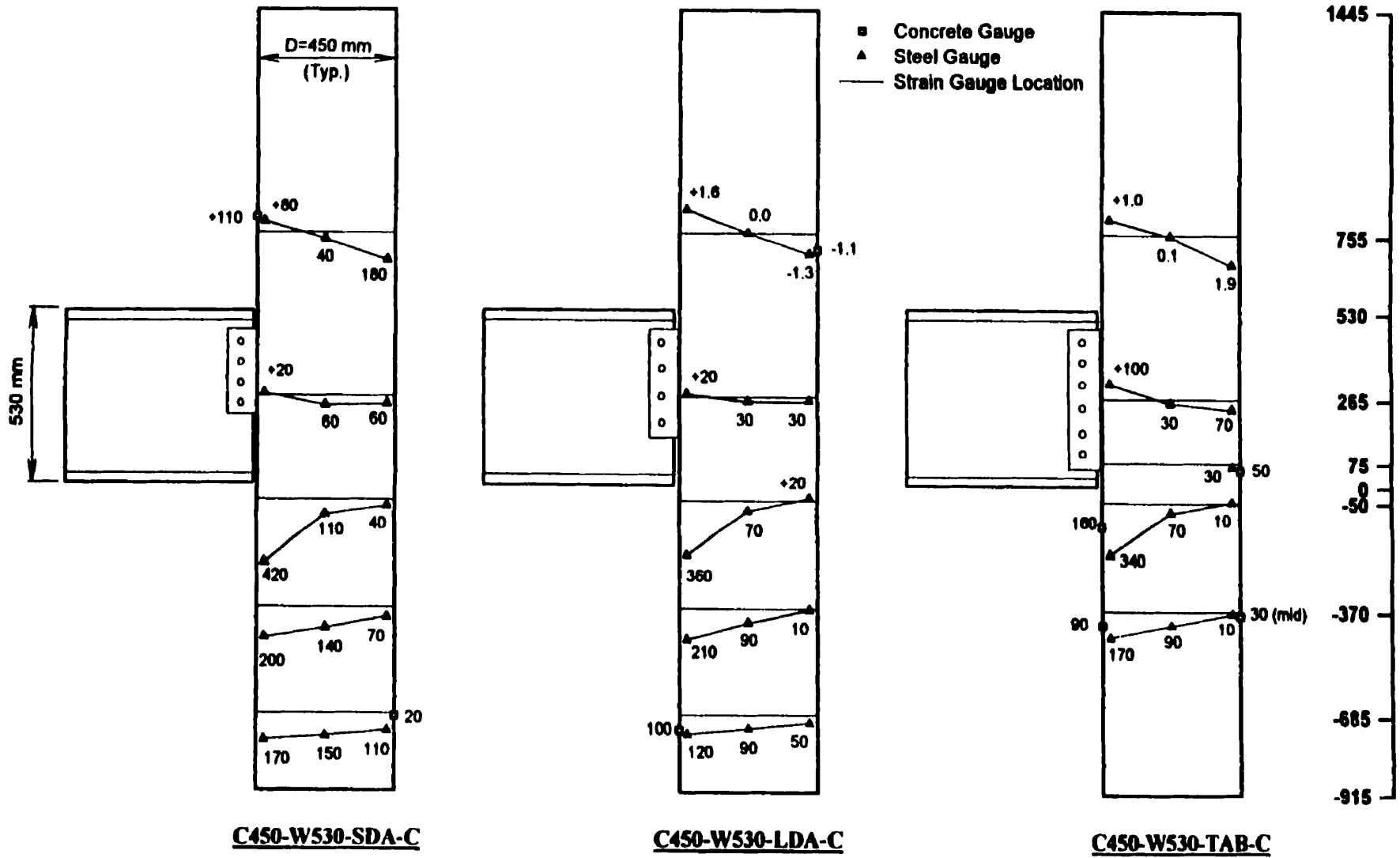
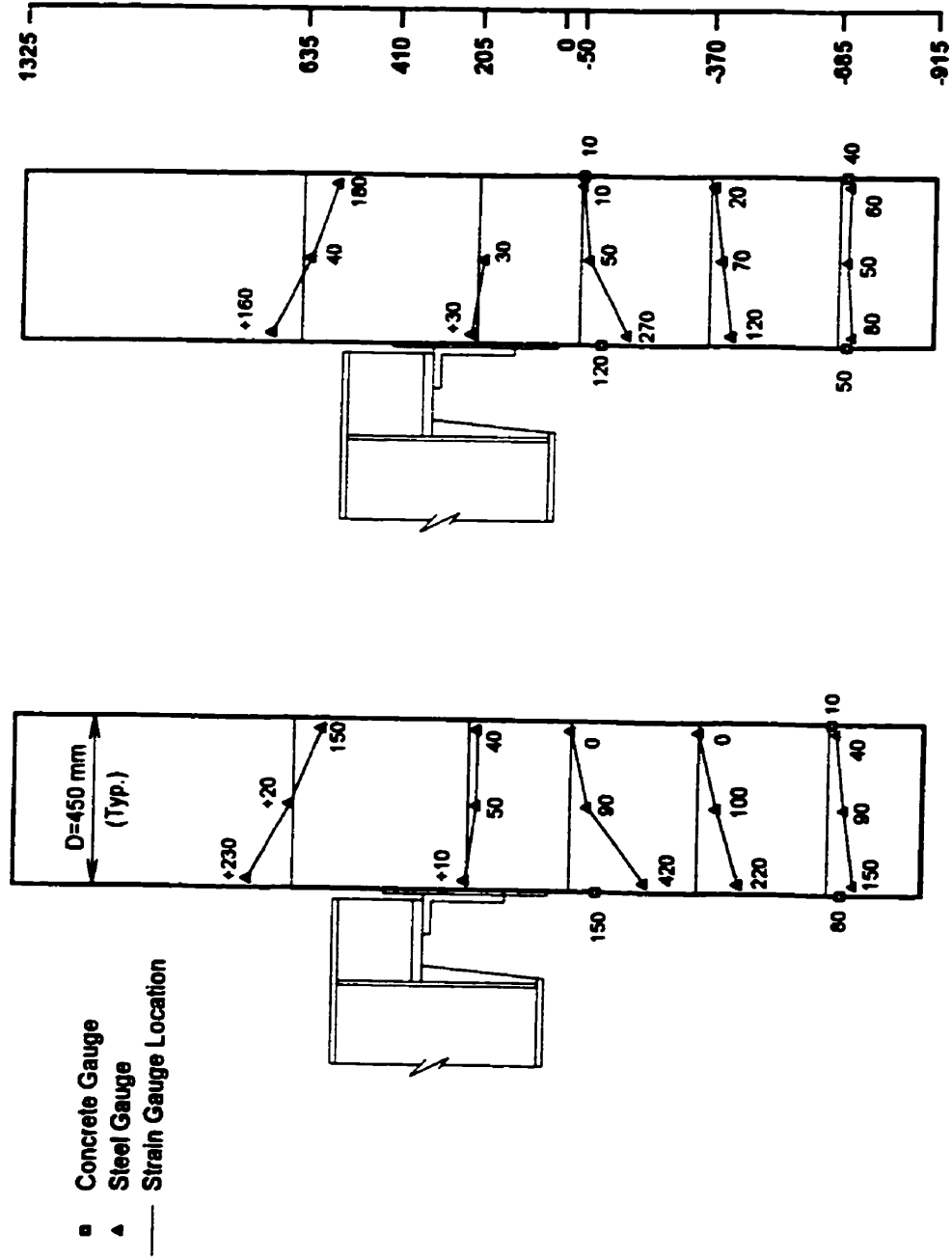


Fig. 4.37: Strain Distribution Over Column Depth: C450-W530 Connection Series with an Applied Connection Load of 500 kN

C450 SEAT CONNECTION SERIES V=500 kN
Microstrain



C450-SEAT-ANC-N
C450-SEAT-ANC
 Fig. 4.38: Strain Distribution Over Column Depth: C450-SEAT Connection Series
 With an Applied Load of 500 kN.

C600-W410 CONNECTION SERIES V=500 kN
Microstrain

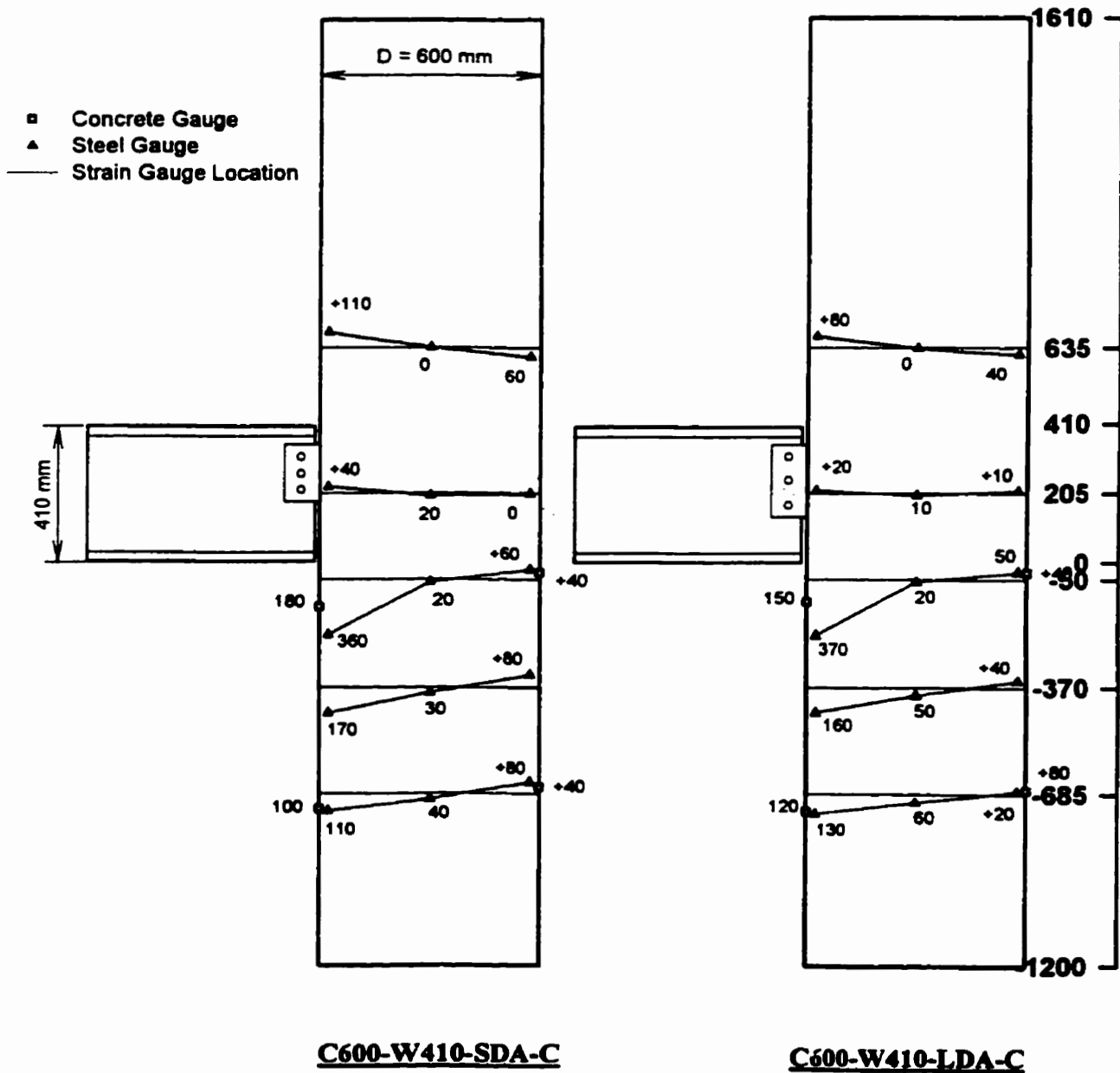


Fig. 4.39: Strain Distribution Over Column Depth: C600-W410 Connection Series With an Applied Load of 500 kN.

Table 4-3: Summary of Composite Results

Specimen	Calculated Ult. (kN) ($\phi=1.0$)	a_1 (mm)	a_2 (mm)	d_{MTS} (mm)	L (mm)	Floor Slab Restraint	$\frac{\Delta M}{\Delta V}$ (mm)	Test V_{Yield} (kN)	Test V_{Ult} (kN)	Comments
C450-W410-SDA-C	466	595	3834	1330	5350	No	41	365	480	Excessive Deformation
C450-W410-LDA-C	613	565	3870	1330	5350	No	21	360	650	Excessive Deformation
C450-W410-TAB-C	567	605	3817	1345	5315	Yes	78	450	576	Bolt Failure
C450-W530-SDA-C	684	627	4173	1348	7013	Yes	121	450	678	Net Section
C450-W530-LDA-C	797	615	4235	1345	7015	Yes	69	580-620	-	
C450-W530-TAB-C	851	560	4035	1350	6937	Yes	86	630	-	
C450-Seat1-NoAnch	-	557	4210	1344	6935	Yes	58	620	-	
C450-Seat20Anch	-	554	4205	1345	3938	Yes	94	-	-	
C600-W410-SDA-C	466	568	3672	1275	5097	Yes	106	360	471	Net Section
C600-W410-LDA-C	613	561	3726	1277	5101	Yes	123	380	735	Excessive Deformation

4.5 Non-composite Tests

A total of four non-composite tests were performed. Three 450x450 mm column specimens with a common b/t ratio of 23 and a single 600 x 600 mm column specimen with a b/t ratio of 31 were tested. Each specimen was loaded axially to a typical story load of 700 kN, the connection loaded to the typical floor load and the column load then increased until a buckling failure occurred. While the column was being loaded, the connection load was manually held constant, with the MTS still on displacement control. During the C450-W410-TAB-N test the load was inadvertently not maintained, and the connection load dropped as the column load increased.

4.5.1 General Observations

All specimens exhibited a similar failure pattern as shown photographically in Figure 4.40. Local buckling occurred in the column flanges, between the connection plate and the tension stirrup. The stirrups were placed to improve buckling of the flange, and were regularly spaced at distance, D . Local buckling initiated at a point equidistant to the support points, $0.5 D$ below the connection plate. In all cases the flanges buckled inwards, and as it progressed was accompanied by the formation of an outward buckle on the east (unloaded) side of the column, between the other connection plate and the tension stirrup. As loading increased the buckle progressed to the bottom portion of the column, just above the bearing endplates, as seen in Fig. 4.41. There was no buckling in the column web until the latter stages of failure.

Two specimens (C450-W410-SDA-N, C450-W530-LDA-N) had a buckling pattern form above the connection at approximately 60% of the maximum axial load. This was due to a seating problem at the top of the column, where there was no spherical head. As the load was increased the buckled shape did not advance as it did below the connection, rather the lateral deflection of the column flange remained relatively constant.

As with the composite connection tests the column shifted slightly in the test fame as the connection load was applied. Although a roller was in place at the top to prevent the lateral movement, it rested against the spacer plate and did not bear directly on the specimen. The specimen was held in place by a block that was positioned flush to the column specimen and then bolted to the spacer plate. At the bottom a similar bracing system as the composite test was used (Figure 3.13).

The column rotated about the bottom spherical head, with a horizontal displacement of 3-4 mm at the top of the specimen. The column returned to the original alignment when the column load was again increased. This was a common observation made of all bare steel tests in which the spherical head

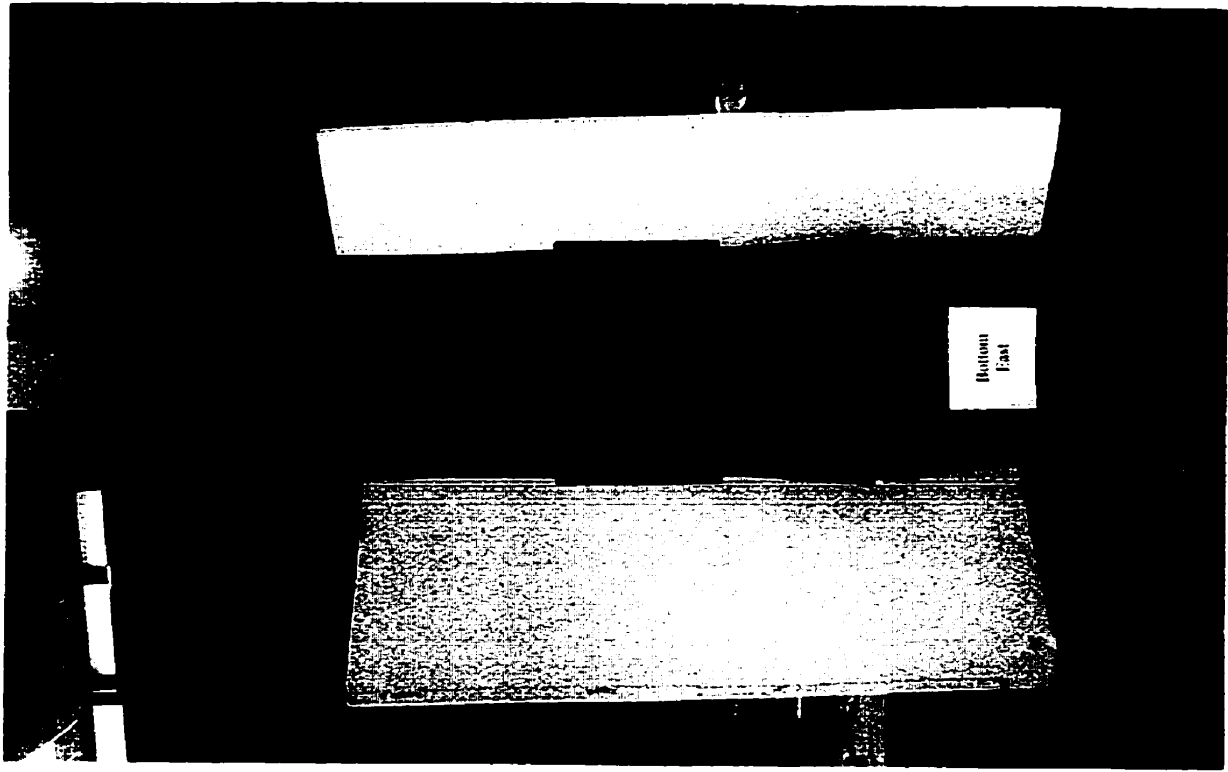


Figure 4.41: Typical Buckling Pattern - East View

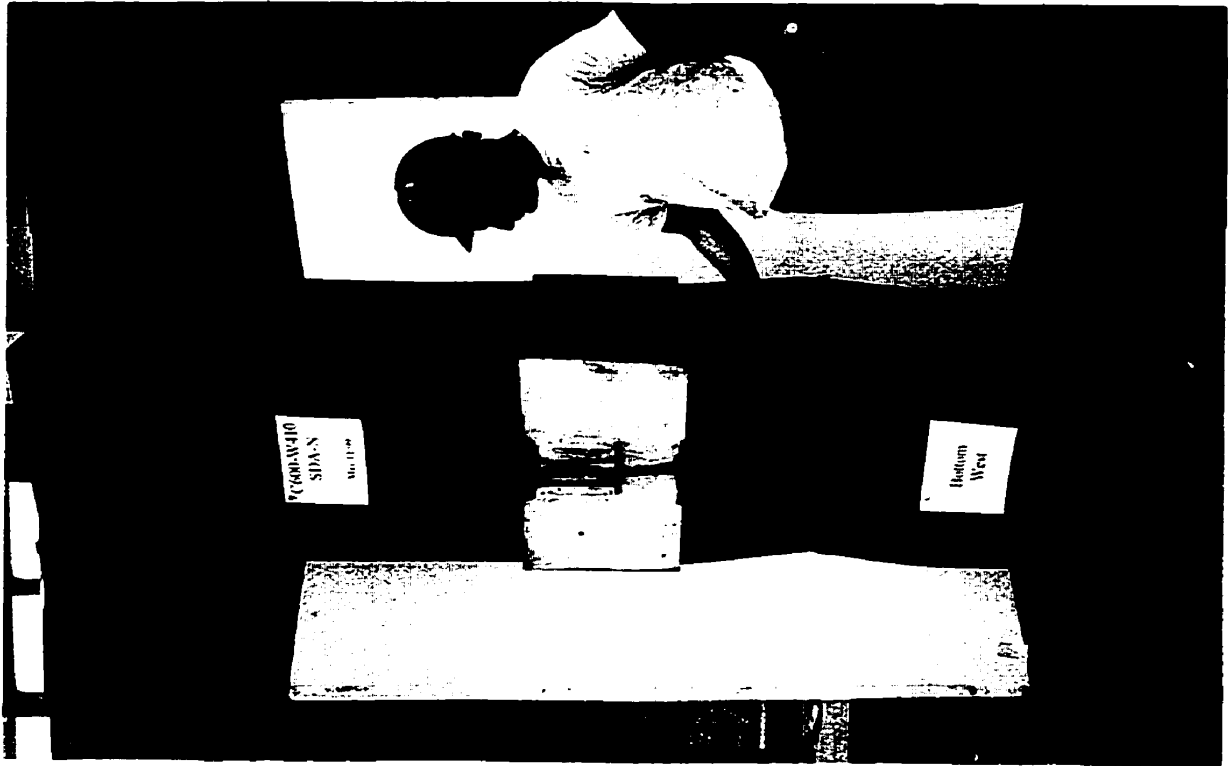


Figure 4.40: Typical Buckling Pattern of Non-Composite Specimen

was used at the bottom. The spherical head was not used for C600-W410-SDA-N and this lateral movement was not observed.

For the larger 600 x 600 mm column the connection plate (600 x 410 x 9.53 mm) noticeably distorted from pretensioning the bolts. As a result of the welding the framing legs were slightly skew to the plate. During bolt pretensioning the cleat angles were forced together, introducing a moment that deformed the plate. Prior to testing the connection plate was 2 mm offline, at centre.

An ANSYS finite element model was developed to help determine the probable buckling pattern (to aid in placing strain gauge locations) and whether yielding could be anticipated under the load combination. The preliminary model indicated that yielding could be expected at the connection weld line, being most likely for the TAB connection. After the C450-W410-TAB-N test there was no evidence of yielding in the connection end plate, nor in any of the non-composite tests.

4.5.2 Non-Composite Results

The instrumentation was designed to monitor both the advancement of buckling in the column flanges, and the response of the connection under the combined loading. As with the composite tests LVDTs were in place to measure the beam flange movement from the original column face, and the vertical displacement of the beam end. In the C450 tests the beam end rotated, as did the connection plate, with the bottom beam flange moving towards and the top flange moving away from the face. The centre of rotation was near the centre of the connection end plate for the C450 tests. This was not true for the C600 test. As the connection was loaded the bottom flange originally moved towards the column face but as the load reached 130 kN - 150 kN the bolts gradually slipped and the entire beam moved away from the column face. This is apparent from the plot of flange displacement versus connection load shown in Figure 4.42, where both flanges are moving away at the same rate. Under a load of 320 kN the top flange had moved 3.8 mm from the original column face and the bottom flange 2 mm away.

There was no abnormal or unexpected response of the connection system that might prove to be a concern for designers in detailing the connection for the construction gravity loads. The major interest in the non-composite test was the evaluation of the connection load on the bare steel column performance. It was important to determine the maximum axial load the column could withstand while subject to the connection load, and to compare that to results from the concentric compression tests¹.

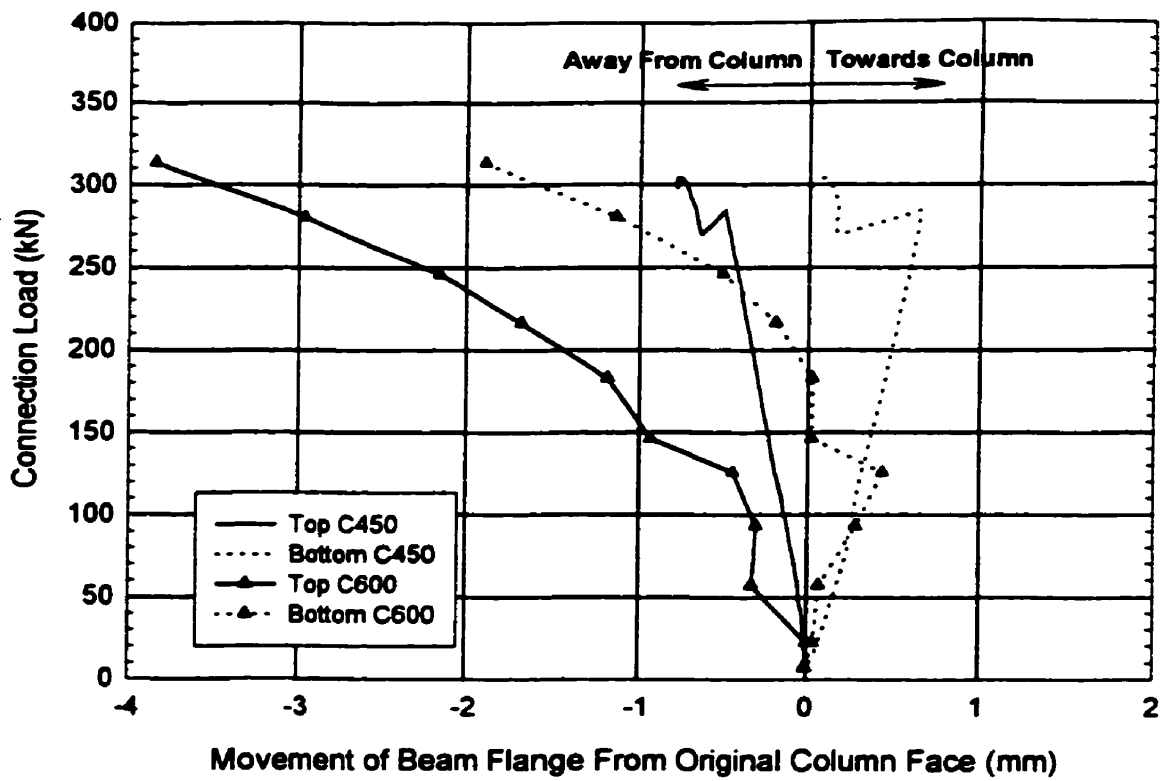


Fig. 4.42: Non-Composite: Connection Load Vs. Beam Flange Movement From Column Face

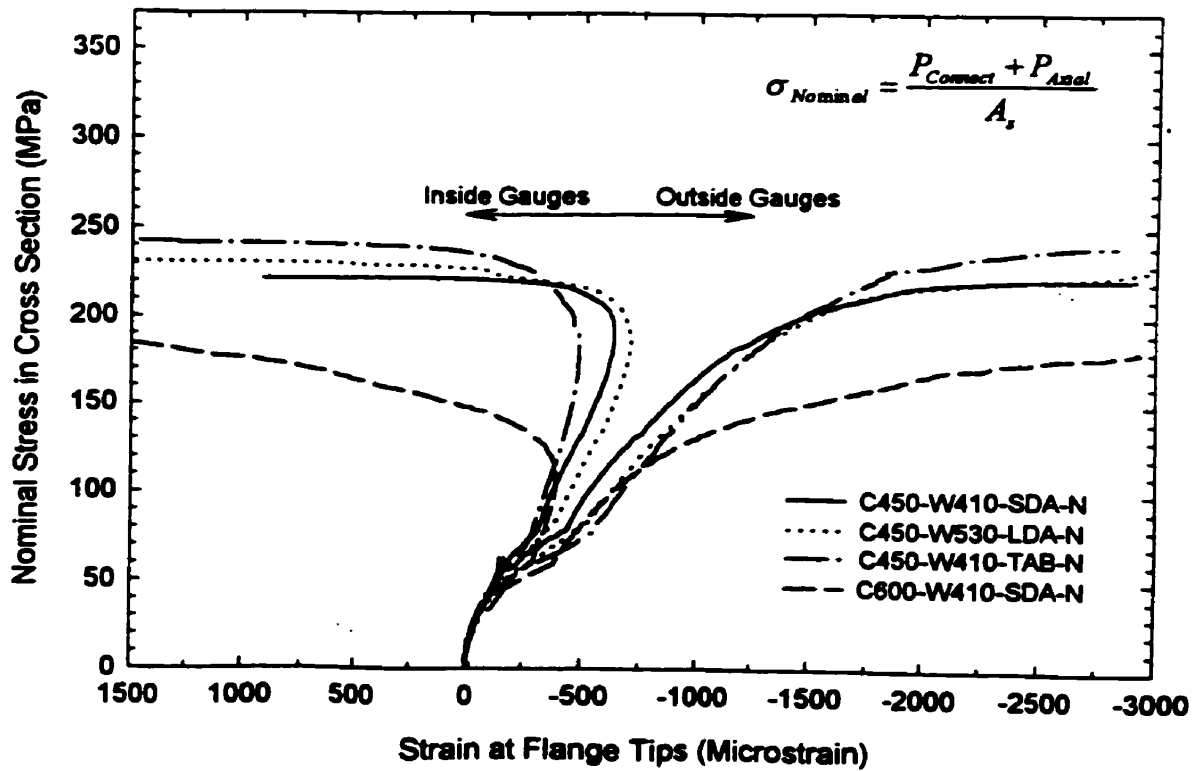


Fig. 4.43: Nominal Stress in Column Cross Section vs. Strain in Flange Tips

To monitor the progression of buckling in the column flanges, strain gauges were placed at the column flange tips, 0.5 D below the connection plate. This was the mid-point between the supports provided by the stirrups and the plate, and where lateral deformation would be most critical. With gauges placed at these locations and on opposite sides of the flange, progression of the buckling could be monitored. Figure 4.43 shows the plot of nominal stress in the cross section versus the strain recorded in gauges located on opposite sides of the south flange. The nominal stress is calculated as:

$$\sigma_{Nominal} = \frac{P_{Connect} + P_{Axial}}{A_s} \quad (\text{Eqn. 4.7})$$

Deviation in the linear response is first observed in the 450 x 450 mm specimens at a nominal stress of approximately 185 MPa, with a maximum stress of 220 MPa. The higher stress observed in the C450-W410-TAB-N test can be attributed to the lower connection load, as discussed in the previous section (connection load dropped from 300 kN to 222 kN). For test C600-W410-SDA-N local buckling was observed at approximately 100 MPa. Unlike the C450 non-composite specimens there is considerable post buckling strength, as indicated by the increasing nominal stress after the clear buckle formation. This is because the spherical head was not used for the C600 test as it was for the other tests. With the spherical head the column base is free to rotate as a buckle forms. Without the spherical head the load is redistributed to the east flanges upon formation of the buckle in the western flanges. Because of the restraint of the column end, there is considerable post-buckling strength in the larger column.

4.5.3 Non-Composite Test Summary

The results of this study have been superimposed with the previous concentric test results¹ in Figure 4.44. The column parameter, λ_p , has been defined in Equation 2.14, where the k factor refers to the plate stability coefficient, which can be calculated from Equation 2.5:

$$k = \frac{12(1-\nu^2)(b/t)^2}{\pi^2 E} F_\sigma \quad (\text{Eqn. 4.8})$$

As part of the Ecole Polytechnique research into the bare column behaviour they have developed equations for F_σ based on the 2 observed buckling shapes in of the columns under concentric loading. The column flanges buckled generally buckled over a span, S, or over 2S. In the tests reported herein, the buckled length was over S only. Thus F_σ can be taken as¹:

$$F_\sigma = \frac{S}{bt} \left(\frac{3}{2\pi^2 + 6} \right) \left[2\pi^2 \left(\frac{Et^3}{12(1-\nu^2)} \right) \left(\frac{\pi^2 b}{3S^3} + \frac{(5-4\nu)}{2bs} + \frac{b}{s^3} + \frac{s}{16b^3} \right) + \frac{\pi^4 EI_y}{2bS^2} \right] \quad (\text{Eqn. 4.9})$$

Table 4.4 contains a summary of the variables used to determine the column parameter λ_p .

The test results in Figure 4.44 have been plotted against the ultimate loads predicted by CAN/CSA S136 – Design of Cold Formed Steel Structural Members²³. The predicted resistance is based on concentric loading, and $\phi = 1.0$. As discussed in Chapter 2, the resistance is based on the capacities of each of the comprising elements, with local buckling accounted for by a reduced cross sectional area. The capacity is based on section properties only and does not consider the influence of the regularly spaced tension stirrups. A summary of the calculations used in calculating the predicted capacity of the columns included in this study is given in Table 4.5.

Table 4-4: Summary of Column Parameters

Column	S (mm)	b (mm)	I_y ($\times 10^3 \text{mm}^4$)	F_{cr} (MPa)	k	λ_p
450 x 450 x 9.53	450	220	16.3	328.9	1.01	1.06
	450	220	16.3	328.9	1.01	1.06
600 x 600 x 9.53	600	295	21.64	184.5	1.01	1.41

Table 4-5: Summary of Design Variables - S136

Column	L (mm)	F_u (MPa)	Flange		Web		A_e (mm^2)	$C_{\text{Predicted,S136}}$ ($\phi=1.0$) (kN)	C_{Test} (kN)
			k_2	b_e (mm)	k_2	w_e (mm)			
C450-W410-SDA-N	2358	360.4	0.43	121.5	4	331	7786	2806	2936
C450-W530-LDA-N	2238	361.3	0.43	121.5	4	331	7786	2813	2823
C600-W410-SDA-N	2810	362	0.43	123.9	4	355	8106	2934	3370

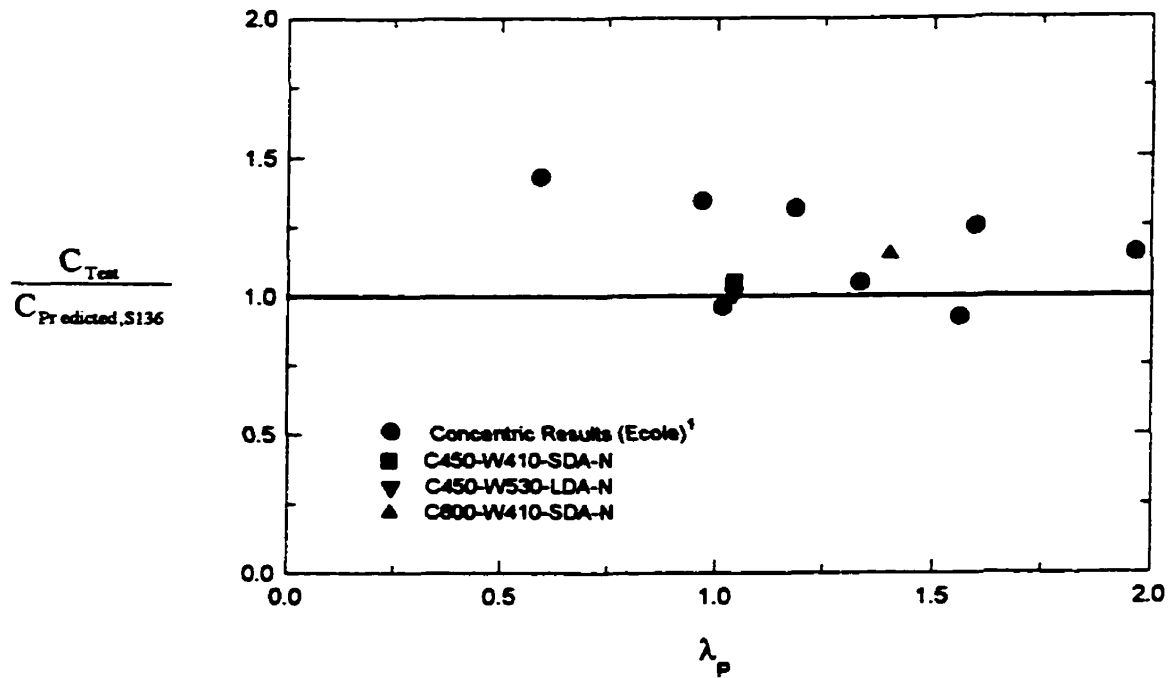


Figure 4.44 : Summary of Non-Composite Test Results

4.6 Effects of Increasing Column Loads

In an attempt to introduce failure in the column, the axial load was increased following the testing of the second connection on each of the C450 column specimens. Generally, the second test had the higher expected load and the connection could either not be brought to complete failure, or the test was terminated with the connection still having reserve strength. Thus as the axial load was increased to the limits of the Fox Jack, a considerable connection load could be maintained. Tests where the column load was increased include: C450-W410-LDA-C, C450-W530-TAB-C, C450-W530-LDA-C and C450-Seat2-Anch.

Several of the specimens had concrete failures on the east side of the specimen (opposite of the loaded connection), and above the beam level. In test C450-W530-LDA the concrete spalling was noticed at an applied column load of 6631 kN, this was associated with a reduction in the concrete strain readings in that quadrant, and the simultaneous increase in steel strains throughout the column height. The test was terminated when the column load reached 6750 kN ($V_{app} = 650$ kN). As can be seen from the individual plots contained in Appendix D there was yielding at the strain gauges, located 50 mm below the connection plate. The total applied load ($P_{Applied} + V_{connect}$) equalled 7400 kN, compared to the pure squash load of 10750 kN calculated from the material properties. The photo of the failure is given in Figure 4.45. It appears as if the failure initiated at the top of the

column and ended along the first tension stirrup from the top. This was typical of the failure pattern also observed in C450-Seat2, but failure was more catastrophic and located on both sides of the column web.

Although there was no concrete failure C450-W530-TAB-C was loaded axially to 6806 kN, with a 720 kN connection load. Even though the concrete remained intact the steel strains were in excess of yield. The steel gauges located 50 mm below the connection end plate registered strains in excess of the yield strain. The complete strain gauge data is given in Appendix D for each composite test.

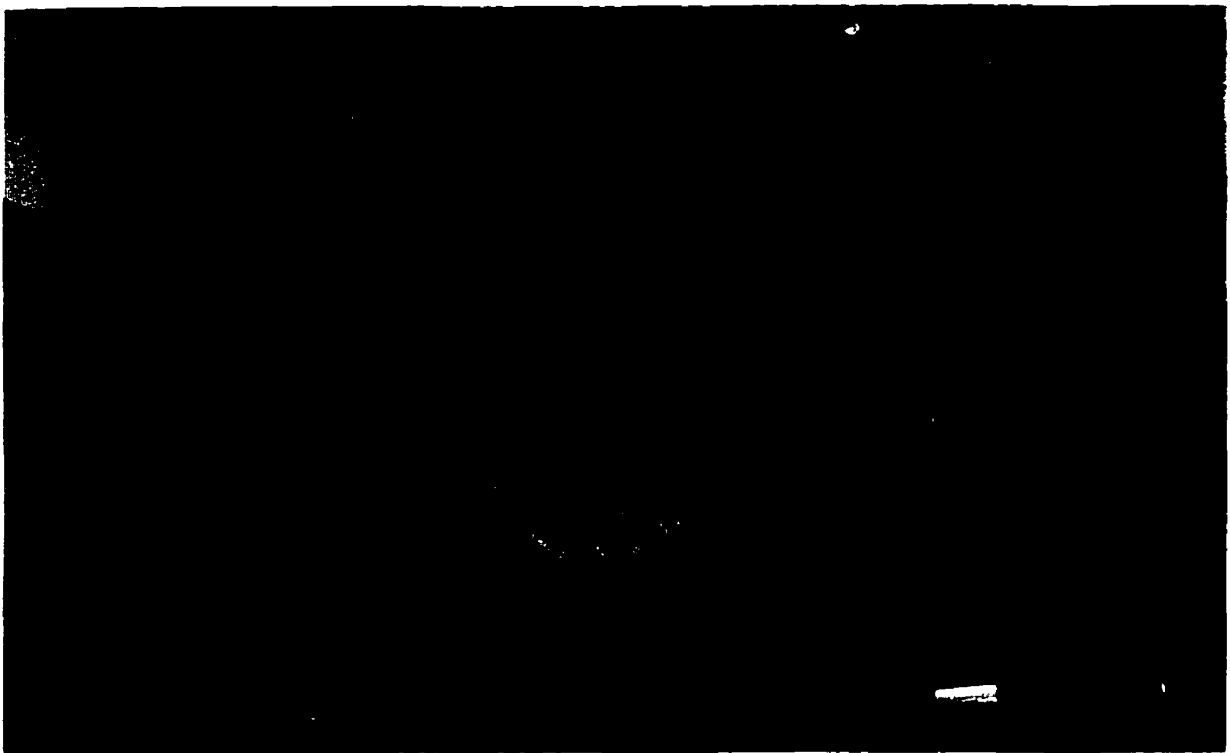


Figure 4.45: Failure Initiated in Specimen C450-W530-LDA-C: $P_{axial} = 6750$ kN; $V_{applied} = 650$ kN

5 Discussion of Results

5.1 Connection Statics – Influence of Beam Restraint

Although it is difficult to quantify the stiffening effects of a concrete slab, and the effects on increasing the rotational stiffness of the connection, it can be assumed that the restraint provided in this experiment is far less than that provided by an actual slab. The restraint provides a lower bound on the problem, and is effective in making the testing program a better reflection of reality. The bracing system used to restrain the longitudinal movement of the load beam has been shown to increase the effective hogging moment at the column face, reduce the rotation of the beam end, and reduce the separation of the beam flange from the original column face. The direct comparison of the test results presented in Section 4.4.3.3 show that although the movement of the beam flange from the column face is reduced, the final separation between the connection end plate, δ_{plate} , remains relatively unchanged. This suggests that the moment at the connection weld line, $M_{Connect}$, is only marginally affected by the presence of the beam restraint, although the total moment at the column face is significantly increased.

The moment developed at the column face, as presented in Chapter 4, was calculated in accordance with the free body diagram of Figure 4.28, and Equation 4.5. This moment is actually the superposition of the moment at the weld line, $M_{Connect}$ and the moment couple from the restraint force.

$$M_{Face} = M_{Connect} + Sj \quad (\text{Eqn. 5.1})$$

Strain gauges were installed on the threaded rods of the restraint system to measure the force, S . The measured force was generally dependant upon the rotation of the beam end, and the tendency of the connection to rotate. The W410 test beam specimens registered higher restraint forces than the W530 beam connection tests due to the higher beam end rotation associated with the lighter beam. As the connection/connection plate yielded, the separation between the beam flange and the column face increased, as did the restraint force, S .

The actual moment developed by the restraint system depends on the moment arm j . As previously mentioned, as the connection and connection plate deformed it rotated near the base of the connection. Thus the moment arm, j can be taken as:

$$j = d_{Connect} + a + 37mm \quad (\text{Eqn 5.2})$$

The variable, a , is the distance between the top of the connection and the top of the beam. For all tests, excluding the two seat connections, $a = 45$ mm. Based on the calculated value of j , an approximation of the restraint moment can be made. These moments have been summarised for all restrained tests in the W410 and W530 beam series, in Figures 5.1 and 5.2.

A summary of the calculated values of j are provided in Table 5.1. The slopes of the M_{Face} - V plots, given for each of the composite specimens in Chapter 4, have also been included. These are a repeat of the values listed in Table 4.3 and are the slope of the curve in the linear portion of the curve, prior to advanced yielding of the connection. The estimated value of the slope of the $M_{Connect}$ - V curve is also given ($M_{Connect}$ is the moment at the weld line). These have been calculated using Equation 5.1, and the restraint moment given in Figures 5.1 and 5.2.

Table 5-1: Summary of Connection Eccentricities

Specimen	No. of Bolts	$d_{connect}$	e_{bolt}	J	$\frac{\Delta M_{Face}}{\Delta V}$	$\frac{\Delta M_{Connect}}{\Delta V}$
	N	(mm)	(mm)	(mm)	(mm)	(mm)
C450-W410-SDA-C	3	190	40	272	41	-
C450-W410-LDA-C	3	250	40	332	21	-
C450-W410-TAB-C	4	310	75	392	78	36
C450-W530-SDA-C	4	265	40	347	121	89
C450-W530-LDA-C	4	325	40	402	69	48
C450-W530-TAB-C	6	445	75	527	86	58
C450-Seat1-NoAnc	-	200	-	247	58	43
C450-Seat2-Anc	-	200	-	247	94	75
C600-W410-SDA-C	3	190	40	272	106	58
C600-W410-LDA-C	3	250	40	332	123	88

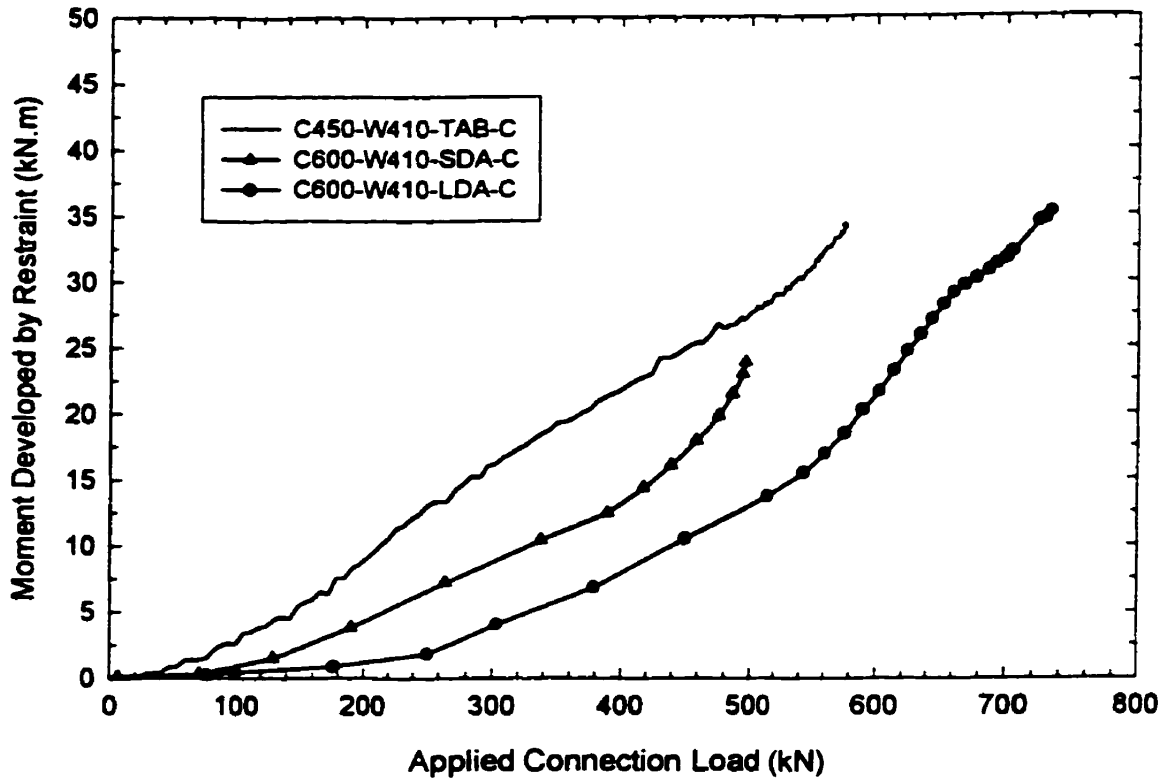


Fig. 5.1: W410 Test Series: Moment Developed by Beam Restraint, S_j , vs. Applied Connection Load

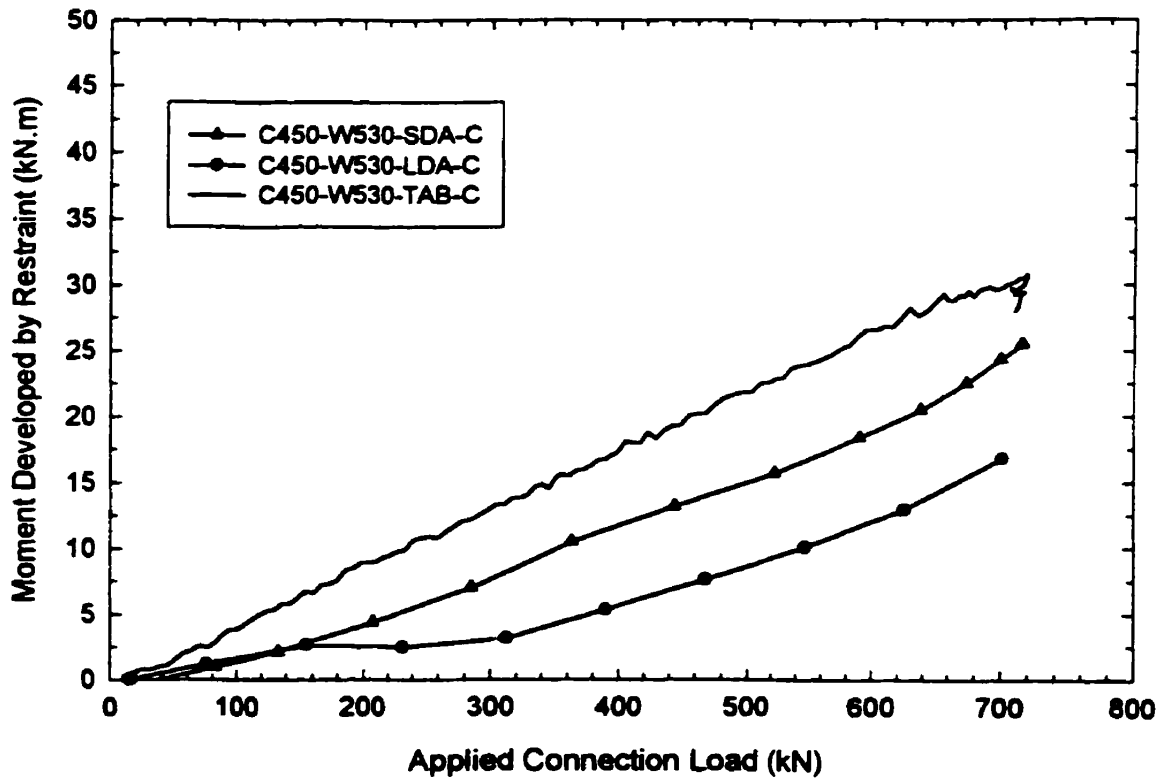


Fig. 5.2: W530 Test Series: Moment Developed by Beam Restraint, S_j , vs. Applied Connection Load

5.2 Evaluation of Original Test Variables

The four primary test variables, as indicated in the test matrix of Table 3.6, were the column size, the connection type, the beam depth and the use of shear studs. In the following sections these parameters will be discussed with reference to the two major objectives of the study: the examination of the connection behaviour under an applied load, and secondly, the investigation of the force transfer mechanism between the steel and the concrete.

5.2.1 Connection Type

In the original test matrix, there were 3 different connection types, the single plate shear tab, the double angle framing connection, and the seat connection. To investigate the role of the connection depth on the overall performance, the bothole spacing was also varied for the double angle connection type.

All composite connections failed at loads in excess of their predicted ultimate, but there was yielding observed in several of the connections within the factored design load range. There was also considerable rotational flexibility observed in the composite beam column connections. The rotational flexibility was largely due to the deformation ability of the connection end plate. As a result the inflection point generally fell between the bolt line and the column face. The connection type was shown to have an influence on the rotational stiffness. The double angle connections appeared to develop lower moments compared to the shear tab connections. All double angle connections consisted of 75 x 75 x 6.4 mm angles, with the outstanding leg welded to the plate. As the connection was loaded the angles deformed away from the plate, as illustrated in Figure 4.7. The shear tabs did not have this deformation capacity, resulting in an increased separation between the cross plate and the concrete face.

The rotational flexibility at the face was the result of the ability of the relatively thin plate to pull away from the concrete face, as the connection was loaded. This was characterized by the formation of a general yield line failure pattern in the connection end plate. Based on test observations, the yield lines tended to form at or near the base of the connection, as this was the centre of in-plane rotation. A sagging yield line then extended from the bottom corners of the connection, to the top of the connection plate at the column flanges. The formation of the yield line pattern was not caused by the shear force at the face, but rather the moment at the weld line, M_{connect} . Since the rotation was centered at the base, the connection length has an important influence in the development of this yield line pattern. Although M_y was influenced by the depth of the connection, the advancement of yielding was limited by the rotation of the beam.

The yield line failure of the connection is not major concern when assessing the performance, as an elastic response is not essential for the effectiveness of the proposed connection. Unlike HSS where localized yielding of the column face may limit the axial capacity of the column, the yielding of the end plate should not adversely affect the column strength. This was confirmed with the test results.

The connection type was also shown to have an influence on the force transfer from the steel to the concrete. As can be seen Figure 3.36 and 3.37 the connection length has a pronounced effect on the steel strain just below the connection plate. Longer connections will transfer the loads over a greater length, and result in a more uniform stress gradient just below the connection. Considering the C450-W530 results, at an applied connection load of 500 kN, the steel strain 50 mm below the connection is 18% higher for the SDA ($L = 250$ mm) compared to the longer TAB connection ($L = 445$ mm). For the W410 beam series, there is a 70% difference in the strain 50 mm below the connection plate between the SDA ($L = 190$ mm) and the TAB connection ($L = 295$ mm).

This indicates that the length of the connection has a pronounced role in the force transfer, with the longer connections outperforming the shorter connections. Although the relative differences are substantial, the actual values are quite small. Even for the W450-W410 test group the difference in the change in strain, due to a 500 kN connection load, is less than 150 microstrain. Although the influence of the connection type is of academic interest, in reality the connection type will have small influence on the transfer of forces, for the range of test variables included in this study.

5.2.2 Depth of Exterior End Plate

The connection plate depth corresponds to the nominal beam size framing into the weak axis of the column. Thus a longer connection plate will generally correspond to a higher range of design loads. But for a given load, a deeper plate should have two effects; it could potentially enhance the force transfer from steel into concrete by providing a longer path, and secondly, it should improve the load-deformation response of the connection plate. For the latter, it appears that the load deformation response of the composite connection is influenced more by the depth of the connection, than the depth of the connection end plate.

For connections of similar characteristics the increase in strain in the column flange, just below the connection end plate, should be less for the longer connection plate. Figure 5.3 shows the change in strain 50 mm below the connection plate for the three tests C450-W410-LDA, C600-W410-LDA, and C450-530-SDA-C. These three specimens consist of consist of 76 x 76 x 6.35 double angles, with lengths of 250, 250, and 265 mm respectively. It appears that the depth of the connection plate

has minimal effect on the strain distribution. This is contrary to the effects of the connection length on strain distribution. This suggests that if the plate is considerably deeper than the connection, the bottom portion of the plate is ineffective in distributing the shear force.

The connection plate depth may be more important when considering the stability of the non-composite columns. As shown in Figure 4.43, the tests results indicate that the connection depth has minimal effect on the overall column strength. But it must be remembered that the connection load was slightly higher for the W530 load beam, compared to the W410 load beam. The higher load represented the construction loads for the girder, rather than the beam framing into the weak axis. The higher connection loads would minimize any positive effects of the increased plate depth.

5.2.3 Column Size

The influence if the column size is most important when considering the steel only state, which was thoroughly discussed in Chapter 4. In the composite state, a SDA and LDA connection type was tested for both a C450 and C600 column size. Although there were differences discussed in Chapter 4 the column size, specifically W, has a minor role in the overall behaviour of the composite connection. It is difficult to directly compare the data because the test performed on the smaller column, C450, did not have the restraint in place, whereas the C600 test did.

5.2.4 Presence of Shear Studs

The shear studs were shown to enhance the force transfer between the steel and the concrete, and to stiffen the deformation response of the connection plate. Results presented in Figure 4.38 indicate a considerable improvement in the transfer of load from the steel into the concrete. At strain gauges located just beneath the loaded connection (50 mm below the west plate) the strain measured in the column flange was 35% lower with the addition of the shear studs. Remembering the general economy of connection design, although beneficial, the use of shear studs has not been shown to be necessary for satisfactory connection performance.

Although, not observed in the anchored seat connection test, there is a possibility of the shear studs causing a failure in the concrete. There are three possible failure modes, a bearing failure of the concrete, a shear failure of the shear studs and a pullout failure of the studs due to the moment developed at the column face. The first two failure modes are related to the shear transfer of the beam loads into the column. If the studs are positioned near the connection, their relatively stiff support would cause the force to flow through the stirrups into the concrete, as opposed to being gradually transferred through the connection plate edge welds. The actual load distribution is.

dependant upon the bearing stiffness of the studs in the concrete, but the shear stud pattern should be designed to resist the entire gravity load introduced at the connection.

Considering the four stud pattern of Figure 3.7, the factored shear resistance of the shear studs can be calculated using the CAN/CSA S16.1 provisions². The shear resistance of the stud (i.e.; Full Slab) can be taken as the lesser of:

$$1) \quad 0.5\phi_{sc} A_{sc} \sqrt{f'_c E_c} \quad (\text{Eqn. 5.3})$$

$$2) \quad 415\phi_{sc} A_{sc} \quad (\text{Eqn. 5.4})$$

$$3) \quad 0.6\phi_s A_{sc} f_{y,stud} \quad (\text{Eqn. 5.5})$$

The shear resistance of a single 19.05 mm (3/4") diameter shear stud used in the seat connection was 94 kN. The total factored resistance of the group would be 376 kN. In the test C450-Seat2-Anch the connection was loaded to 756 kN, without obvious distress in the shear studs. As the connection was loaded, there was a shear deformation of the studs/concrete and the load was distributed to the column flanges. This was reflected in the strain data from the column flanges just below the connection plate (Note Figure 4.38).

For simple connections that develop higher moments at the face, such as shear tabs, there is a possibility of the headed shear stud pulling out of the concrete. From Astaneh's results⁹ on shear tab tests to a stiff column flange; there was a moment of about 70 kN m developed at the weld line for a five bolt shear tab, at a connection load of 500 kN. Using the stud spacing in Figure 3.7 the force in each stud would equal 157 kN.

The pullout capacity of a headed shear stud may be calculated as³⁵:

$$f_{pullout} = 0.3A_{pull}\phi_c \sqrt{f'_c} \quad (\text{Eqn. 5.6})$$

Where the area of the pullout is based on the effective pyramid concept and equals:

$$A_{pull} = \pi \frac{l^2}{\cos 45^\circ} \quad (\text{Eqn. 5.7})$$

For the 120 mm long, 19 mm diameter shear studs used in this experimental program, with a concrete strength of 30 MPa, the pullout strength of each stud is 105 kN ($\phi = 1.0$). This shows that if a simple framing connection is to have shear studs placed on the connection plate, or in the vicinity of the connection plate, then the designer must be conscious of the pullout forces that could potentially develop in the shear studs.

5.3 Tension Stirrups

There has been considerable discussion regarding the effectiveness of the regularly spaced tension ties between column flange tips, as shown in Figure 1.2. Their primary role is preventing local buckling in the construction stages, but their role in the enhancement of the composite connection is yet to be discussed. There are two immediate issues, the effects of the stirrups in preventing and outward buckling of the column flange, due to the superimposed connection and axial loads, and the role of the stirrups in provided a path for the transfer of the forces from the steel into the concrete.

To evaluate the effectiveness in preventing outward buckling of the flanges the stirrups were instrumented with strain gauges placed at the midpoint, on specimens C450-W410-SDA-C and C450-W410-LDA-C. Gauges were placed on both the east and west stirrups (connection loaded on west side) below the connection. The results from the test C450-W410-LDA-C are included in Figure 5.4. Following the connection test, the connection load was reduced (reserve strength in connection) and the column load increased to 6100 kN. Under the combined loading the stirrups developed a minor tensile force, and there was no evidence of outward buckling of the column flanges.

The stirrups also act as a method of force transfer between the steel and the concrete. It can be considered analogous to a shear stud that is welded to the column flange. From the test results it is difficult to ascertain the role of the stirrup in the transfer of forces. Although the gauges reported in Figure 4.36 to 4.39 are located both above and below the stirrups, there is generally good compatibility between the concrete and steel at a distance D above or below the connection plate (stirrup locations). It is unclear if this is due to the tension stirrup itself or the flow of forces over the depth due to the bond between the steel and the concrete.

Although the stirrups will be regularly spaced, their locations will not be referenced to the storey elevations. Thus it is possible that there would be stirrups located just above and below the connection plate. It is suggested that in subsequent studies it might be suggested to investigate these possible failure modes involving a stirrup welded adjacent to the connection. It is possible that the presence of a stirrup in the connection region may lead to two possible failures; where the stirrup or welds fail in shear, or secondly, a bearing related failure in the concrete.

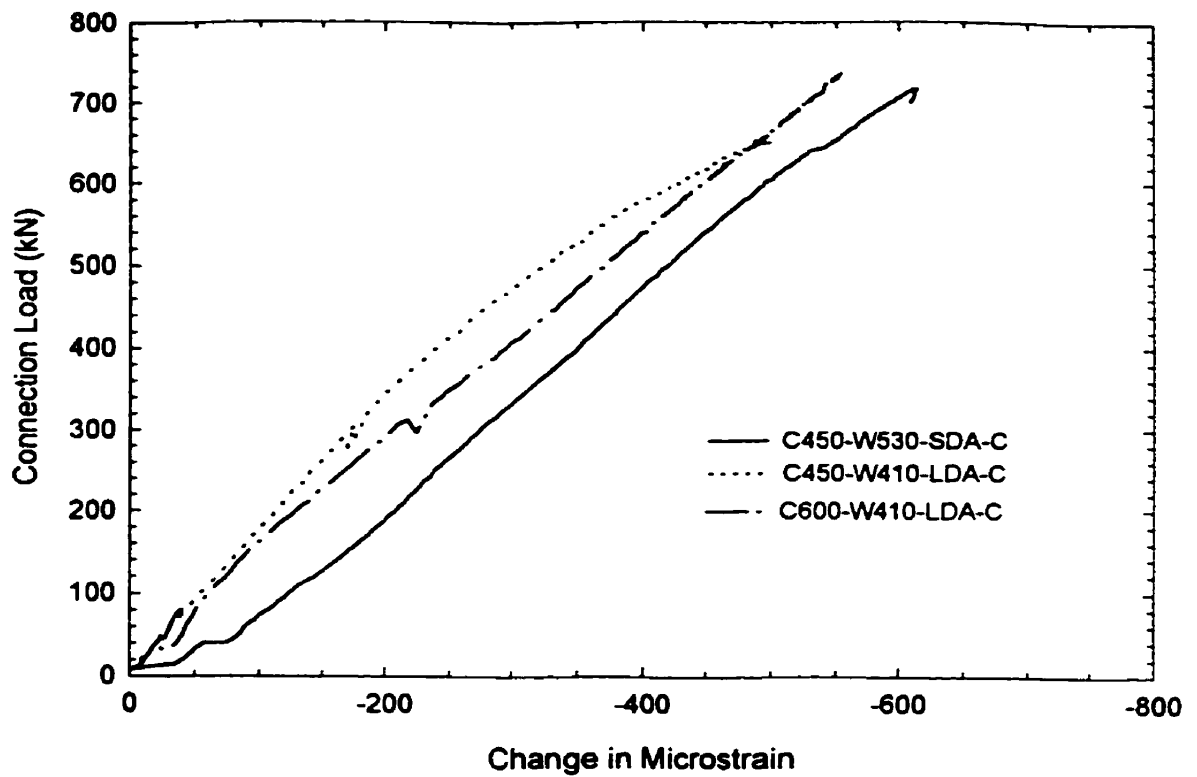


Fig. 5.3: Applied Connection Load vs. Change in Steel Strain in Column Flange (-50 mm) for Various End Plate Depths

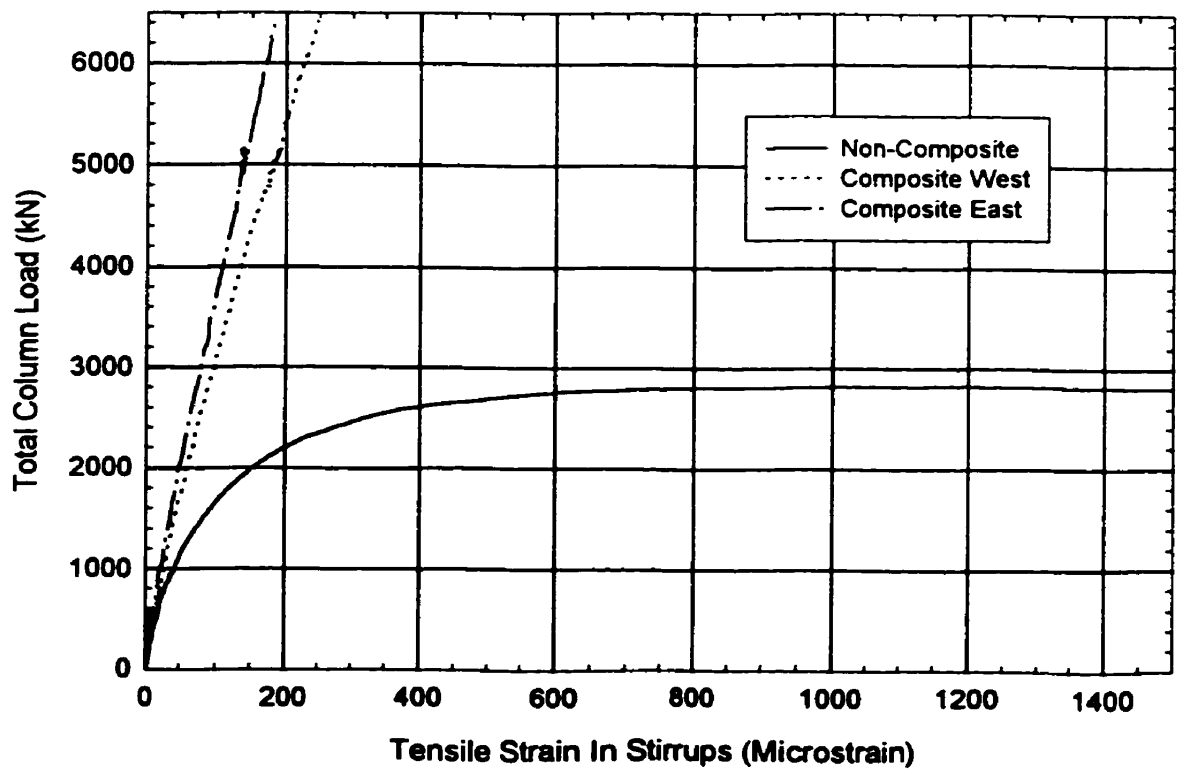


Fig. 5.4: Total Column Load vs. Tensile Strain in Stirrups 0.5D Below Connection Plate

5.4 Use of Exterior Columns

In gravity frames the majority the columns will be loaded on four sides, negating the moments that result from the one-sided connection loads. There are exceptions such as exterior columns or in cases of pattern loading. Although the moment at the column face is generally quite small, with the geometric offset of $D/2$ a significant moment at the column centreline results. If you consider several stories where the column is unsymmetrically loaded along the weak axis, there is potential for a cumulating moment in the column. This moment cannot necessarily neglected in design. This is especially true in the column type included in this study, which has an especially low resistance to weak axis bending.

Although there have been eccentric tests³⁶ on the columns with an eccentricity of 25 mm, the eccentricity was based on loading jack limits. Thus it is important to consider what could be a typical range of eccentricity for an exterior column. Using the design loads and column spacing summarised in Chapter 3, a typical eccentricity can be calculated based on the connection eccentricities determined in this experimental program. Using the same 36 storey gravity frame of Appendix A, a 14 m x 8 m column spacing will be assumed. The girder will be framing into the weak axis, on one side of the column, with the beam loads framing into the connection on both sides, along the strong axis. A schematic of the proposed layout is contained in Figure 5.5.

A series of floor heights will be considered for the column sizes included in this study. The framing loads from the beams will be considered concentric, with the only eccentric loading being that of the girder framing into the weak axis. Respecting the Live Load reduction factor for tributary areas in excess of 20 m² as outlined by the National Building Code of Canada³⁷, the live load at each floor level will be reduced by 50%.

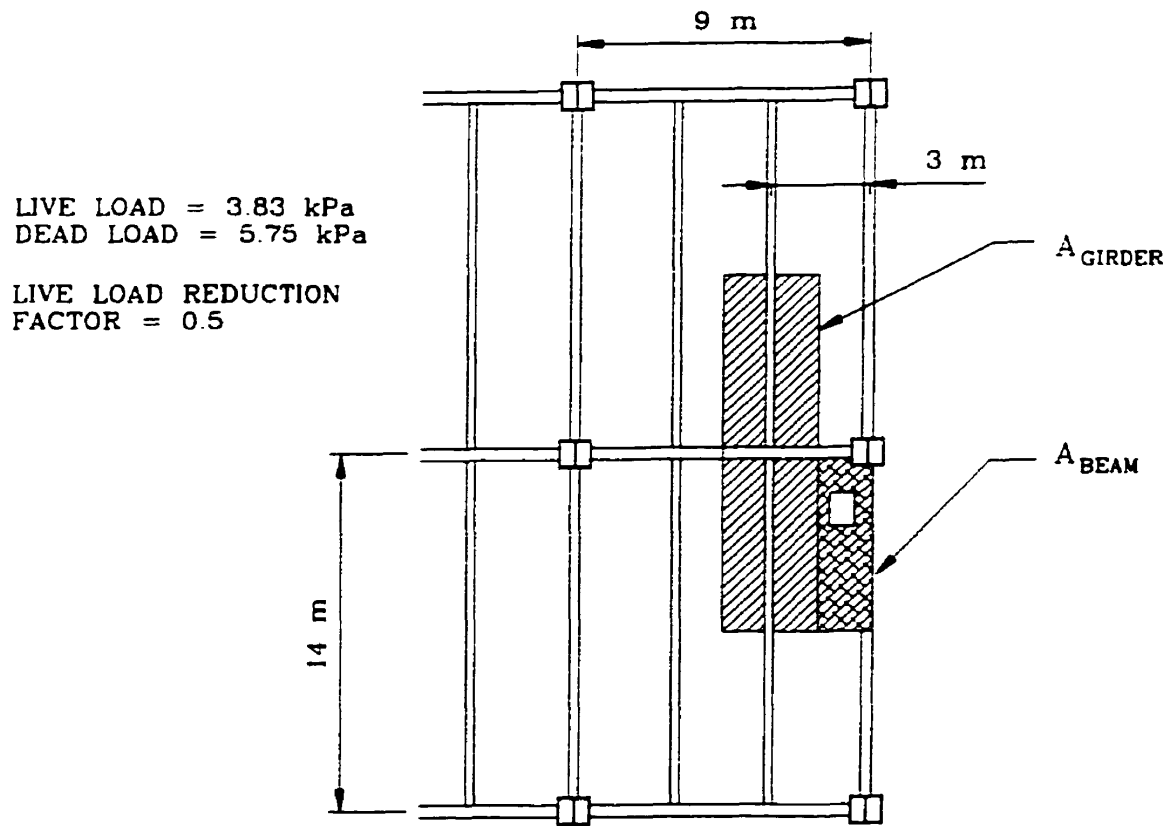


Figure 5.5 : Exterior Column Layout

With a full dead load factor of 1.25 along with a live load factor of 1.5 the framing loads are:

$$Girder\ Load = 1.25(3 \times 14 \times 5.75) + 1.5 \times 0.5(3 \times 14 \times 3.83) = 422\text{ kN} \quad (\text{Eqn. 5.9})$$

$$Beam\ Load = 1.25(1.5 \times 7 \times 5.75) + 1.5 \times 0.5(1.5 \times 7 \times 3.83) = 106\text{ kN} \quad (\text{Eqn. 5.10})$$

In this calculation the minimal composite column size has been taken as 300 x 300 mm, and it is assumed that same column size will be used for up to 3 storeys. The top floors would be framed with steel columns, and the axial load will be concentric. At each storey a total load of 634 kN will be introduced, with a moment caused by the girder load. The eccentricity has been taken as $D/2 + 60$ mm to reflect results from this testing. Table 5.3 summarises the calculation.

Table 5-2: Summary of Column Eccentricity: Exterior Column

Column Size	Beam (kN)	Girder (kN)	Axial Load(kN)	e_{load} (m)	M (kNm)	M_{total} (kNm)	e_{axial} (mm)
300 x 300	212	422	2500	0.21	88.62	0	28
			3134	0.21	88.62		
	212	422	3768			177.24	47
450 x 450	212	422	4402	0.285	120.27	297.51	68
	212	422	5036	0.285	120.27	417.78	83
	212	422		0.285	120.27		
	212	422	5670	0.285	120.27	538.05	95
	212	422	6304			658.32	104
600 x 600	212	422	6938	0.36	151.92	810.24	117
	212	422	7572	0.36	151.92	962.16	127

Although the maximum eccentricity is less than $D/4$ it does exceed the eccentricity that has been tested to date. More importantly in the “worse case scenario” the eccentricity lies outside the Kern point, indicating that a tension stress in concrete is indeed possible. Further experimental validation of the column under bending should be performed to validate the potential use of the columns in perimeter frames.

6 Conclusions and Recommendations

6.1 Review of Scope of Work

This report summarises the University of Toronto's contribution to the collaborative research effort between Lehigh University, École Polytechnique, and Canam Steelworks in the experimental validation of a new composite gravity framing system. The innovation of the new system is the composite column, which consists of a built-up H section member partially encased in concrete. The scope of the University of Toronto's work has been the testing of several types of simple framing connections to the weak axis of the proposed column. In the new system the beam does not frame into the column web, but terminates at an end plate welded between the column flange tips. The plate is nominally the same depth of the beam, and there are no provisions for direct shear anchorage, other than the regularly spaced tension rods connecting the column flange tips.

This was intended as a pilot study, thus the objective was not to test a full range of design parameters, and develop refined design equations. Rather the goal was to develop a test program that reflected the reality of construction, and in-service conditions, and in doing so, determine if the connection system is indeed viable. The final test matrix agreed to by all involved parties, attempted to make the experimental program as realistic and complete as possible. All specimens were full scale, and were proportioned based on a typical frame design, provided by Canam.

A total of 14 tests were performed, in both the composite and non-composite state. The four bare steel tests were included to represent the conditions existing during construction. In the non-composite tests the connection was loaded to a typical construction load, and the column load increased until buckling failure occurred in the column flanges. This would indicate the number of storeys of steel framing that could be erected prior to casting of the concrete.

The 10 composite connection tests involved the same experimental set-up but with a slightly different loading arrangement. The columns were subjected to a nominal axial load of 1.0 Dead Load + 0.5 Live Load, while the connections were loaded to failure. This nominal axial load corresponded to approximately 50% of the ultimate squash load of the column. The major objectives of the composite connection tests were to investigate any failure that could be initiated in a column due to a locally introduced connection load, and to evaluate the force transfer from the steel into the concrete.

Other variables in the final test matrix included the connections types, beam size and the column size. Although all major types of simple connections were considered, the double angle, shear tab and seat connection were included. There was also two beam depths, a W410 beam size representing the case when a floor beam frames into the weak axis, and a heavier W530 beam, representing the girder framing into the column. Although the primary column size was 450 x 450 mm there were two 600 mm x 600 mm columns included to investigate the role of the column size on connection performance.

6.2 Major Conclusions

Of the 10 composite connection tests included in this study, six specimens were loaded to failure, defined by either rupture or excessive bolthole deformation in the connection. The remaining four connections had ultimate capacities in excess of the test frame capacity. Although these specimens could not be brought to failure, there was yielding observed in the test data, and limited permanent deformation visible in the connection and connection end plate.

In all cases where the specimens were loaded to failure, the loads were in excess of the calculated ultimate loads ($\phi=1.0$). For the SDA connections with their shorter bolt spacing, there was loss of proportionality in the load deformation response while still within in the factored load range (As defined in Table 3.2). The SDA bolt spacing of 60 and 65 mm, for the W410 and W530 beam sizes respectively, are shorter than that used in general practice, but still meet S16.1 minimum spacing of $3d_{\text{bolt}}$. With the more common bolthole spacing of 80-90 mm in the LDA connections there was no gross yielding of the connection within the factored design load range.

For all composite tests there was a general yield line failure pattern observed in the connection end plate, similar to that experienced in similar connections to HSS columns. Yielding of the connection end plate occurred at relatively low loads, but appeared to have minor effect on the column in the connection region. The extent of yielding was dependant upon the connection stiffness and was ultimately limited by the rotation of the beam. The additional rotational flexibility from the deformation of the outstanding legs of the double angle connections appeared to reduce the observed separation between the concrete and steel at the end plate. The TAB connection without this deformation ability caused a larger amount of separation at the column face. The ability of the double angles to deform will be reduced, with thicker connection angles. As with all double angle framing connections used in design, there should be an upper limit in angle thickness to allow for rotational flexibility at the beam column connection.

At a distance of $1.5D$ below the connection endplates there was a general state of strain compatibility observed between the steel and the concrete. The actual change in strain in the column from the connection load was actually quite small. At a connection load of 500 kN, there was a maximum change in strain of 420 microstrain in the column flanges, just below the connection. This value was dependant upon the depth of the connection, but the difference was less than 200 microstrain regardless of the connection type.

From these test results it can be concluded that for the design of the connection types included in this study, for the range in loads given in Table 3.2, no extra provisions are required for the simple framing connections to the weak column axis, through an exterior end plate. Standard practice for connection design to any flexible column support may be followed. The designer must take extra precautions if the loads are in excess of the range included in this study, or if design loads are beyond simple shear. This is specifically referring to an applied moment, or horizontal force resulting from lateral loads, or exterior bracing.

Although the connection load had minimal effect on column behaviour in the composite state, this was not true in the non-composite testing. In the testing of the steel connection the connection load had a pronounced effect on the axial load carrying capacity of the column. The connection load introduced at a single side of the column, created a stress gradient in the column and initiated buckling in the column flange, just under the loaded endplate, at total axial loads less than those experienced in the concentric tests. Deviation in the linear response is first observed in the 450 x 450 mm specimens at a nominal stress of approximately 185 MPa, with a maximum stress of 220 MPa. For test C600-W410-SDA-N local buckling was observed at approximately 100 MPa.

6.3 Recommendations for Further Study

The experimental program summarised in this report serves as a solid foundation for further work into the behaviour of the beam column connection made to the weak axis of a partially concrete encased WWF section. During the course of the research there were several issues that would warrant further experimental and analytical research. Potential research work could include, but not be limited to the following:

- 1) Finite Element Analysis of the non-composite column. Testing has been limited to b/t ratios of 23 and 31, with a stirrup spacing of D . Once a F.E. model has been developed and calibrated against these test a full parametric study could be performed and eventually modified to include a full cruciform loading situation.

- 2) At larger stirrup spacing, S , the non-composite column is susceptible to damage resulting from lateral impact. Impact of the column flange during construction is a definite possibility, and the response of the axially loaded column subjected to a variable load should be explored.
- 3) If the proposed columns are intended for exterior applications compression tests should be performed with the range of eccentricities proposed in section 5.4.
- 4) Testing should be performed to assess the influence of time factors (i.e.; creep, concrete shrinkage) on the force transfer mechanism at the connection.
- 5) Several simple framing connections to the column strong axis (in-line to web) should be performed to examine the force transfer from steel into concrete. Because the connection will not rotate as observed in the weak axis connection the direct transfer of forces to the concrete may not occur.

7 References

- [1] Tremblay, R., Massicotte, B., Filion, I., and Maranda, R., "Experimental Study on the Behaviour of Partially Encased Composite Columns Made With Light Welded H Steel Shapes Under Compressive Axial Loads", Proceedings of the Annual Technical Session, SSRC, Atlanta, Georgia, 1998, pp. 195-204.
- [2] CSA. 1994. **Limit States Design of Steel Structures, CAN/CSA-S16.1-94**. Canadian Standards Association, Rexdale, Ontario.
- [3] AISC. 1993. **Load and Resistance Factor Design Specification for Structural Steel Buildings**. American Institute of Steel Construction, Chicago, Illinois, U.S.A.
- [4] Viest, I.M., Colaco, J.P., Furlong, R.W., Griffis, L.G., Leon, R.T., and Wylie, L.A., "Composite Construction Design for Buildings", ASCE Press, N.Y., 1997, 460 pp.
- [5] Oehlers, D.J., and Bradford, M.A., "Composite Steel and Concrete Structural Members, Fundamental Behaviour", Pergamon, 1995.
- [6] Griffis, L.G., "Future Directions and Needs for Composite Construction", Proceedings of Structures Congress XIII, ASCE, Boston, 1995, pp. 1309-1312.
- [7] Astaneh, A., "Demand and Supply of Ductility in Steel Shear Connections", Journal of Construction Steel Research, V. 14 (1), 1989, pp. 1-19.
- [8] Sherman, D.R., and Ales, J.M., "The Design of Shear Tabs with Tubular Columns." AISC Proc. National Steel Construction Conference, 1991, pp. 23-1-23-14.
- [9] Astaneh, A, McMullin, K., and Call, S., "Behavior and Design of Steel Single Plate Shear Connections", AISC Engineering Journal., 1st Quarter 1989, pp. 21-32.
- [10] CISC. 1995. **Handbook of Steel Construction, 6th Edition**. Canadian Institute of Steel Construction, Willowdale, Ontario.
- [11] Sherman, D.R., "Simple Framing Members to HSS Columns," AISC Proceedings National Steel Construction Conference, 1995, pp. 30.1-30.16
- [12] Sherman, D.R., "Designing with Structural Tubing", AISC Engineering Journal, 3rd Quarter, 1996, pp. 101-109.
- [13] Richard, R.M., Gillet P.E., Kreigh, J.D., and Lewis, B.A., "The Analysis and Design of Single Plate Framing Connections", AISC Engineering Journal, 2nd Quarter, 1980, pp. 38-52.
- [14] Lipson, S.L.. "Single Angle Welded-Bolted Connections", ASCE Journal of Structural Division 193(ST3), March 1977, pp. 559-571.
- [15] Birkemoe, P.C., and Gilmor, M.L., "Behaviour of Bearing Critical Double Angle Beam Connections", AISC Engineering Journal, 4th Quarter, 1978.
- [16] Leon, R.T., and Deierlein, G.G., "An Overview of Codes, Standards, and Guidelines for Composite Construction", Proceedings of Structures Congress XIII, ASCE, Boston, 1995, pp. 1297-1300.
- [17] Ammerman, D.J., and Leon, R.T., "Behavior of Semi-Rigid Composite Connections", AISC, Engineering Journal, 2nd Quarter, 1987, pp. 53-61.
- [18] Leon, R.T. and Ammerman, D.J., "Semi-Rigid Composite Connections for Gravity Loads", AISC, Engineering Journal, 1st Quarter, 1990, pp. 1-11.
- [19] Ahmed, B., and Nethercot, D.A., "Design of Composite Finplate and Angle Cleated Connections", Journal of Construction Steel Research, V. 41, No. 1, 1997, pp 1-29.

- [20] Li, T.Q., Nethercot, D.A., and Choo, B.S., "Behaviour of Flush End-plate Composite Connections with Unbalanced Moment and Variable Shear/Moment Ratios-I. Experimental Behaviour". *Journal of Construction Steel Research*, V. 38, No. 2, 1996, pp. 125-164.
- [21] Zandonini, R. and Zanon, P., "Semi-Rigid Joint Action in Composite Frames: Numerical Analysis and Design Criteria", *Proceedings of an Engineering Foundation Conference, ASCE, Potosi, Missouri, 1992*, pp. 397-412.
- [22] Timoshenko, S. P., and Gere, J.M., "Theory of Elastic Stability, 2nd Edition", McGraw Hill Book Company, New York, 1961.
- [23] CSA. 1989. *Cold Formed Structural Steel Members, CAN/CSA-S136-M89*. Canadian Standards Association, Rexdale, Ontario.
- [24] Schnieder, S.P., "Experimental Behavior of Connections to Concrete Filled Steel Tubes", *Proceedings of Structures Congress XV, ASCE, Portland, Oregon, 1997*, pp. 954-958.
- [25] Kato, B., Kimura, M., Ohta, H., and Mizutani, N., "Connection of Beam Flange to Concrete Filled Tubular Column", *Proceedings of an Engineering Foundation Conference, ASCE, Potosi, Missouri, 1992*, pp. 528-538.
- [26] Azizinamini, A., and Prakash, B., "A Tentative Design Guideline for a New Steel Beam Connection Detail to Composite Tube Columns", *AISC Engineering Journal*, 3rd Quarter, 1993.
- [27] Azizinamini, A, and Shekar, Y., "Rigid Beam to Column Connection Detail for Circular Composite Columns", *Proceedings of Structures Congress, ASCE, Atlanta, Georgia, 1994*, pp. 1155-1160.
- [28] Lawrence, W.S., and Lu, L.W., "Partially Restrained Composite Connection Using a Tubular Column and ATCLASS Connectors", *Proceedings of Structures Congress XIII, ASCE, Boston, 1995*, pp. 1297-1300.
- [29] Alostaz, Y.M., and Schneider, S.P., "Analytical Behavior of Connections to Concrete Filled Steel Tubes", *Journal of Construction Steel Research*, V. 40, No. 2, 1996, pp. 95-127.
- [30] Dunberry, E., Leblanc, D., and Redwood, R.G., "Cross Section Strength of Concrete Filled HSS Columns at Simple Beam Connections", *Canadian Journal of Civil Engineering*, V. 14, 1987, pp. 408-417.
- [31] Shakir-Khalil, H.S. "Full Scale Tests on Composite Connections", *ASCE Proceedings Composite Construction of Steel and Concrete II, 1992*, pp. 539-554.
- [32] Kennedy, S.J., MacGregor, F., "Effects of End Connections on the Strength of Concrete Filled HSS Beam Columns", *Proceedings of the Canadian Society of Civil Engineering Annual Conference, Saskatoon, Sask., 1985*, pp. 617-637.
- [33] Hunaita, Y.M., and Fattah, B.A., "Design Considerations of Partially Encased Composite Columns", *Proc. Institution of Civil Engineers Structures and Buildings*, V106, Feb., 1994, pp. 75-82.
- [34] Galambos, T.V., "Guide to Stability Design Criteria for Metal Structures, 4th Edition, Wiley, New York, 1988
- [35] CSA. 1994. *Design of Concrete Structures for Buildings, CSA-CAN3-A23.3-M84*. Canadian Standards Association, Rexdale, Ontario.
- [36] Chicoine, T., Tremblay, R., Massicotte, B., Ricles, J., Le-Wu Lu, and Mehmet Yalcin, "Experimental Program on Partially Encased Built-Up Three Plate Composite Columns" *Ecole Polytechnique de Montreal and Lehigh University, January 2000*. [in press].
- [37] "National Building Code of Canada", *Canadian Commission on Building and Fire Codes, National Research Council of Canada, Ottawa, 1990*.

APPENDIX A

Design of Test Program

A1 Test Set-up

Before the specimens could be designed it was important to first determine the nature of the test set-up and the rig capacities. From the onset it was decided to test a simple framing connection, to a single side of the proposed composite column, through an exterior endplate. There were two primary loads required; the axial load on the column and the load required to bring the connection to failure. The University of Toronto possesses a 8890 kN Fox column tester, mounted on the strong floor of the Mark Huggin's Lab. The jack is mounted on four columns, which are bolted to the strong floor. This is the largest capacity jack at the University of Toronto, and was used to apply a nominal load on the test column.

There were several options considered to load the connection. Recent tests (Astaneh, 1989) have provided two actuators: one located at the beam-column connection to apply the load, and a second, displacement controlled actuator at the end of the load beam to control the beam end rotation. Due to the size of the Fox Jack and its support frame, it was impossible to position a jack near the beam column joint. Thus, the second alternative of a load beam connected at the column, and supported at a distance away from the test connection had to be used. A series of loads, or a single load could be applied along the load beam. Based on available equipment, the load beam could be loaded by either several 675 kN actuators located at adjacent bolt lines, 1524 and 3048 mm from the connection face. Alternatively, the 1000 kN MTS universal testing machine could be positioned adjacent to the Fox Jack frame. The centreline of the MTS would be 1550 mm from the centreline of the Fox Jack (and the centre of the test column). This meant that only a portion of the MTS 1000 kN capacity was available to fail the connection. This was an important consideration in the design of both the load beams, and detailing the connections to be tested.

A2 Design Parameters

The size of the test specimens would be in the range used by Canam engineers, with an upper limit provided by the apparatus limitations. To aid in the specimen design Canam provided an example of a gravity frame they had previously designed. A typical floor pattern is shown graphically in Figure A1. The columns are spaced 7.6↔9.2 m (25↔30 ft.) in one direction and 12↔15 m (40↔50 ft) in the other. The girders running along the shorter dimension have beams framing into them. Beam spacing varies from 3↔3.75 m. The floor slab consists of a 75 mm deep slab, with a 75 mm metal deck (total depth = 150mm). The beams are not to be shored during construction, and the decking will act as lateral bracing for the beam. Either the beams or girders could potentially frame into the weak column axis (as seen in Figure A1). The design loads are given in Table A1.

DEAD			LIVE		
DL stl.frame	0.38	kPa	Construction		
DL columns	0.3	kPa	LL concrete&form	0.6	kPa
DL concrete	2.77	kPa	LL apron	0.3	kPa
DL mech+elec	0.24	kPa	LL finishing	0.3	kPa
DL ceiling	0.24	kPa	LL erection	1	kPa
DL flooring	0.15	kPa	Service		
DL walls.int	1	kPa	LL occupation	3.83	kPa
DL walls.ext	1	kPa			
$\alpha_{DL} =$	1.25		$\alpha_{LL} =$	1.5	

Table A-1

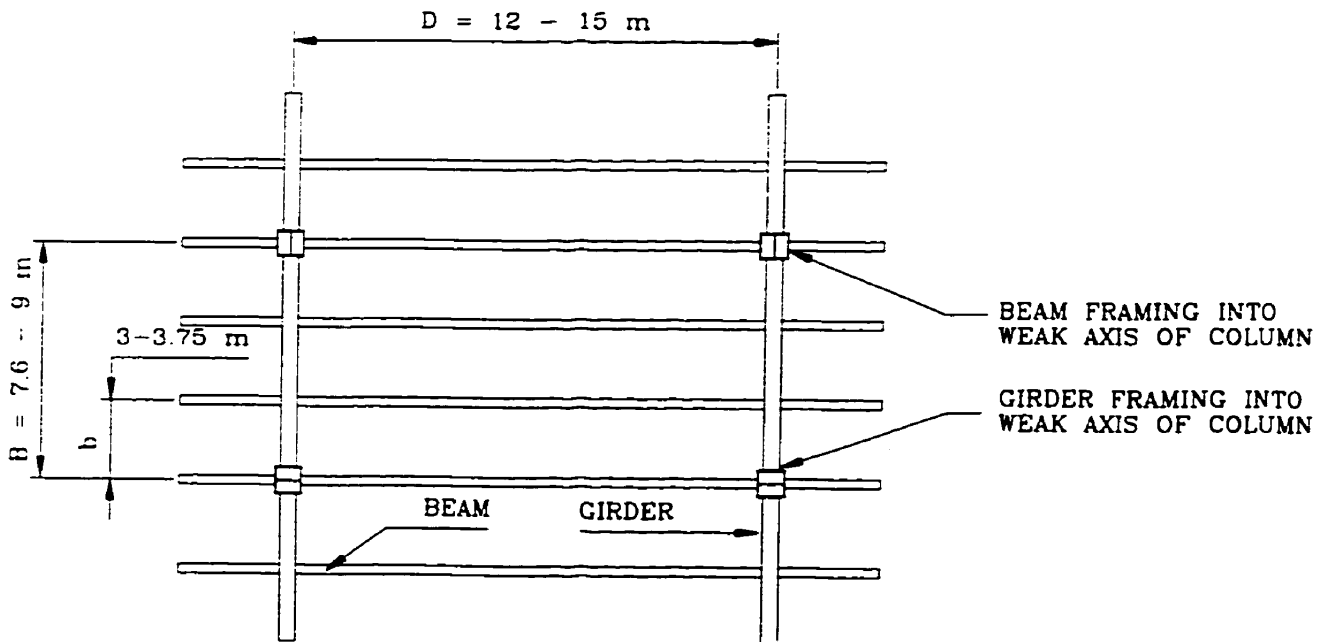


Figure A1: Typical Floor Layout

It is conceivable that up to 10 stories of steel structure could be erected prior to the concrete being cast. Thus the experimental examination of the connection behaviour must also include the stability of the column in the bare steel state, under the expected range of construction loads.

For the design of the test specimens the following material properties were assumed:

Steel Profiles: Grade 300W, $F_y = 300$ MPa, $F_u = 450$ MPa

Concrete: Columns: 25 MPa

Slabs: 25 MPa

A3 Connection Reactions

To design the test connections it was important to first determine a realistic range of the factored connection loads. There are two classifications, when the beams frame into the weak axis and when the girders frame into the weak axis. A summary of the factored design loads is given for each case in Tables A2 and A3. One (1) way slab action is assumed throughout.

Sample Calculation

$$D = 13 \text{ m}$$

$$B = 8 \text{ m}$$

$$b = 2.67 \text{ m}$$

$$\begin{aligned}\omega_{\text{construction}} &= \alpha_{\text{DL}} [\text{DL Steel Frame} + \text{DL Concrete}] + \alpha_{\text{LL}} [\text{LL Concrete Formwork} + \text{LL Apron} + \text{LL} \\ &\quad \text{Finish} + \text{LL Erect}] \\ &= 1.25[0.38 \text{ kPa} + 2.77 \text{ kPa}] + 1.5[0.6 \text{ kPa} + 0.3 \text{ kPa} + 0.3 \text{ kPa} + 1 \text{ kPa}] \\ &= 7.26 \text{ kPa}\end{aligned}$$

$$\begin{aligned}\omega_{\text{full load}} &= \alpha_{\text{DL}} [\text{DL Steel Frame} + \text{DL Concrete} + \text{DL Mech} + \text{DL Ceil} + \text{DL Flooring} + \text{DL interior}] + \\ &\quad \alpha_{\text{LL}} [\text{LL Occupation}] \\ &= 1.25[0.3 \text{ kPa} + 2.77 \text{ kPa} + 0.24 \text{ kPa} + 0.24 \text{ kPa} + 0.15 \text{ kPa} + 1 \text{ kPa}] + 1.5 [3.83 \text{ kPa}] \\ &= 11.62 \text{ kPa}\end{aligned}$$

Floor Type I: Beam Framing into Weak Axis

$$\begin{aligned}\text{Construction Load} &= \omega \times b \times D \times 1/2 \\ &= 7.26 \text{ kPa} \times 2.67 \text{ m} \times 13 \text{ m} \times 0.5 \\ &= 125.6 \text{ kN}\end{aligned}$$

$$\begin{aligned}\text{Full Load} &= 11.62 \text{ kPa} \times 2.67 \times 13 \times 0.5 \\ &= 202 \text{ kN}\end{aligned}$$

Floor Type II: Girder Framing into Weak Axis

For a beam spacing of 2.67 m there would be two interior beams that frame into each side of the girder. The connection would have to resist 1/2 of this load.

$$\begin{aligned}\text{Construction Load} &= [\omega \times b \times D \times 1/2] \times 4 \times 1/2 \\ &= [7.26 \text{ kPa} \times 2.67 \text{ m} \times 13 \text{ m} \times 0.5] \times 4 \times 1/2 \\ &= 252 \text{ kN}\end{aligned}$$

$$\begin{aligned}\text{Full Load} &= 202 \text{ kN} \times 4 \times 1/2 \\ &= 404 \text{ kN}\end{aligned}$$

Clause 21.4 of CAN/CSA S16.1-94² states that connections should develop the force due to the factored loads but should also be designed for not less than 50 % of the resistance of the member. Thus, to properly detail the test connections it is important to check if the factored connection load or the 50 % $V_{r,\text{beam}}$ would govern the actual design process.

****Nomenclature does not necessarily correspond to main body of report**

Table A2: Connection Loads and Tentative Beam Sizes for Floor Type I (Beams into Weak Axis)

D (m)	B (m)	b (m)	b _c (m)	Connection Load		Max. Moment		Tentative Beam
				Steel (kN)	Composite (kN)	Steel (kN.m)	Composite (kN.m)	
12	7.5	3.75	3	162.8	263.7	488.5	791.0	W460X74
		2.5	2.5	108.6	175.8	325.7	527.0	W410X54
	8	4	3	173.7	281.3	521.1	843.8	W460X82
		2.67	2.67	115.9	187.8	347.8	563.3	W410X60
	8.5	4.25	3	184.6	298.9	553.7	896.6	W460X82
		2.83	2.83	122.9	199.0	368.7	597.0	W410X60
	9	4.5	3	195.4	316.4	586.2	949.3	W530X82
		3	3	130.3	211.0	390.8	632.9	W460X61
	9.5	4.75	3	206.3	334.0	618.8	1002.1	W530X82
		3.2	3	139.0	225.0	416.9	675.1	W410X67
	2.4	2.4	104.2	168.8	312.7	506.3	W410X54	
13	7.5	3.75	3.25	176.4	285.7	573.3	928.4	W460X82
		2.5	2.5	117.6	190.5	382.2	619.0	W460X61
	8	4	3.25	188.2	304.7	611.6	990.3	W530X82
		2.67	2.67	125.6	203.4	408.2	661.1	W410X67
	8.5	4.25	3.25	199.9	323.8	649.8	1052.2	W530X82
		2.83	2.83	133.1	215.6	432.7	700.7	W460X67
	9	4.5	3.25	211.7	342.8	688.0	1114.1	W610X91
		3	3	141.1	228.5	458.7	742.8	W460X67
	9.5	4.75	3.25	223.5	361.9	726.2	1176.0	W610X91
		3.2	3.2	150.5	243.8	489.3	792.3	W460X74
	2.4	2.4	112.9	182.8	366.9	594.2	W410X60	
14	7.5	3.75	3.5	190.0	307.7	664.9	1076.8	W610X91
		2.5	2.5	126.7	205.1	443.3	717.9	W460X67
	8	4	3.5	202.7	328.2	709.3	1148.6	W610X91
		2.67	2.67	135.3	219.0	473.4	766.7	W410X74
	8.5	4.25	3.5	215.3	348.7	753.6	1220.3	W610X91
		2.83	2.83	143.4	232.2	501.8	812.6	W460X74
	9	4.5	3.5	228.0	369.2	797.9	1292.1	W610X91
		3	3	152.0	246.1	532.0	861.4	W460X82
	9.5	4.75	3.5	240.6	389.7	842.3	1363.9	W610X101
		3.2	3.2	162.1	262.5	567.4	918.8	W460X82
	2.4	2.4	121.6	196.9	425.6	689.1	W410X67	
15	7.5	3.75	3.75	203.6	329.6	763.3	1236.1	W610X91
		2.5	2.5	135.7	219.8	508.9	824.1	W460X74
	8	4	3.75	217.1	351.6	814.2	1318.5	W530X101
		2.67	2.67	144.9	234.7	543.5	880.1	W460X82
	8.5	4.25	3.75	230.7	373.6	865.1	1400.9	W610X101
		2.83	2.83	153.6	248.8	576.1	932.8	W530X82
	9	4.5	3.75	244.3	395.6	916.0	1483.3	W610X113
		3	3	162.8	263.7	610.7	988.9	W530X82
	9.5	4.75	3.75	257.8	417.5	966.9	1565.7	W610X113
		3.2	3.2	173.7	281.3	651.4	1054.8	W530X82
	2.4	2.4	130.3	211.0	488.5	791.1	W460X74	

Table A3: Connection Loads and Tentative Beam Sizes for Floor Type II (Girder into Weak Axis)

B (m)	D (m)	b (m)	b _c (m)	Connection Load		Load Per Joist		Max. Moment		Tentative Beam
				Steel (kN)	Composite (kN)	Steel (kN)	Composite (kN)	Steel (kN)	Composite (kN)	
7.5	12	3.75	1.875	162.8	263.7	325.7	527.4	610.7	988.9	W530X82
		2.50	1.875	217.1	351.6	217.1	351.6	542.8	879.0	W460X82
	13	3.75	1.875	176.4	285.7	352.8	571.4	661.6	1071.3	W610X91
		2.50	1.875	235.2	380.9	235.2	380.9	588.0	952.3	W530X82
	14	3.75	1.875	190.0	307.7	380.0	615.3	712.4	1153.7	W610X91
		2.50	1.875	253.3	410.2	253.3	410.2	633.3	1025.5	W610X91
15	3.75	1.875	203.6	329.6	407.1	659.3	763.3	1236.1	W610X101	
	2.50	1.875	271.4	439.5	271.4	439.5	678.5	1098.8	W610X91	
8	12	4.00	2	173.7	281.3	347.4	562.6	694.8	1125.1	W610X91
		2.67	2	231.6	375.0	231.6	375.0	617.6	1000.1	W530X82
	13	4.00	2	188.2	304.7	376.4	609.4	752.7	1218.9	W610X91
		2.67	2	250.9	406.3	250.9	406.3	669.1	1083.4	W610X91
	14	4.00	2	202.7	328.2	405.3	656.3	810.6	1312.6	W610X101
		2.67	2	270.2	437.5	270.2	437.5	720.5	1166.8	W610X91
15	4.00	2	217.1	351.6	434.3	703.2	868.5	1406.4	W610X101	
	2.67	2	289.5	468.8	289.5	468.8	772.0	1250.1	W610X91	
8.5	12	4.25	2.125	184.6	298.9	369.1	597.7	784.4	1270.2	W610X91
		2.83	2.125	246.1	398.5	246.1	398.5	697.2	1129.0	W610X91
	13	4.25	2.125	199.9	323.8	399.9	647.5	849.7	1376.0	W610X101
		2.83	2.125	266.6	431.7	266.6	431.7	755.3	1223.1	W610X91
	14	4.25	2.125	215.3	348.7	430.6	697.3	915.1	1481.8	W610X113
		2.83	2.125	287.1	464.9	287.1	464.9	813.4	1317.2	W610X101
15	4.25	2.125	230.7	373.6	461.4	747.2	980.5	1587.7	W610X125	
	2.83	2.125	307.6	498.1	307.6	498.1	871.5	1411.3	W610X101	
9	12	4.50	2.25	195.4	316.4	390.8	632.9	879.4	1424.0	W610X101
		3.00	2.25	260.6	421.9	260.6	421.9	781.7	1265.8	W610X91
		2.25	2.25	293.1	474.7	195.4	316.4	1099.2	1780.0	W610X140
	13	4.50	2.25	211.7	342.8	423.4	685.6	952.6	1542.6	W610X113
		3.00	2.25	282.3	457.1	282.3	457.1	846.8	1371.2	W610X101
	14	2.25	2.25	317.5	514.2	211.7	342.8	1190.8	1928.3	W610X155
4.50		2.25	228.0	369.2	456.0	738.4	1025.9	1661.3	W610X125	
15	3.00	2.25	304.0	492.2	304.0	492.2	911.9	1476.7	W610X113	
	2.25	2.25	342.0	553.8	228.0	369.2	1282.4	2076.6	W610X174	
	4.50	2.25	244.3	395.6	488.5	791.1	1099.2	1780.0	W610X140	
9.5	12	4.75	2.375	206.3	334.0	412.5	668.0	979.8	1586.6	W610X125
		3.17	2.375	275.0	445.4	275.0	445.4	870.9	1410.3	W610X101
		2.38	2.375	309.4	501.0	206.3	334.0	1224.7	1983.2	W610X155
	13	4.75	2.375	223.5	361.9	446.9	723.7	1061.4	1718.8	W610X140
		3.17	2.375	297.9	482.5	297.9	482.5	943.5	1527.8	W610X113
	14	2.38	2.375	335.2	542.8	223.5	361.9	1326.8	2148.5	W610X174
4.75		2.375	240.6	389.7	481.3	779.4	1143.1	1851.0	W610X140	
15	3.17	2.375	320.9	519.6	320.9	519.6	1016.1	1645.4	W610X125	
	2.38	2.375	361.0	584.5	240.6	389.7	1428.8	2313.8	W610X195	
	4.75	2.375	257.8	417.5	515.7	835.1	1224.7	1983.2	W610X155	
		3.17	2.375	343.8	556.7	343.8	556.7	1088.6	1762.9	W610X140
		2.38	2.375	386.8	626.3	257.8	417.5	1530.9	2479.1	W610X195

For the design loads given in Tables A2 and A3 a spreadsheet was created to determine optimal beam sizes. For each D, B and b the maximum bending moment under construction and full loads was calculated. The moment and shear capacities for each of the commonly available wide flange sections were also listed, and sorted based on their unit weight. A macro selected the lightest steel beam that met all strength criteria. The results of this process are also provided in Tables A2 and A3, for Floor Types I and II respectively. As expected, the beam selection was primarily based on bending moment and not the shear strength. Therefore the connection design was often based on the 50 % V_r restriction, rather than the applied loads.

For each of the beam sizes the minimum double angle connection required to resist the 50 % V_r requirements was designed. The double angle framing connection is the most commonly used type in gravity frame construction and it served as the baseline for the preliminary design of the test matrix. Table A4 gives the minimum connection for each beam, with the ultimate loads for each potential failure mechanism. All calculations assume no eccentricity, with $F_y = 350$ MPa, and $F_u = 450$ MPa.

Based on an upper limit of 800 kN (80% of MTS capacity) it would be impossible to fail connections meeting W610 load requirements with the proposed experimental set-up. Thus, it was decided to test a W410 beam representing the beam framing into the axis and a larger W530 beam size representing the girder framing into the weak axis. The connection reactions are:

Floor Type I:

Construction Loads: 130 - 180 kN

Composite Loads: 211-293 kN

50% V_r Requirement (Probable beam size W410): 300 - 352 kN

Floor Type II:

Construction Loads: 261-360 kN

Composite Loads: 422-586 kN

50% V_r Requirement (Probable beam size W530): 470 - 574 kN

It is important to remember that the depth of the connection plate, between the column flange tips, would be of the same nominal depth as each of the above beam sizes.

A4 Typical Beam End Rotation

The load beam must not only transfer the shear load to the connection, but must also apply a realistic rotation at the face. Although the true shear-rotation response, into the non-linear region, is beyond the scope of this research, a simple elastic rotation model was developed. The elastic rotation was calculated at factored load levels, considering the increased stiffness of the composite beam. These rotations were based on typical column and beam spacing, and the tentative beam selections contained in Tables A2 and A3. It was assumed that the entire construction dead load and only 20% of the live load would account for long-term rotations before the concrete becoming effective in load resistance. The rotations caused by additional post concrete setting dead load (i.e., flooring, mechanical etc) and the occupational live load were calculated using the stiffness of the composite section. To account for reductions in beam stiffness due to long-term effects of creep and shrinkage the I_r value was decreased by 20%. This was reduced for the long-term live load and post construction dead load only. A summary of the rotations at factored load levels are contained in Table A5.

Table A4: Connection Capacities Designed for 50% V_r of Realistic Beam Sizes

Nominal Section	Weight Kg/m	Web Thickness (mm)	50% V_r (kN)	Tentative Connection Angle	Connection Length (mm)	# Bolts	Connection Failures (kN)			Web Failures (kN)		Comments
							Yield	Rupture	Block	Tear	Bear	
W410	54	7.5	300	4x3.5x1/4	230	3	613	572	640	572	579	P=80; Cleat is centred P=80; Cleat is centred P=80; Cleat is centred P=80; Cleat is centred
	60	7.7	308	4x3.5x1/4	230	3	613	572	640	587	594	
	67	8.8	352	4x3.5x1/4	230	3	613	572	640	671	679	
				4x3.5x5/16	230	3	767	715	800	665	679	
W460	61	8.1	364	4x3.5x1/4	230	3	613	572	640	675	625	P=80 P=80 P=80 P=80 P=80 P=80 P=90 P=80
	67	8.5	383	4x3.5x5/16	230	3	767	715	800	669	625	
	74	9	404	4x3.5x1/4	230	3	613	572	640	708	656	
	82	9.9	445	4x3.5x5/16	230	3	767	715	800	702	656	
				4x3.5x1/4	230	3	613	572	640	747	694	
				4x3.5x5/16	230	3	767	715	800	741	694	
				4x3.5x1/4	250	3	667	641	708	876	764	
				4x3.5x5/16	230	3	767	715	800	815	764	
W530	72	8.9	470	4x3.5x1/4	295	4	787	722	790	833	916	P=3" P=3d P=3" P=3d P=3" P=3d P=80 P=65
	82	9.5	500	4x3.5x5/16	250	4	834	711	795	718	916	
	92	10.2	538	4x3.5x1/4	295	4	787	722	790	889	977	
	101	10.9	574	4x3.5x5/16	250	4	834	711	795	767	977	
				4x3.5x1/4	295	4	787	723	790	954	1049	
				4x3.5x5/16	250	4	834	711	795	823	1049	
				4x3.5x1/4	310	4	827	774	842	1064	1121	
				4x3.5x5/16	265	4	884	775	859	924	1121	
W610	84	9	541	4x3.5x1/4	295	4	787	723	790	854	926	P=3" P=3d P=80 P=65
	91	9.7	584	4x3.5x5/16	250	4	834	711	795	738	926	
				4x3.5x1/4	310	4	827	774	842	960	998	
				4x3.5x5/16	265	4	884	775	859	835	998	

Table A5: Typical Elastic Beam End Rotations (radians) at Factored Load Levels
Type I: Beams

B (m)	D (m)	b _c (m)	b (m)	Tentative Beam	I _{steel} × 10 ⁶ mm ⁴	Steel Only Rotations (rad)		Composite Rotations (rad)		Gross	20% Reduction	Net Rotation (rad)
						Dead Load	Live Load	Conc DL	Long Term LL			
12	9	3	3	W460x61	255	0.017	0.014	0.017	0.003	0.002	0.005	0.003
	9.5	3	3.2	W410x67	245	0.018	0.015	0.018	0.003	0.002	0.006	0.004
	10	3	3.33	W460x67	296	0.016	0.013	0.016	0.003	0.002	0.005	0.003
13	9	3	3	W460x67	296	0.018	0.015	0.018	0.003	0.003	0.006	0.004
	9.5	3.2	3.2	W460x74	332	0.017	0.014	0.017	0.003	0.002	0.006	0.004
	10	3.25	3.33	W460x74	332	0.018	0.015	0.018	0.003	0.003	0.006	0.004
14	9	3	3	W460x82	370	0.018	0.015	0.018	0.003	0.003	0.006	0.004
	9.5	3.2	3.2	W460x82	370	0.019	0.016	0.019	0.003	0.003	0.006	0.004
	10	3.25	3.33	W530x82	478	0.016	0.013	0.016	0.003	0.002	0.005	0.003
15	9	3	3	W530x82	478	0.018	0.015	0.018	0.003	0.003	0.006	0.004
	9.5	3.2	3.2	W530x82	478	0.017	0.015	0.017	0.003	0.003	0.006	0.004
	10	3.25	3.33	W610x91	667	0.014	0.012	0.014	0.003	0.002	0.005	0.003

Floor Type II: Girders

D (m)	B (m)	b (m)	b _c (m)	Tentative Beam	I _{steel} × 10 ⁶ mm ⁴	Steel Only Rotations (rad)		Composite Rotations (rad)		Gross	20% Reduction	Net Rotation (rad)
						Dead Load	Live Load	Conc. DL	Long Term LL			
12	7.5	2.5	1.875	W460x82	214	0.01	0.008	0.01	0.002	0.002	0.004	0.021
13	7.5	2.5	1.875	W530x82	479	0.008	0.007	0.008	0.002	0.002	0.004	0.019
14	7.5	2.5	1.875	W610x91	667	0.006	0.005	0.006	0.002	0.001	0.003	0.00165
12	8	2.67	2	W530x82	479	0.009	0.008	0.009	0.002	0.002	0.004	0.021
13	8	2.67	2	W610x91	667	0.007	0.006	0.007	0.002	0.002	0.004	0.0185
13	8	2.67	2	W610x91	667	0.008	0.007	0.008	0.002	0.002	0.004	0.0199
13	8	2.67	2	W610x91	667	0.008	0.002	0.008	0.002	0.002	0.004	0.0203
13	8	2.67	2	W610x91	667	0.008	0.007	0.008	0.002	0.002	0.004	0.022
12	9	2.25	3	W530X101	617	0.011	0.008	0.011	0.002	0.002	0.005	0.02
13	9	2.25	3	W610X101	764	0.009	0.008	0.009	0.002	0.002	0.004	0.0165
14	9	2.25	3	W610X113	875	0.009	0.007	0.009	0.002	0.002	0.004	0.01785
15	9	2.25	3	W610X125	985	0.008	0.007	0.008	0.002	0.002	0.004	0.0172
12	9.5	2.375	3.17	W610X101	764	0.01	0.008	0.01	0.002	0.002	0.004	0.0201
13	9.5	2.375	3.17	W610X113	875	0.009	0.008	0.009	0.002	0.002	0.004	0.018

A5 Beam Selection

Although there has been discussion of realistic beam selection to determine a range of 50% V_r requirements, the actual load beam does not necessarily have to match these sizes. The load beam must be stiff enough to resist the bending moments resulting from the long beam length, but must still provide realistic beam end rotation. It would also be advantageous to have a realistic web thickness as not to preclude failure resulting from bolthole bearing. Another important criteria is that the load beams must be of adequate length to ensure a high portion of the MTS load is available at the connection, but still be within manageable handling lengths in the laboratory. The following is a summary of the load beam criteria:

Floor Type I: Beams Framing into Weak Axis

Non-Composite Factored Connection Load: 130 ↔ 180 kN
Non-Composite Rotation at Factored Load: 0.026 ↔ 0.031 Rad

Composite Factored Connection Load: 211 ↔ 293 kN
Rotation at Composite Factored Load: 0.027 ↔ 0.033 Rad
Net Rotation After Concrete Setting: 0.014 ↔ 0.018 Rad

50% V_r Requirements (Based on W10 Beam Size): 300 ↔ 352 kN
Length of Load Beam Required for Force at Column Face: 5 m

Floor Type II: Girders Framing into Weak Axis

Non-Composite Factored Connection Load: 261 ↔ 362 kN
Non-Composite Rotation at Factored Load: 0.015 ↔ 0.018 Rad

Composite Factored Connection Load: 422 ↔ 586 kN
Rotation at Composite Factored Load: 0.018 ↔ 0.021 Rad
Net Rotation After Concrete Setting: 0.008 ↔ 0.011 Rad

50% V_r Requirements (Based on W530 Beam Size): 470 ↔ 574 kN
Length of Load Beam Required for Force at Column Face: 7.2 m

Although the MTS applies a single point load, with a maximum value of 1000 kN, a spreader beam was used to distribute the load and reduce the maximum bending moment in the load beam (As shown in Figure A2). By positioning the roller locations, the bending moment in the beam and the rotation at the connection face can be controlled. Although the spreader beam is 3.9 m long the maximum possible distance between the centrelines of the rollers was 3.5 m. This allowed for movement of the spreader beam, relative to the load beam during the testing.

Table A6 contains a summary of the rotation response for the commonly available beam sizes for each framing classification. The size of beam required to resist the bending moment will have beam end rotations on the order of 0.01 to 0.13 radians. The actual beam end rotations that could be expected at factored load levels are approximately half that calculated in Table A5. With the minimum beam lengths required for load transfer, it is impossible to have a smaller load beam, and increased rotation at the face.

At the time of designing the test program this was cause of concern. But it considered acceptable for several reasons. First, this is a pilot study on this connection type only and it was not intended as a complete test on shear connectors. Secondly, the main connection type was the double angle framing connection. These are generally shorter in length, and provide lower rotational restraint than other shear connectors (especially those in single shear). Finally, the magnitude of the rotations that will be developed match those calculated in Table A5 for post concrete loading.

The following load beams were selected:

Floor Type I: Beams Framing into the Weak Axis
W410x67, L= 5.1 m

Floor Type II: Girders Framing into Weak Axis
W530X92; L= 7.2 m

From table A6 it appears that W410x67 and W530 x 82 would provide a higher rotation, while still meeting bending moment demands. Since each of these beams could potentially be used for up to eight tests, it was decided to use a slightly heavier section as an extra precaution to avoid excessive distortion (i.e.: shear, bending moment, lateral torsional effects). A slightly longer length was also provided to make allowances for removing the local deformation at the ends.

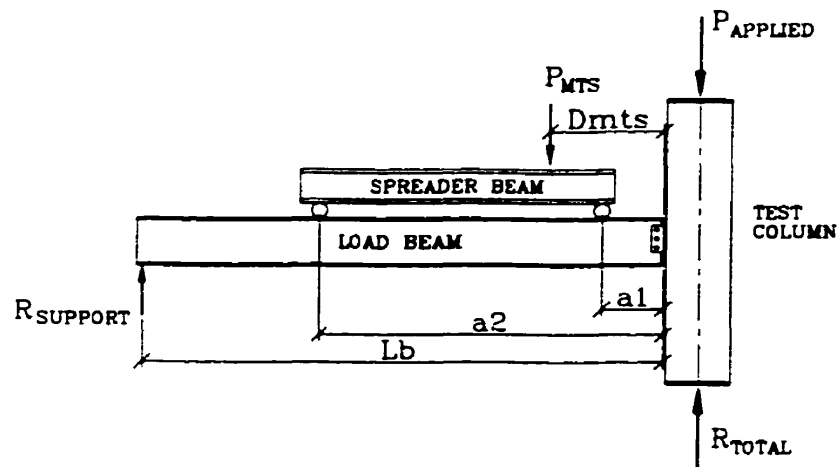


Figure A2: Schematic of Proposed Set-up

Table A6: Calculated Rotations for Possible Load Beams and Test Geometry: Rotations Calculated at Factored Loads.

**Floor
Type I:**

Beam	S $\times 10^3$ mm ³	I $\times 10^6$ mm ⁴	L (mm)	a ₁ (mm)	a ₂ (mm)	V _{factored} (kN)	MTS _{factored} (kN)	V _{max} (kN)	MTS _{max} (kN)	Rotation (rad)
W410x54	924	186	5000	0.445	3.81	350	480	730	1000	0.0093
x60	1060	216	5000	0.505	3.63	350	480	730	1000	0.0104
x67	1200	246	5000	0.575	3.45	350	480	730	1000	0.0089
W460x61	1130	255	5000	0.542	3.6	350	180	730	1000	0.0080
x67	1300	296	5000	0.62	3.31	350	480	730	1000	0.0078
x67	1300	296	6000	0.55	4.1	350	450	730	940	0.0085

**Floor
Type II:**

Beam	S $\times 10^3$ mm ³	I $\times 10^6$ mm ⁴	L mm	a ₁ (mm)	a ₂ (mm)	V _{factored} (kN)	MTS _{factored} (kN)	V _{max} (kN)	MTS _{max} (kN)	Rotation (rad)
W530x72	1530	402	7200	0.55	4.35	550	675	813	1000	0.0129
x82	1810	479	7200	0.78	3.82	550	675	813	1000	0.0132
x92	2070	552	7200	0.89	3.35	550	675	813	1000	0.0125
x101	2300	617	7200	0.99	2.91	550	675	813	1000	0.0119
W610x84	2060	613	7200	0.885	3.37	550	675	813	1000	0.0112
x91	2230	667	7200	0.99	2.91	550	675	813	1000	0.0110

A6 Final Connection Details

Following discussions with Canam it was decided to test two primary connection types; namely, double angle framing connections and single shear plates (shear tabs). To investigate the influence of connection length on overall connection behaviour, both a short and long double angle connection was included for each beam depth (varied bolt spacing). An additional two seat connections were added to the test matrix during the course of the testing program. As discussed in the main body of this report, one seat connection was tested with four ¼" shear studs welded on the back of the connection end plate.

For all connections an edge distance of 35 mm was maintained. The first bolthole was located 80 mm from the top of the beam. All connection angles, for the double angle connections consisted of 75 x 75 x 6.25 mm sizes. The capacities of these connections are given in the main body of this report. The predicted failure loads given in Tables 3.4 and 3.5 in the main report are based on the tested material properties. The effects of load eccentricity were neglected in the calculations.

A7 Test Columns

At the commencement of this research program, Canam provided a copy of a spreadsheet used to calculate column loads in a gravity frame. This spreadsheet was used to determine the number of floors where the nominal load of 1.0 D.L. and 0.5 L.L. is less than 6750 kN test rig capacity (Fox Jack capacity reduced to account for MTS being anchored to the floor bolts). Once the number of supported floors was determined the full factored design load was calculated. The actual design of the test columns was based on the full factored axial loads.

In the calculations a 14 m x 8 m column spacing was assumed, and the live loads were reduced in accordance to the National Building Code of Canada³⁷:

$$A_{\text{reduced}} = A_{\text{Tributary}} \times \left[0.3 + \sqrt{\frac{9.8}{A_{\text{Tributary}}}} \right]$$

Table A7 contains the elevation in a multi-story building where the nominal load is within testing limits. The nominal loads represents approximately 67% of the full factored load. The nominal column size can then be estimated based on the simple squash load:

$$P_R = \phi_{\text{steel}} A_{\text{Steel}} f_y + 0.85 \phi_{\text{concrete}} A_{\text{Concrete}} f'_c$$

Assuming that the column web and flange are both from 9.53 mm (3/8 inch) plate material, and the concrete strength is 25 MPa, the maximum column dimension can be readily calculated:

$$\frac{6750 \times 10^3}{0.67} = 0.9(350)(30D - 200) + 0.6(0.85)(25)[(D - 10)(D - 20)]$$
$$D = 605 \text{ mm}$$

École Polytechnique has tested specimens with nominal dimensions of 300 mm, 450 mm and 600 mm. To evaluate the influence of the connection load on the overall behaviour of the column, the columns sizes for the University of Toronto testing would corresponded to these sizes; the capacities of which are listed in Table A8. To allow for the ability to increase the applied column load during the composite tests, above the 1.0 D.L. + 0.5 L.L. level, it was decided to conduct the majority of the tests on the 450 mm column size. Two 600 mm x 600 mm specimens were also provided to investigate the influence of column size.

Table A7: Nominal and Factored Loads for Various Numbers of Supported Floors (8 x 14 m Column Spacing).

Number of Supported Floors	Nominal Load 1.0 D.L. + 0.5 L.L. (kN)	Factored Load 1.25 D.L. + 1.5 L.L. (kN)
8	4982	7443
9	5589	8333
10	6196	9222
11	6802	10110

Table A8: Column Properties and Loads – Nominal Sizes Correspond to Previous Work¹

Column (mm x mm)	b/t flange	w/t	P _{Nominal} (67%) (kN)	P _{Resist} (kN)	P _{Ultimate} (kN)
300 x 300	24	46	1890 kN	2821 kN	3732 kN
450 x 450	22.5	43	4423 kN	6602 kN	8676 kN
600 x 600	30	58	6679 kN	9970 kN	13502 kN

- All steel plates are 9.53 mm thick

APPENDIX B

Additional Design Calculations For Test Set-up

B1 Lateral Beam Bracing

The load beams are not supported along their length, thus may be subjected to lateral torsional buckling. To prevent this from happening, and ensuring multiple use of the load beams, lateral bracing will be designed based on Winters Design Criteria (Galambos, 1997). The two (2) load beams used in this testing are:

W410 x 67; L = 5.2 m

W530 x 93; L = 7.2 m

Both are class 1 in bending

For a simply supported beam subjected to a constant moment the moment at which lateral buckling will occur is given as (S16.1):

$$M_u = \frac{\pi}{L} \sqrt{EI_y GJ + \left(\frac{\pi E}{L}\right)^2 I_y C_w}$$

Where: L Unbraced Length
 I_y Moment of Inertia Along Weak Axis
 J Torsional Constant
 C_w Warping Constant

The value of M_r can be taken as ϕM_u when it is less than ϕM_p . Also to account for the presence of high residual strains in the flange tips M_r is modified when $M_u > 0.67 M_p$.

$$M_r = 1.15\phi M_p \left(1 - \frac{0.28M_p}{M_u}\right)$$

For the purpose of evaluating whether lateral bracing is required, the ϕ factor will be taken as 1, and M_p will be replaced by M_y . The relevant beam properties are:

W410 x 67:	$S_x = 1200 \times 10^3 \text{ mm}^3$	$J = 469 \times 10^3 \text{ mm}^4$
	$I_y = 13.8 \times 10^6 \text{ mm}^4$	$C_w = 540 \times 10^9 \text{ mm}^6$
	$G = 77 \times 10^3 \text{ MPa}$	$E = 200 \times 10^3 \text{ MPa}$
W530 x 92:	$S_x = 2070 \times 10^3 \text{ mm}^3$	$J = 762 \times 10^3 \text{ mm}^4$
	$I_y = 23.8 \times 10^6 \text{ mm}^4$	$C_w = 1590 \times 10^9 \text{ mm}^6$
	$G = 77 \times 10^3 \text{ MPa}$	$E = 200 \times 10^3 \text{ MPa}$

Based on the following information the two graphs of M_r Vs Unbraced length can be produced

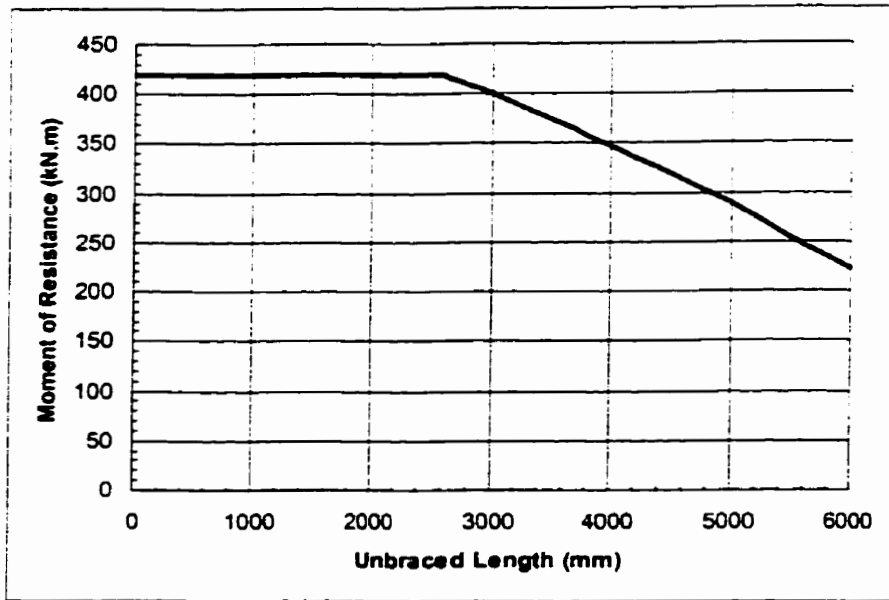


Figure B1: Moment Capacity Vs. Unbraced Length: W410 x 67

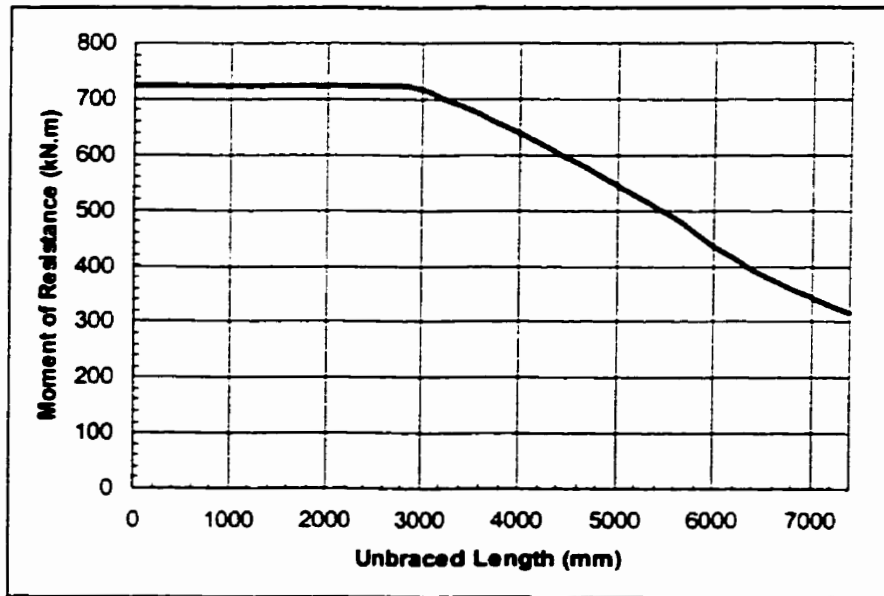


Figure B2: Moment Capacity Vs. Unbraced Length: W530 x 92

The number of brace points can now be determined by first determine the critical bending moment diagram for each of the load beams. Assuming a load beam length of 5.2 m, and the MTS centreline is located 1.35 m from the column face the following bending moment diagram can be produced for the maximum loading condition.

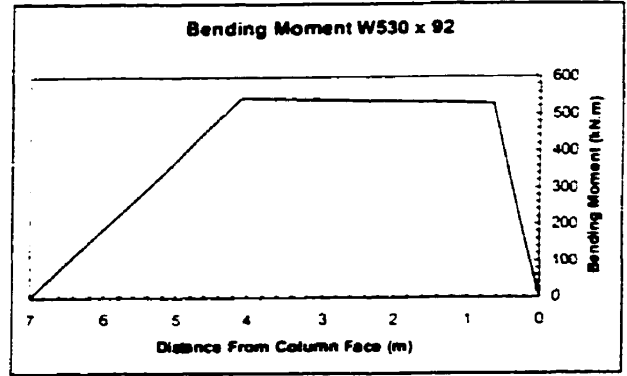
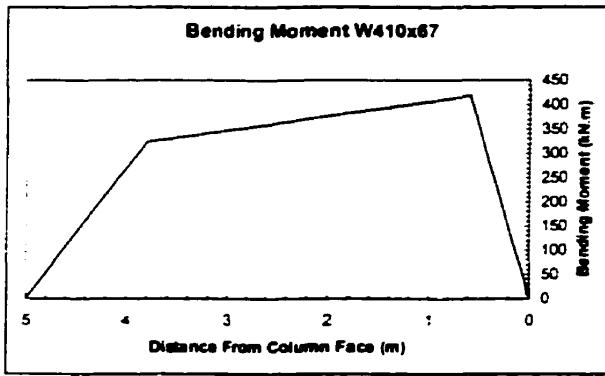


Figure B3: Bending Moments Under Maximum Loading

Prior to the analysis it was decided to provide lateral bracing at the connection end. This bracing will be located 200 mm from the column face. Bracing could also be conveniently placed some 2 m from the column face, at the next set of floor bolts. The large floor bolts will be in place for the MTS tie down mechanism, and the beam bracing can be conveniently anchored.

For the W410 load beam, with a 5 m length, the unbraced lengths will then equal 2 and 3 meters. From Figure B1 it can be seen than for the 2 m the strength is governed by the section capacity M_y , and a 3 m the strength is slightly reduced to 390 kN.m. Therefore braces located at these two points are adequate.

For the W530 load beam, with the same brace points the unbraced lengths are 2 and 5 m respectively. For 5 meters the bending resistance is approximately 550 kN.m ($\phi=1.0$), which corresponds to approximately the same bending moment under the applied test loads. This was considered adequate since the bending moment is not constant throughout the length.

The two afore mentioned brace points are all that is required. The bracing system must now be designed based on both strength and stiffness criteria (Galambos, 1997)

$$stiffness \geq \frac{10M_f C_d}{L_b h}$$

$$F_{brace} \geq \frac{0.01M_f C_d}{h}$$

W410

$$stiff > (10 \cdot 390E6 \cdot 1.0) / (3000 \cdot 410) = 3200 \text{ N/mm}$$

$$Force = (0.01 \cdot 390E6 \cdot 1.0) / 410 = 9.51 \text{ kN}$$

W530

$$2075 \text{ N/mm}$$

$$10.4 \text{ kN}$$

The lateral beam braces must be designed for a specified stiffness of 3200 N/mm and a force of 10.5 kN. The braces must also be designed to accommodate longitudinal movement of the beam, and well as the vertical displacement. A common method of accomplishing this is with the swivel mechanism shown in Figure 3.11 in the main report. The rods and rod ends were from University of Toronto stock and the rods are 600 mm long and 31 mm in diameter.

$$stiffness = \frac{AE}{L} = \frac{\pi(31/2)^2 200000}{2(600)} = 125 \times 10^3 \geq 3200$$

Strength Check based on one rod in tension only

$$P_y = \sigma_y A = 300 \frac{N}{mm^2} \times \frac{\pi(31)^2}{4} mm^2 = 226 kN$$

Thus the "in stock" bracing material is more than adequate.

B2 Design of Column Bracing

Due to the eccentricity of the connection load there will be a moment applied to the column at the beam connection. To resist this moment horizontal braces are required at the column ends as shown in Figure 1.3. To design these braces a connection eccentricity of 250 mm was first assumed for a maximum load of 820 kN. The moment applied on the column then equals:

$$M = V \left(e + \frac{D}{2} \right)$$

$$M = 820 kN \left(0.250 m + \frac{0.450 m}{2} \right) = 389.5 kN.m$$

Conservatively taking the shortest column length of 2.258 m the horizontal force that must be resisted equals $389.5 kN.m / 2.258 m = 172.5 kN$. It was decided that the bracing system would consist of tension rods that connected the top plate of the spherical heads to the Fox Jack frame. Since the load is monotonic the rods will always be in tension. Universal rod ends would be pinned at the spherical head, but directly bolted to the test frame. Thus the spherical head was free to rotate. The tension rods were not directly connected to the test specimen, rather the horizontal force was assumed to be transferred by both friction, and by a stop that was connected to the spherical head (As shown in Figure 3.13). Although there was no spherical head on the top of the column the system would be the similar for the composite specimens, where only small displacements would have to be accommodated. For the non-composite specimens the tension braces at the top were removed. A roller, anchored to the test frame, was used to prohibit lateral motion of the specimen.

The rod ends were purchased for this experiment and the rods machined. For conformity to other apparatus the same diameter rods as in the lateral beam bracing.

Existing Rod Diameter 1.25" = 31.7 mm

Strength of Rod Material = 300 MPa

Rod End Capacity = 116 kN

Since two rods will be used at both the top and bottom the total capacity of the system is:

$$P_r = 2[A_{rod} f_v]$$

$$P_r = 2 \left[\frac{\pi(31.7)^2}{4} 300 * 0.001 \right] = 473.2kN$$

The capacity is governed by the rod ends, but still exceeds the design load of 172.5 kN.

B3 Longitudinal Beam Bracing

Following the first two tests it was decided to use a longitudinal beam restraint for the remainder of the composite specimens. The restraint system was self-equating with the beam tied directly to the column specimen. A schematic of the set-up is shown in Figure B4.

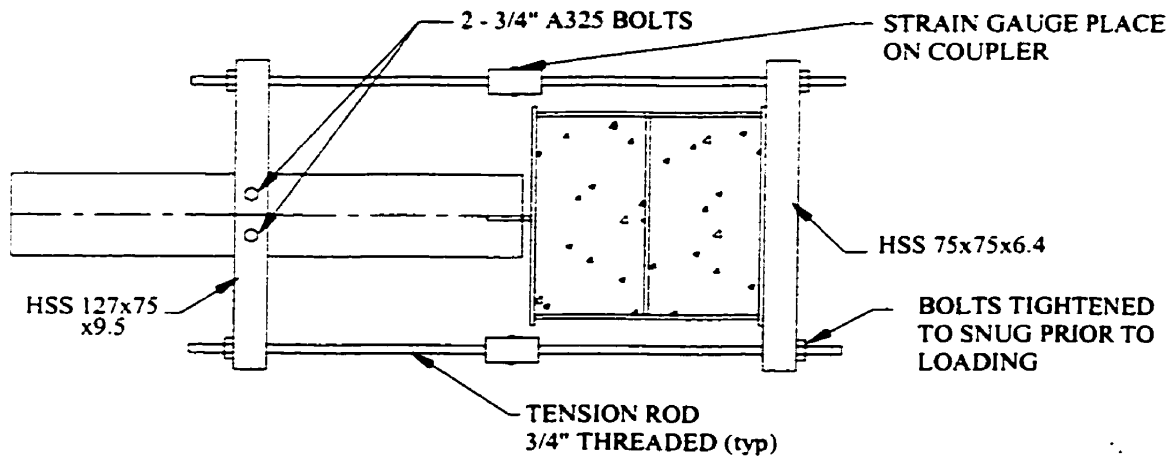


Figure B4: Schematic of Proposed Longitudinal Bracing

The capacity of the above system can now be calculated, with the moment arm can be taken as the distance from the tension rod to the centre of the connection element. For the purpose of design this will be taken as 225 mm.

$$T_{rod} = A_{rod} \sigma_y = 2 \frac{\pi(19.05)^2}{4} (350MPa) 0.001 = 200kN$$

$$M_{max} = T_{rod} xj = 200x0.225 = 45kNm$$

For the analysis of the test data it was important to know the load in restraining system. Two strain gauges were installed on the tension rods, mounted on a machined coupler.

APPENDIX C

Graphical Material Property Results

C1 Summary of Results

The material properties for both the concrete and steel have been reported in tabular form in the main body of this report. In this appendix the stress-strain plots will be presented for all steel coupons, and all concrete cylinders tested in the 5000 kN MTS Stiff Frame testing machine. The nomenclature matches that used in Table 4.1 in the main body of this report.

For all steel coupons the entire stress-strain curve is given until rupture, but there is an inset with the stress strain curve for strains up to 0.03 provided at a more convenient scale. All values given in the tables have been measured graphically from these source curves.

In the first concrete batch there were two cylinders tested at 141 days in the stiff frame. This corresponded to the time of the full-scale specimen tests. Their stress strain curves are given in Figures C15 and C16. For the second concrete batch there were two cylinders tested at both 40 and 90 days. The stress strain curves have been shown in Figures C17 and C18 respectively, with both cylinders superimposed on the same plot.

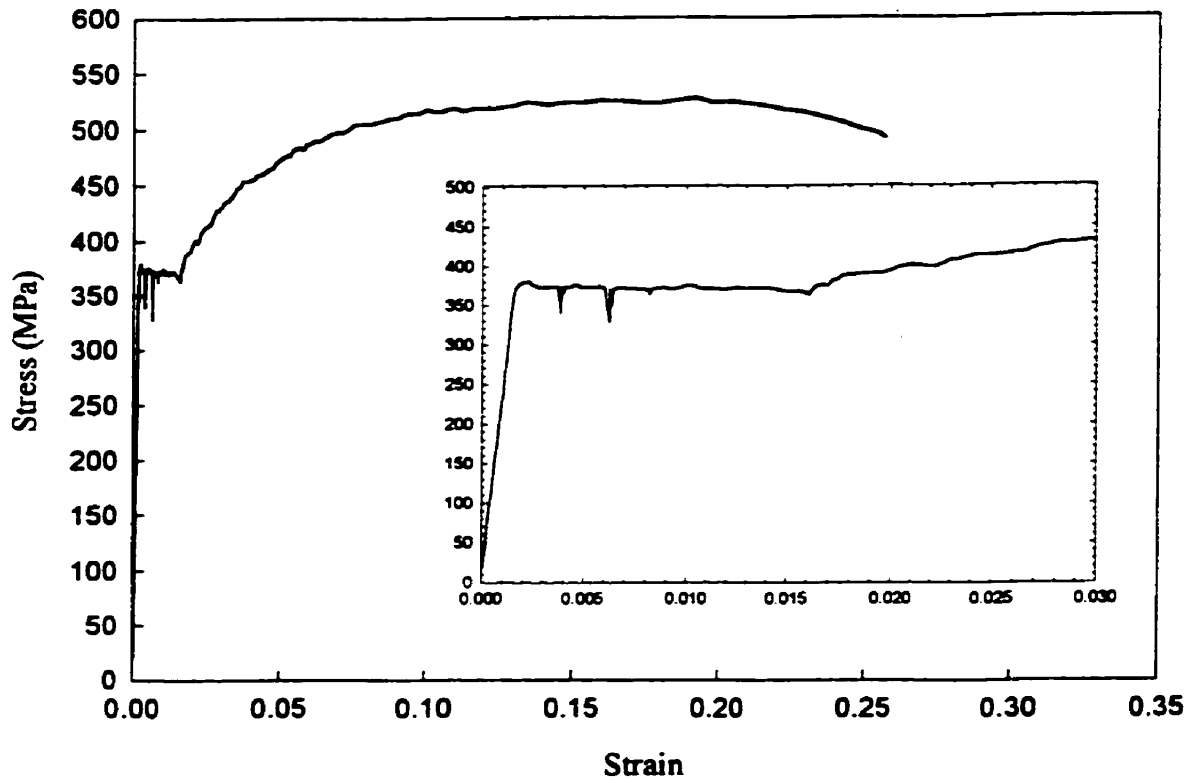


Fig. C1: Load Deformation Response of Coupon P1 - Column Plate Material

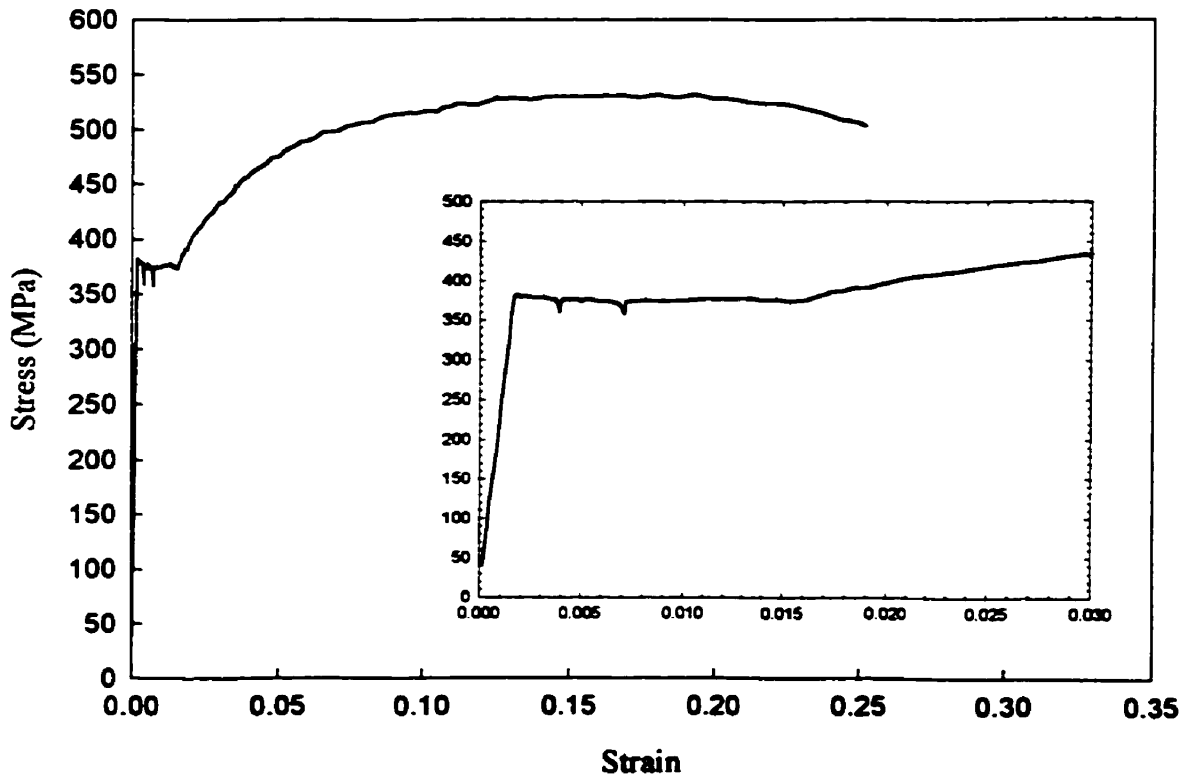


Fig. C2: Load Deformation Response of Coupon P2 - Column Plate Material

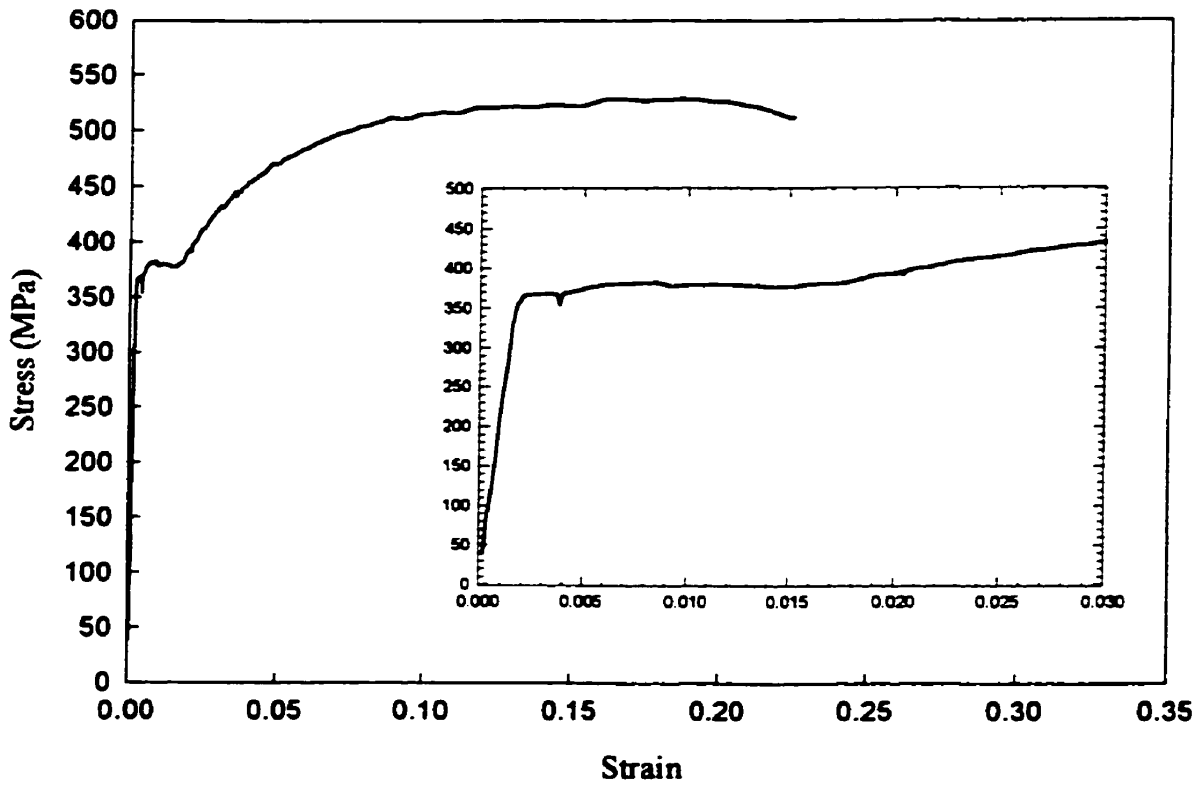


Fig. C3: Load Deformation Response of Coupon P3 - Column Plate Material

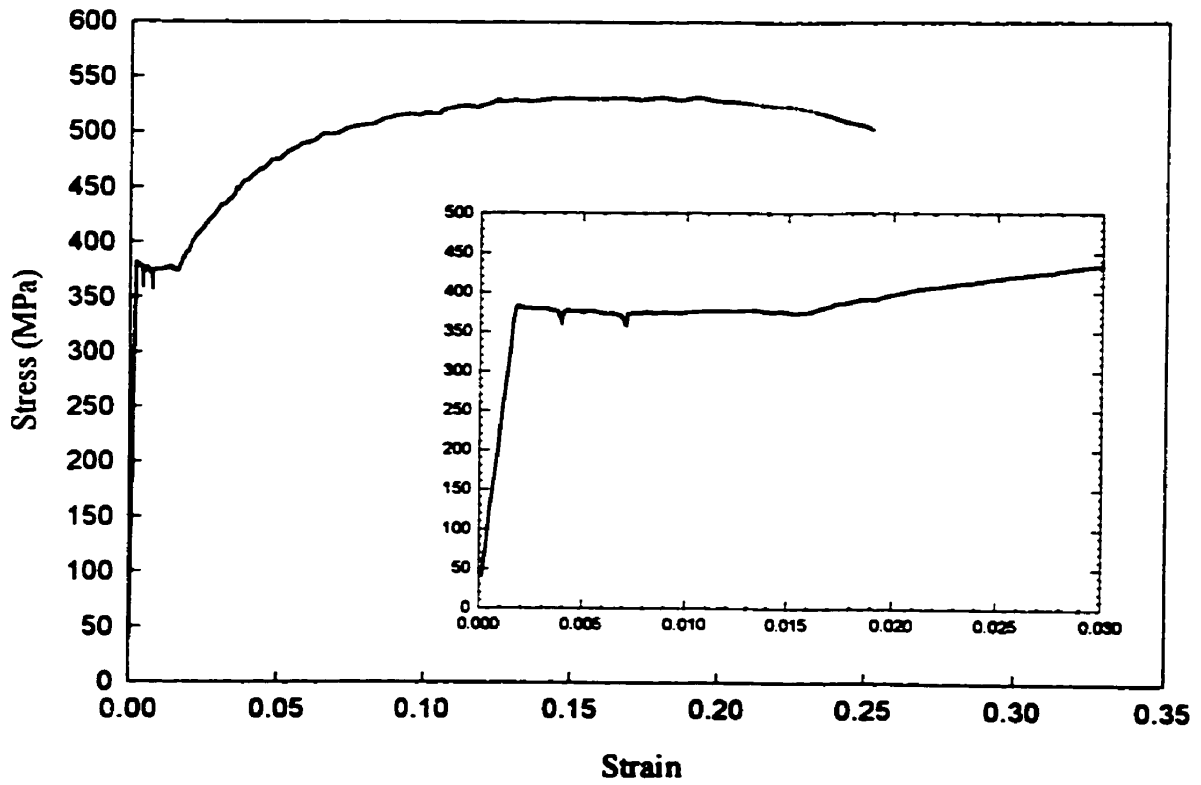


Fig. C4: Load Deformation Response of Coupon P4 - Column Plate Material

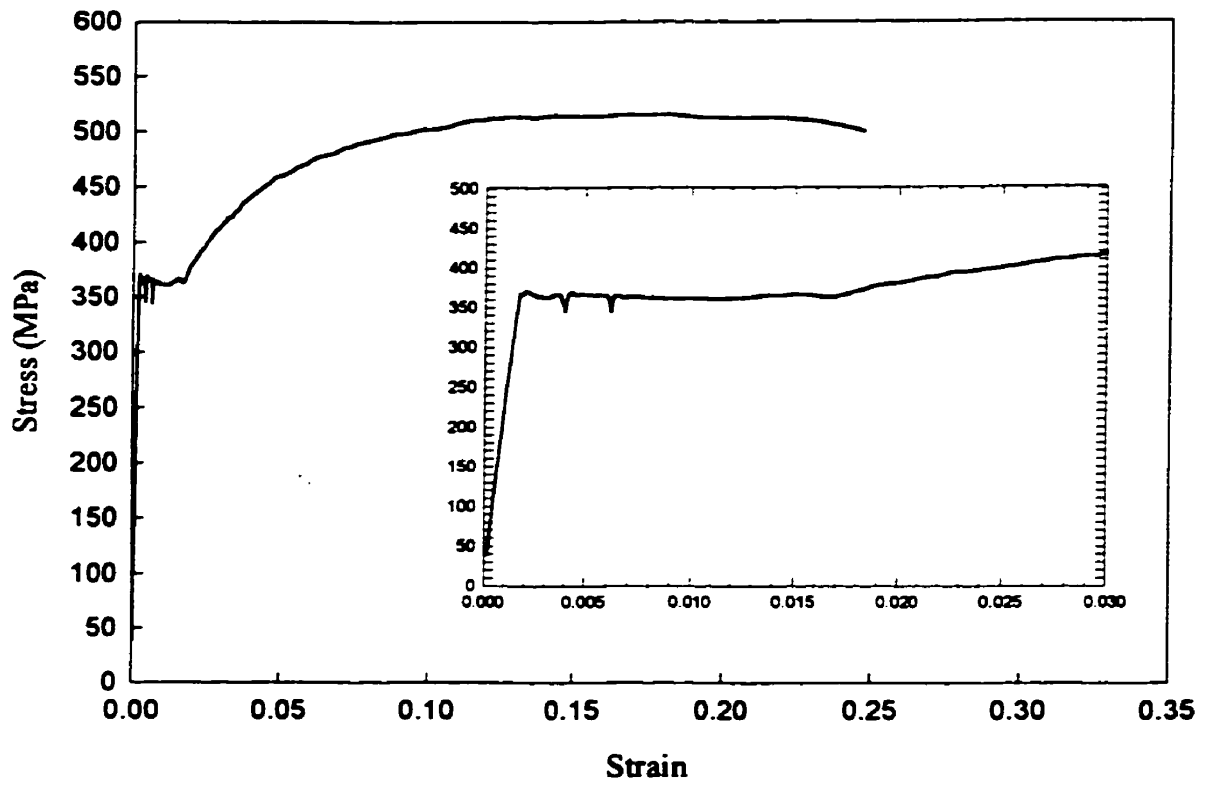


Fig. C5: Load Deformation Response Coupon P5 - Column Plate Material

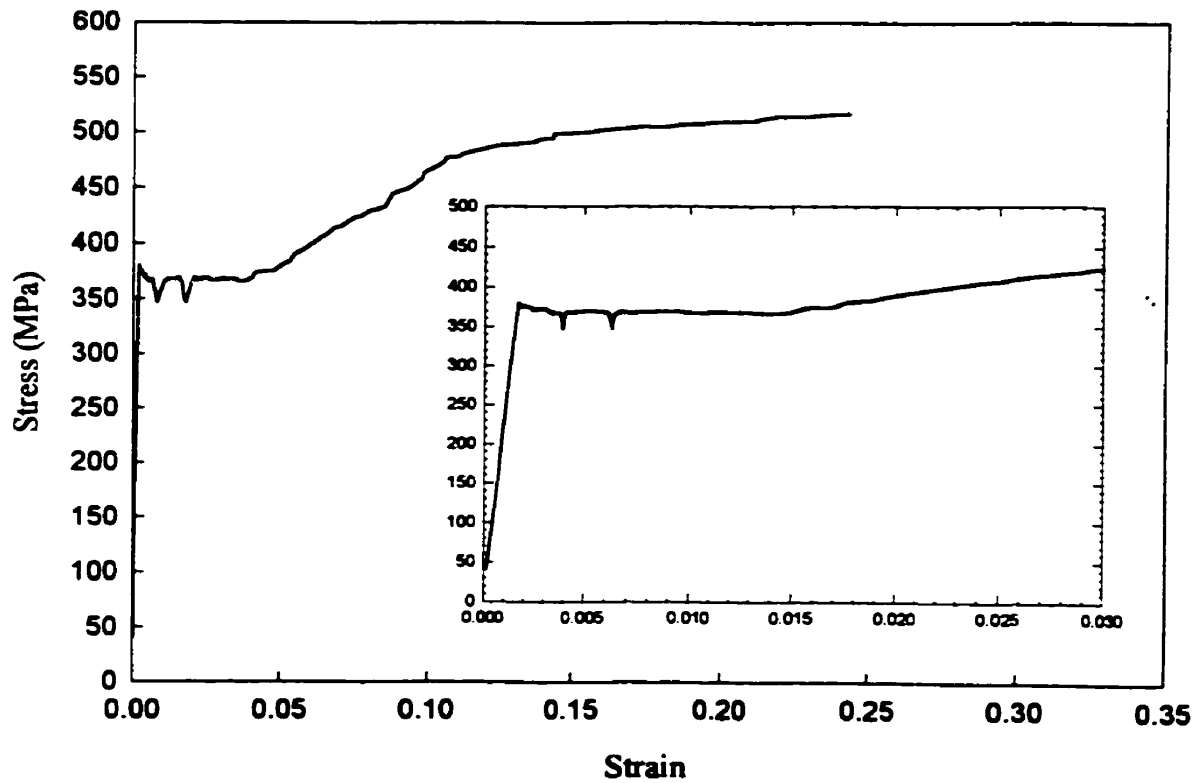


Fig. C6: Load Deformation Response Coupon P6 - Column Plate Material

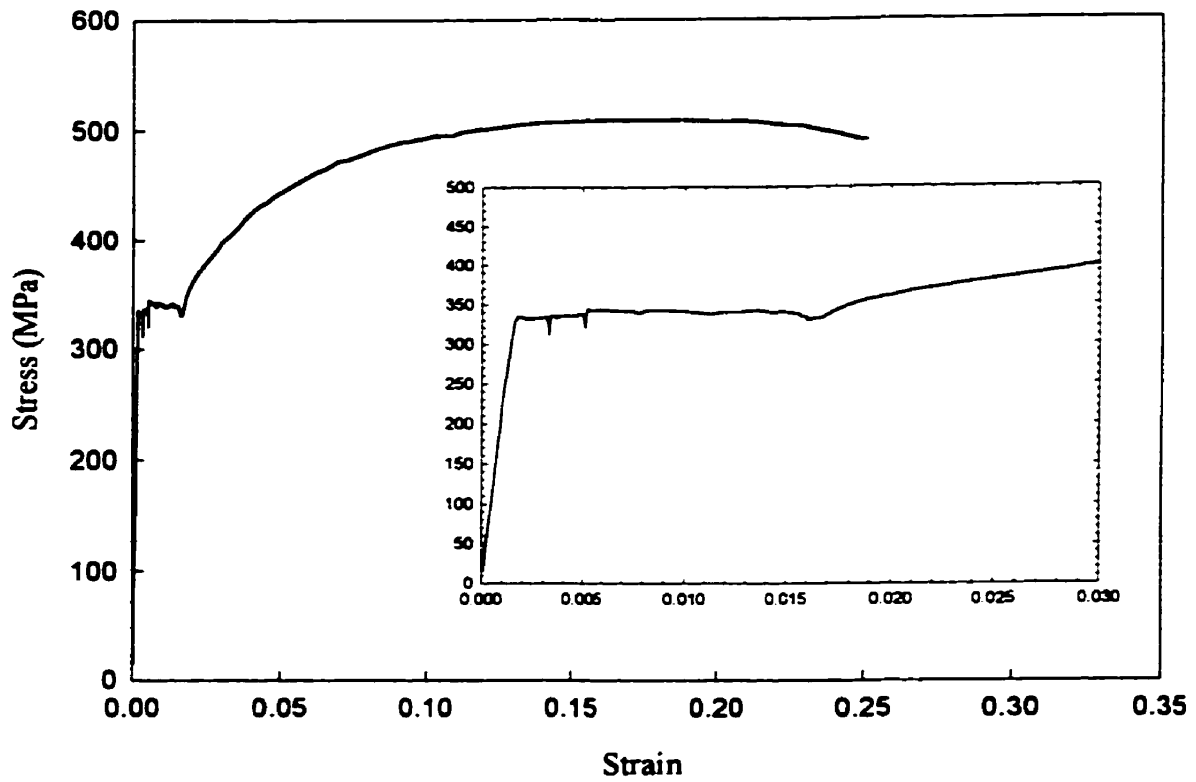


Fig. C7: Load Deformation Response of Coupon CA1 - Connection Angle

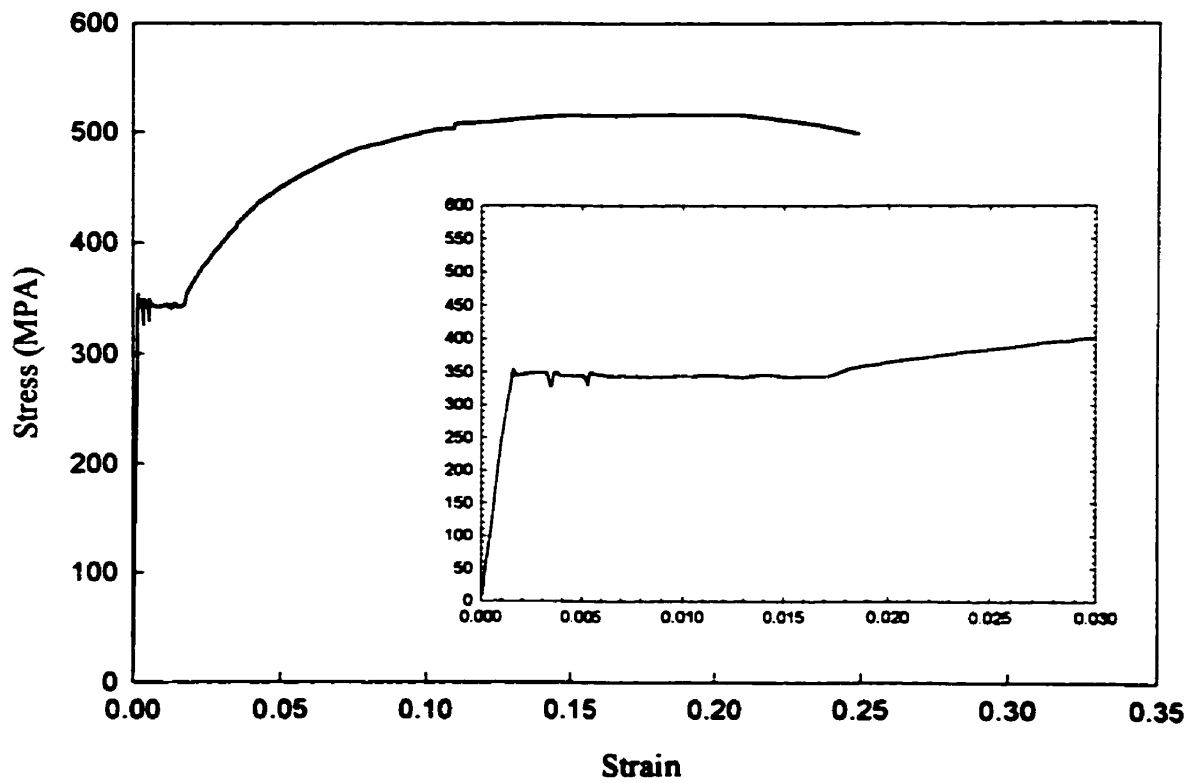


Fig. C8: Load Deformation Response of Coupon CA2 - Connection Angle

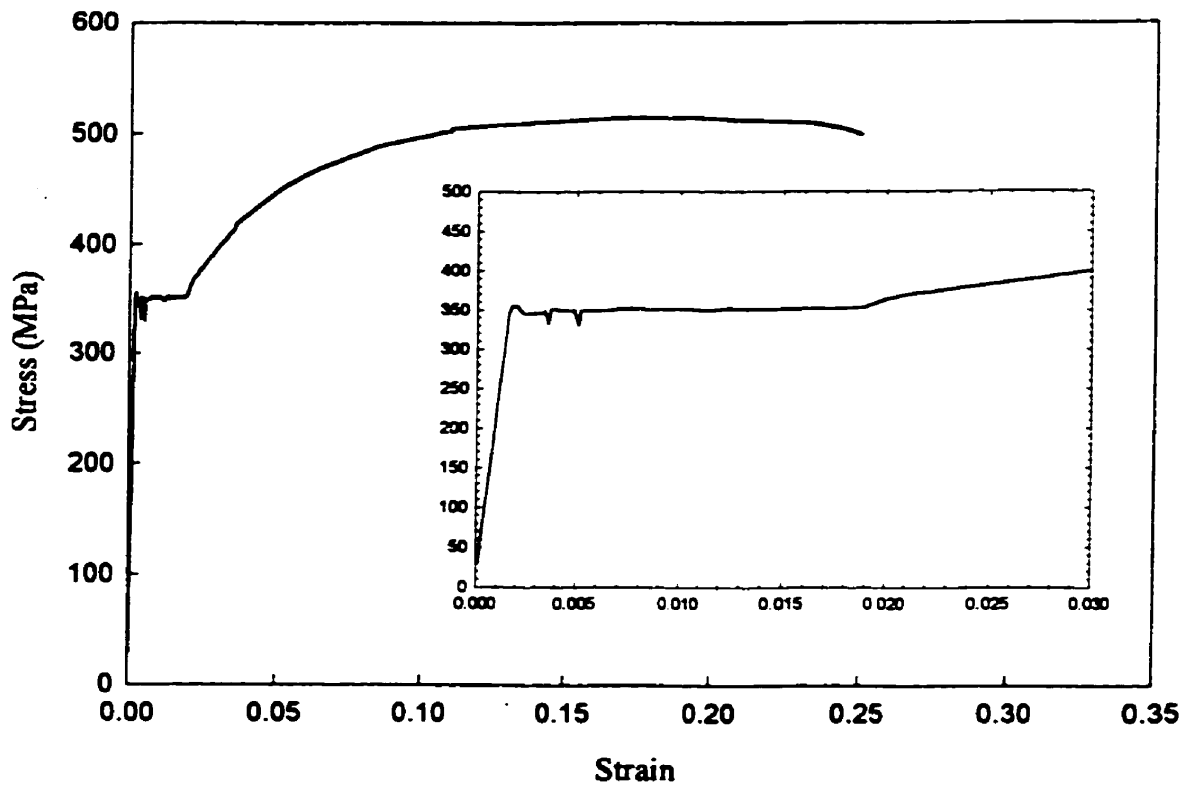


Fig. C9: Load Deformation Response of Coupon CA3 - Connection Angle

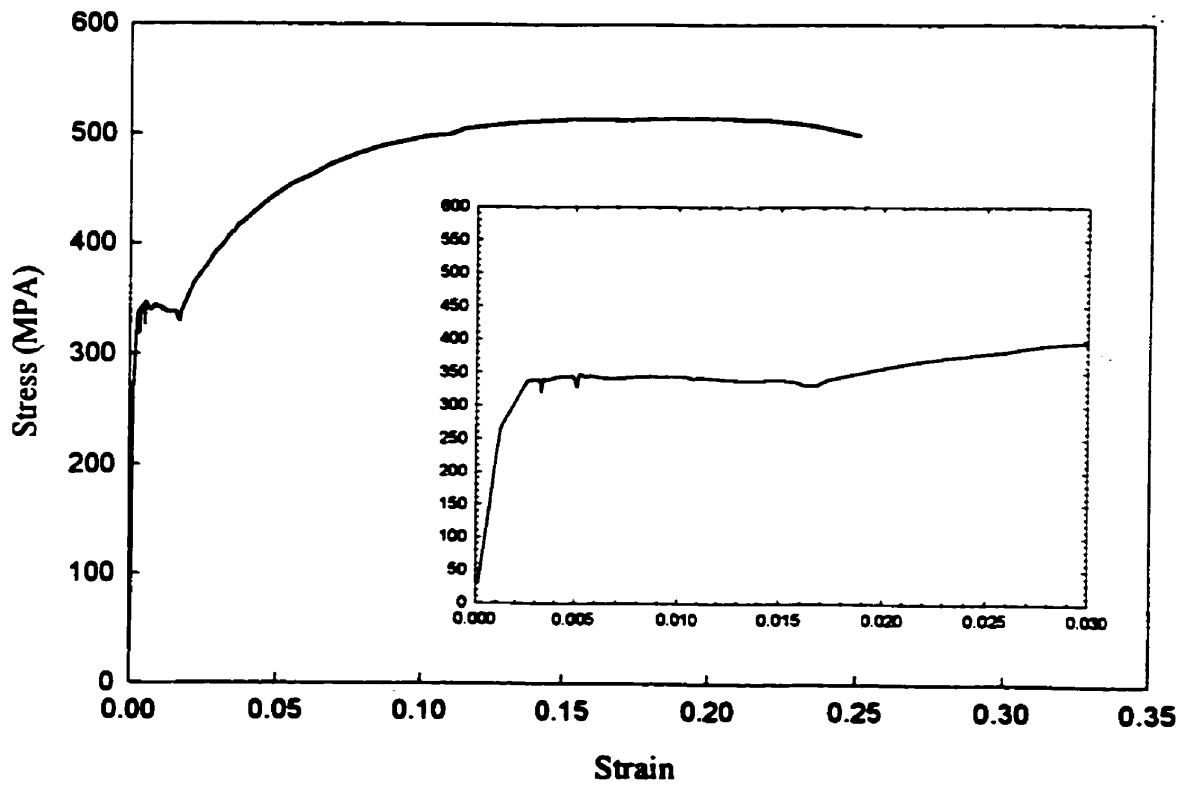


Fig. C10: Load Deformation Response of Coupon CA4 - Connection Angle

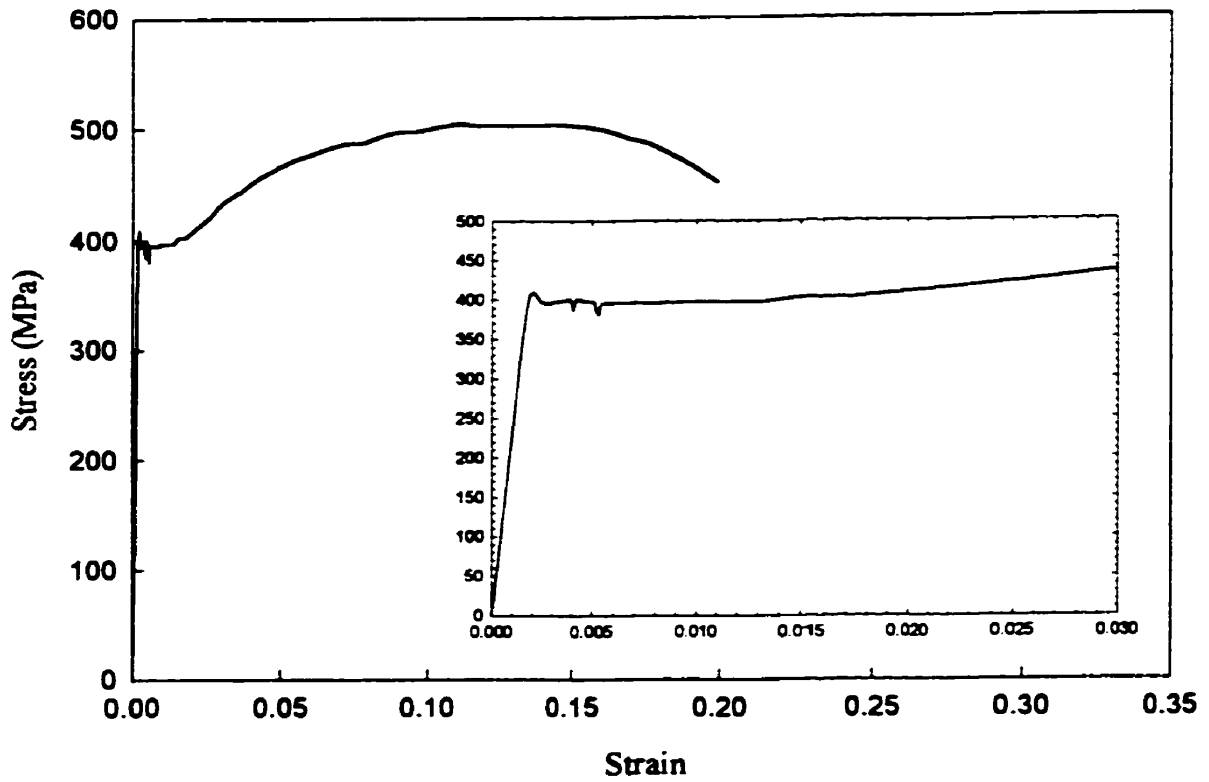


Fig. C11: Load Deformation Response of Coupon W410-1: Web of Load Beam

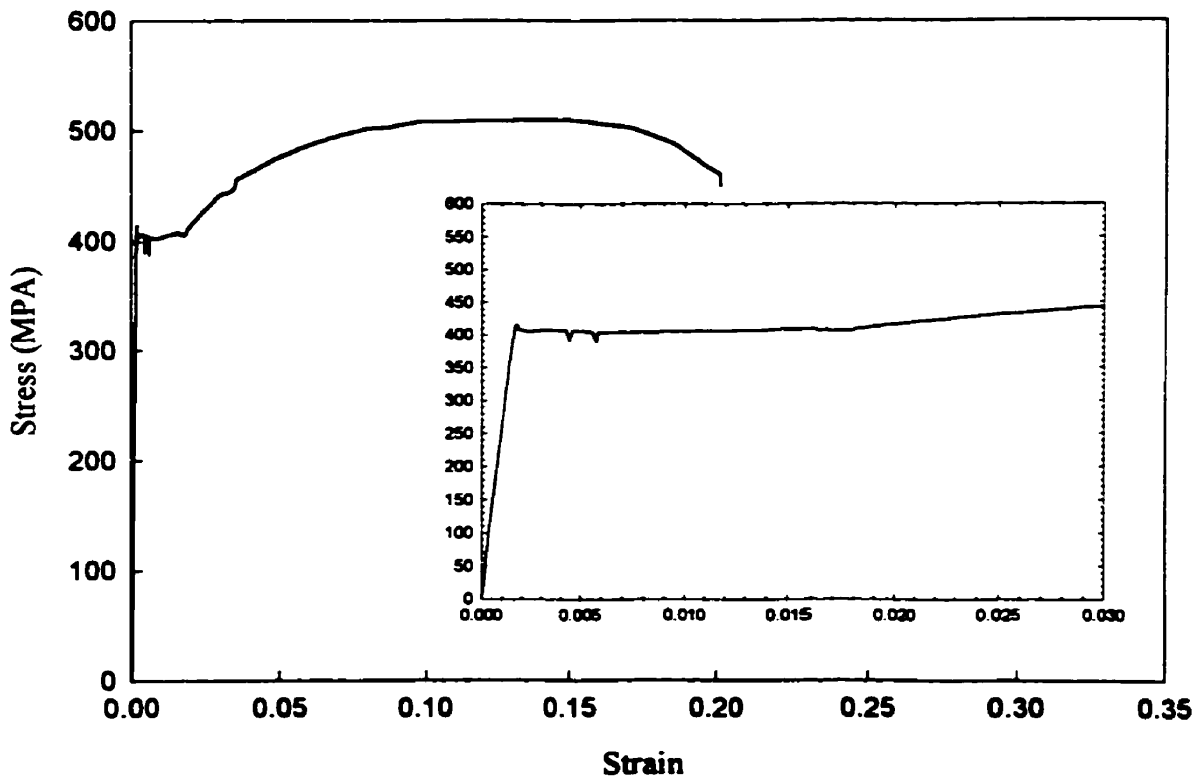


Fig. C12: Load Deformation Response of Coupon W410-2: Web of Load Beam

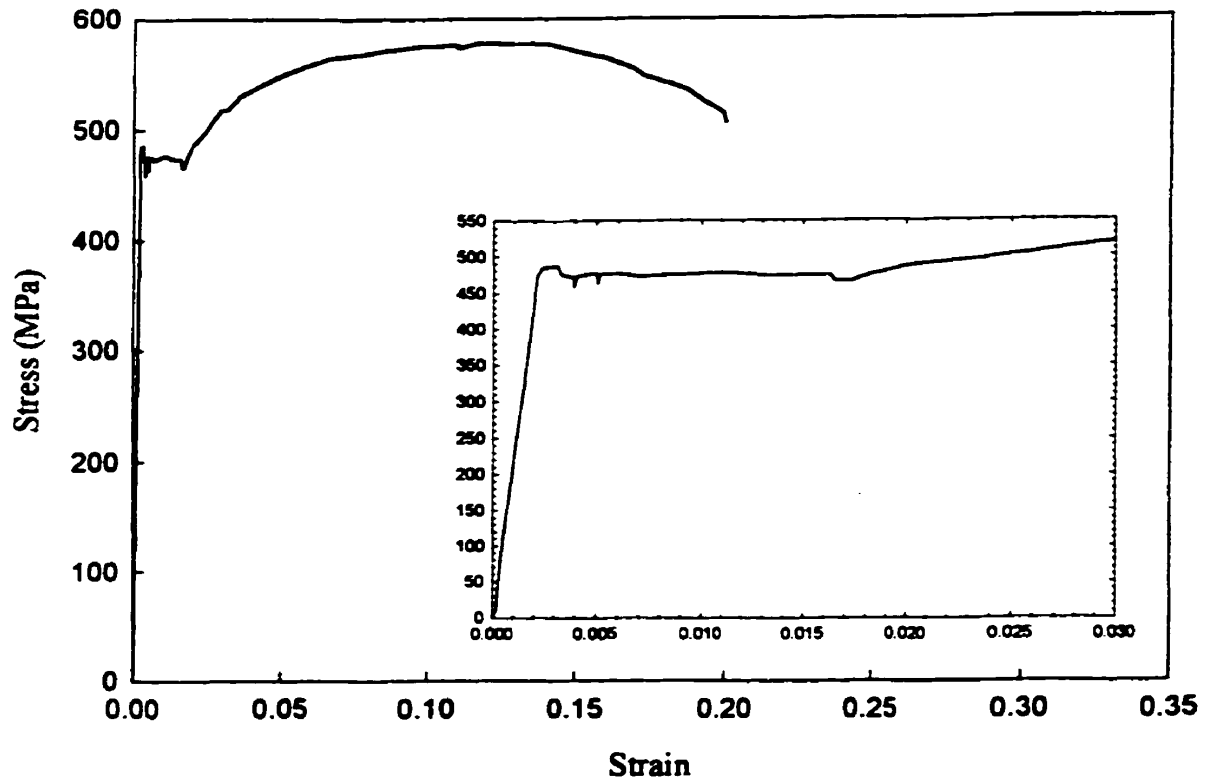


Fig. C13: Load Deformation Response of Coupon W530-1: Web of Load Beam

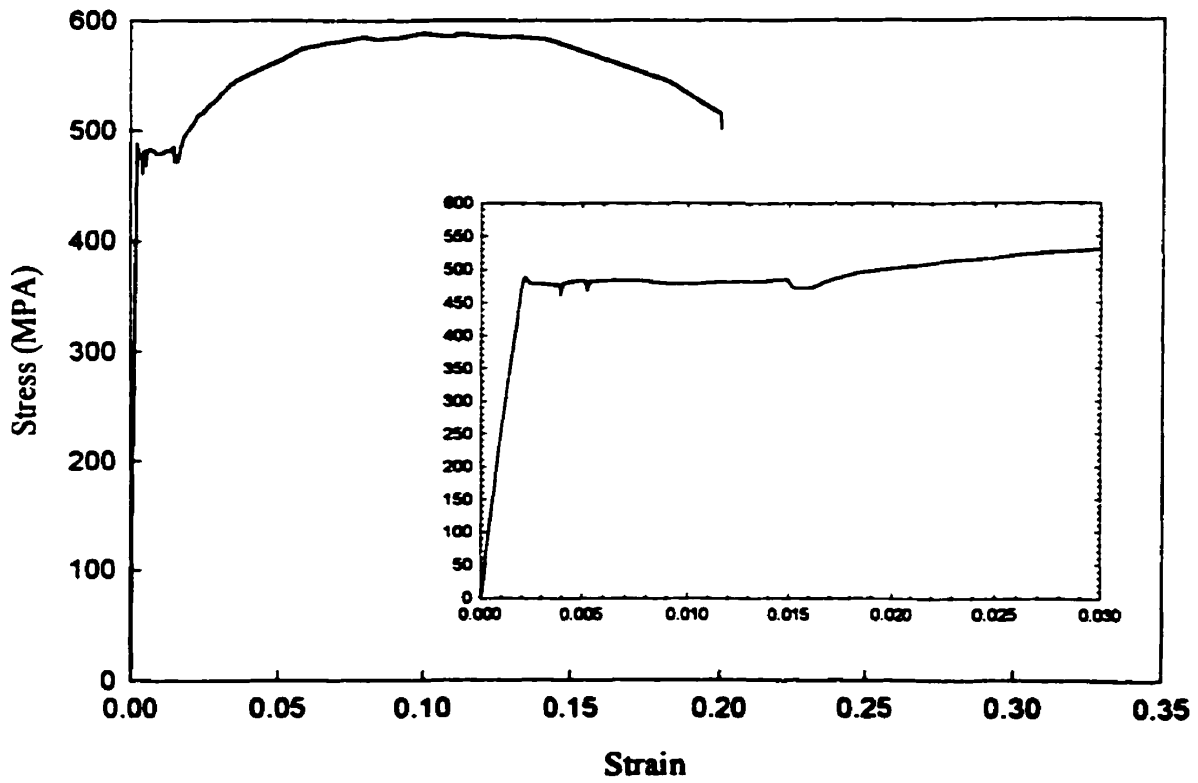


Fig. C14: Load Deformation Response of Coupon W530-2: Web of Load Beam

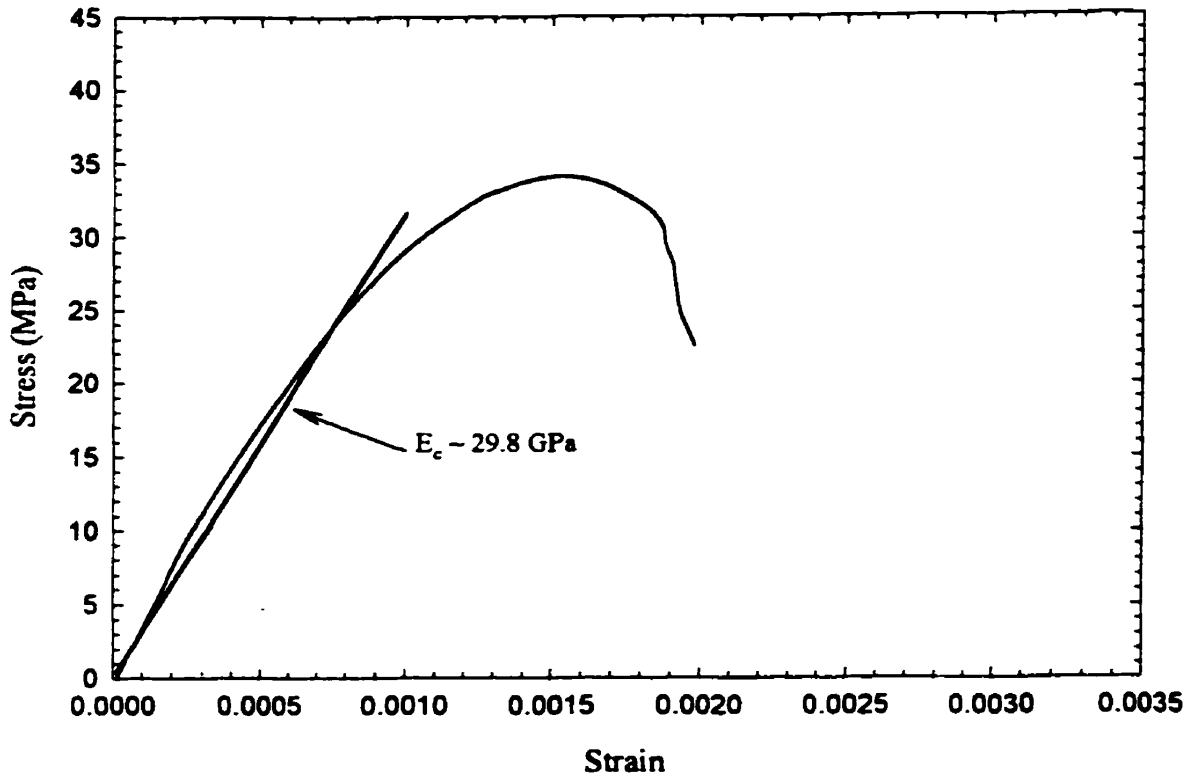


Fig. C15: Load-Deformation Response for Concrete Cylinder Batch 1- No. 1

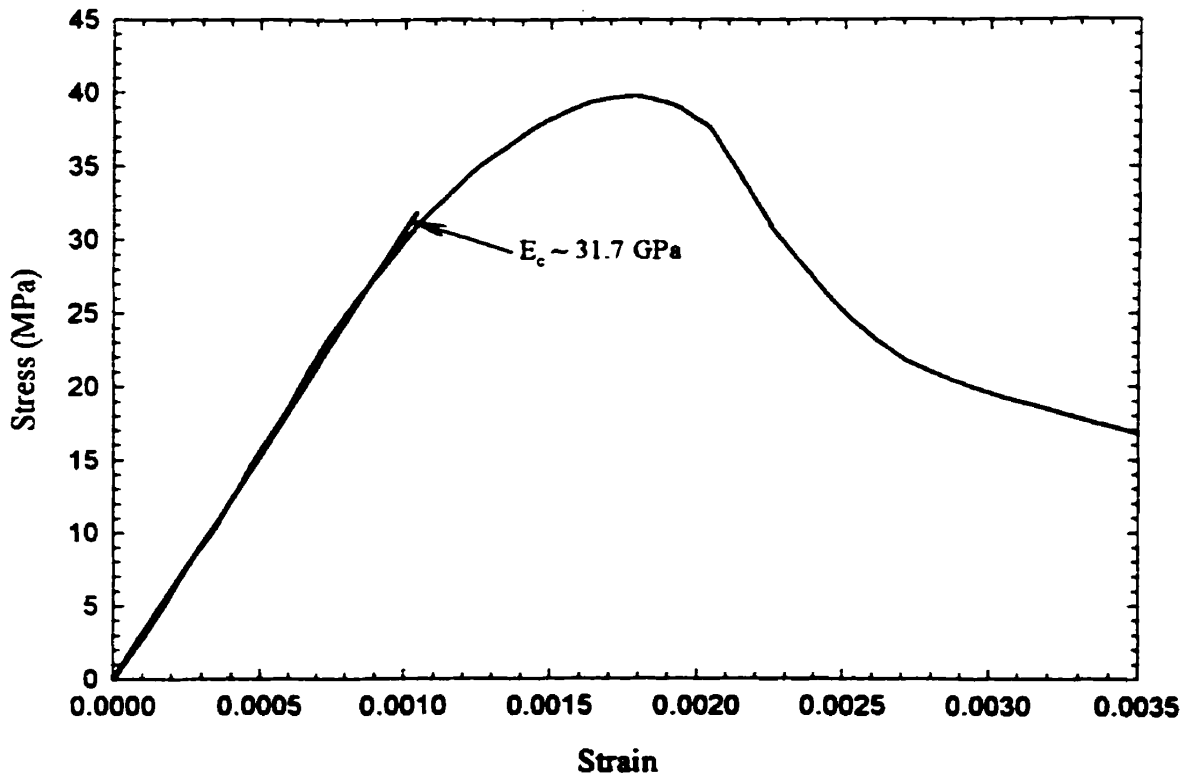


Fig. C16: Load Deformation Response for Concrete Cylinder Batch 1 - No. 2

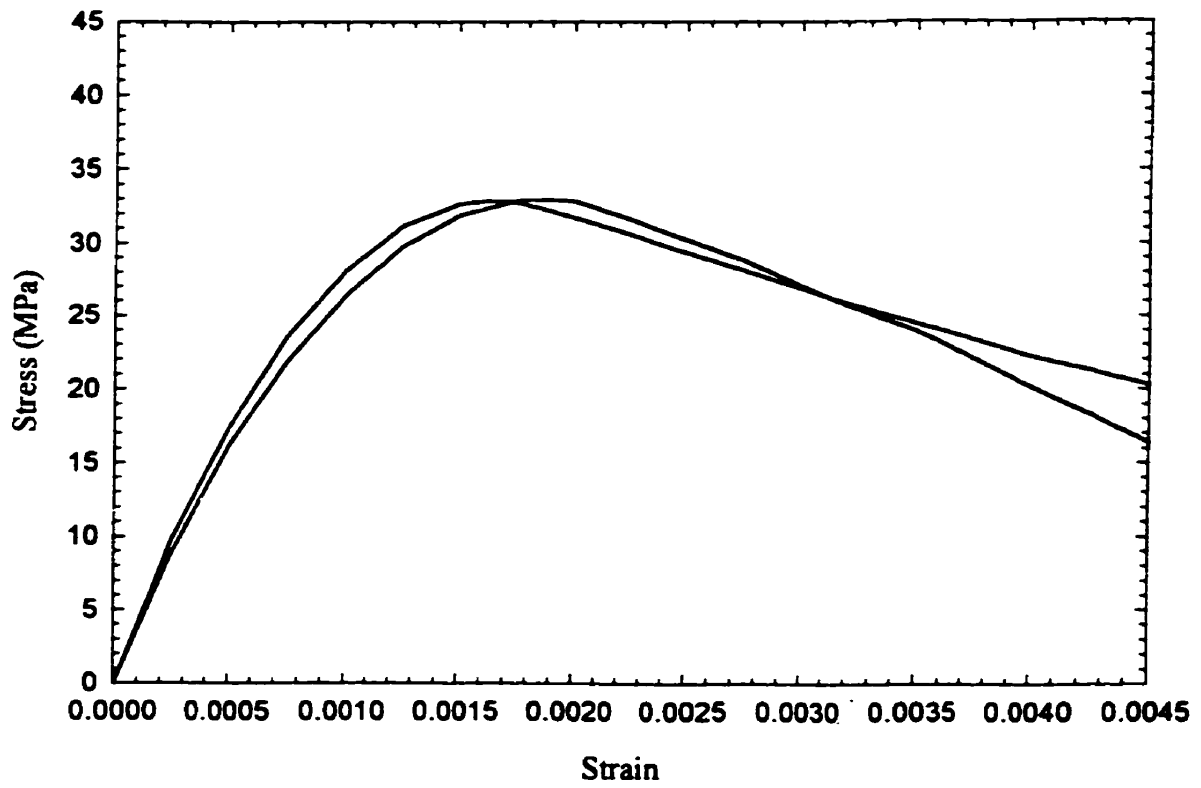


Figure C17: Load Deformation Response for Concrete Batch 2 - 40 d

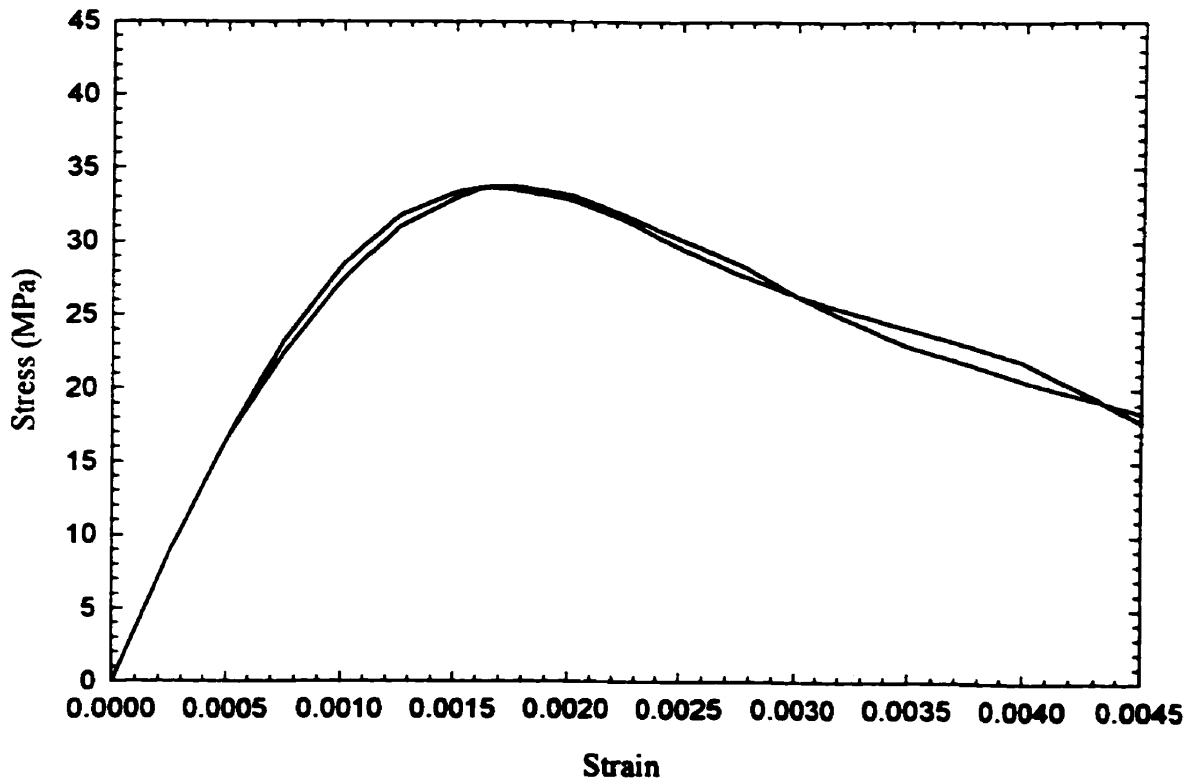


Figure C18: Load Deformation Response for Concrete Batch 2 - 90 d

APPENDIX D
Individual Test Results

D1 Summary of Appendix D

The data presented in the following pages does not provide a complete summary of the tests results: rather it includes data that has not been presented in the main body of this paper. For each specimen there is a single summary sheet summary provided; including such details as the test geometry and the various recorded observations. This is followed by a photo of the test specimen in the frame prior to loading, and schematic of the instrumentation used for that particular test.

For each test there are several data plots, which compliment the data presented in the main body of the report. For the composite tests this has been limited primarily to strain gauge data. For the non-composite specimens the load deformation response of the connection has been included, with strain gauge and LVDT data. The plots give test data only, so the reader must consult the instrumentation figure to interpret the results.

There are also several photos showing each of the specimens following the tests. It was attempted to make these photos as consistent as possible. Several of the photos appear in the main body of the report, but have been included for completeness.

Test No. 1: **C450-W410-SDA-NON**
FEB. 1, 1999

Description: 450 x 450 x 2234 mm Column Short Double Angle Connection
 W410 x 67 Load Beam 3 - 3/4" A325 Bolts (70% Yield).
 Non - Composite State Total Cleat Length = 190 mm

Testing Procedure: 1) Loaded the column to 700 kN (typical 1 story construction load)
 2) Proceeded to load the connection to 300 kN
 3) While maintaining the connection load, the axial load was increased until buckling failure occurred in the column.

Geometry: $A_1 = 590 \text{ mm}$ $d_{MTS} = 1330 \text{ mm}$
 $A_2 = 3836 \text{ mm}$ $L = 5330 \text{ mm}$

RESULTS:

<u>Dataset</u>	<u>Load Stage</u>	<u>Description</u>
134	Applied Axial Load = 1000 kN Connection Load = 300 kN	There was some distortion of the South East column flange, above the connection.
164	Applied Axial Load = 1505 kN Connection Load = 300 kN	Buckling in the top SE flange continues to become more pronounced. No visible buckling noted elsewhere.
172-173	Applied Axial Load = 1700 kN Connection Load = 300 kN	Buckling noticed in both the SW and NW flanges below the connection plate. Stress ~ 110 MPa
215	Applied Axial Load = 2526 kN Connection Load = 300 kN Total Column Load = 2826 kN	Load on column drops, test terminated.

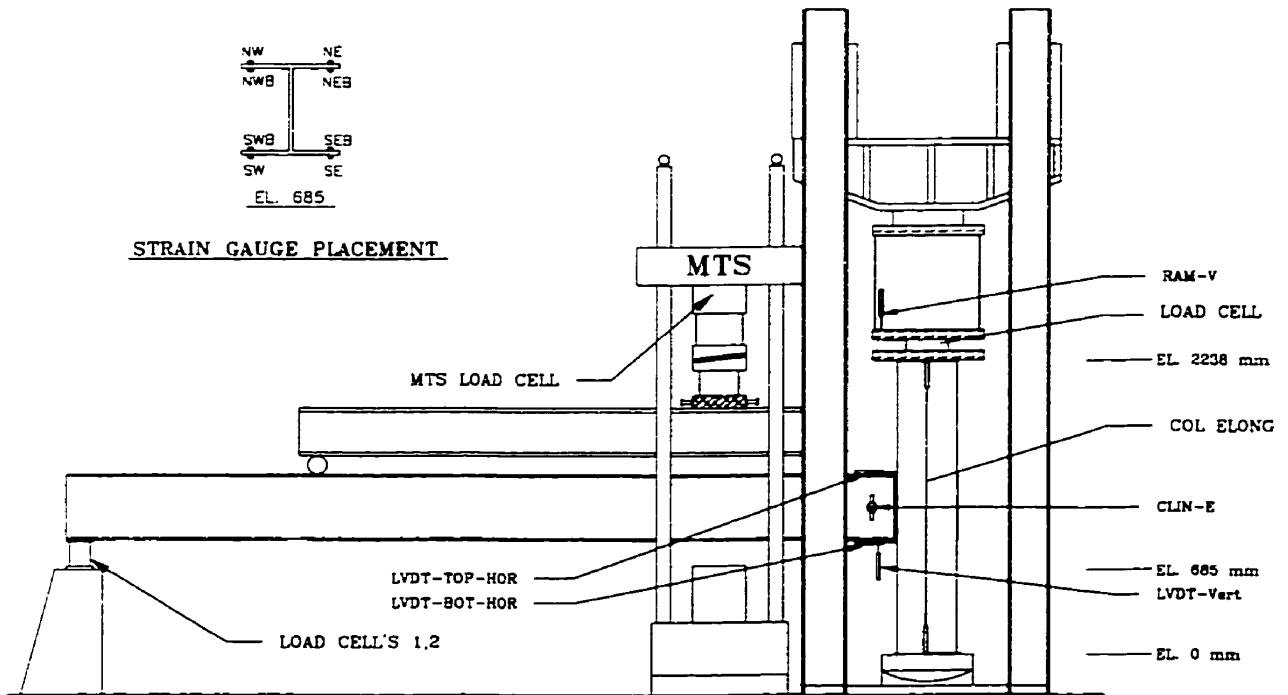
Comments:

Neither the top nor bottom of the column had Hydrostone grout capping, resulting in initial seating problems. The Hydrostone was not used since it appeared as if there was good contact between the column head and the top of the column. Buckling above the connection plate at relatively low axial loads (ie: 1200 kN) was likely due to the lack of grout.

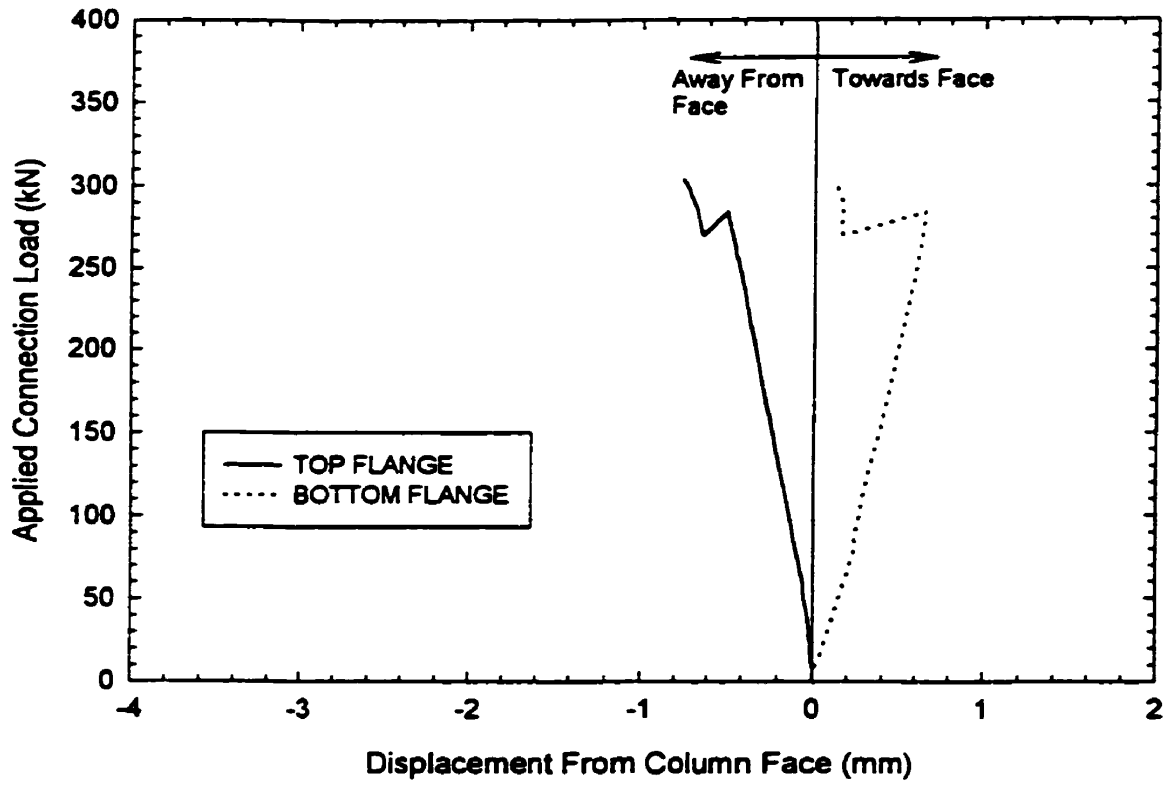
The first test was attempted three times, the first two being terminated early due to lateral displacement of the column. It was thought that friction alone would be adequate to sustain the horizontal forces at the column ends, but due to hydraulic oil between the specimen and the loading plates this frictional forces could not be mobilized. Thus, the horizontal bracing intended for use in the composite testing was installed. To accommodate the larger column shortening, a roller was used to brace the column at the top. The second attempt at Test 1 was terminated due to discrepancy between the axial load cell and the line pressure readings (due to incorrect range selection in the Data Acquisition).



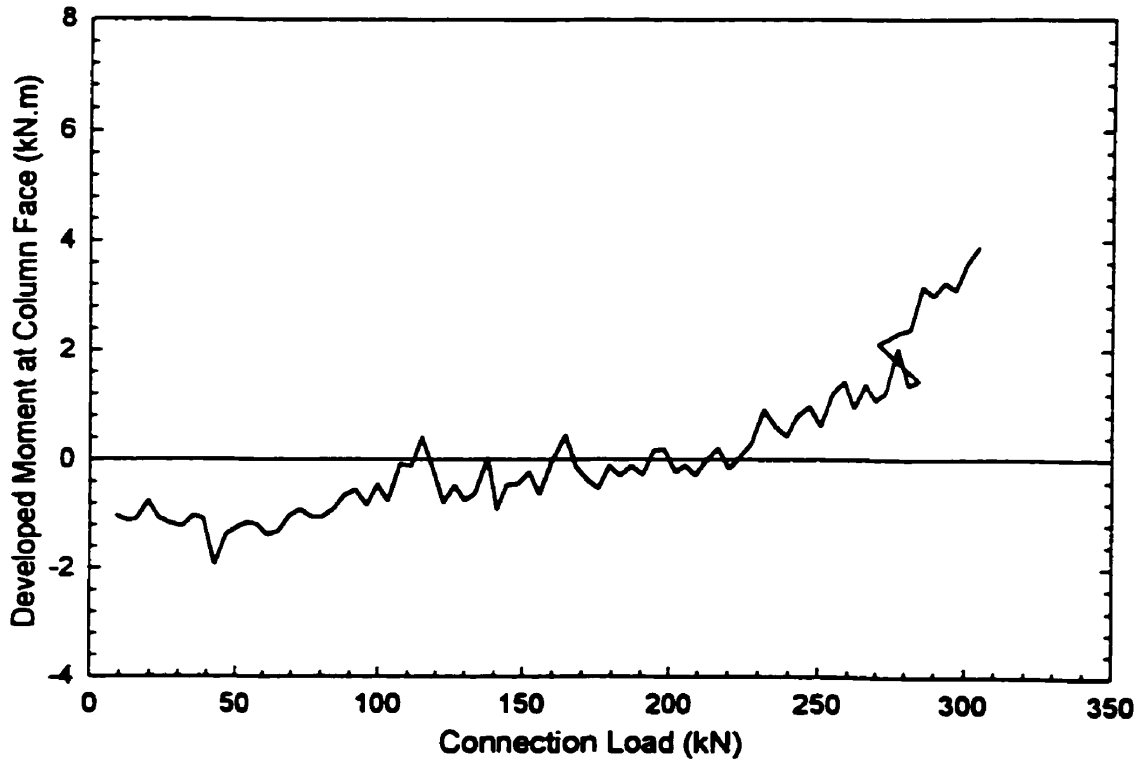
C450-W410-SDA-N: Photographic View of Test Set-up



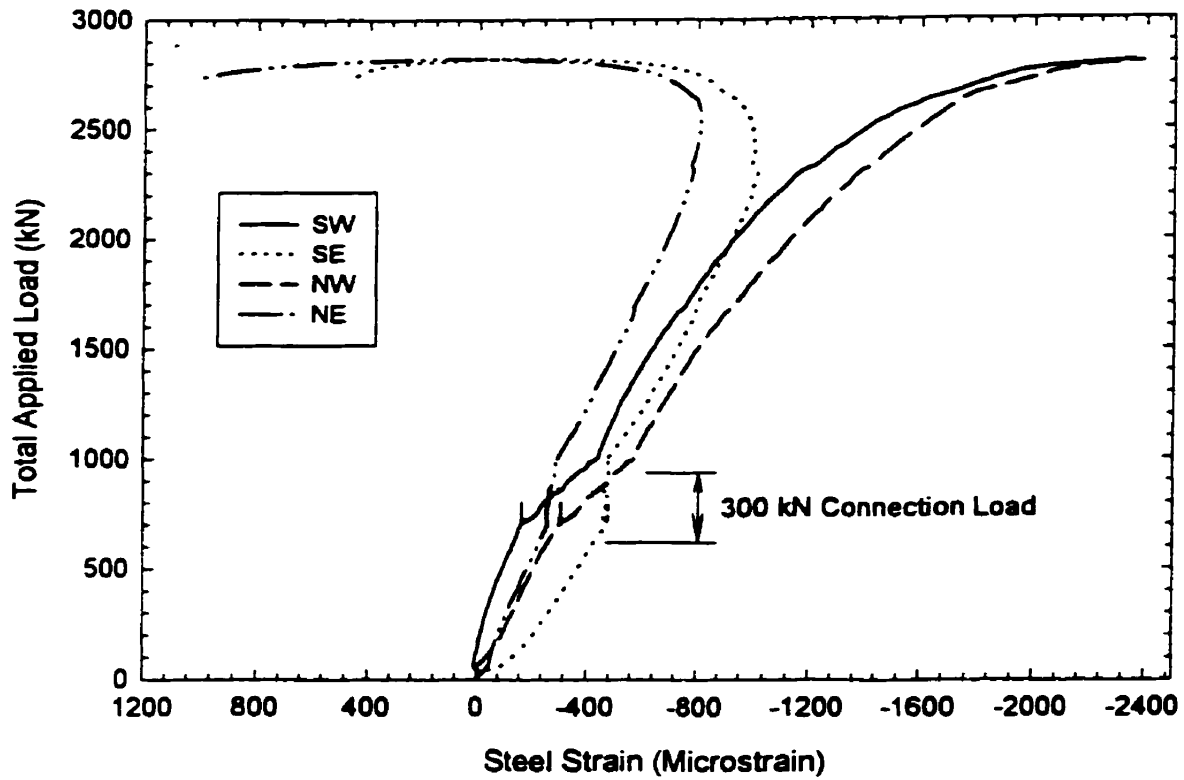
C450-W410-SDA-N: Instrumentation Layout of Test Specimen



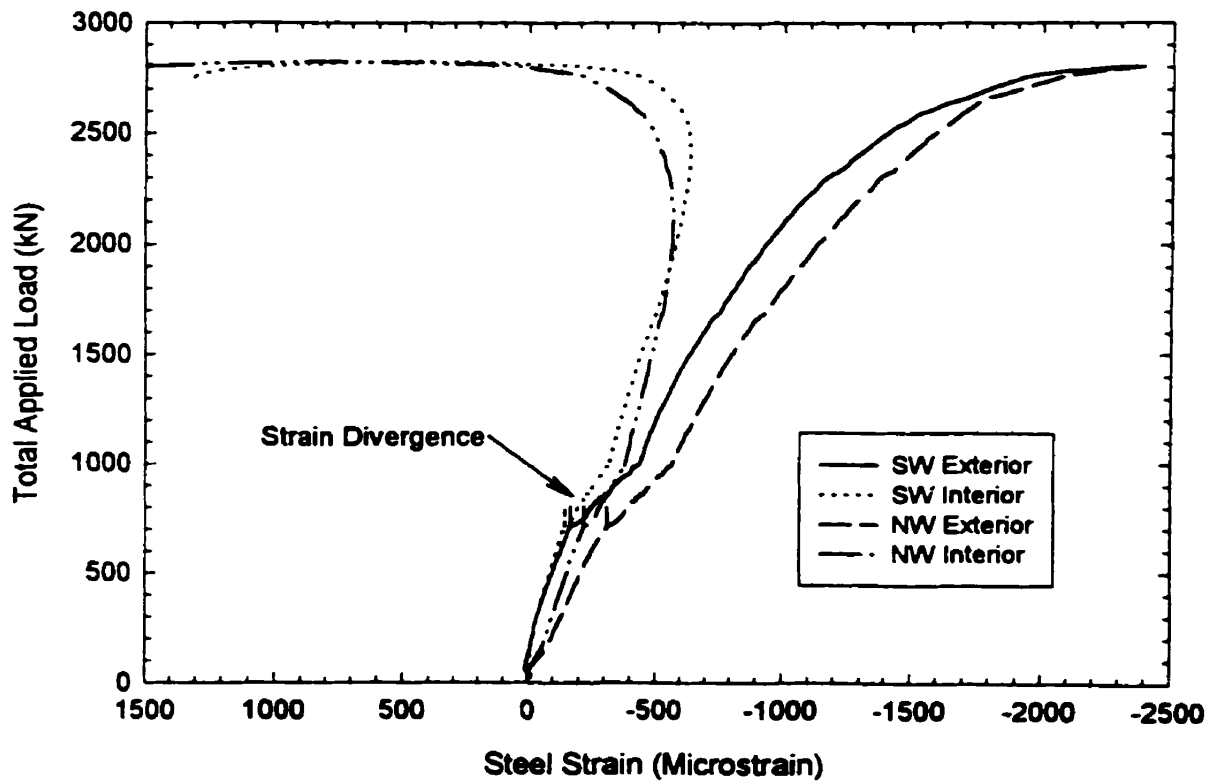
C450-W410-SDA-N: Applied Connection Load vs. Displacement of Beam Flange From Column Face



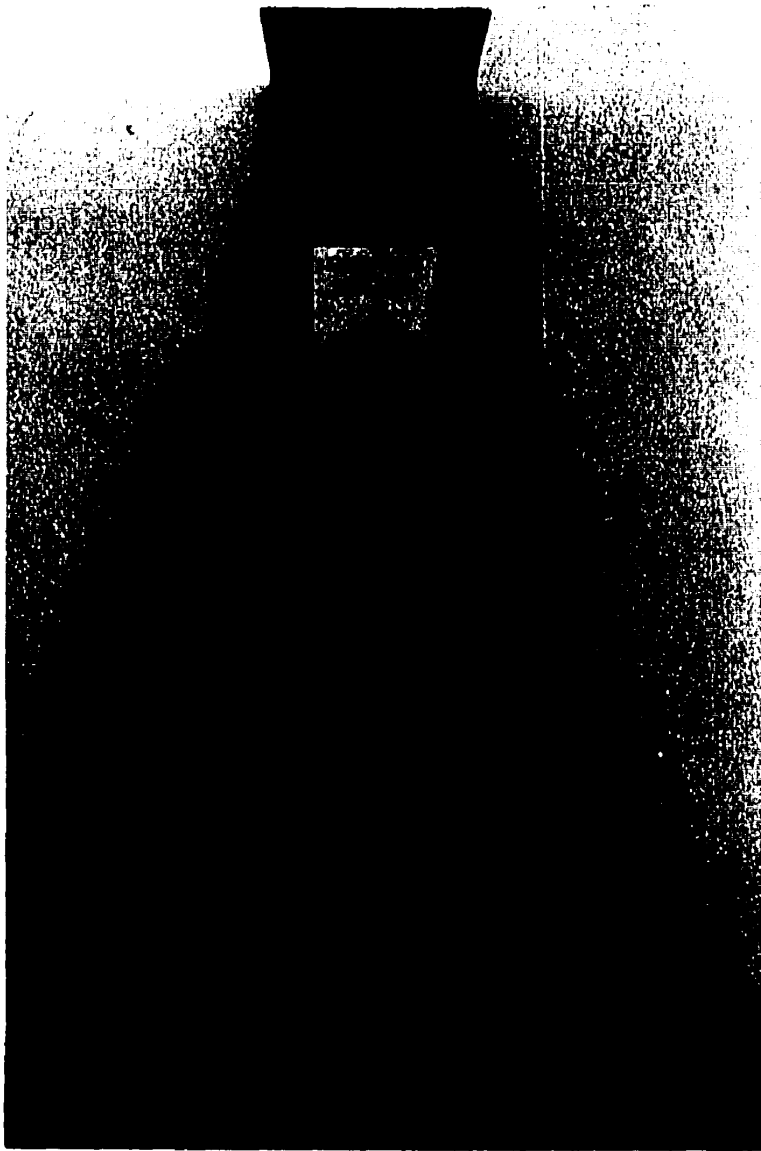
C450-W410-SDA-N: Developed Moment at Column Face vs. Connection Load



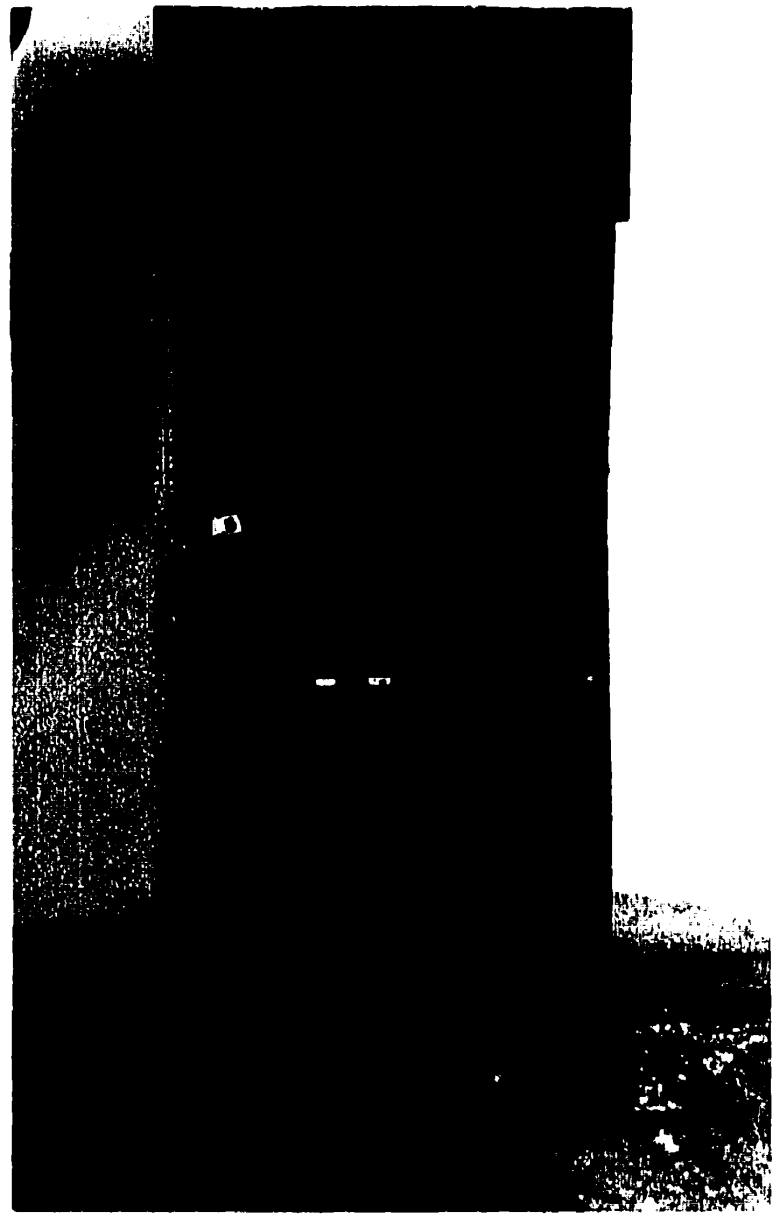
C450-W410-SDA-N: Total Applied Load vs. Strain 225 mm Below Connection (El. 685)



**C450-W410-SDA-N: Total Applied Load vs. Strain 225 mm Below Connection
West Side of Column, Interior and Exterior of Flange Tips**



C450-W410-SDA-N: Full View of Failed Specimen



C450-W410-SDA-N: View of Bottom West Quadrant

Test No. 2: C450-W410-SDA-COMP
FEB. 9, 1999

<u>Description:</u>	450 x 450 x 2234 mm Column W410 x 67 Load Beam Composite State	Short Double Angle Connection 3 - 3/4" A325 Bolts (70% Yield). Total Cleat Length = 190 mm
----------------------------	--	--

Testing Procedure:

- 1) Load the column to a nominal load of 4500 kN. This approximately represents 1.0 DL + 0.5 LL.
- 2) Proceed to load the connection unto failure

Geometry:

$A_1 = 595 \text{ mm}$	$d_{MFS} = 1330$
$A_2 = 3834$	$L = 5320$

RESULTS:

<u>Dataset</u>	<u>Load Stage</u>	<u>Description</u>
119	Applied Axial Load = 4500 kN	<ul style="list-style-type: none"> • Column exhibits linear response. No distortion evident in the concrete or steel.
155	Applied Axial Load = 4500 kN Connection Load = 252 kN	<ul style="list-style-type: none"> • Bolts Slipped • Separation of the connection plate and concrete obvious
179	Applied Axial Load = 4500 kN Connection Load = 330 kN	<ul style="list-style-type: none"> • 5 mm of separation observed between the connection plate and the concrete.
195	Applied Axial Load = 4500 kN Connection Load = 394 kN	<ul style="list-style-type: none"> • Yielding observed in the cleats, both sides
250	Applied Axial Load = 4500 kN Connection Load = 452 kN	<ul style="list-style-type: none"> • Reset Vertical Beam LVDT
301	Applied Axial Load = 4500 kN Connection Load = 478 kN Total Applied Load = 4978 kN	<ul style="list-style-type: none"> • Test Terminated - Bearing/Tearing Failure of the connection • No distortion of the test column, aside from the connection plate was observed.

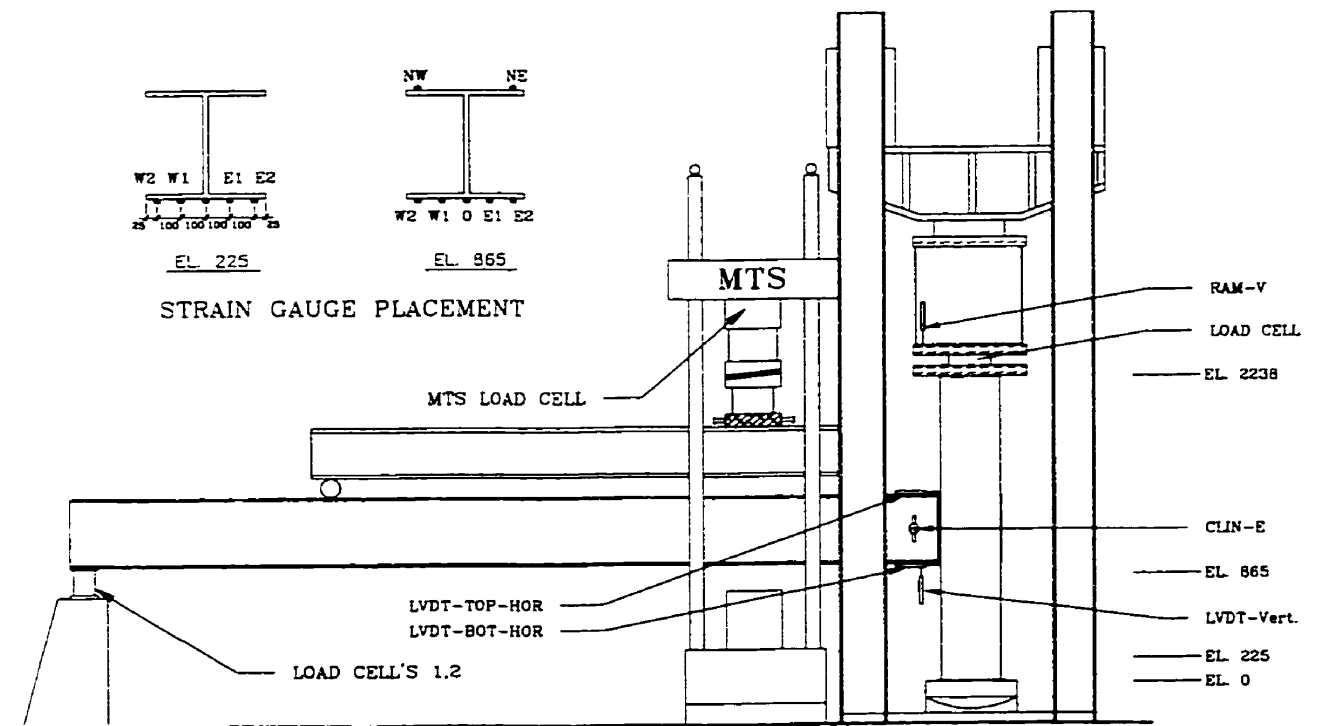
Comments:

Hydrostone was placed between the top end plate and the loading plate. Unlike other composite columns tested, the first prototype column specimen (Tests: C600-W410-SDA-C and C600-W410-LDA-C) had the column cap plate welded back onto the specimen. This plate was removed for the concrete casting. The heat generated by the welding caused a separation between the concrete and steel near the top of the column. This seemed to have no effect on the results.

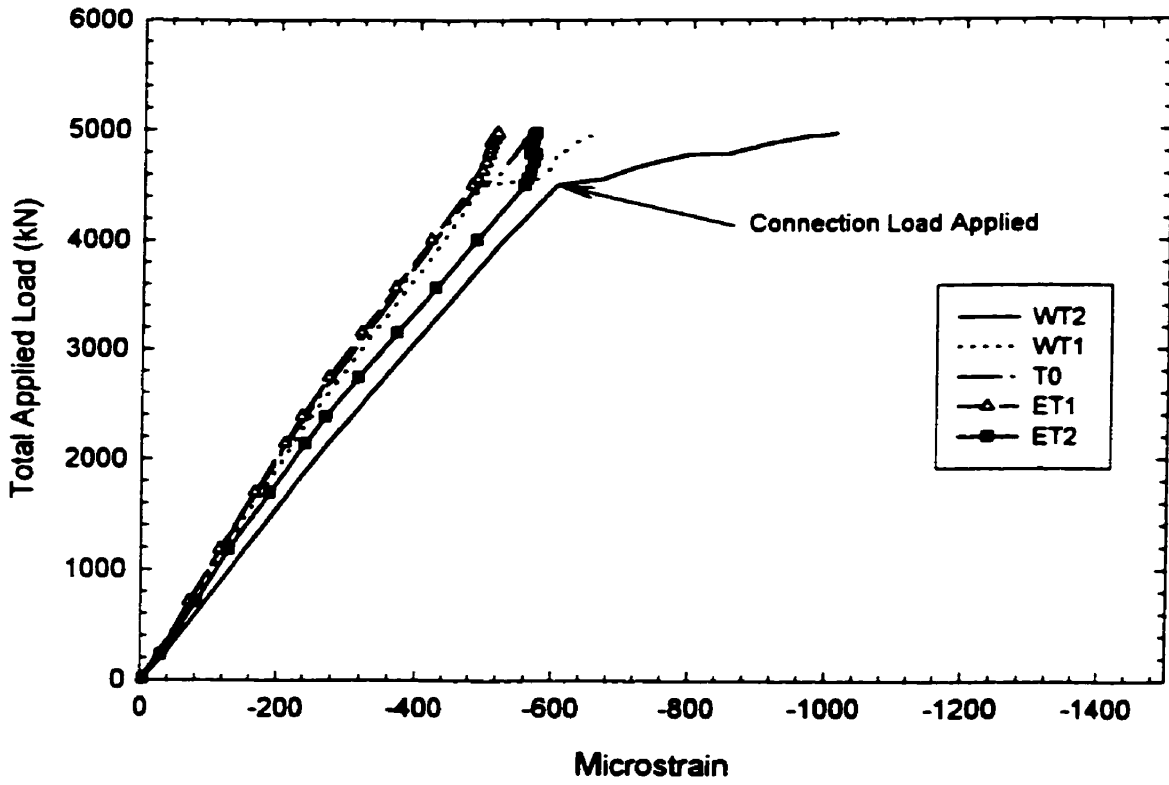
There was considerable movement of the load beam. The far end roller moved about 1/8 of a revolution, about 20 mm longitudinally.



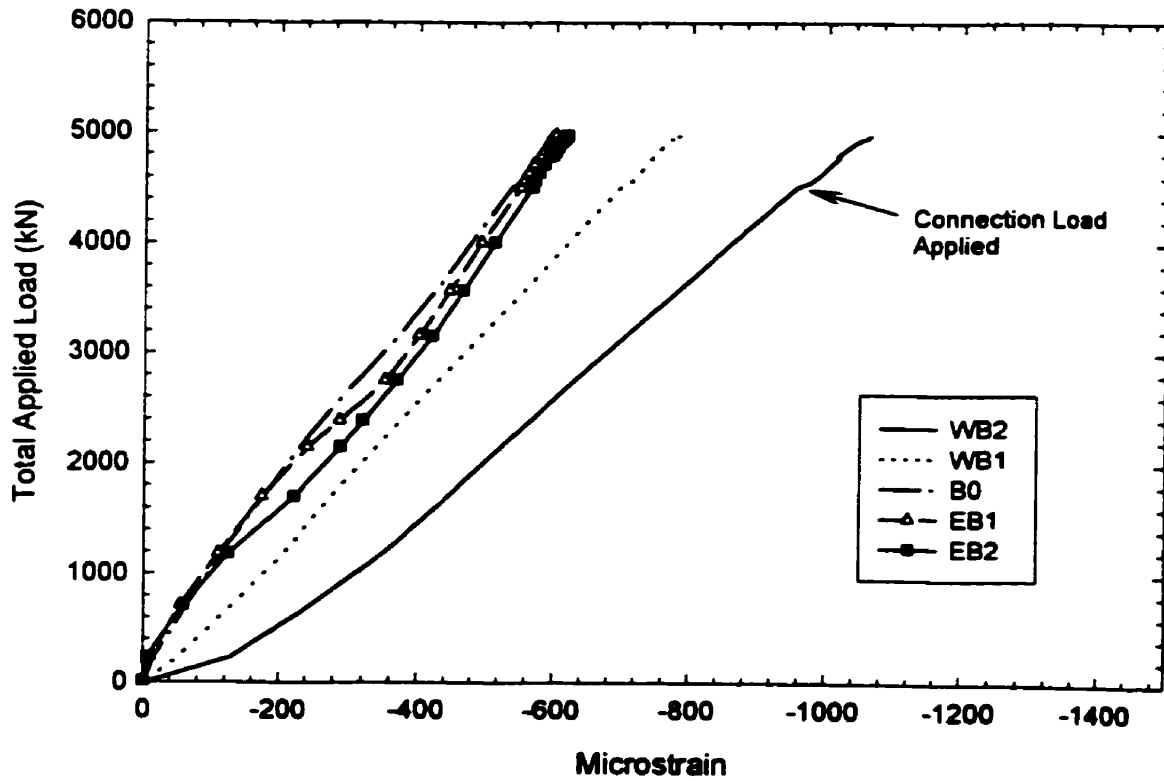
C450-W410-SDA-C: Photographic View of Test Set-up



C450-W410-SDA-C: Instrumentation Layout of Test Specimen



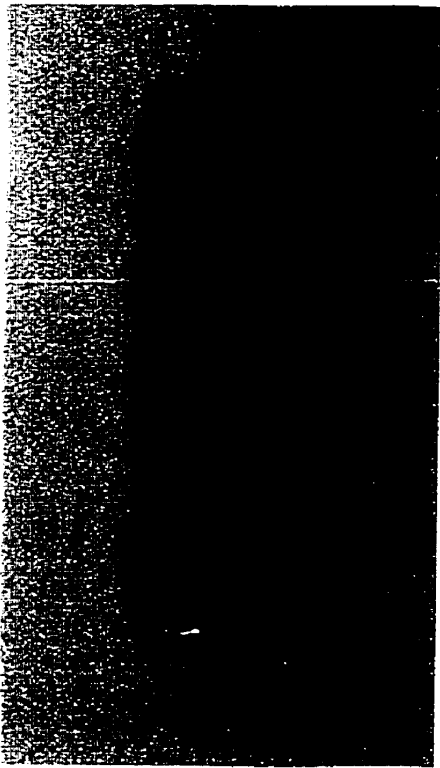
C450-W410-SDA-C: Total Applied Load vs. Strain 50 mm Below Connection (El. 865)



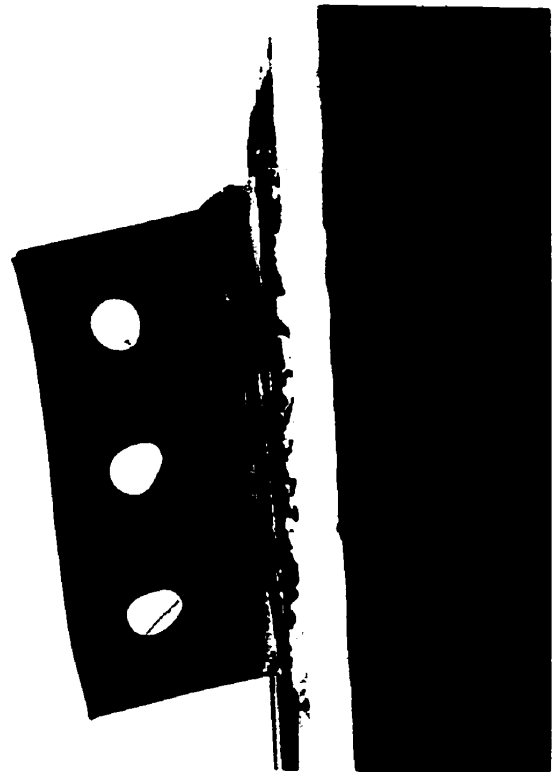
C450-W410-SDA-C: Total Applied Load vs. Strain 685 mm Below Connection (El. 225)



**C450-W410-SDA-C: Oblique View of Connection Area-
Note Separation Between Connection Plate and Concrete**



**C450-W410-SDA-C: Beam Web Showing
Bolt Hole Distortion**



**C450-W410-SDA-C: Connection Side
Profile – Note Tear at Weld and Bolt Hole**

Test No. 3: C450-W410-LDA-COMP
FEB. 9, 1999

Description: 450 x 450 x 2234 mm Column Long Double Angle Connection
W410 x 67 Load Beam 3 - 3/4" A325 Bolts (70% Yield).
Composite State Total Cleat Length = 250 mm

Testing Procedure:

- 1) Load the column to a nominal load of 4500 kN. This approximately represents 1.0 DL + 0.5 LL.
- 2) Proceed to load the connection unto failure.
- 3) This was the second and last test with this column specimen. Since the connection had not ruptured (it was essentially failed due to excessive deformation) the connection load was reduced and the axial column load increased to jack limits.

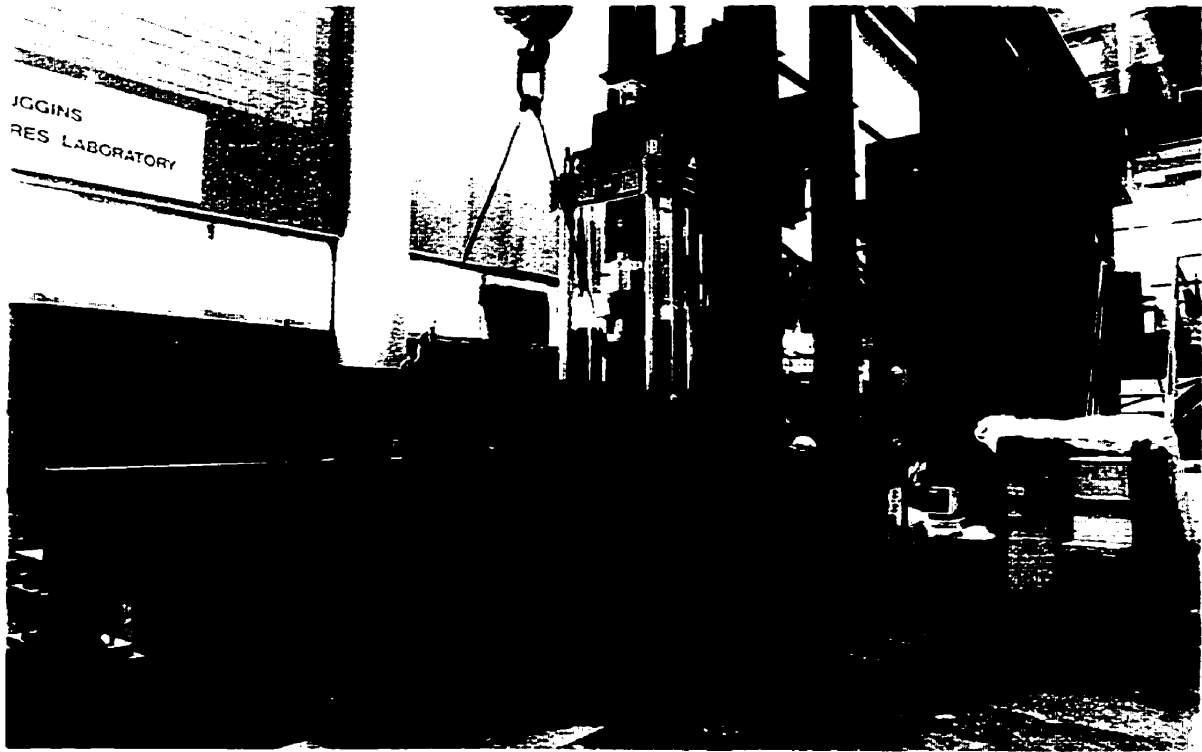
Geometry: $A_1 = 565 \text{ mm}$ $d_{\text{MTS}} = 1330 \text{ mm}$
 $A_2 = 3870$ $L = 5350 \text{ mm}$

<u>Dataset</u>	<u>Load Stage</u>	<u>Description</u>
89	Applied Axial Load = 4500 kN	<ul style="list-style-type: none"> • Column exhibits elastic response. No distortion evident in the concrete or steel.
128	Applied Axial Load = 4500 kN Connection Load = 300 kN	<ul style="list-style-type: none"> • Bolts Slipped
140	Applied Axial Load = 4500 kN Connection Load = 412 kN	<ul style="list-style-type: none"> • No yielding observed in cleats • Separation observed between the connection plate and the concrete.
160	Applied Axial Load = 4500 kN Connection Load = 470 kN	<ul style="list-style-type: none"> • Yielding observed at bolt line
186	Applied Axial Load = 4500 kN Connection Load = 530 kN	<ul style="list-style-type: none"> • Yielding observed in both legs
241	Applied Axial Load = 4500 kN Connection Load = 608 kN	<ul style="list-style-type: none"> • Beam Vertical LVDT Adjusted
256	Applied Axial Load = 4500 kN Connection Load = 620 kN	<ul style="list-style-type: none"> • Shear Distortion of Beam Observed (0.96 V_r)
319	Applied Axial Load = 4500 kN Connection Load = 650 kN Total Applied Load = 5150 kN	<ul style="list-style-type: none"> • Connection is essentially failed, excessive deformation.
334-392	Column Load reduced and brought back up to 4500 kN. Connection load dropped to 410 kN	<ul style="list-style-type: none"> • Delay caused by increasing hydraulic pressure for Fox Jack
438	Applied Axial Load = 6005 kN Connection Load = 410 kN Total Applied Load = 6415 kN	<ul style="list-style-type: none"> • Test Terminated - Bearing/Tearing Failure of the connection. Fox Jack capacity exceeded, with no distortion of the column

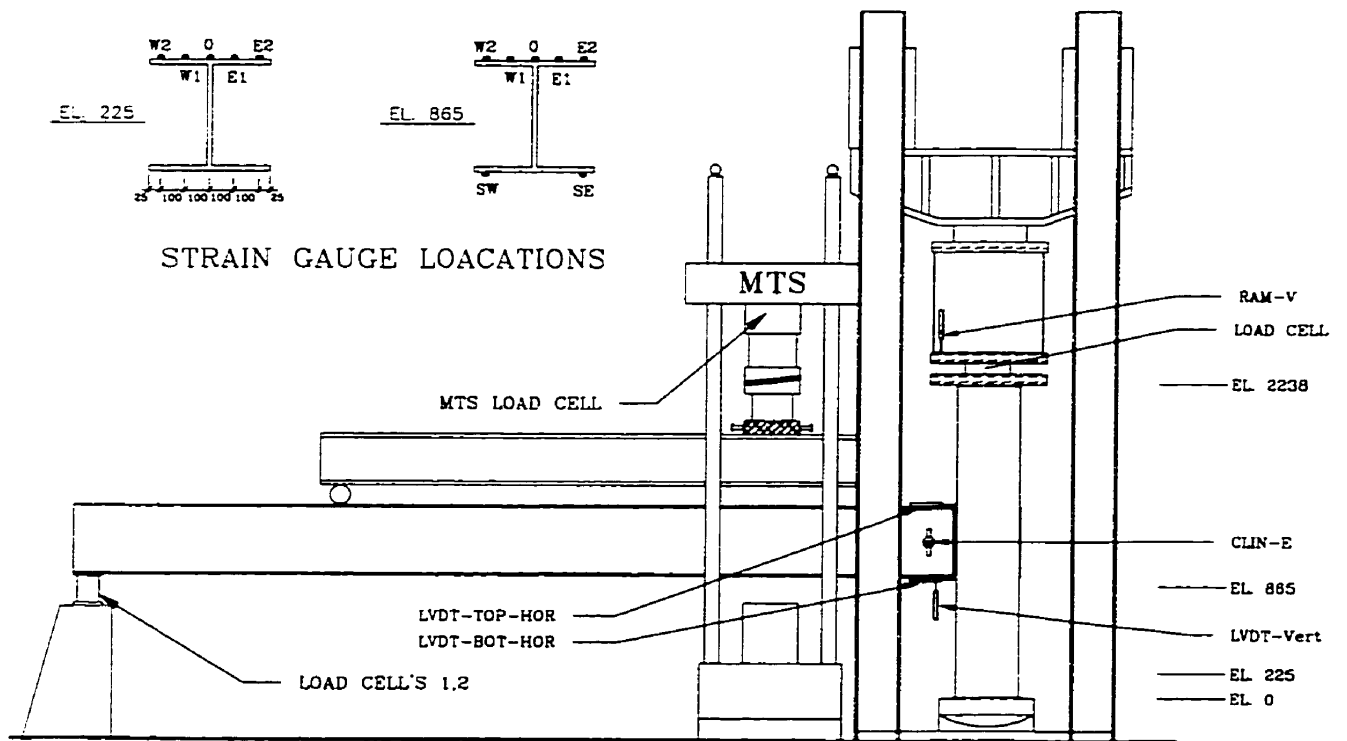
Comments:

During the test the MTS tie down frame was monitored as well as the effectiveness of the lateral beam braces. The MTS tie down did not show any visible sign of distress. At a MTS load of 450 kN the lateral bracing system at the column face was mobilized, whereas the outer bracing system was still loose (as installed). The latter brace became effective as the MTS load was increased (checked at 800 kN).

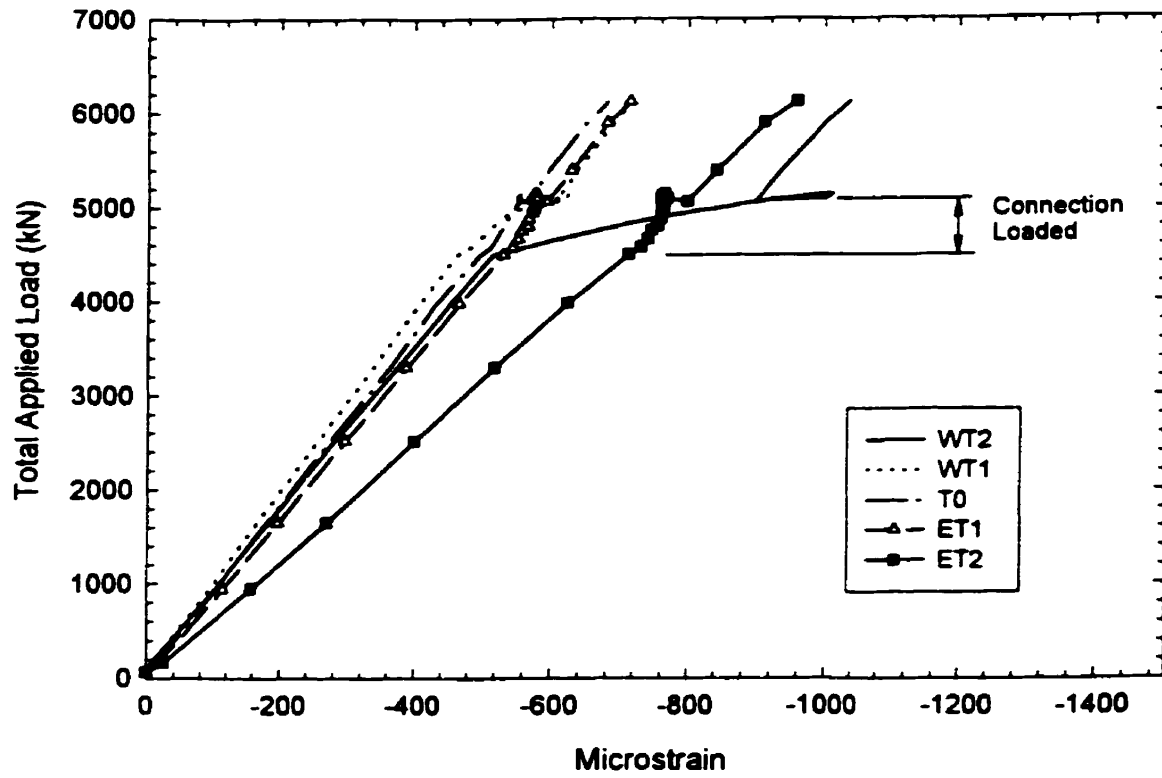
For this test a strain gauge was placed on the test beam, on the bottom flange near the east roller. The maximum strains reached in the beam were on the order of 0.78 ϵ_y . This corresponded well with the calculated strain levels. There was no distress caused in the column at the increased load levels. The load was limited to 6100 kN as this was the capacity of the Fox Jack pump. For later test a second higher capacity pump was used.



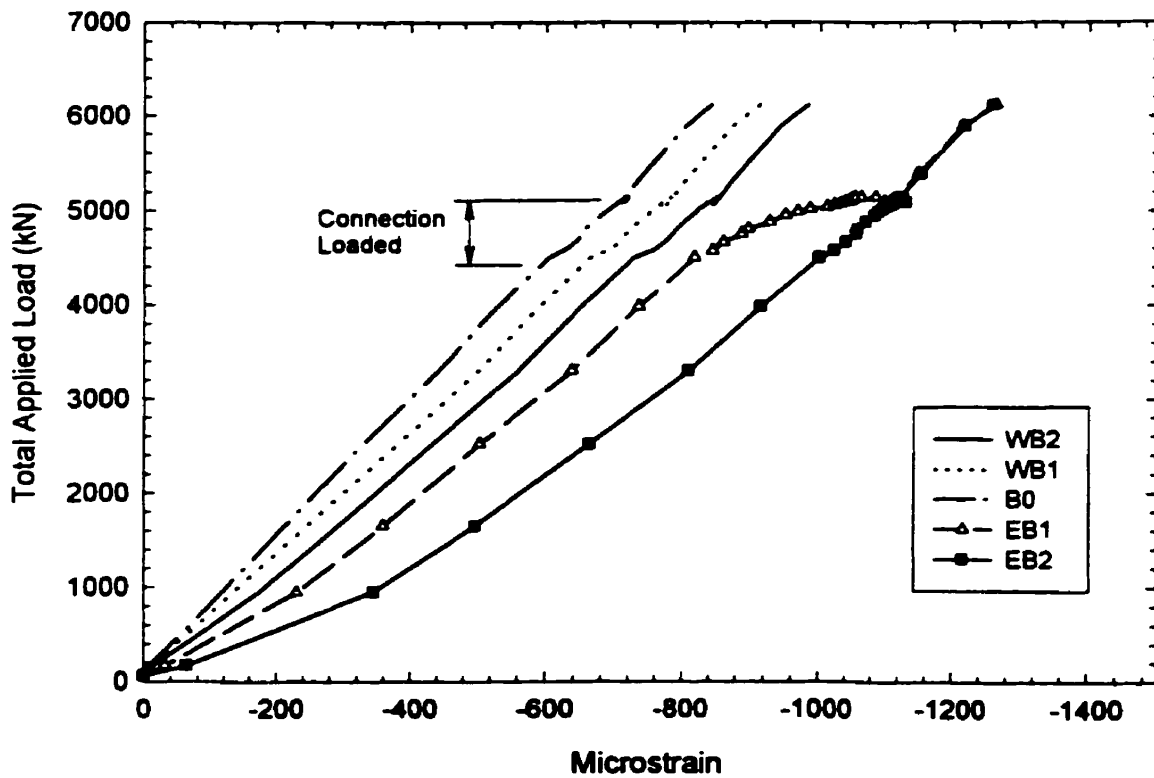
C450-W410-LDA-C: Photographic View of Test Set-up



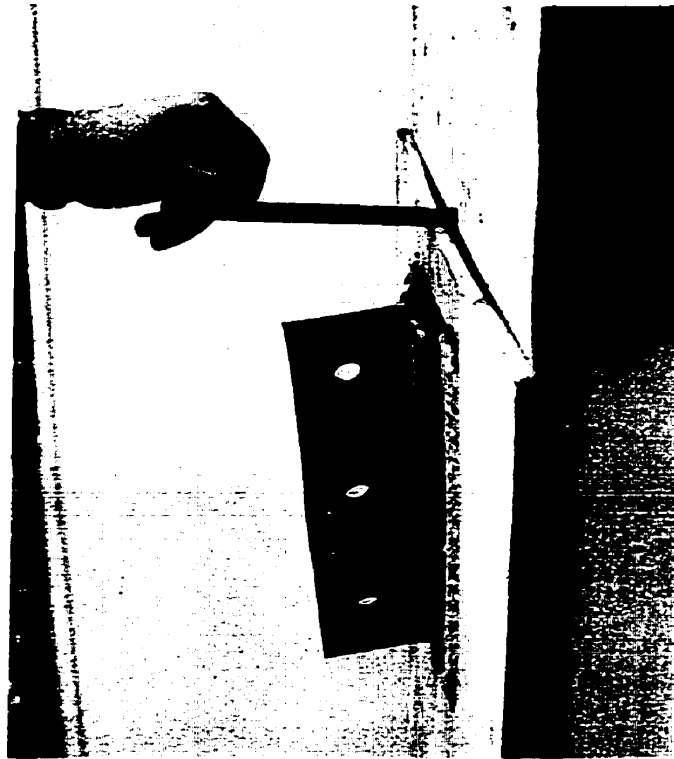
C450-410-LDA-C: Instrumentation Layout of Test Specimen



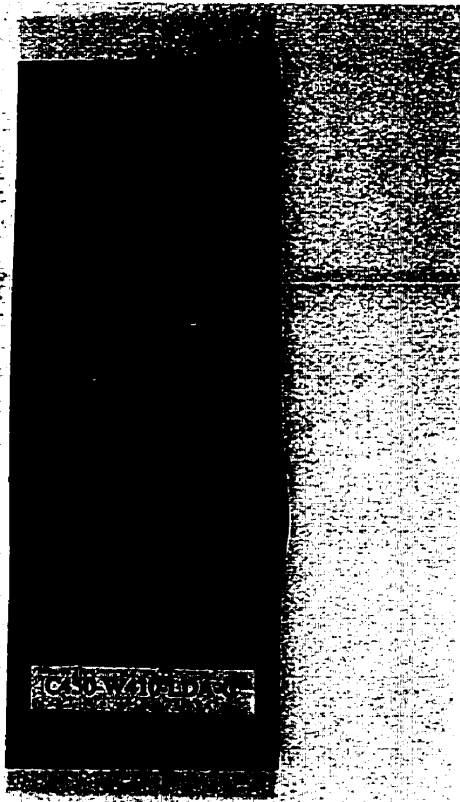
C450-W410-LDA-C: Total Applied Load vs. Strain 50 mm Below Connection (El. 865)



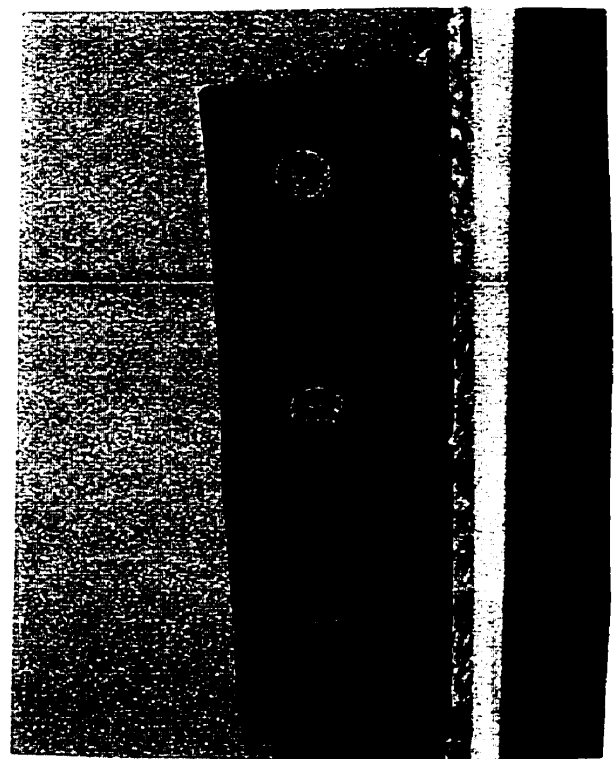
C450-W410-LDA-C: Total Applied Load vs. Strain 685 mm Below Connection (El. 225)



**C450-W410-LDA-C: Oblique View of Connection Area-
Note Separation Between Connection Plate and Concrete**



**C450-W410-LDA-C: Beam Web Showing
Bolt hole Distortion**



**C450-W410-LDA-C: Side Profile of
Connection – Note Tear at Weld**

Test No. 4: C450-W530-LDA-NON
FEB. 23, 1999

<u>Description:</u>	450 x 450 x 2358 mm Column W530 x 92 Load Beam Non - Composite State	Long Double Angle Connection 3 - 3/4" A325 Bolts (70% Yield). Total Cleat Length = 325 mm
----------------------------	--	---

Testing Procedure:

- 1) Loaded the column to 700 kN (representing a typical 1 story construction load).
- 2) Proceeded to load the connection to a construction load of 375 kN
- 3) While maintaining the connection load, axial load was increased until buckling failure of the column occurred.

Geometry: $A_1 = 625\text{mm}$ $d_{\text{MTS}} = 1320\text{ mm}$
 $A_2 = 4227\text{ mm}$ $L = 7015\text{ mm}$

RESULTS:

<u>Dataset</u>	<u>Load Stage</u>	<u>Description</u>
15	Axial Load = 690 kN $V_{\text{app}} = 5\text{ kN}$ (initial load of beam + spreader)	<ul style="list-style-type: none"> ● Prior to loading the connection there was no noticeable distortion
38	Axial Load = 700 kN $V_{\text{app}} = 190\text{ kN}$	<ul style="list-style-type: none"> ● Bolts Slipped
62	Axial Load = 700 kN $V_{\text{app}} = 360\text{ kN}$	<ul style="list-style-type: none"> ● No Visible Distortion ● Column End Bracing (Bottom only) is not effective. Lateral beam bracing adjacent to the connection is effective.
65	Axial Load = 700 kN $V_{\text{app}} = 375\text{ kN}$	<ul style="list-style-type: none"> ● Column Load increased, the MTS load was still on displacement control $V_{\text{app}} \pm 10\text{ kN}$
84	Axial Load = 1250 kN $V_{\text{app}} = 375\text{ kN}$	<ul style="list-style-type: none"> ● No Visible Distortion
99	Axial Load = 1680 kN $V_{\text{app}} = 375\text{ kN}$	<ul style="list-style-type: none"> ● Observed a buckling pattern in column flanges below the connection on the west side only.
103	Axial Load = 1850 $V_{\text{app}} = 375\text{ kN}$	<ul style="list-style-type: none"> ● Bottom West LVDT showing yielding
117	Axial Load = 2400 kN $V_{\text{app}} = 375\text{ kN}$	<ul style="list-style-type: none"> ● No buckling beside BW Quadrant ● Buckling observed in top East Flange above the stirrup
128	Axial Load = 2554 kN $V_{\text{app}} = 375\text{ kN}$ Total Load = 2929 kN	<ul style="list-style-type: none"> ● Maximum load, test terminated.

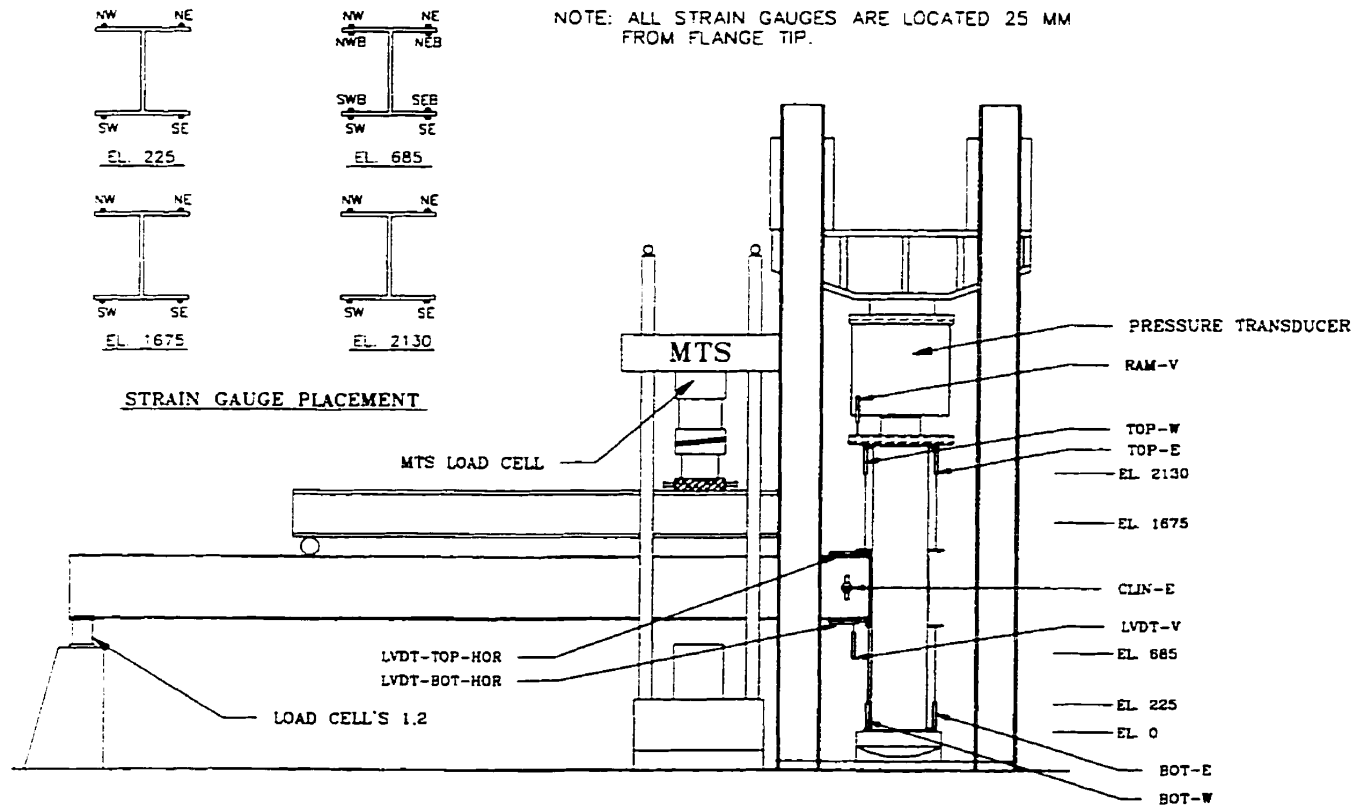
Comments:

For this test Hydrostone was applied at both column ends. It was obvious that seating problems associated with C450-W410-SDA-NON was corrected with the grouting between the loading head, column and spherical head. A general observation was that although a buckling pattern was obvious directly below the connection (Bottom West Column Flange above the stirrup) at an axial load of 1680 kN there was considerable load carrying capacity before other obvious buckling occurred in other quadrants. This is reinforced with the results from the 4 LVDT's included in this test (LVDT TW, TE, BW, and BE).

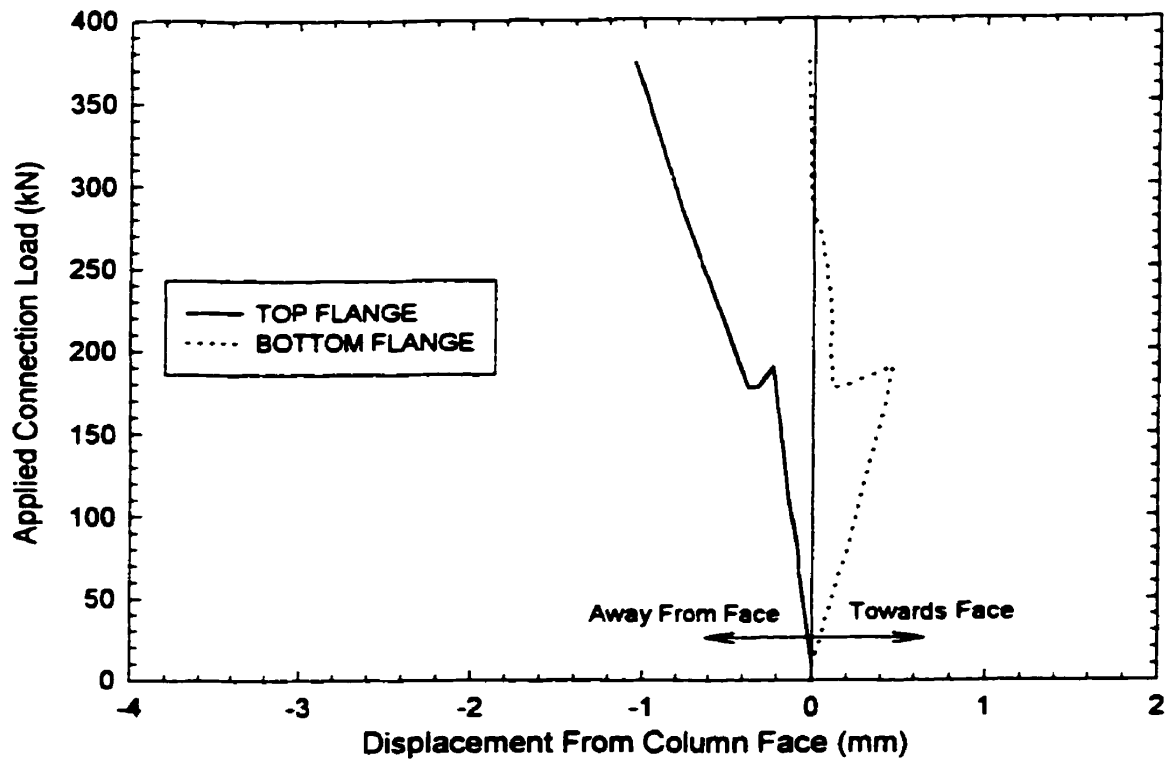
Due to the longer column length the load cell used in C450-W410-SDA-NON was removed and the axial load was calibrated based on line hydraulic pressure. There was little lateral movement.



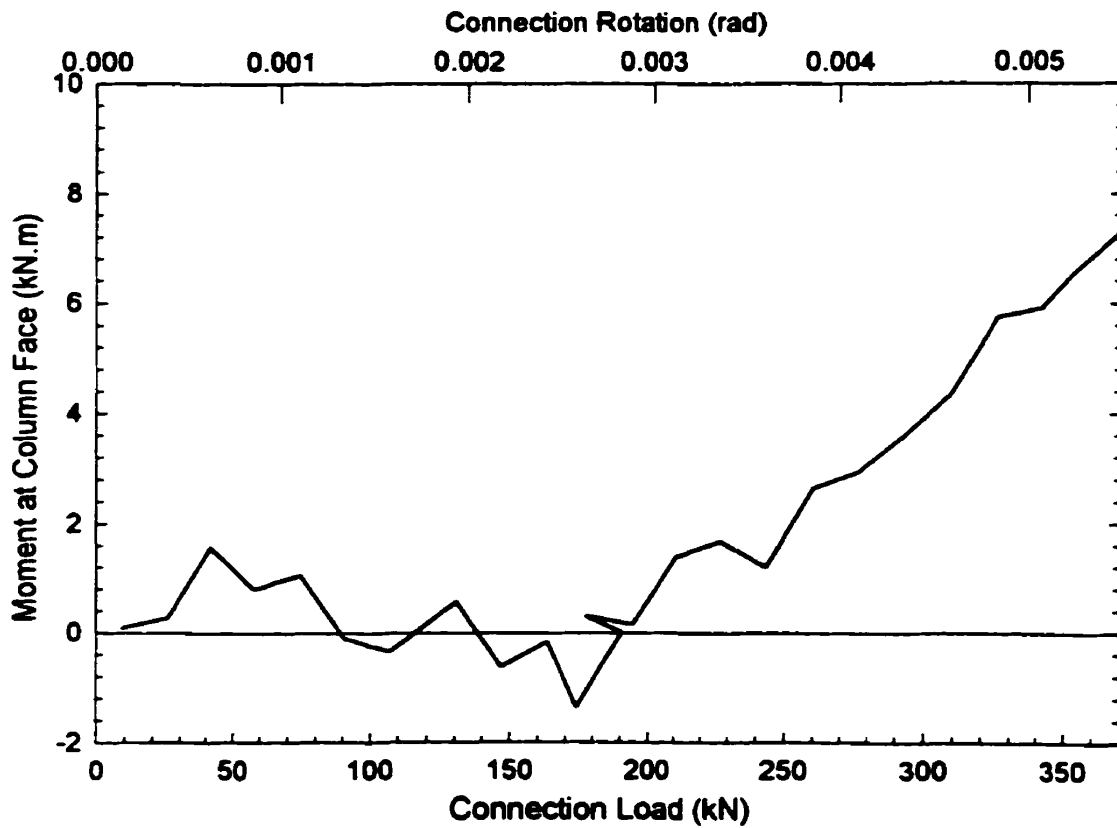
C450-W530-LDA-N: Photographic View of Test Set-up



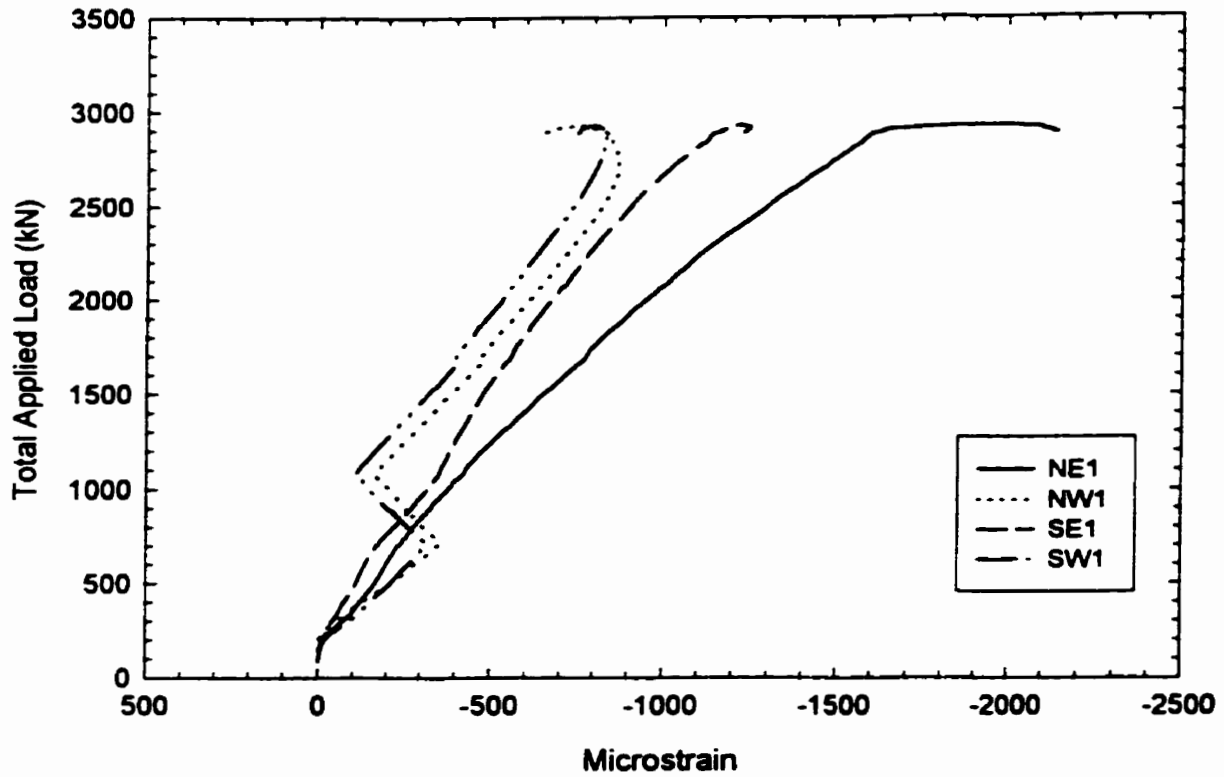
C450-W530-LDA-N: Instrumentation Layout of Test Specimen



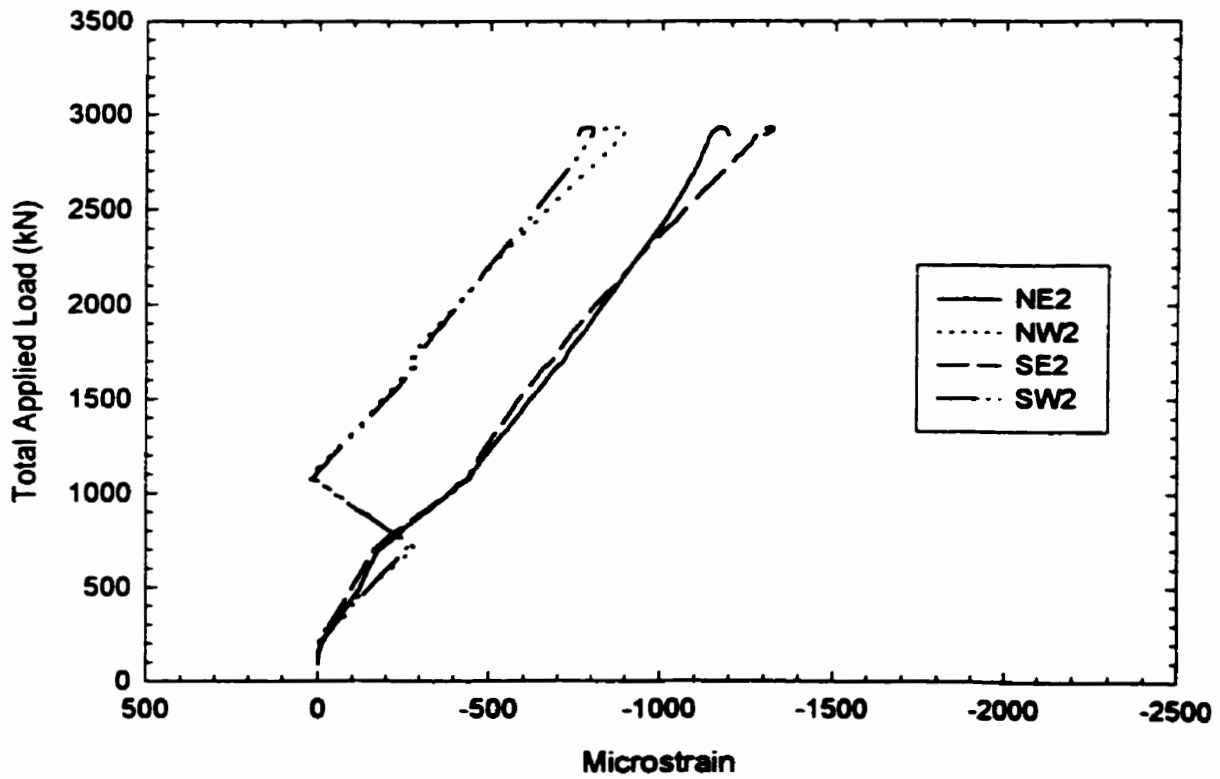
C450-W530-LDA-N: Connection Load vs. Displacement of Beam Flange From Column Face



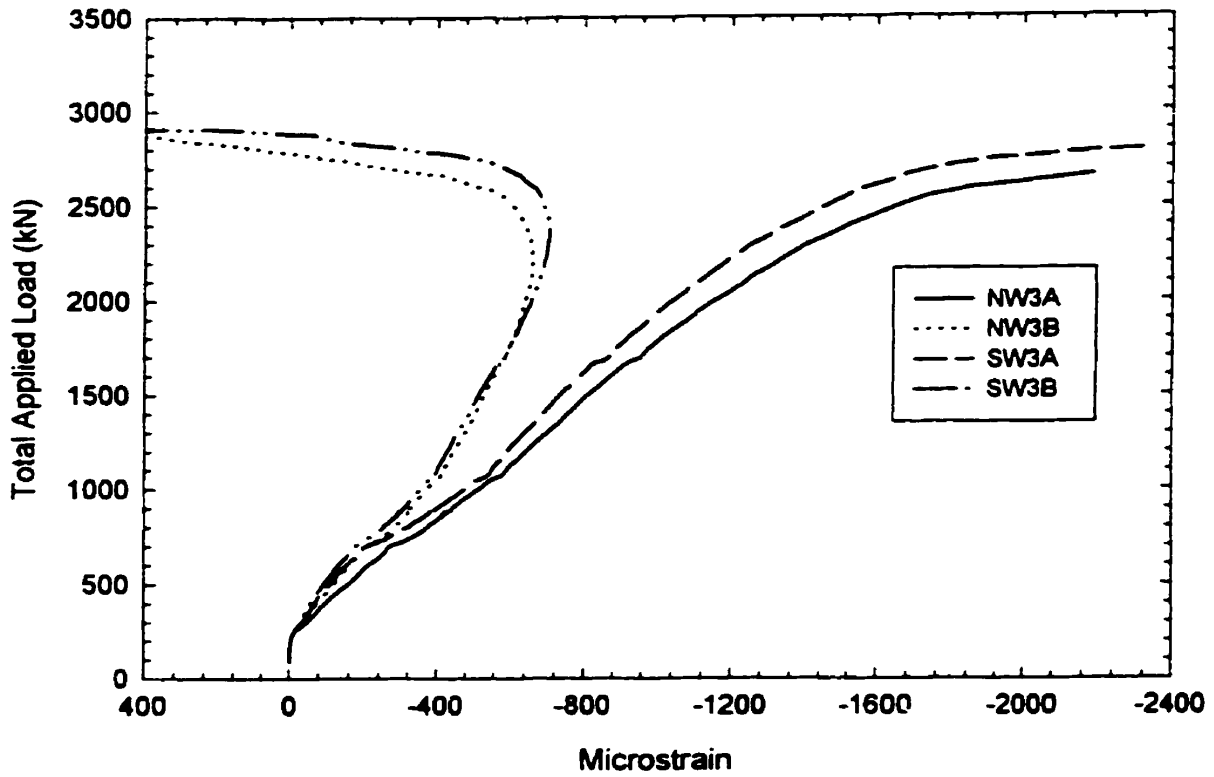
C450-W530-LDA-N: Developed Moment at Column Face vs. Rotation and Connection Load



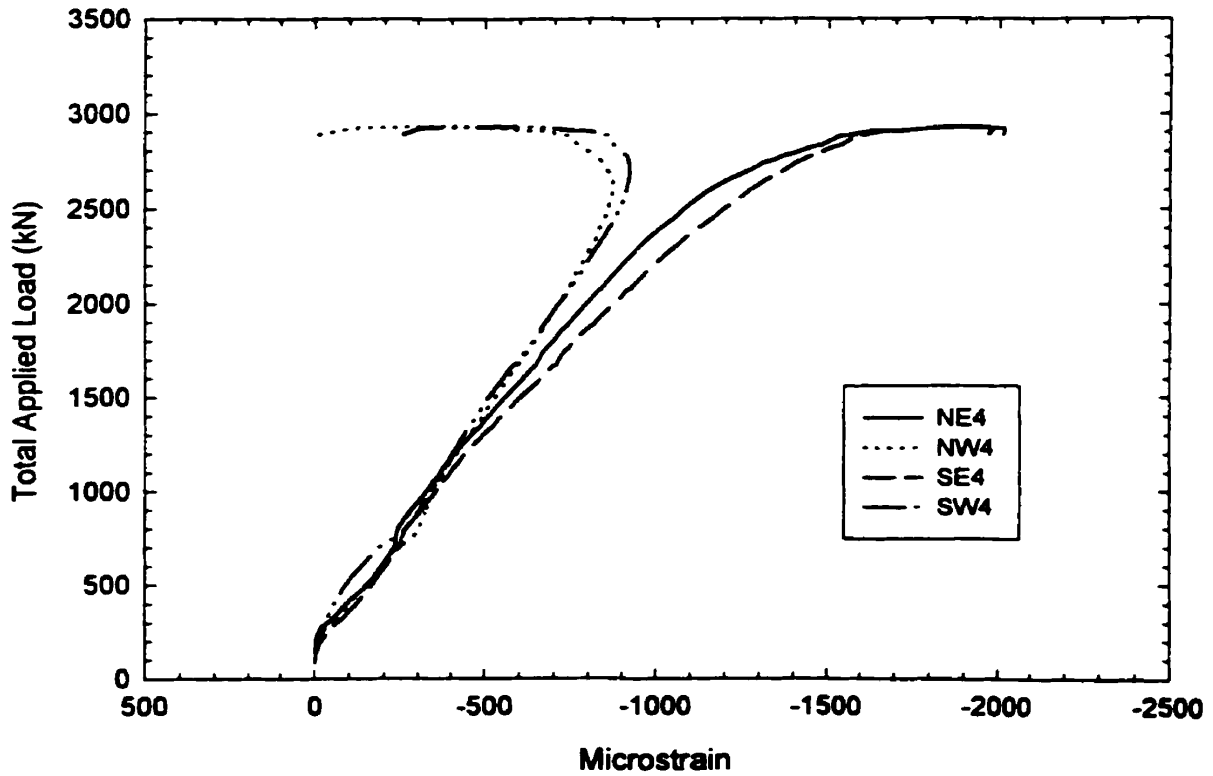
C450-W530-LDA-N: Total Applied Load vs. Strain 675 mm Above Connection Plate (El. 2130)



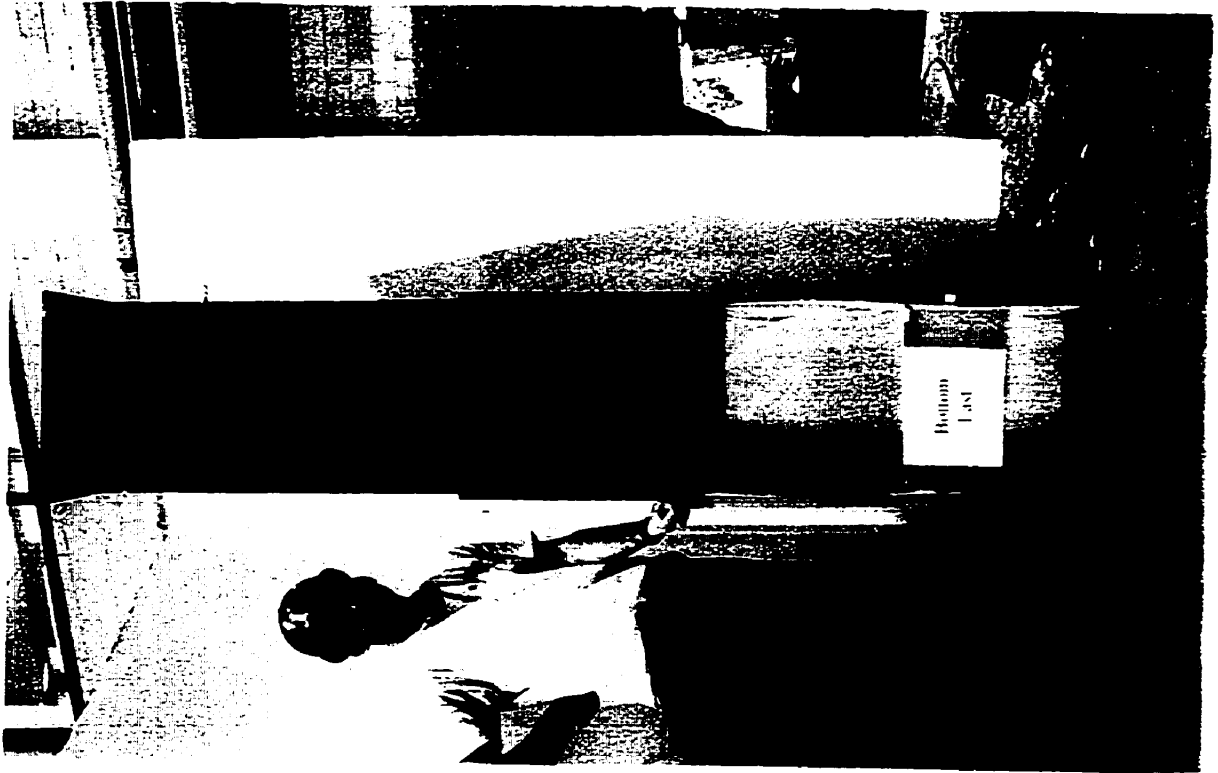
C450-W530-LDA-N: Total Applied Load vs. Strain 225 mm Above Connection Plate (El. 1675)



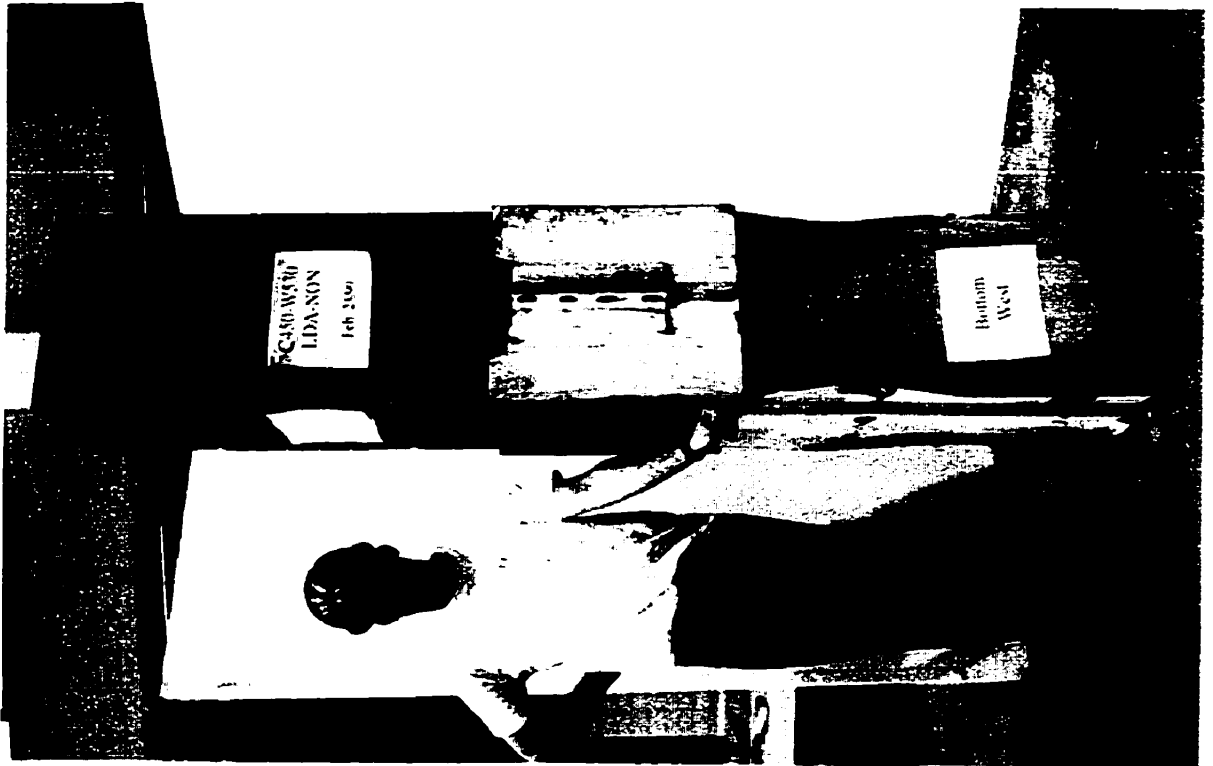
C450-W530-LDA-N: Total Applied Load vs. Strain 225 mm Below Connection (El. 685)



C450-W530-LDA-N: Total Applied Load vs. Strain 675 mm Below Connection (El. 225)



C450-W530-LDA-N: View of Bottom East Quadrant



C450-W530-LDA-N: Full View of Failed Specimen

Test No. 5: C450-W530-SDA-COMP

April 29, 1999

Description: 450 x 450 x 2358 mm Column Short Double Angle Connection
W530 x 92 Load Beam 3 - 3/4" A325 Bolts (70% Yield).
Composite State Total Cleat Length = 265 mm

Testing Procedure: 1) Load the column to a nominal load of 4500 kN. This approximately represents 1.0 DL + 0.3 LL.
2) Proceed to load the connection unto failure

Geometry: $A_1 = 627 \text{ mm}$ $d_{\text{MTS}} = 1348 \text{ mm}$
 $A_2 = 4173 \text{ mm}$ $L = 7013 \text{ mm}$

RESULTS:

<u>Dataset</u>	<u>Load Stage</u>	<u>Description</u>
99	Axial Load = 4500 kN	● Begin loading connection, no problems
156	Axial Load = 4500 kN $V_{\text{app}} = 332 \text{ kN}$	● Lateral beam bracing is mobilized
169	Column Load = 4500 kN $V_{\text{app}} = 417 \text{ kN}$	● 2mm of separation between cross plate and column face above beam
205	Column Load = 4500 kN $V_{\text{app}} = 622 \text{ kN}$	● Observed cleat yielding
252	Column Load = 4500 kN $V_{\text{app}} = 700 \text{ kN}$	● Unable to maintain load on MTS
261	Column Load = 4500 kN $V_{\text{app}} = 678$	● Violent Failure, Net Section along bolt line

Comments:

Painting the beam web, prior to framing into the test column proved effective in eliminating the violent bolt slip as experienced in the earlier test.

This was the first test that used the longitudinal beam restraint. The net section failure was a result of the restraint. It's absence would have caused the more ductile response as seen in tests without the restraint.

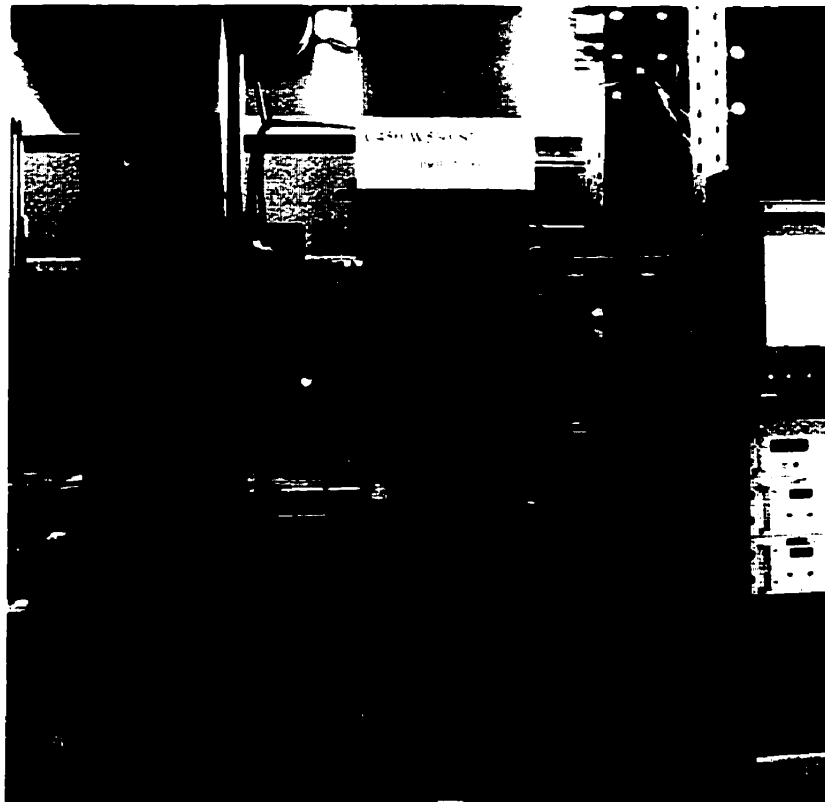


Figure D.5.1: Photographic View of Specimen C450-W4530-SDA-C

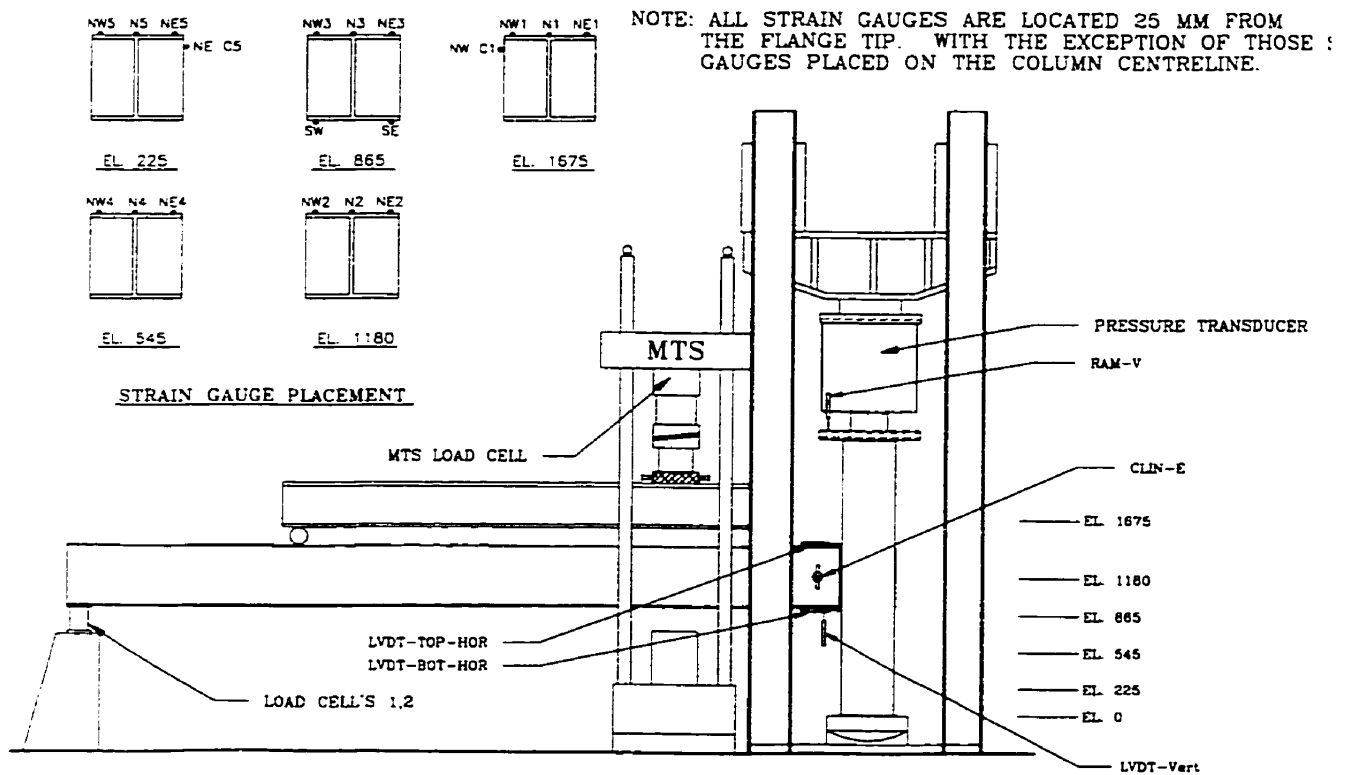
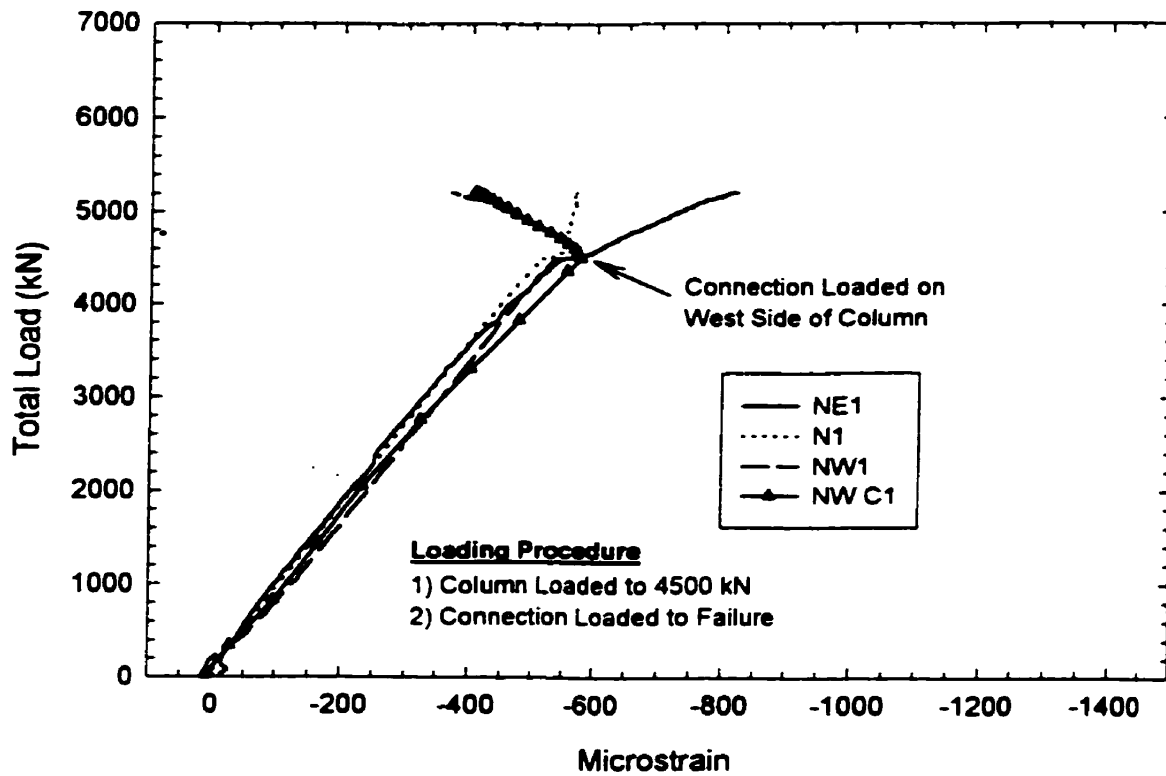
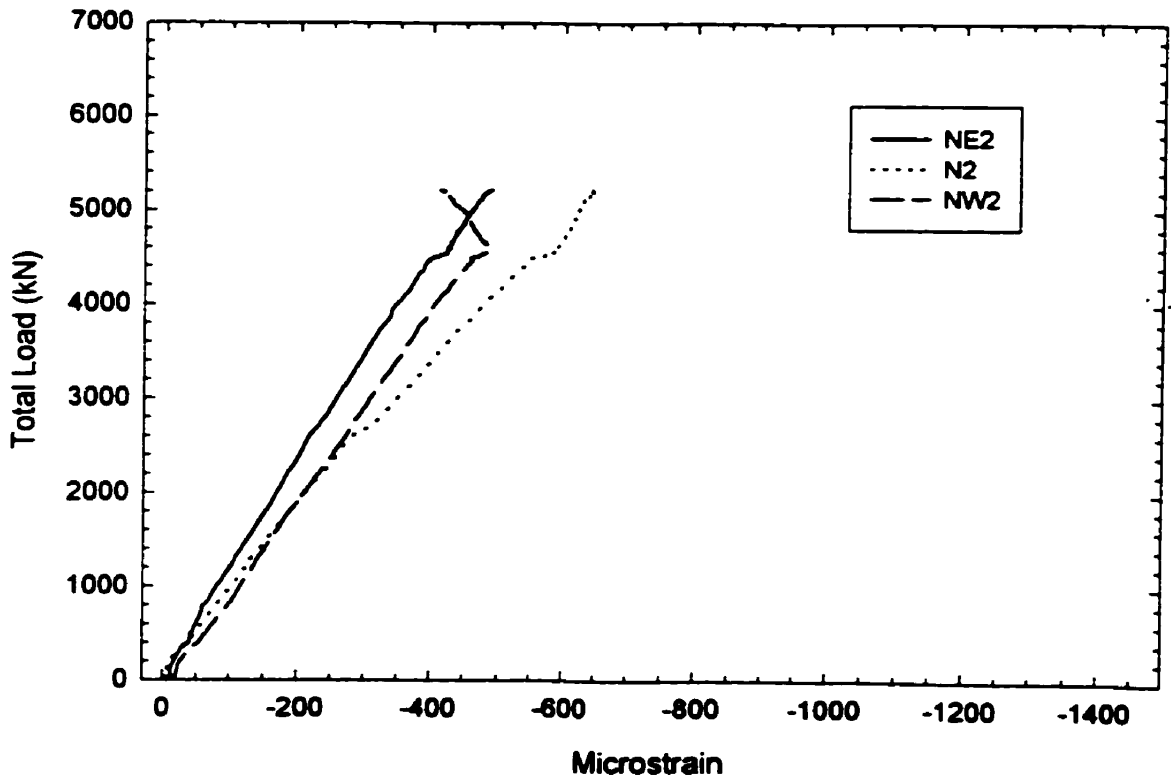


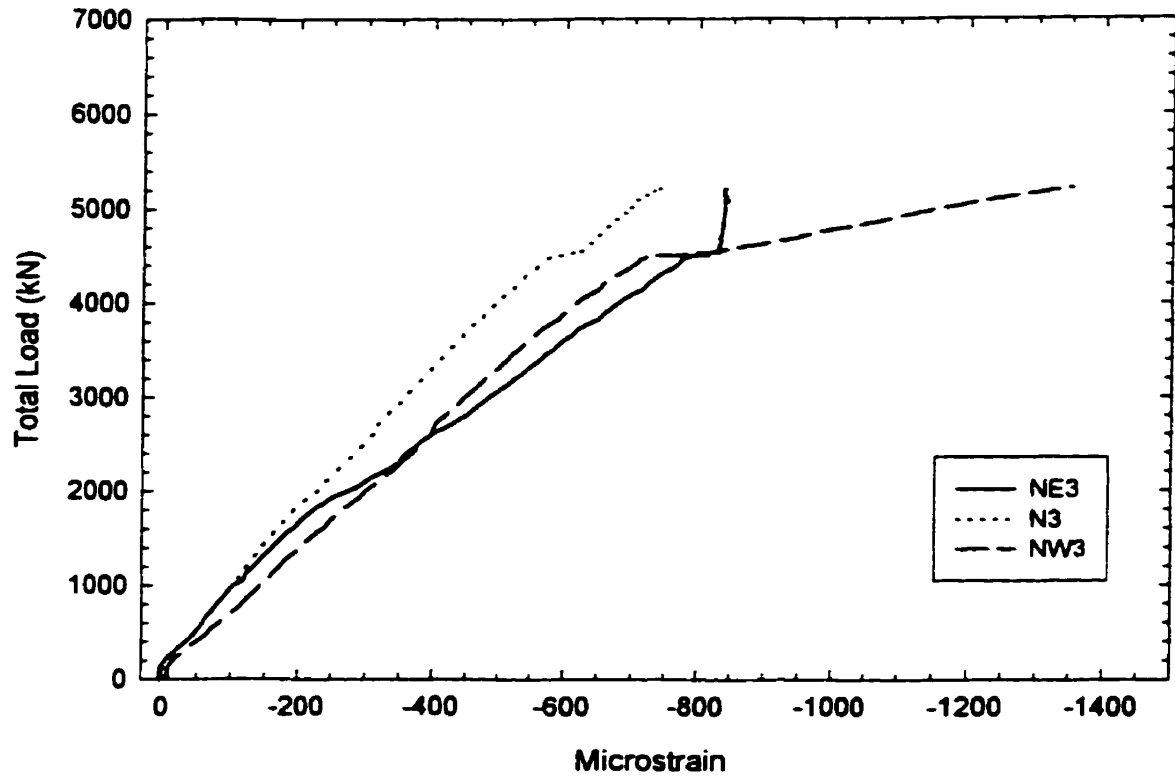
Figure D.5.2: Instrumentation Layout of Test Specimen C450-W530-SDA-C



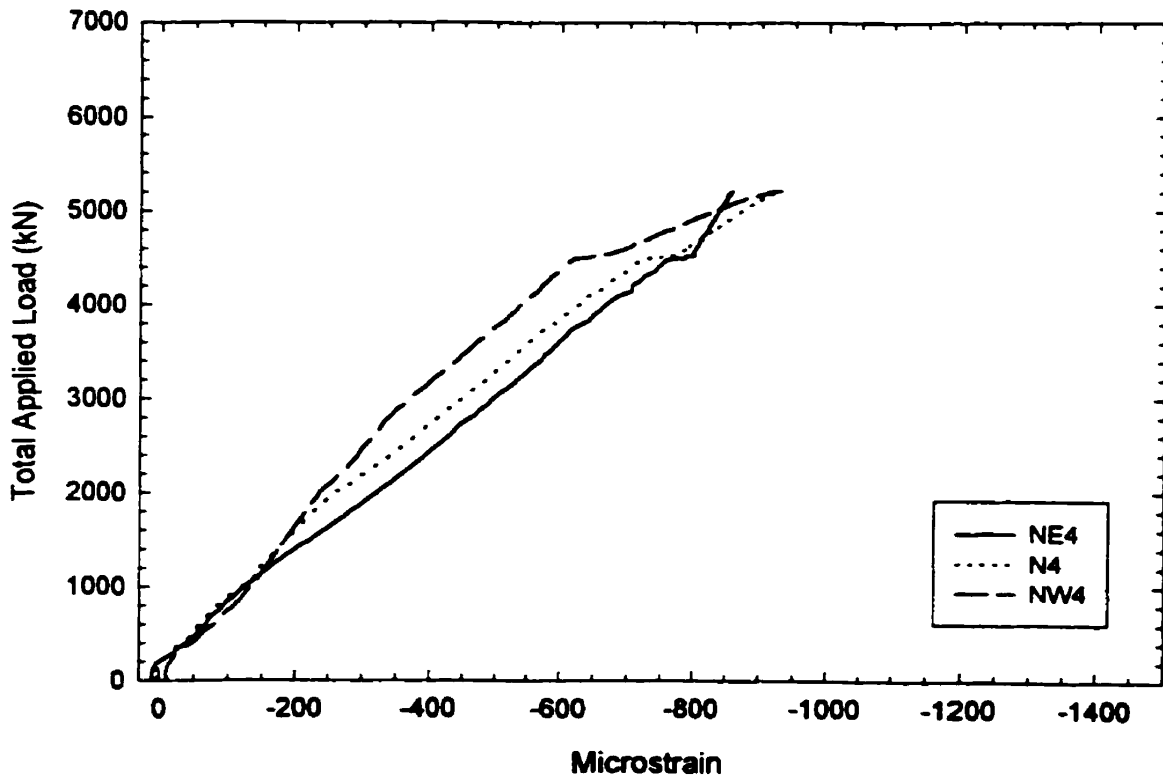
C450-W530-SDA-C: Total Applied Load vs. Strain at Elevation 1675 mm



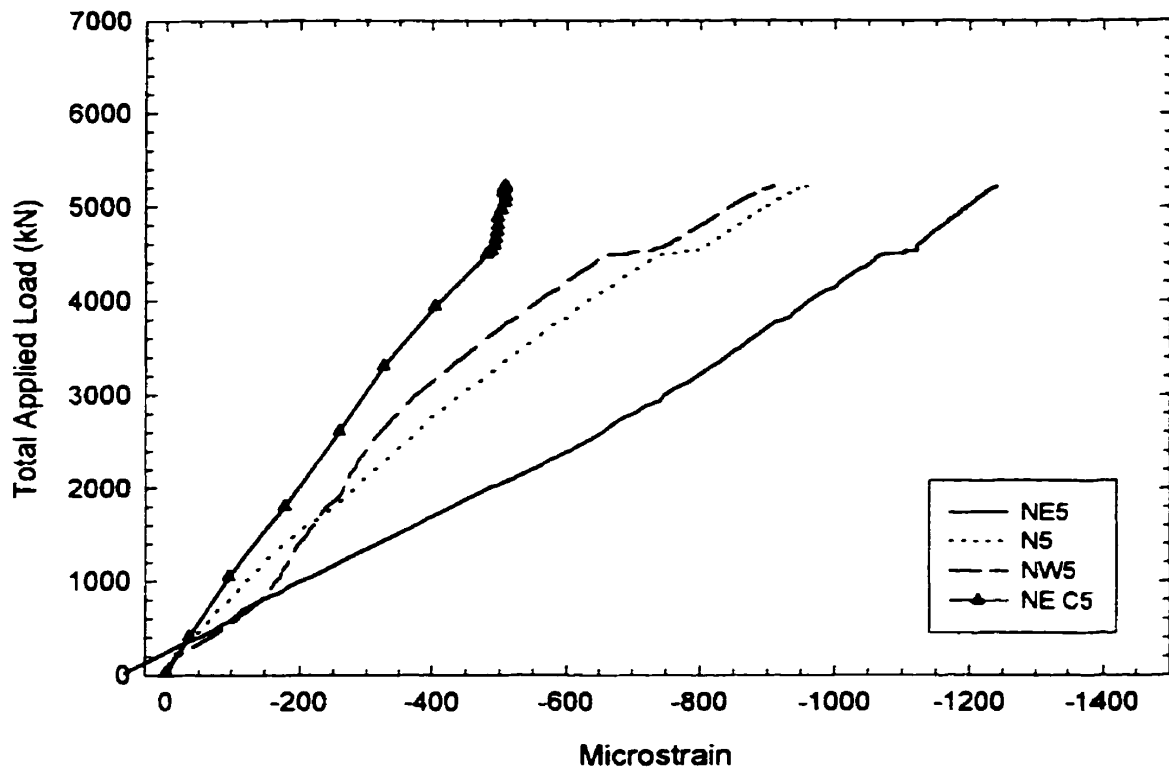
C450-W530-SDA-C: Total Applied Load vs. Strain at Middle of Connection Plate (EL. 1180mm)



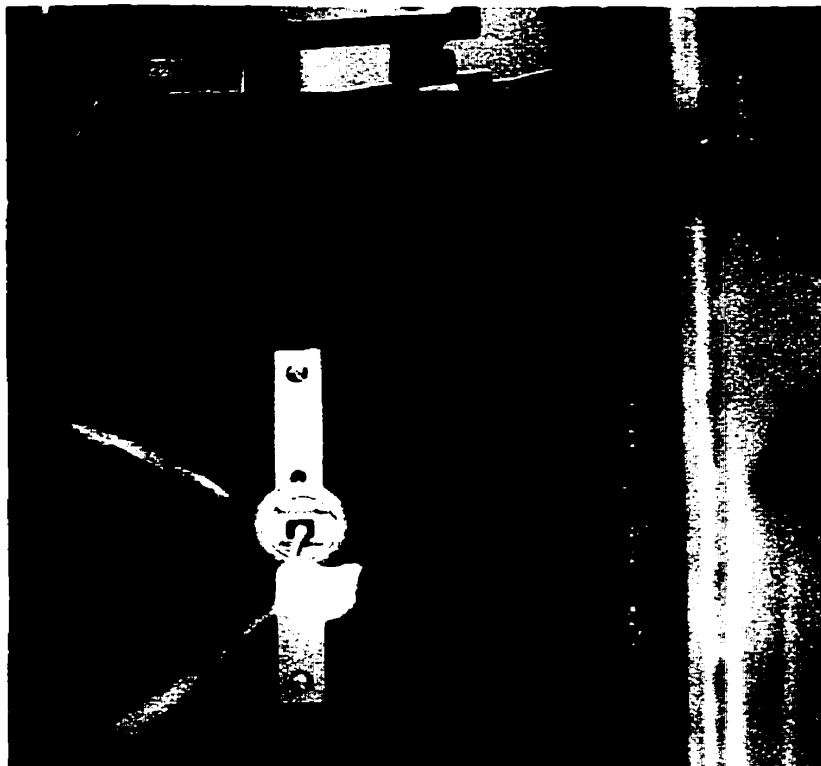
C450-W530-SDA-C: Total Load vs. Strain 50 mm Below Connection Plate (El. 865mm)



C450-W530-SDA-C: Total Load vs. Strain 370 mm Below Connection Plate (El. 545mm)



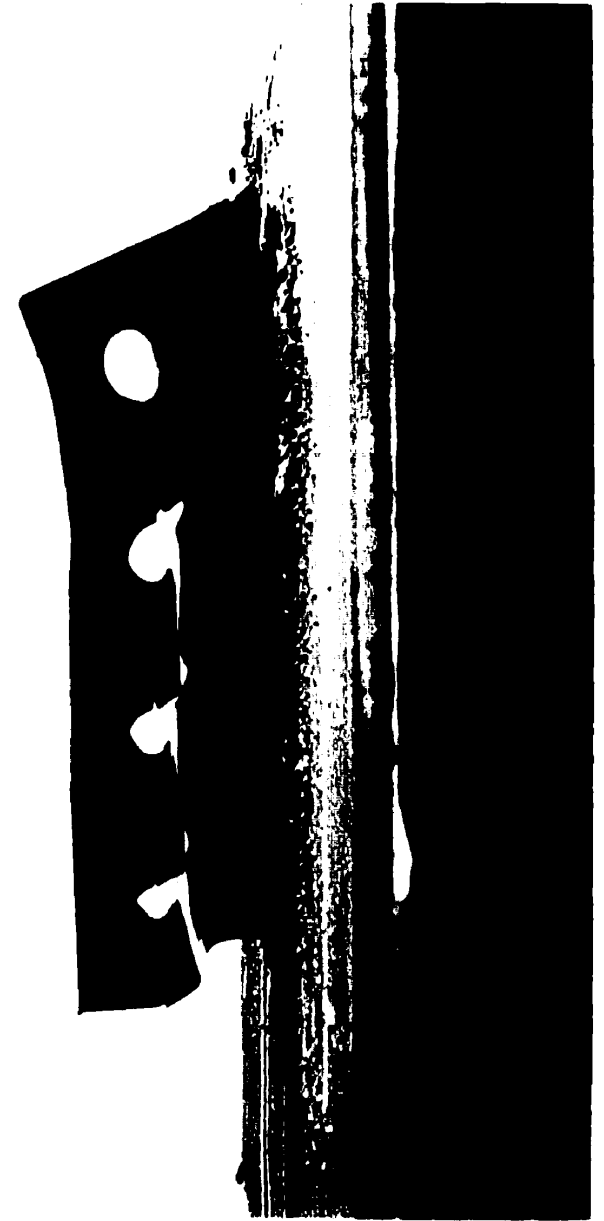
C450-W530-SDA-C: Total Applied Load Vs. Strain 685 mm Below Connection Plate (El. 225)



C450—W530-SDA-C: Photo of Failed Specimen Before Removal of Load Beam – Note Tearing of the Header Connection Along the Bolt Line



C450-W530-SDA-C: Oblique View of Failed Specimen Showing Tearing at the Weld line and the Boltline.



C450-W530-SDA-C: Side Profile of Connection Angle

Test No. 6: C450-W530-LDA-COMP

May 4, 1999

Description: 450 x 450 x 2358 mm Column Long Double Angle Connection
W530 x 92 Load Beam 4 - 3/4" A325 Bolts (70% Yield).
Composite State Total Cleat Length = 325 mm

Testing Procedure:

- 1) Loaded the column to a nominal load of 4500 kN. This approximately represents 1.0 DL + 0.5 LL.
- 2) Proceeded to load the connection to upper MTS limits ($V_{app} = 750$ kN).
- 3) The connection load was reduced to 650 kN and the column load was increased. As the axial load = 6750 kN the connection load was increased back up to 650 kN (Displacement controlled resulted in some loss of connection load during column loading).

Geometry: $A_1 = 615$ mm $d_{MTS} = 1345$ mm
 $A_2 = 4235$ mm $L = 7015$ mm

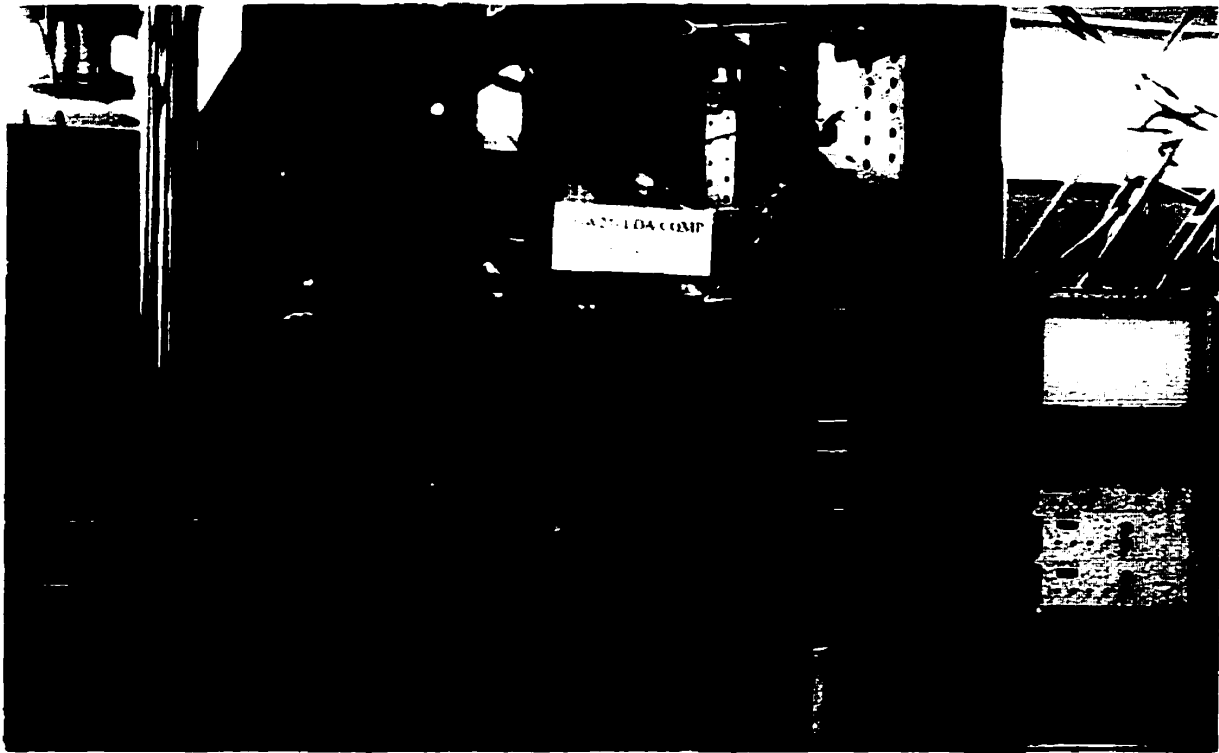
RESULTS:

<u>Dataset</u>	<u>Load Stage</u>	<u>Description</u>
69	Column Load = 4500 kN	<ul style="list-style-type: none">• Begin Connection Loading
173	Column Load = 4500 kN $V_{app} = 676$ kN	<ul style="list-style-type: none">• Although no yielding visible the MTS Load Vs MTS Displacement plot indicates yielding
187	Column Load = 4500 kN $V_{app} = 750$ kN	<ul style="list-style-type: none">• Decided to lower V_{app} to 650 kN and increase column load
259	Column Load = 6631 $V_{app} = 600$ kN	<ul style="list-style-type: none">• There was concrete spalling observed
265	Column Load = 6600 kN	<ul style="list-style-type: none">• Connection Load brought back to 650 kN
281	Column Load = 6750 kN $V_{app} = 637$	<ul style="list-style-type: none">• Maximum column load, connection load again brought back to 650 kN
289	Column Load = 6750 kN $V_{app} = 650$ kN	<ul style="list-style-type: none">• Test terminated

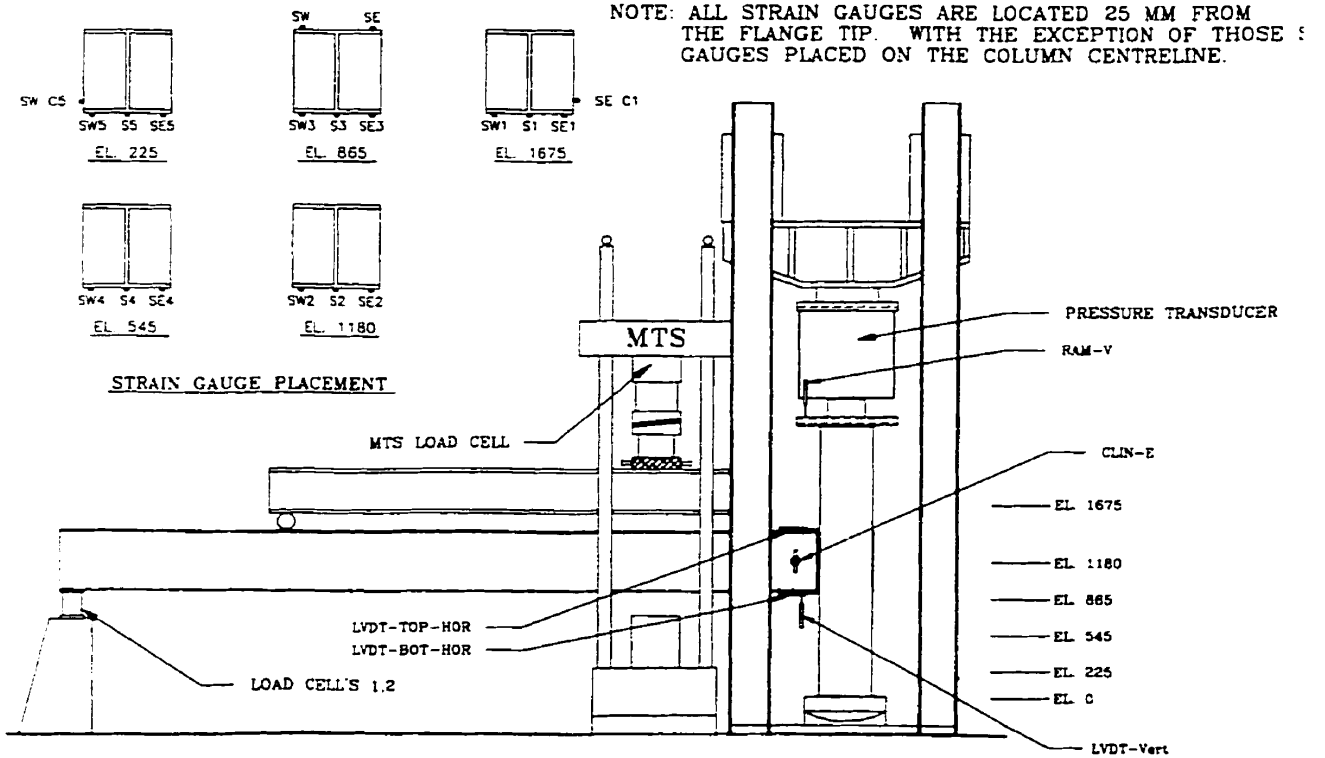
Comments:

As the load was increased there was some observed spalling of the concrete, that corresponded with a slight decrease in the axial load at DS 259. Following the test it was discovered that there was a failure initiated in the concrete at the top, and propagated to the stirrup in the top east column quadrant. This crack initiated about 75 mm from the side of the column.

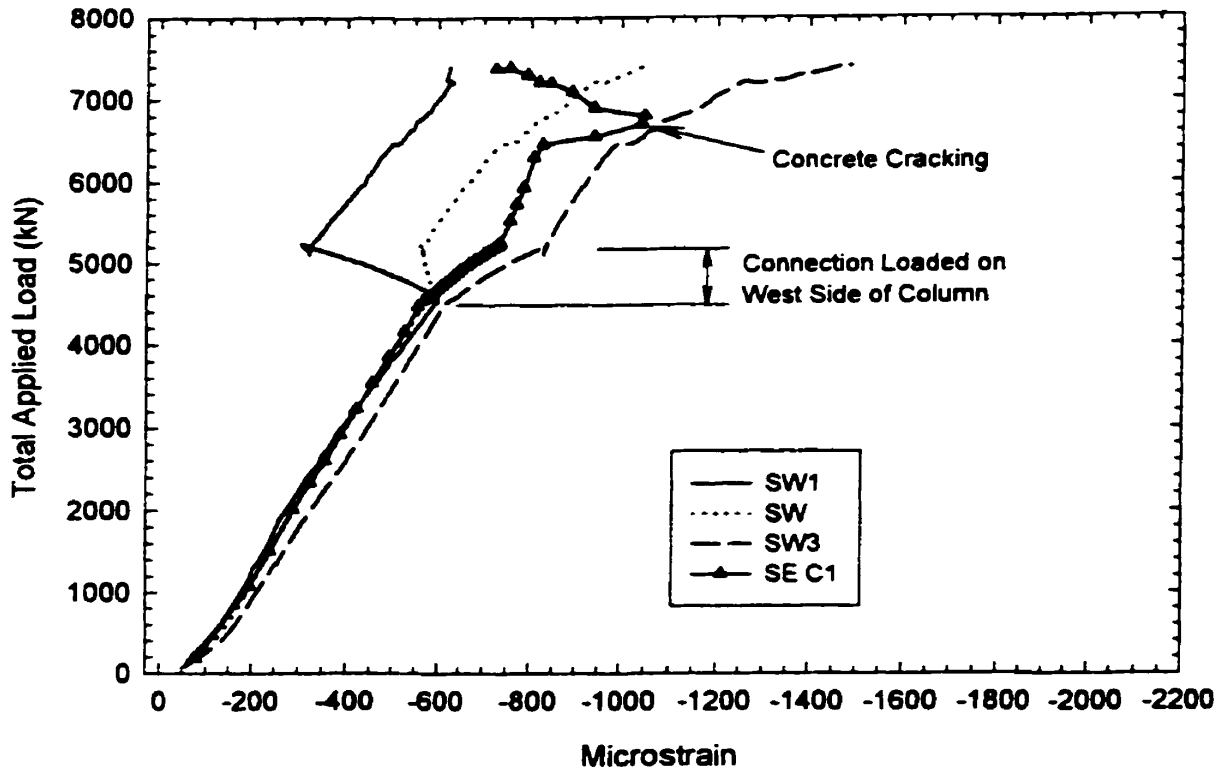
Also under the combined loading there were strains in excess of ϵ_y at the strain gauge locations 50 mm below the connection plate.



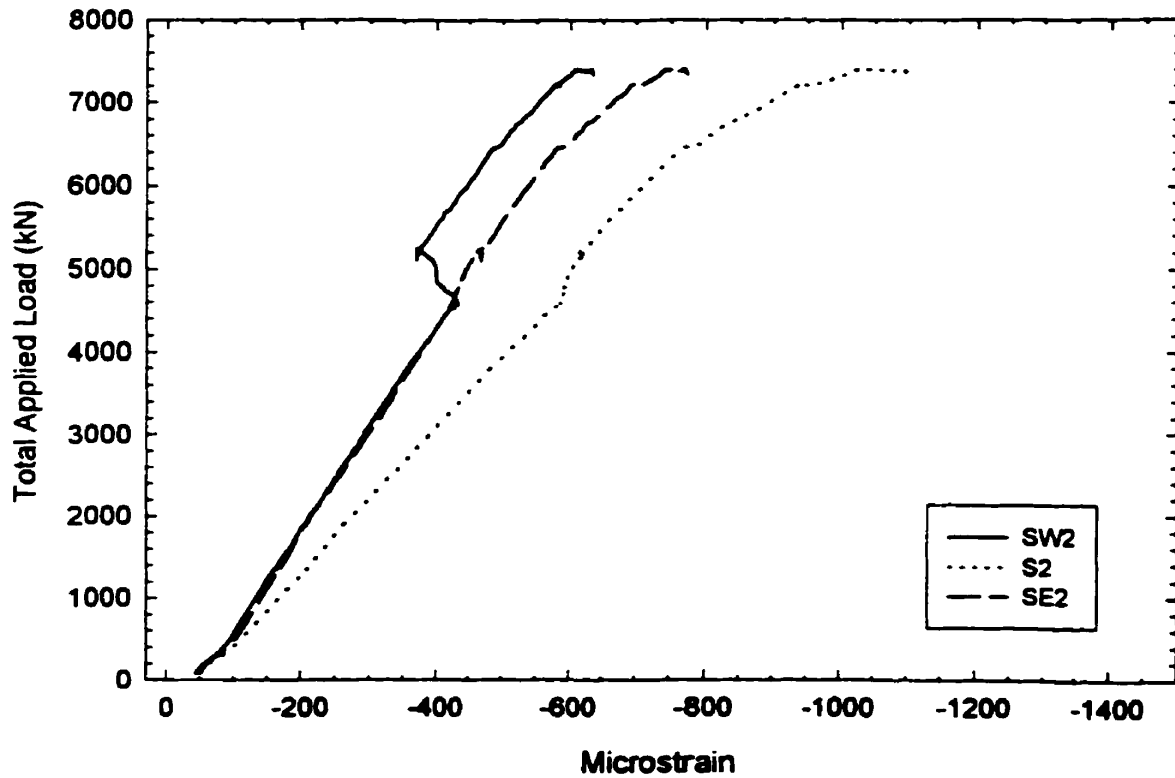
C450-W530-LDA-C: Photographic View of Test Set-up



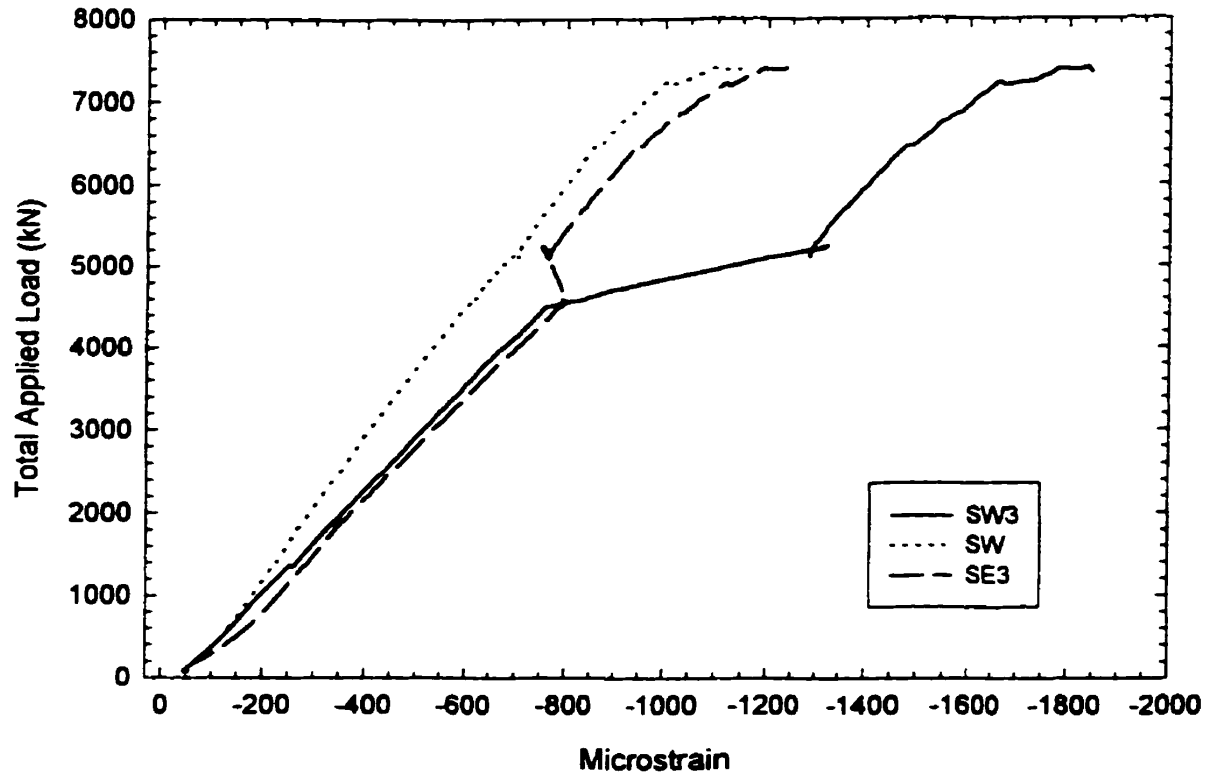
C450-W530-LDA-C: Instrumentation Layout of Test Specimen



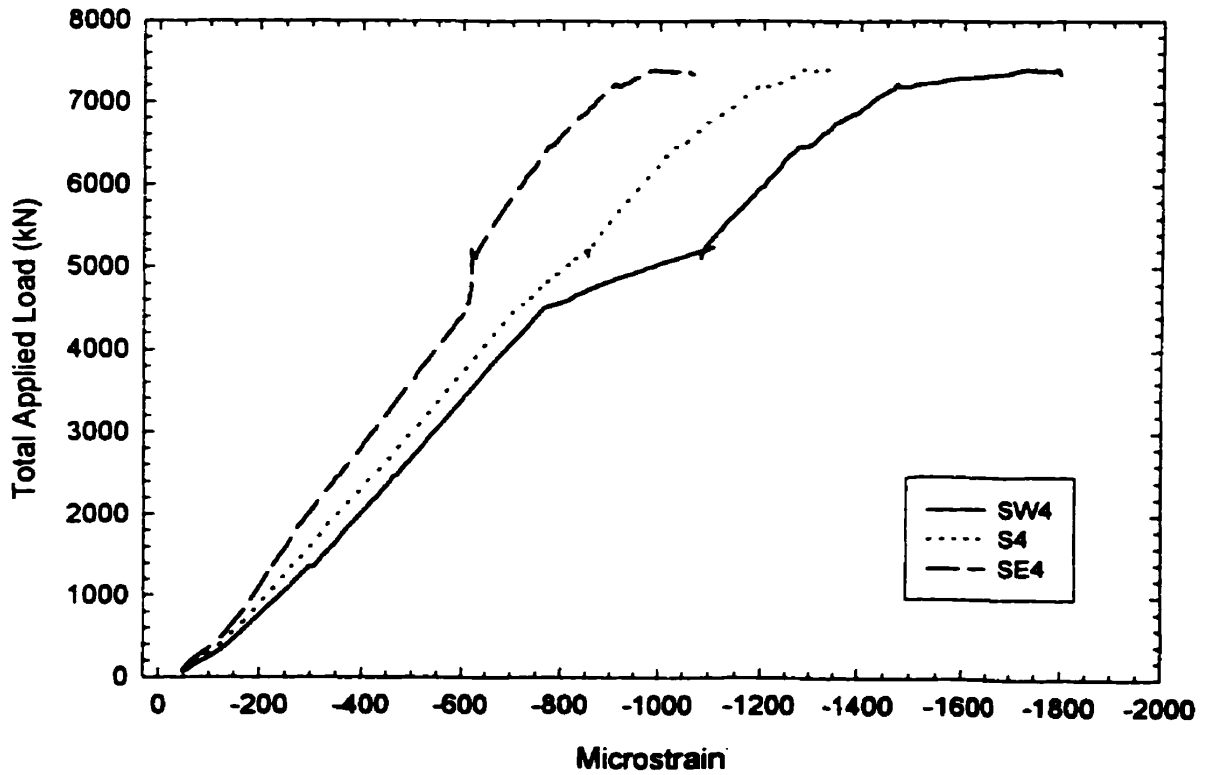
C450-W530-LDA-C: Total Applied Load vs. Strain at El. 1675



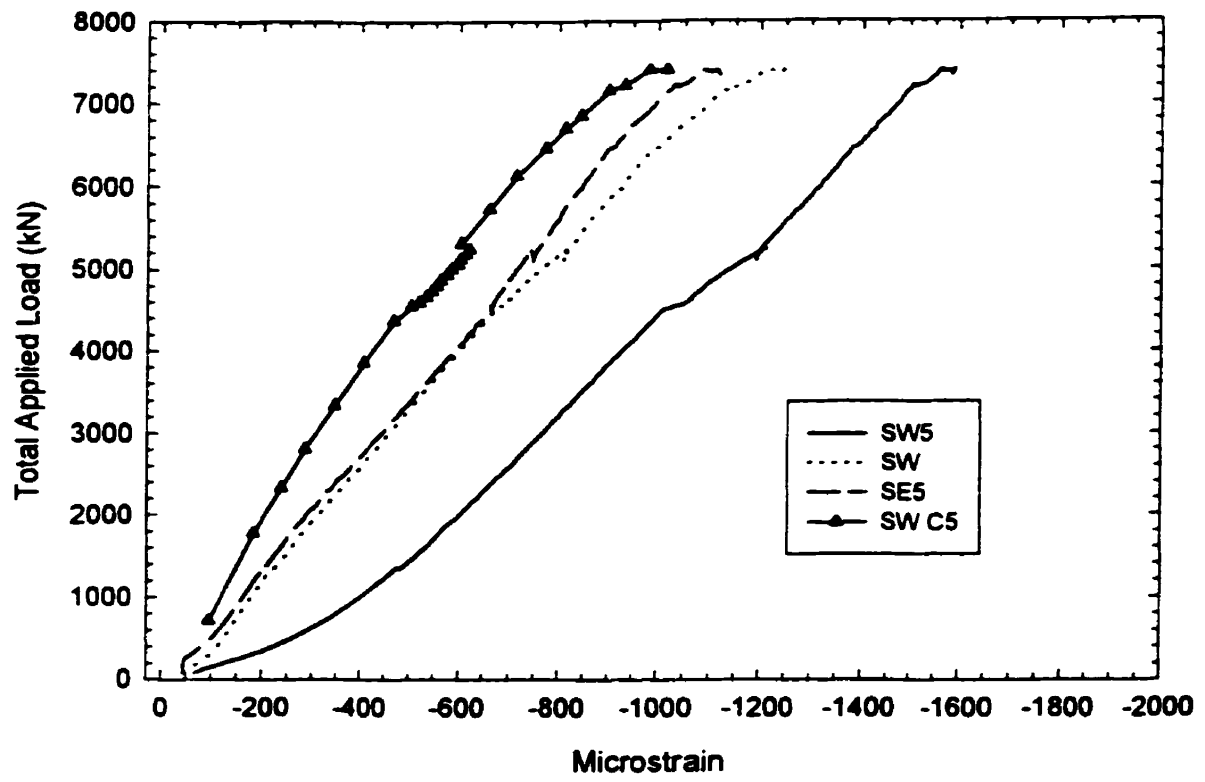
C450-W530-LDA-C: Total Applied Load vs. Strain at Middle of Connection Plate (El. 1180)



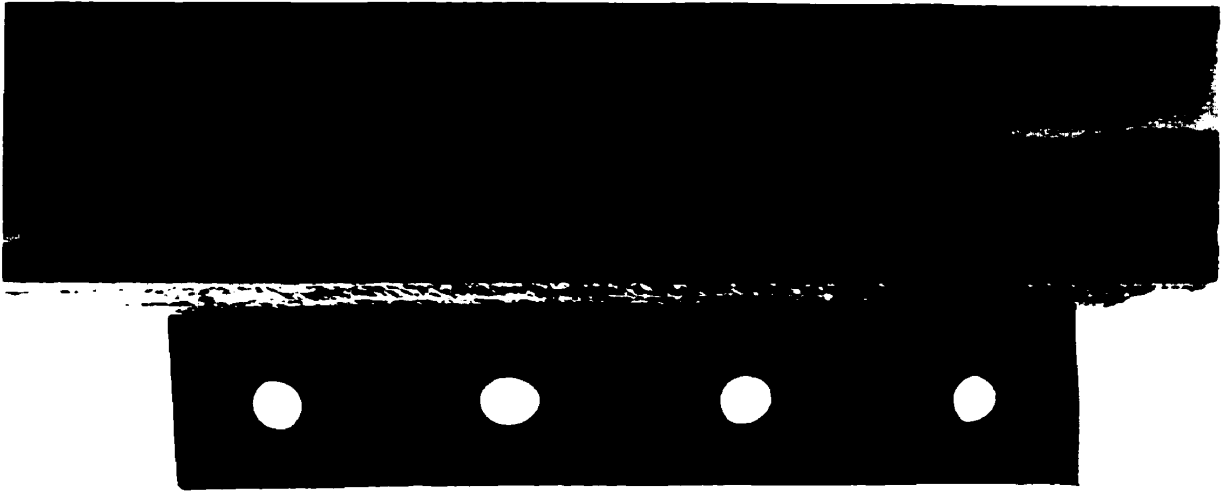
C450-W530-LDA-C: Total Load vs. Strain 50 mm Below Connection Plate (El. 865)



C450-W530-LDA-C: Total Load vs. Strain 370 mm Below Connection Plate (El. 545)



C450-W530-LDA-C: Total Applied Load vs. Strain 685 mm Below Connection Plate (El. 225)



C450-W530-LDA-C: Side Profile of Connection Angle



C450-W530-LDA-C: Oblique View of Tested Specimen Showing Little Deformation

Test No. 7: C450-W410-TAB-NON
May 5, 1999

Description: 450 x 450 x 2234 mm Column Single Shear Plate (TAB) Connection
 W410 x 67 Load Beam 4 - 3/4" A325 Bolts (70% Yield).
 Non - Composite State PL 295 x 110 x 9.53 Connection

Testing Procedure: 1) Load the column to that representing a typical 1 story construction load (700 kN).

 2) Proceed to load the connection to a construction load of 300 kN

 3) While maintaining the connection load increase the applied axial load (Fox Jack applies load above the connection) until a buckling failure in the column occurred.

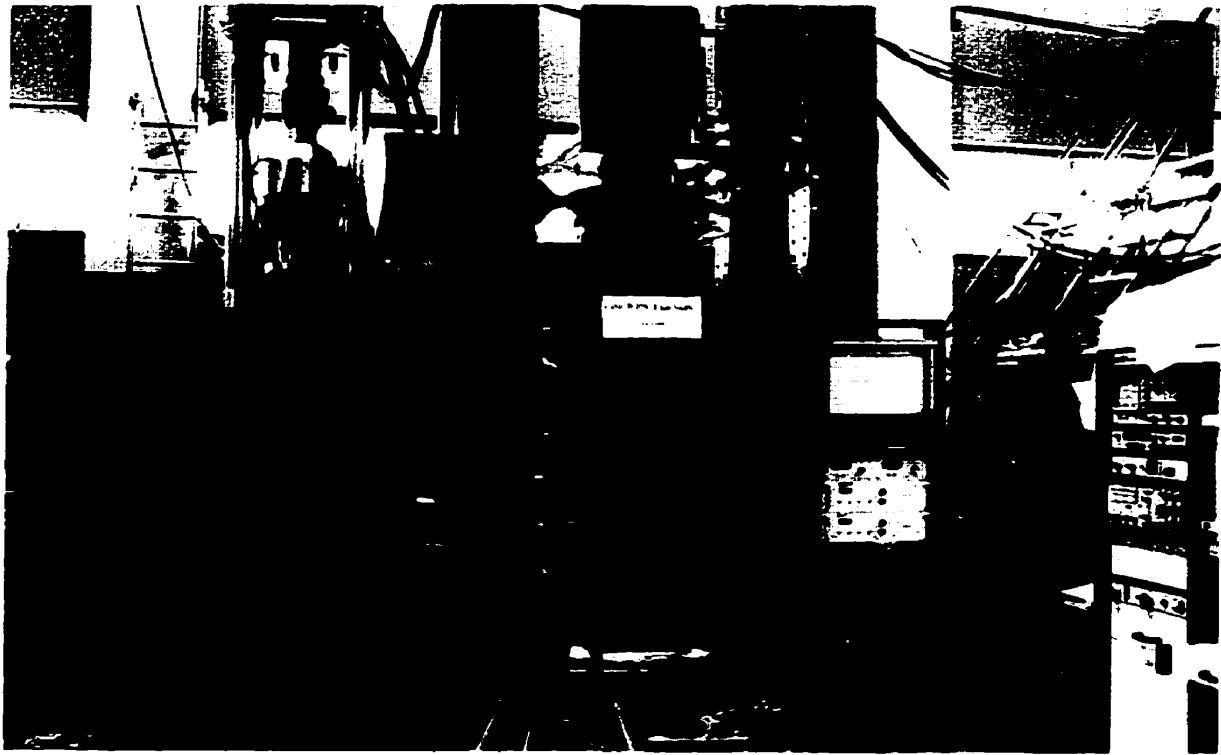
Geometry: $A_1 = 622 \text{ mm}$ $d_{\text{MTS}} = 1347 \text{ mm}$
 $A_2 = 3813 \text{ mm}$ $L = 5340 \text{ mm}$

RESULTS:

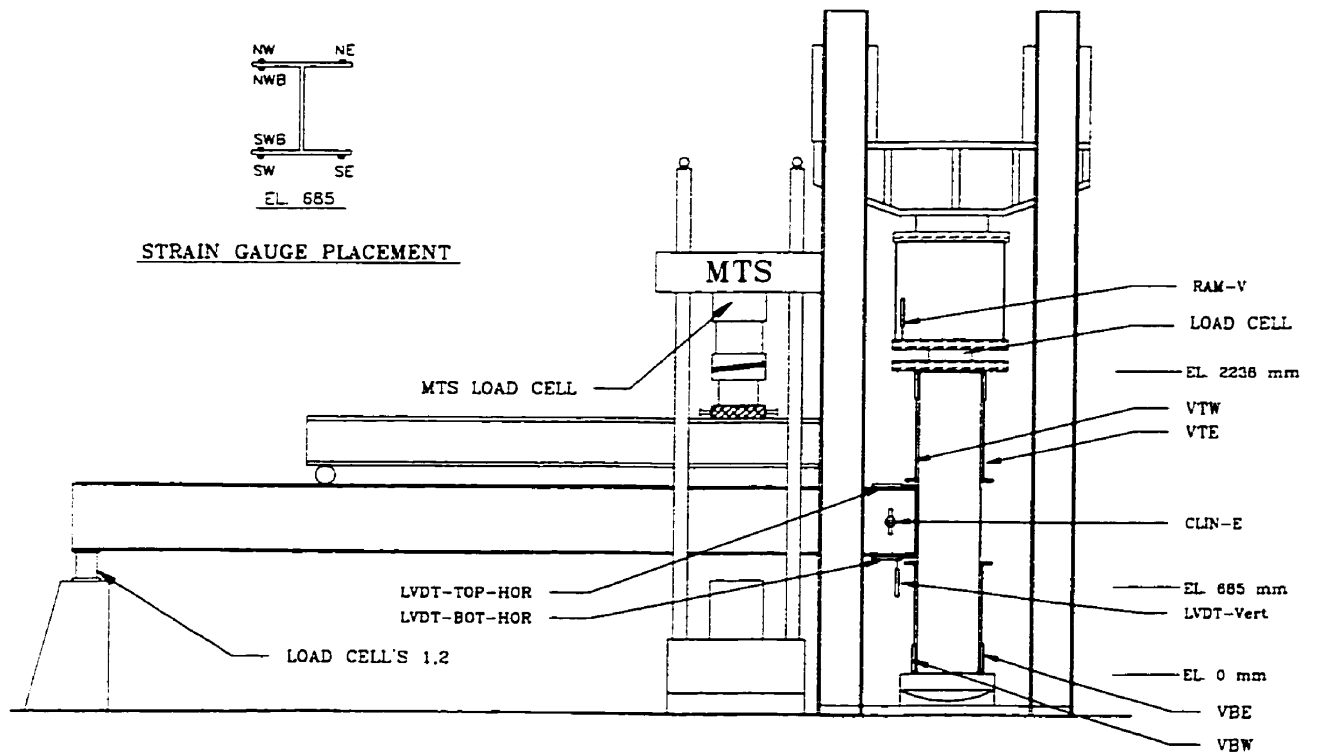
<u>Dataset</u>	<u>Load Stage</u>	<u>Description</u>
31	Column Load = 700 kN	● No Distortion, begin connection loading
82	Column Load = 700 kN $V_{\text{app}} = 300 \text{ kN}$	● Begin to increase column load
120	Column Load = 1875 kN $V_{\text{app}} = 275 \text{ kN}$	● No Distortion. connection load not maintained (displacement control)
209	Column Load = 2825 kN $V_{\text{app}} = \text{Dropped to } 222 \text{ kN}$	● Maximum loading, test terminated.

Comments:

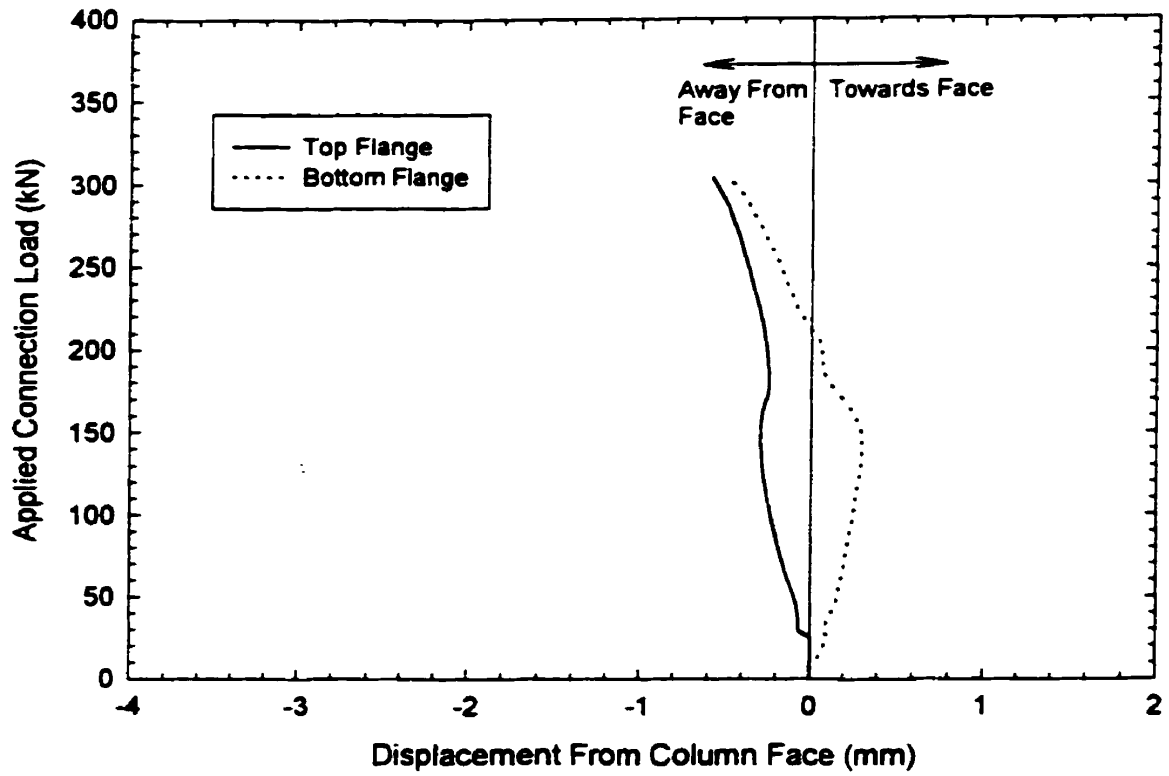
In other non-composite tests the MTS universal machine was kept on displacement control while the column load was increased. To maintain the connection load the MTS was adjusted during the column loading. For test C450-W410-TAB-NON the MTS load was not adjusted throughout the increased column load, thus the connection load dropped from 300 to 222 kN.



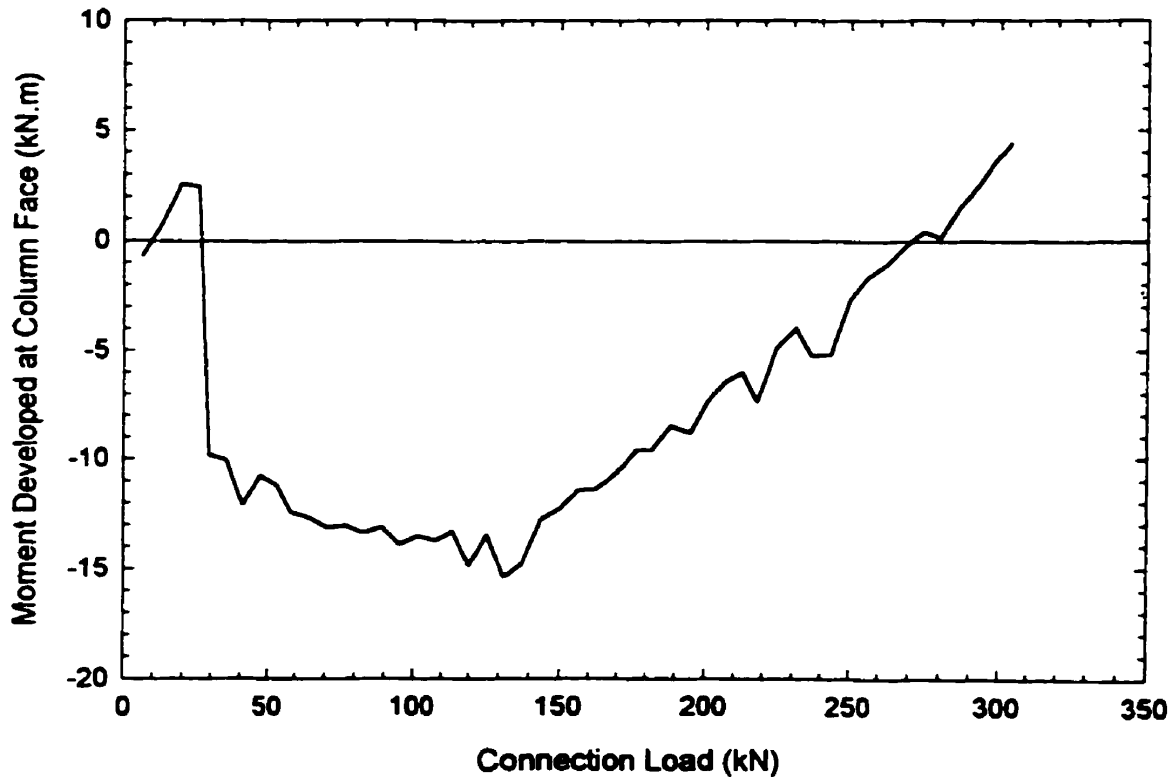
C450-W410-TAB-N: Photographic View of Test Set-up



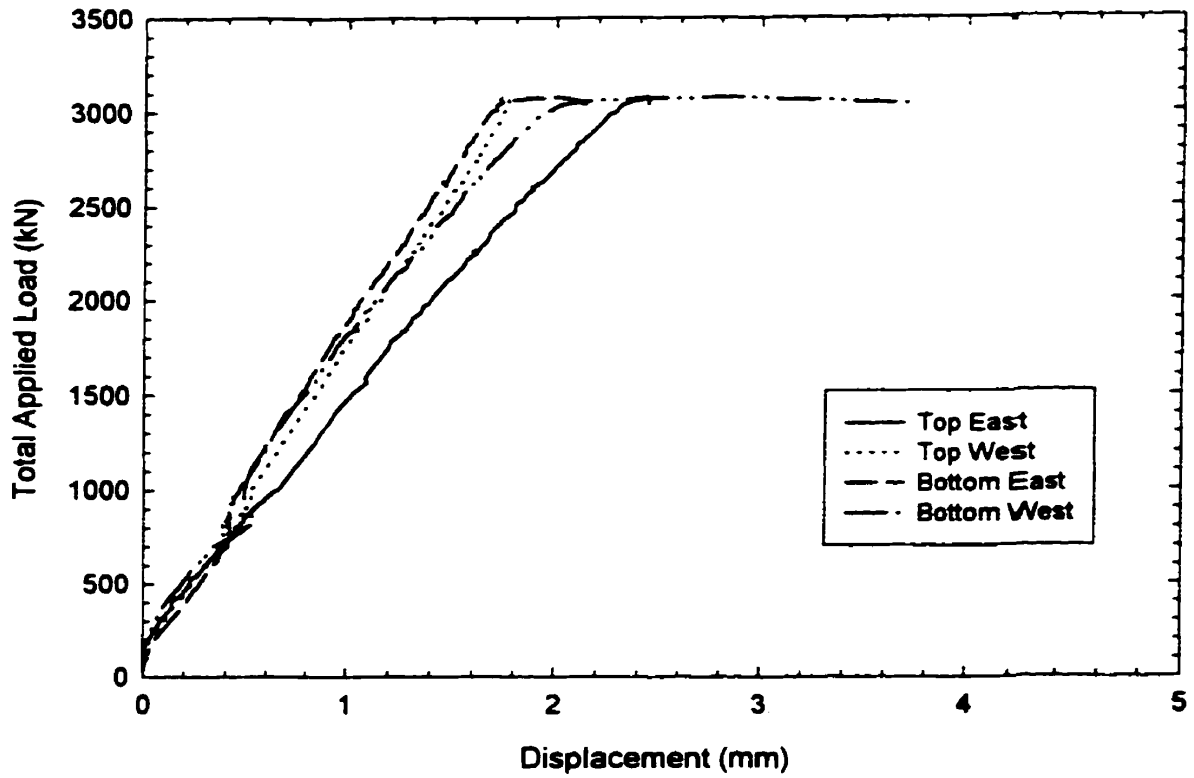
C450-W410-TAB-N: Instrumentation Layout of Test Specimen



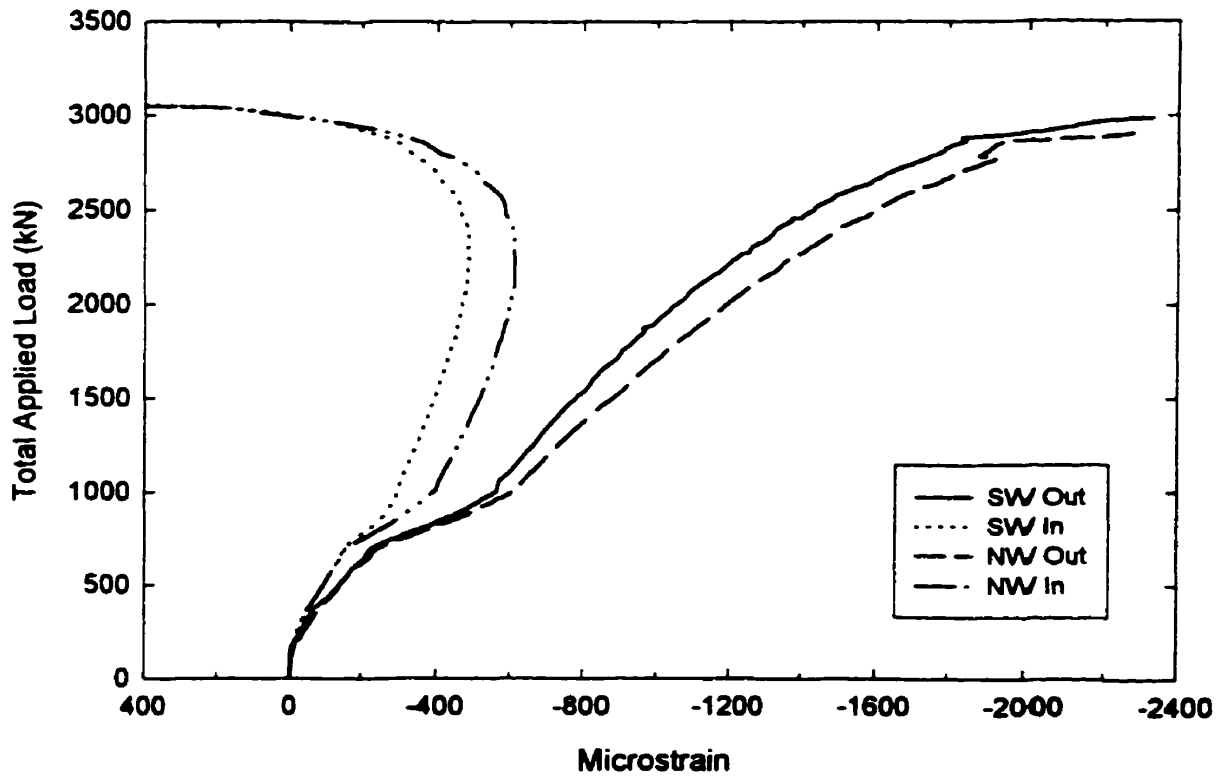
C450-W410-TAB-N: Applied Connection Load vs. Displacement of Beam Flange From Column Face



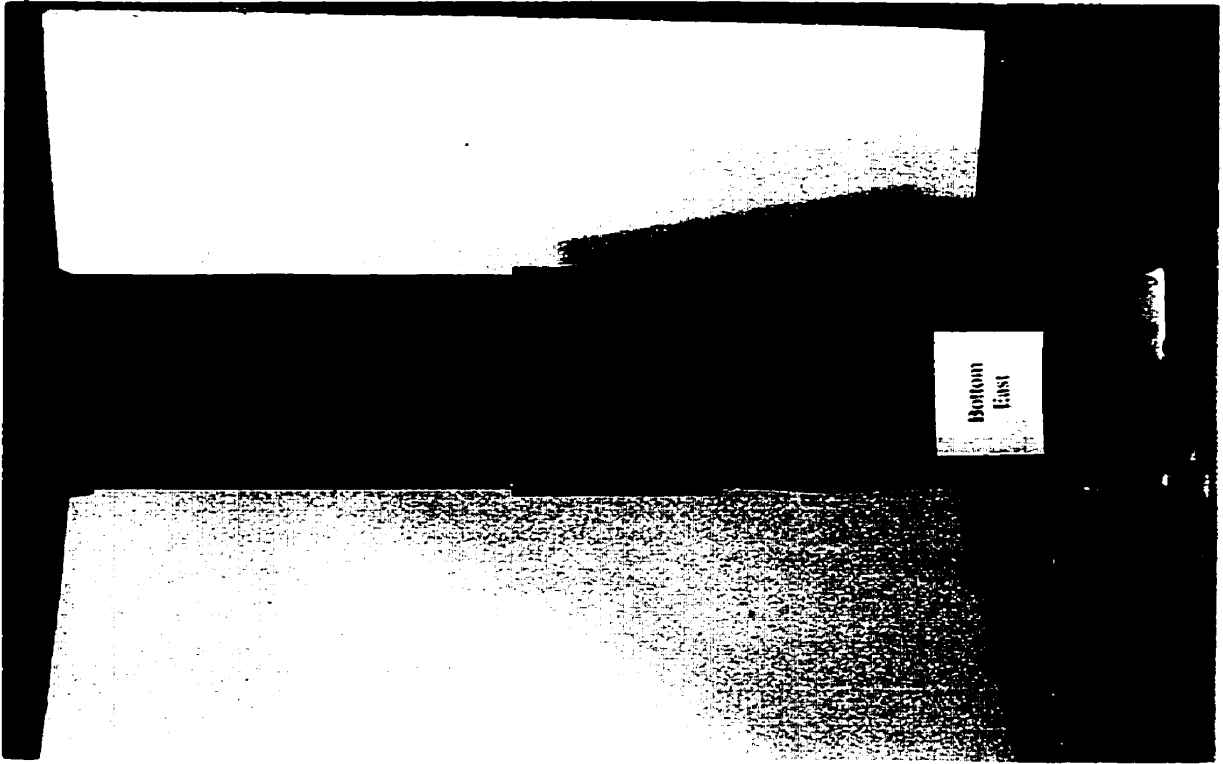
C450-W410-TAB-N: Developed Moment at Column Face vs. Connection Load



C450-W410-TAB-N: Total Applied Load vs. Quadrant LVDT Displacement



C450-W410-TAB-N: Total Applied Load vs. Strain in Column Flange 225 mm Below Connection Plate (El. 685)



C450-W410-TAB-N: View of Bottom East Quadrant



C450-W410-TAB-N: Full View of Failed Specimen

Test No. 8: C600-W410-SDA-NON
MAY 11, 1999

Description: 600 x 600 x 2806 mm Column Short Double Angle Connection
W410 x 67 Load Beam 3 - 3/4" A325 Bolts (70% Yield).
Non - Composite State Total Cleat Length = 190 mm

Testing Procedure:

- 1) Load the column to a typical 1 story construction load (700 kN).
- 2) Proceed to load the connection to a construction load of 320 kN
- 3) While maintaining the connection load increase the applied axial load (Fox Jack applies load above the connection) until buckling occurs in the column.

Geometry: $A_1 = 582 \text{ mm}$ $d_{MTS} = 1275 \text{ mm}$
 $A_2 = 3900 \text{ mm}$ $L = 5270 \text{ mm}$

RESULTS:

Dataset	Load Stage	Description
42	Column Load = 700 kN	<ul style="list-style-type: none">• Begin Loading Connection
50	Column Load = 700 kN $V_{app} = 60 \text{ kN}$	<ul style="list-style-type: none">• The rollers (3) were unlocked. Harder than usual to remove bolts.
100	Column Load = 700 kN $V_{app} = 320 \text{ kN}$	<ul style="list-style-type: none">• Column Load Increased• No Distortion in specimen
189	Column Load = 1712 kN $V_{app} = 320 \text{ kN}$	<ul style="list-style-type: none">• Bottom East Column Flange showing buckling pattern
208	Column Load = 2008 kN $V_{app} = 320 \text{ kN}$	<ul style="list-style-type: none">• Buckling Pattern becoming obvious in bottom west
353	Column Load = 3044 kN $V_{app} = 320 \text{ kN}$	<ul style="list-style-type: none">• Axial load could not be maintained• Test Terminated

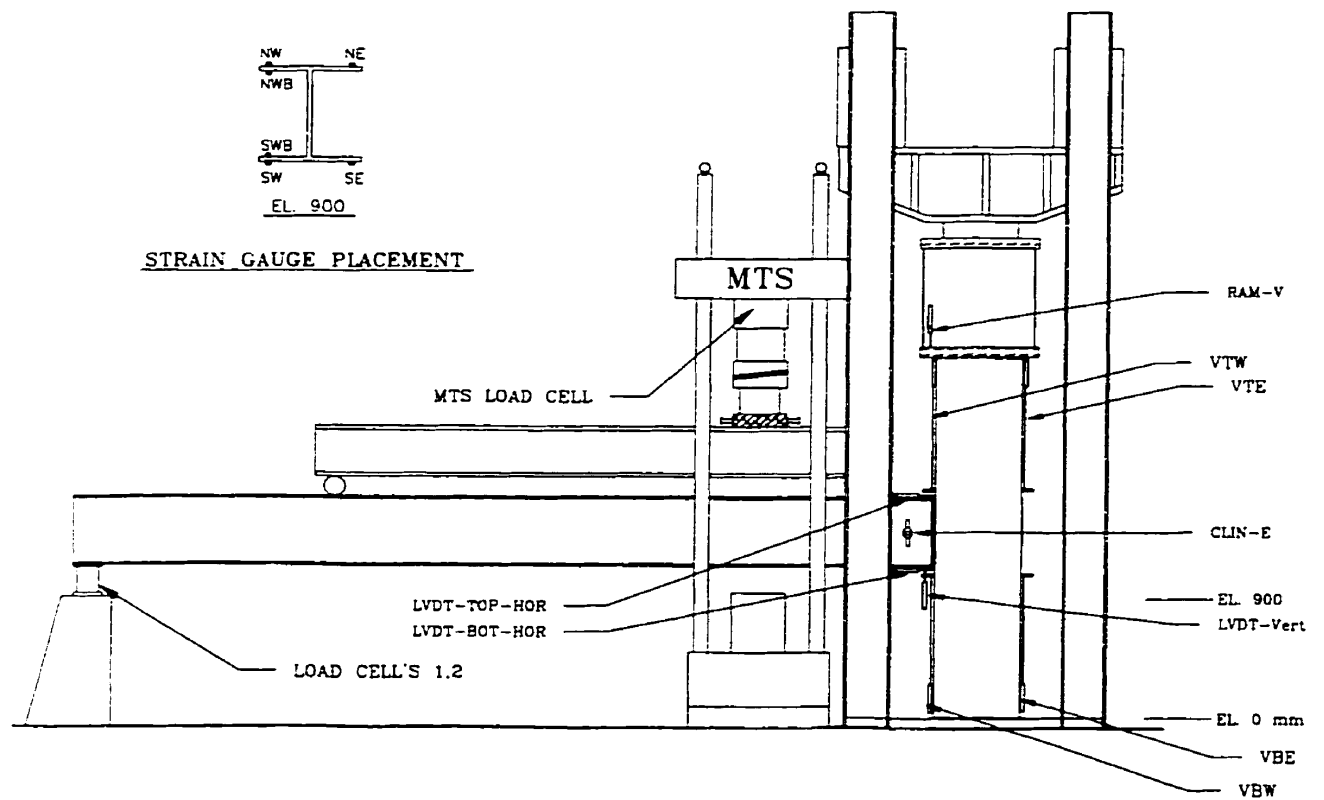
Comments:

There was initial distortion in the connection plate from the pretensioning of the 3 - 3/4" A325 Bolts. As the 2 cleats were clamped together the connection plate deflected on the order of 2 mm.

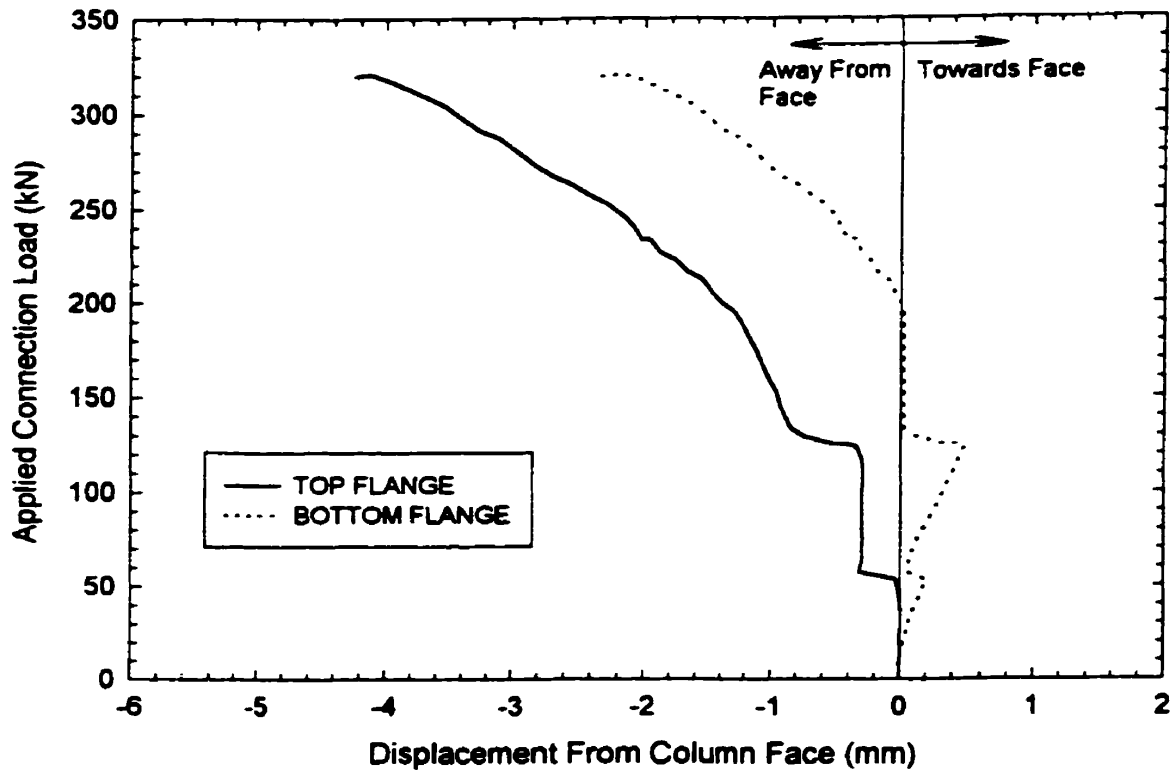
As with other specimens, although there were a buckling pattern in quadrants other than that below the connection at relatively low loads, as the column load was increased the buckling did not advance. The bottom west quadrant eventually did become the dominant failure zone.



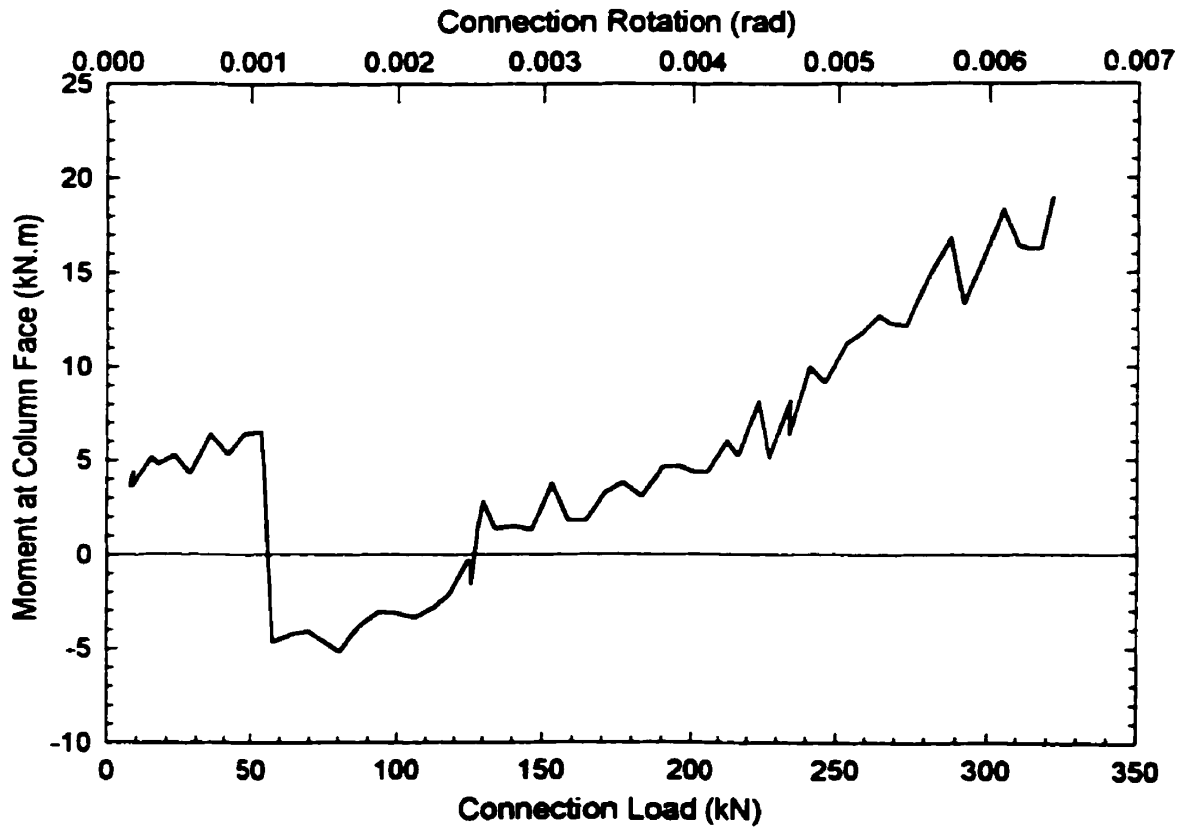
C600-W410-SDA-N: Photographic View of Test Set-up



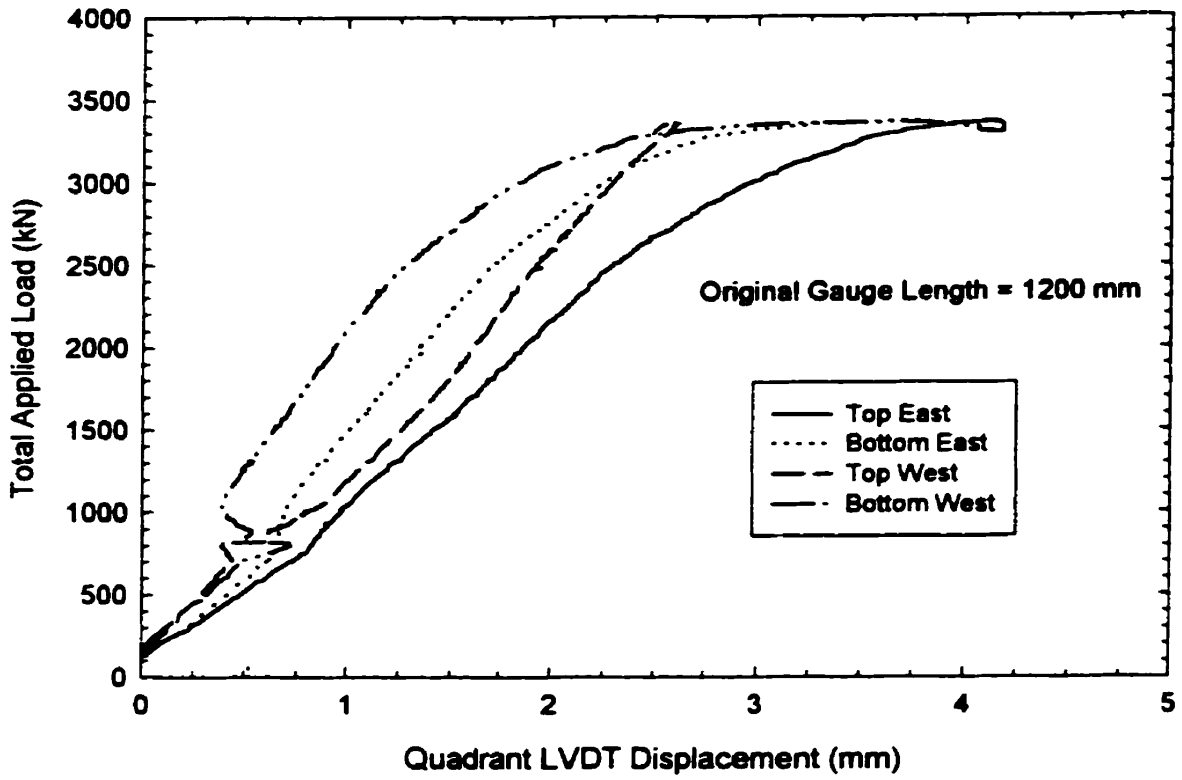
C600-W410-SDA-N: Instrumentation Layout of Test Specimen



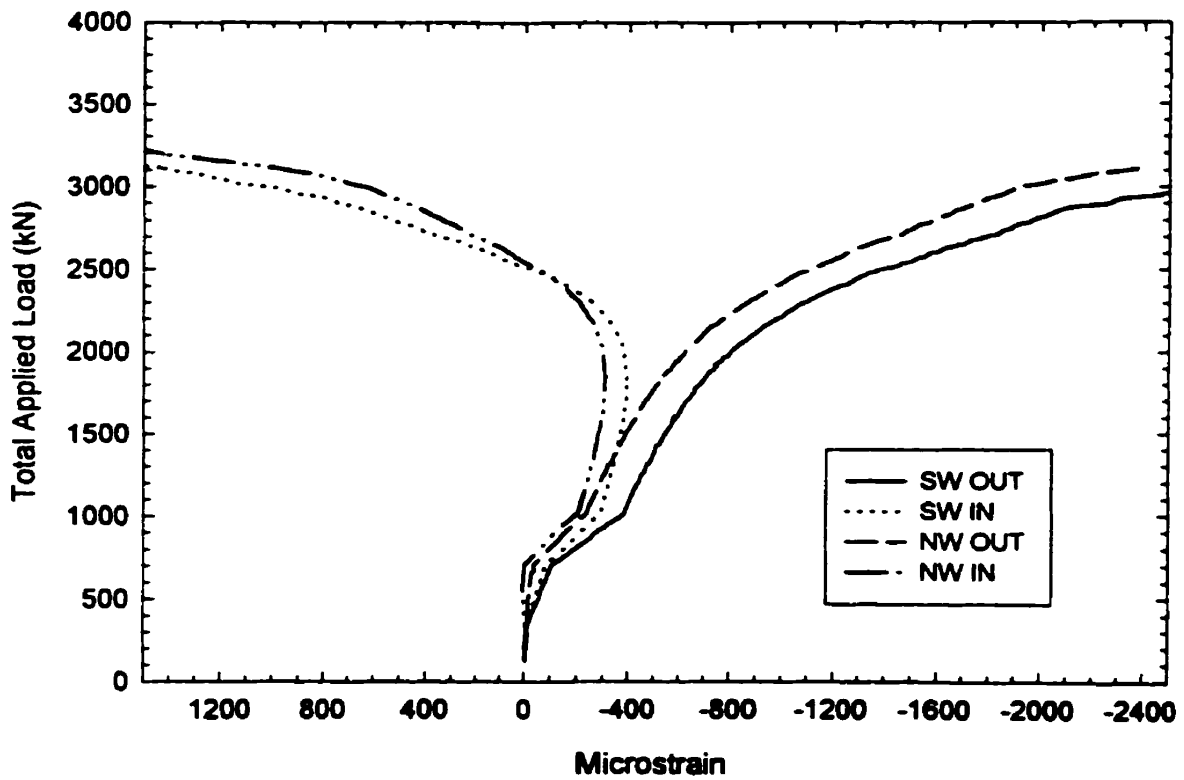
C600-W410-SDA-N: Connection Load vs. Displacement of Beam Flange From Column Face



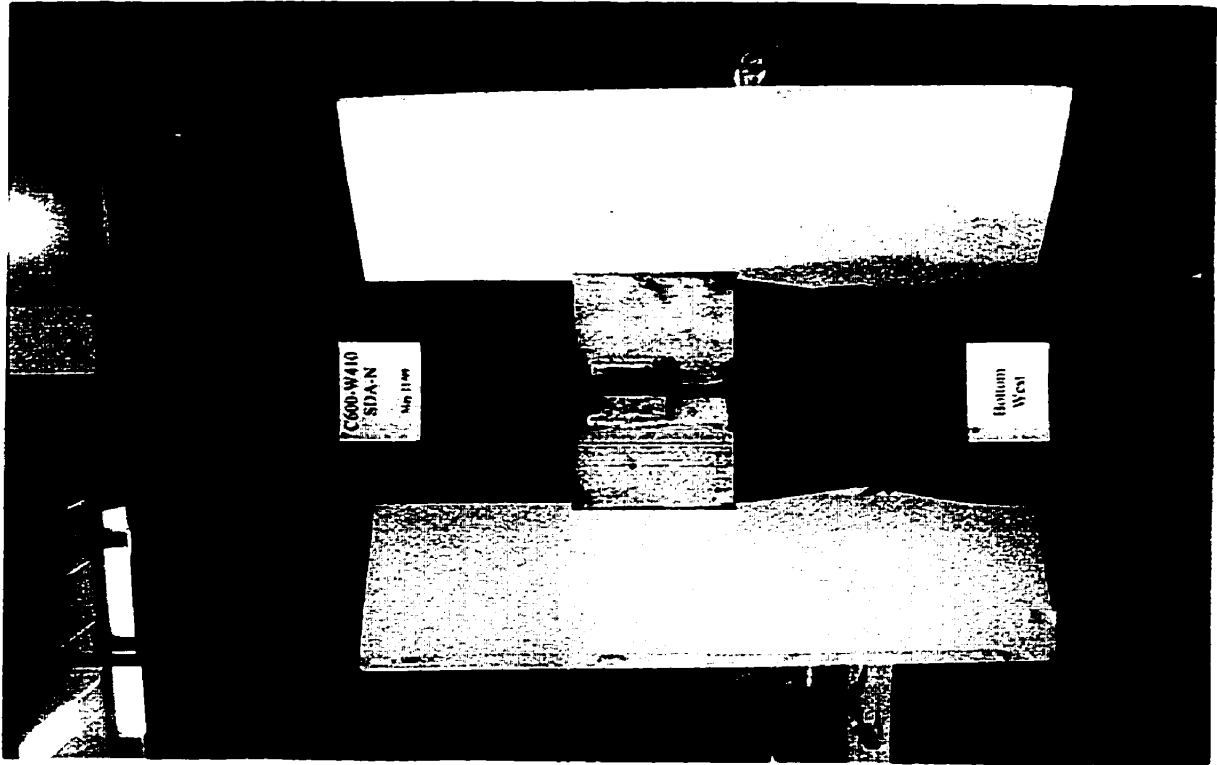
C600-W410-SDA-N: Developed Moment at Column Face Vs Rotation and Connection Load



C600-W410-SDA-N: Total Applied Load vs. Quadrant LVDT Displacement



C600-W410-SDA-N: Total Applied Load vs. Strain 300 mm Below the Connection (EL. 900)



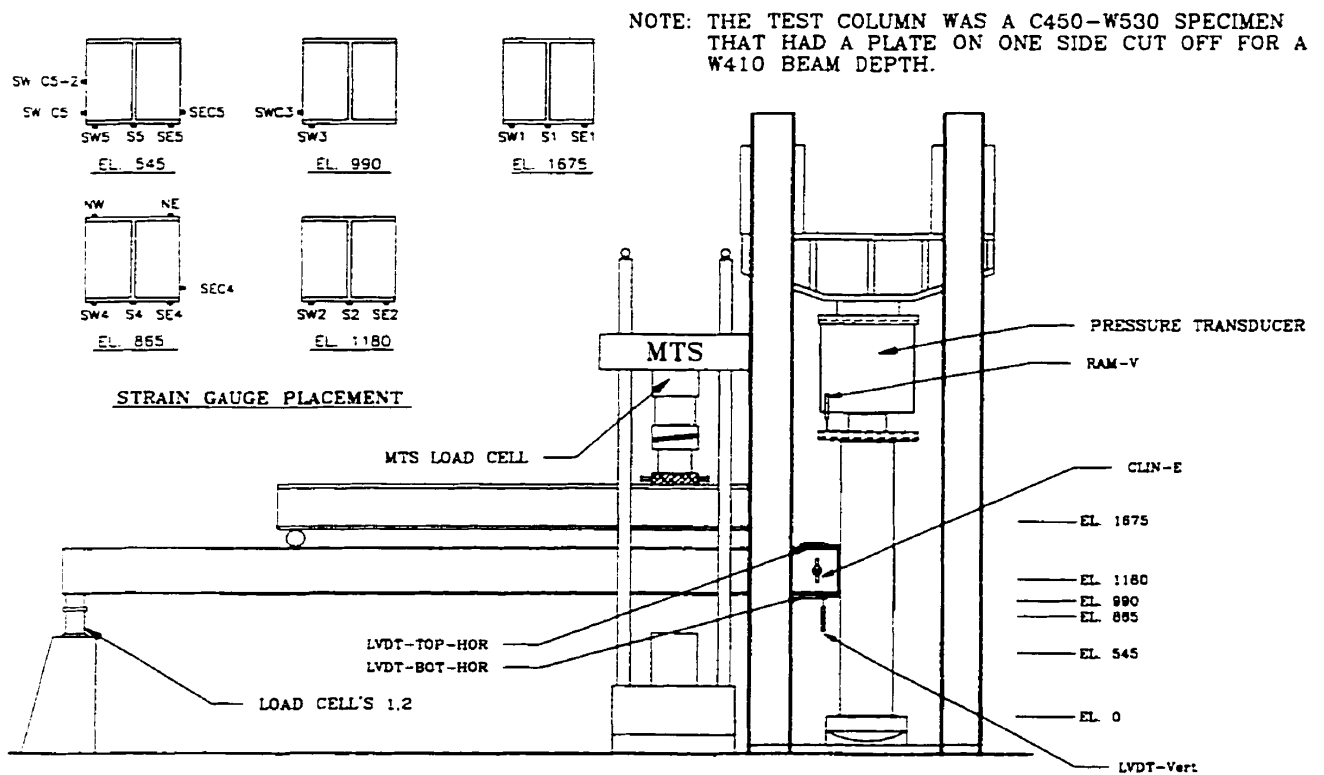
C600-W410-SDA-N: View of Bottom West Quadrant



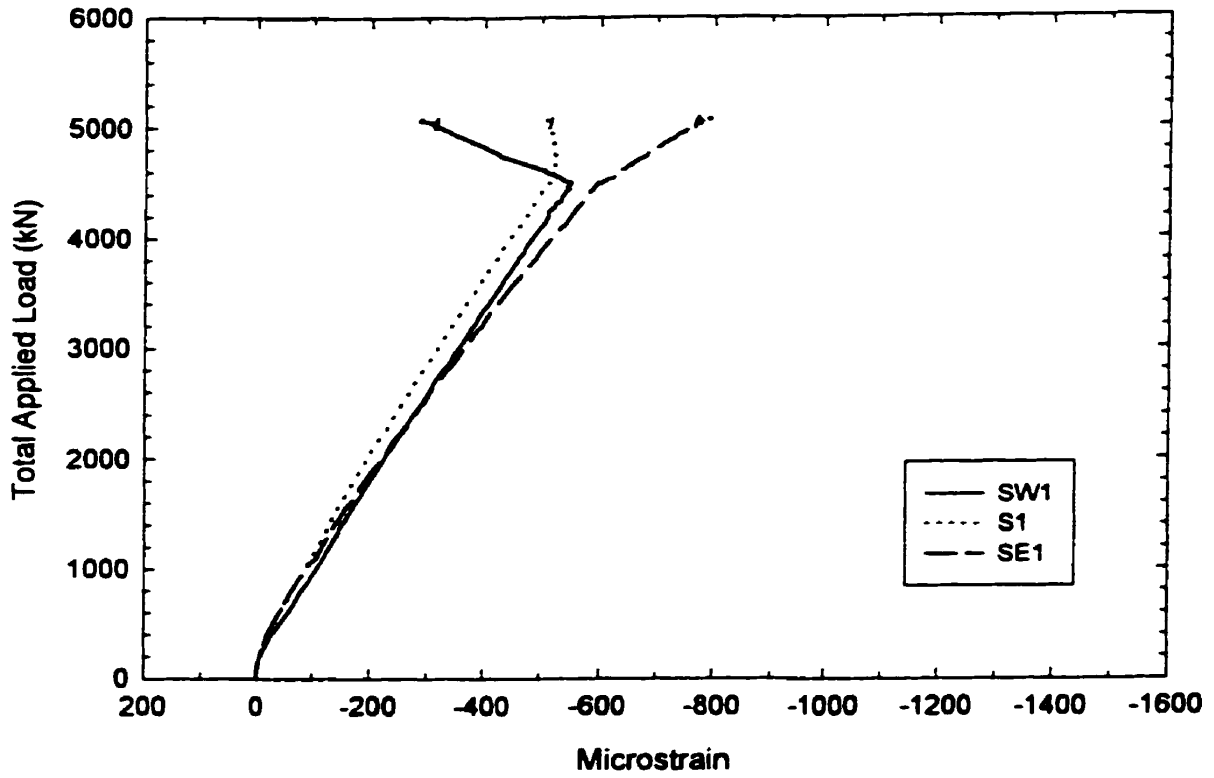
C600-W410-SDA-N: Full View of Failed Specimen



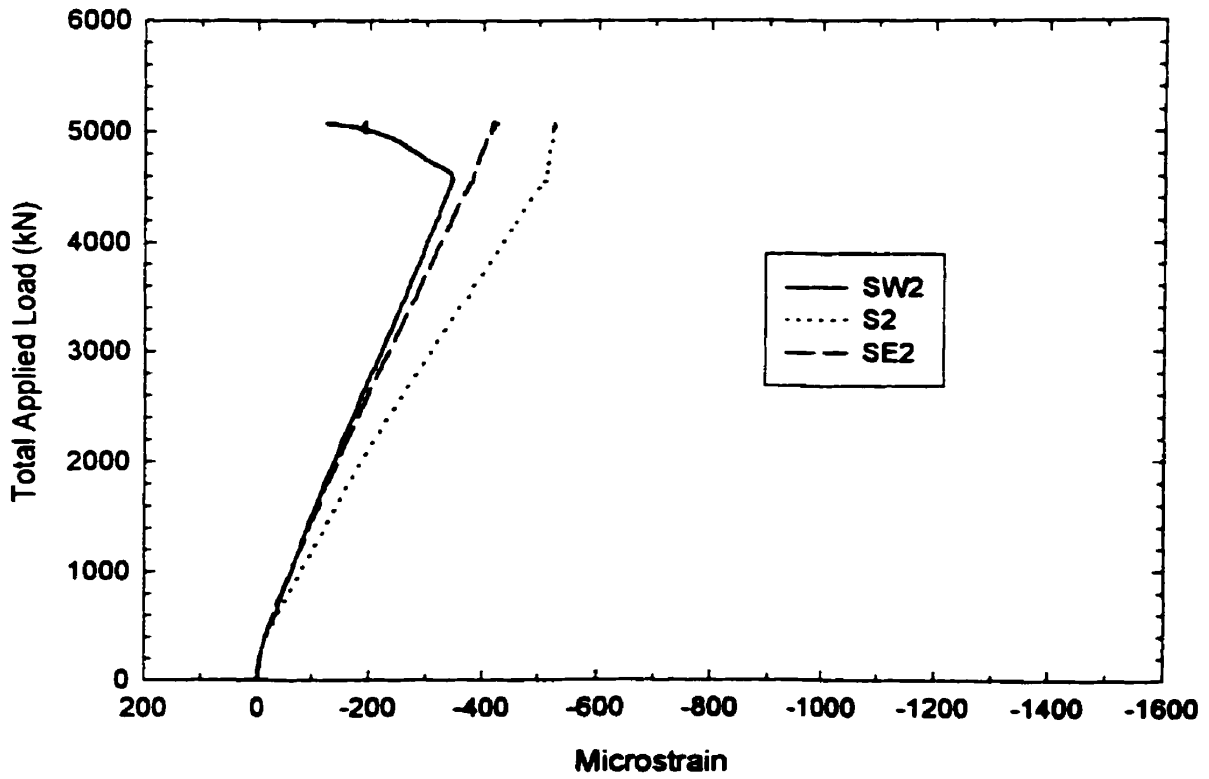
C450-W410-TAB-C: Photographic View of Test Set-up



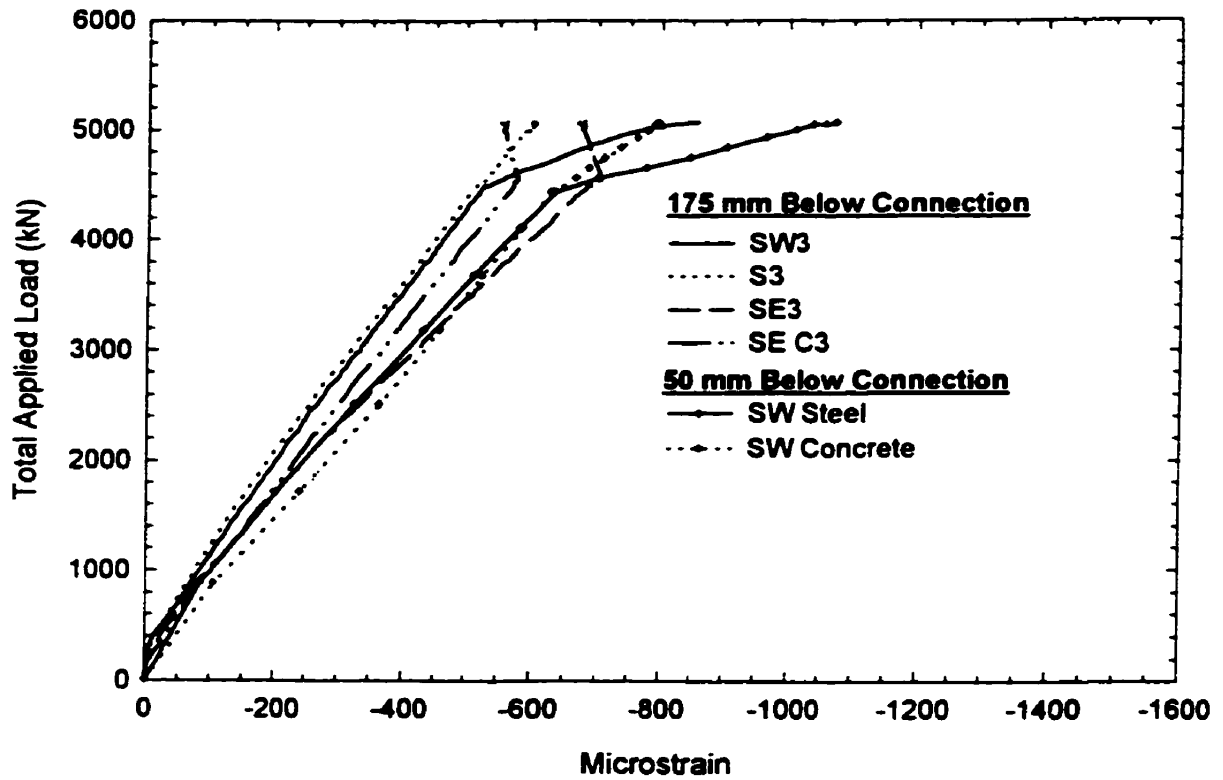
C450-W410-TAB-C: Instrumentation Layout of Test Specimen



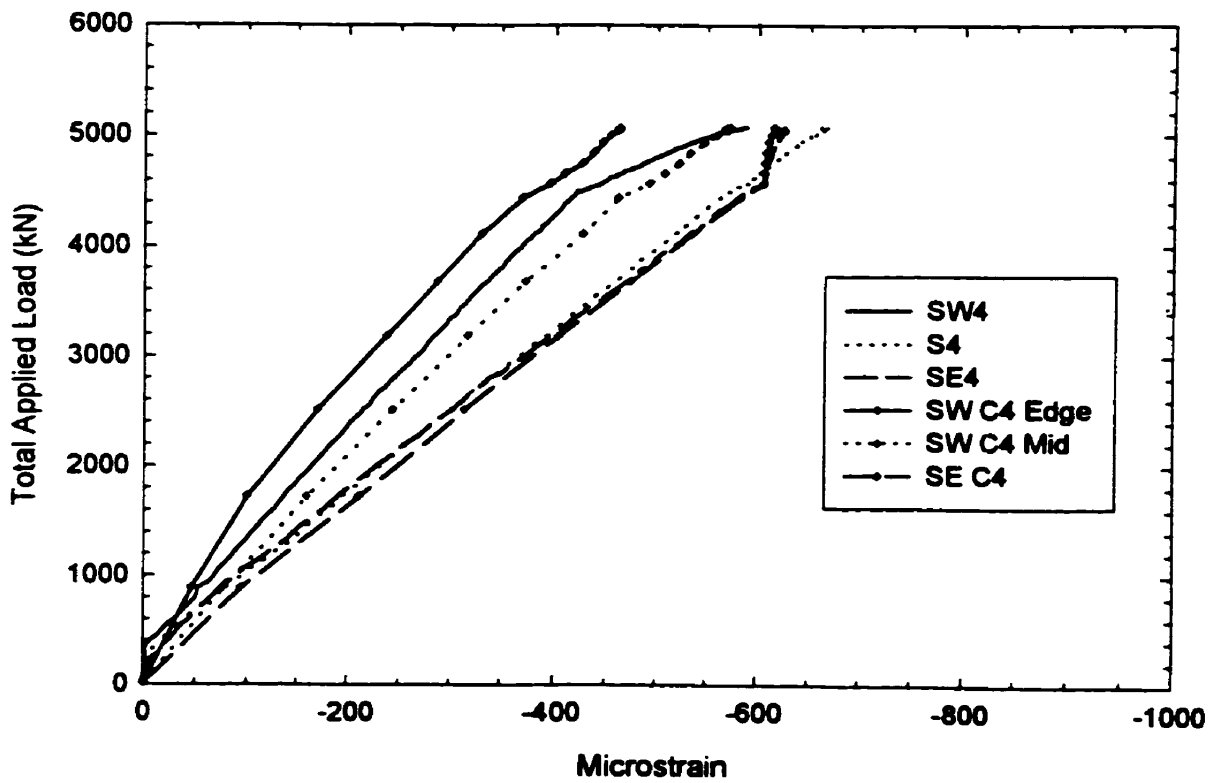
C450-W410-TAB-C: Total Applied Load vs. Strain above Connection (El. 1675)



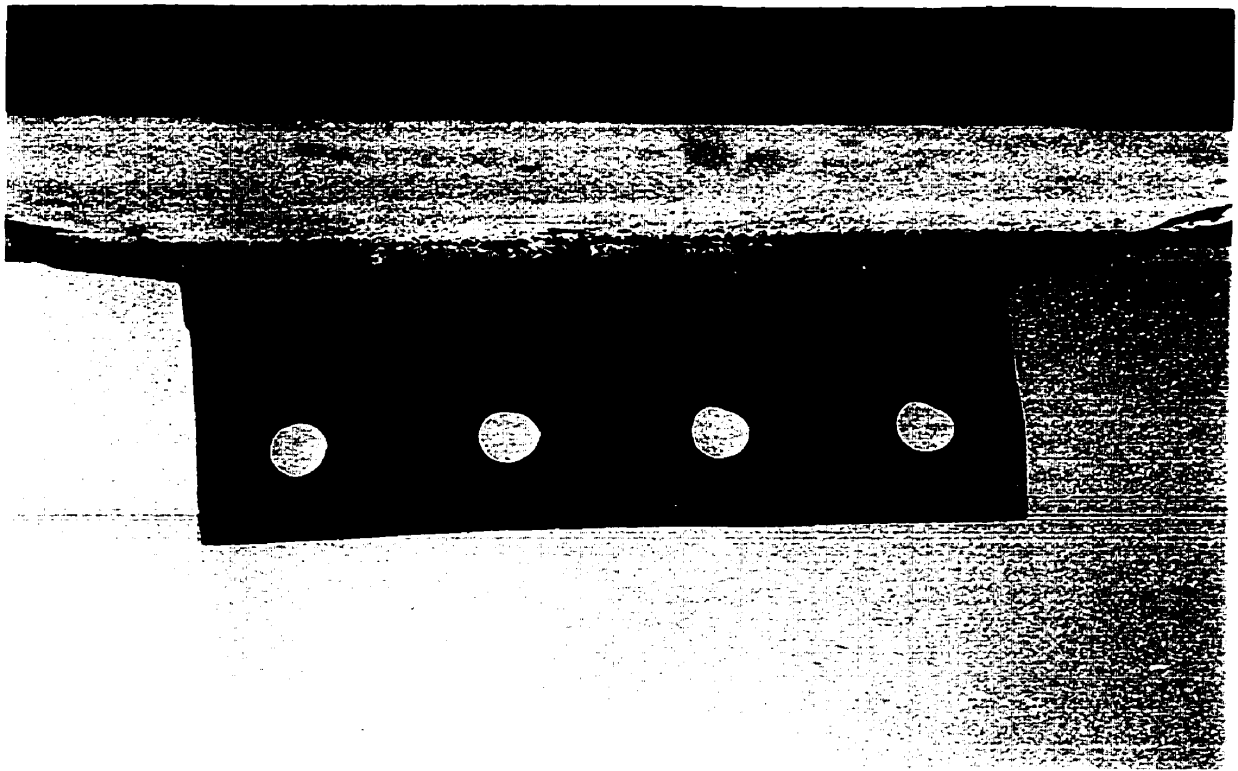
C450-W410-TAB-C: Total Applied Load vs. Strain at Middle of Connection Plate (El. 1180)



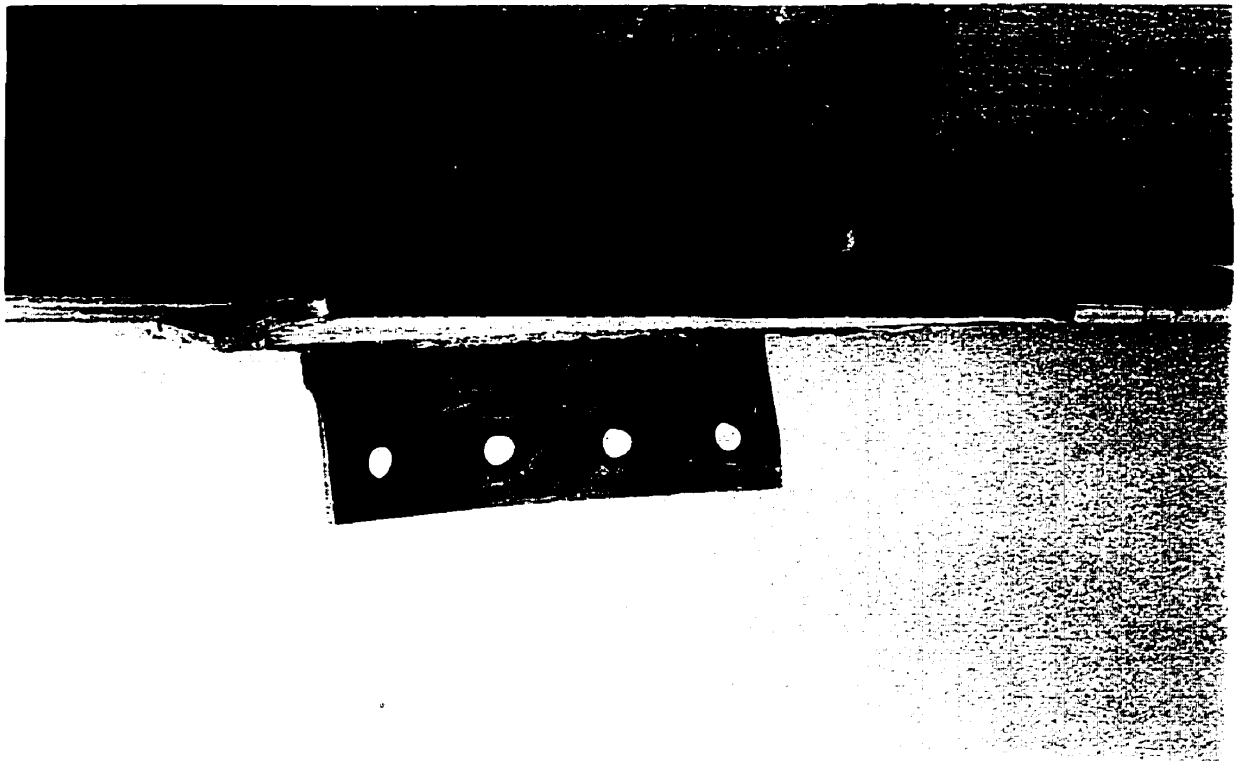
C450-W410-TAB-C: Total Load vs. Strain Below Connection Plate (El. 990 and 865)



C450-W410-TAB-C: Total Load vs. Strain 495 mm Below Connection Plate (El. 545)



C450-W410-TAB-C: Side View of Connection



**C450-W410-TAB-C: Oblique View of Tested Specimen
Note the Out of Plane Distortion**

Test No. 10: C450-W530-TAB-COMP
May 26, 1999

Description: 450 x 450 x 2358 mm Column Single Shear Plate (TAB) Connection
 W530 x 92 Load Beam 6 - 3/4" A325 Bolts (70% Yield).
 Composite State PL 445 x 110 x 9.53 Connection

Testing Procedure:

- 1) Load the column to a nominal load of 4500 kN. This approximately represents 1.0 DL + 0.5 LL.
- 2) Proceeded to load the connection to 720 kN. Stopped at this point because it was desired to load the column to higher loads.
- 3) The column load was increased to the Fox Jack Limits. At which point the column showed no obvious distress (although strain readings were in the yielded zone). Thus the column load was decreased to 4500 kN and the connection reloaded to MTS limits.

Geometry: $A_1 = 560 \text{ mm}$ $d_{\text{MTS}} = 1360 \text{ mm}$
 $A_2 = 4035 \text{ mm}$ $L = 6937 \text{ mm}$

RESULTS:

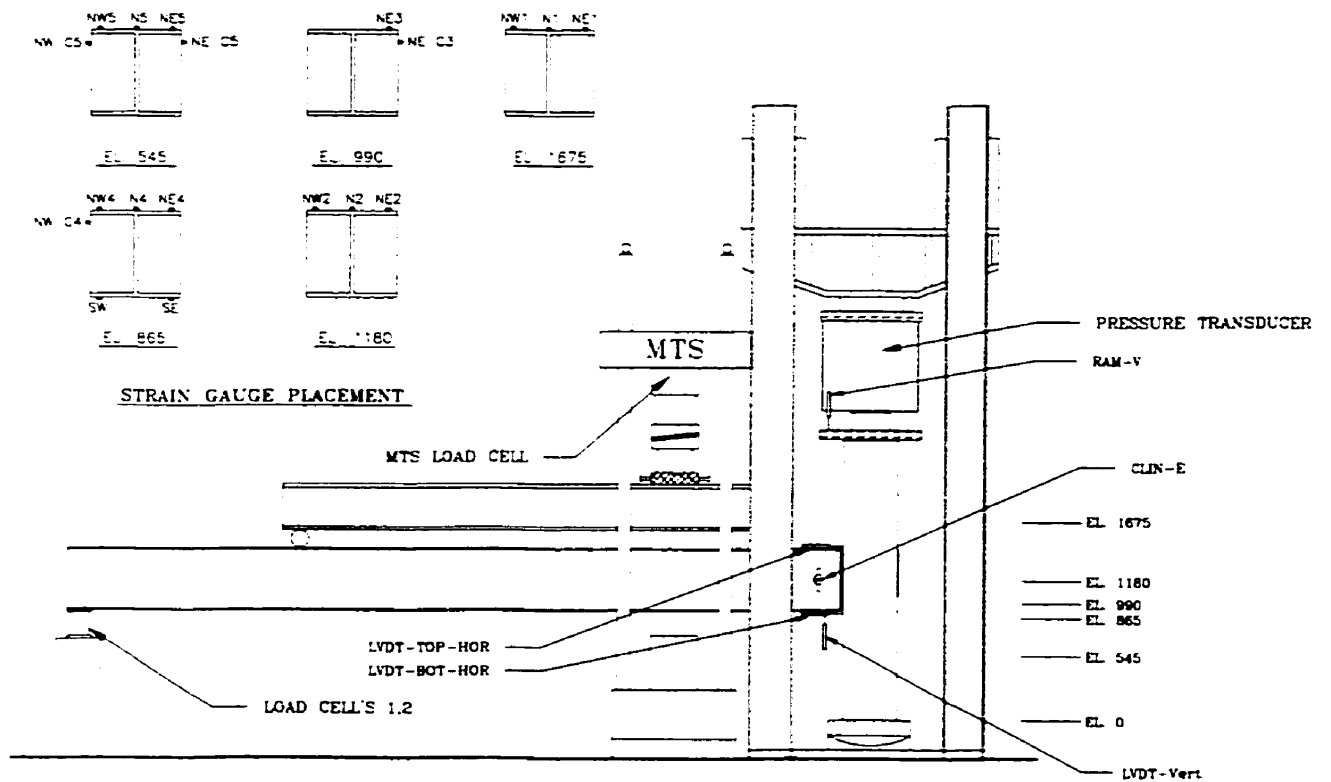
<u>Dataset</u>	<u>Load Stage</u>	<u>Description</u>
77	Column Load = 4500 kN	<ul style="list-style-type: none">• Begin Loading Connection
197	Column Load = 4500 kN $V_{\text{app}} = 720 \text{ kN}$	<ul style="list-style-type: none">• Begin to increase column load, keeping V_y constant.
301	Column load = 6806 kN $V_{\text{app}} = 716 \text{ kN}$	<ul style="list-style-type: none">• Maximum loading. Yielding strain at gauges but no visible distress.
341	Column Load = 4500 kN $V_{\text{app}} = 710 \text{ kN}$	<ul style="list-style-type: none">• Decided to load the connection to MTS limits.
377	Column Load = 4500 kN $V_{\text{app}} = 792 \text{ kN}$	<ul style="list-style-type: none">• MTS at maximum load, pump shut off• Test Terminated.

Comments:

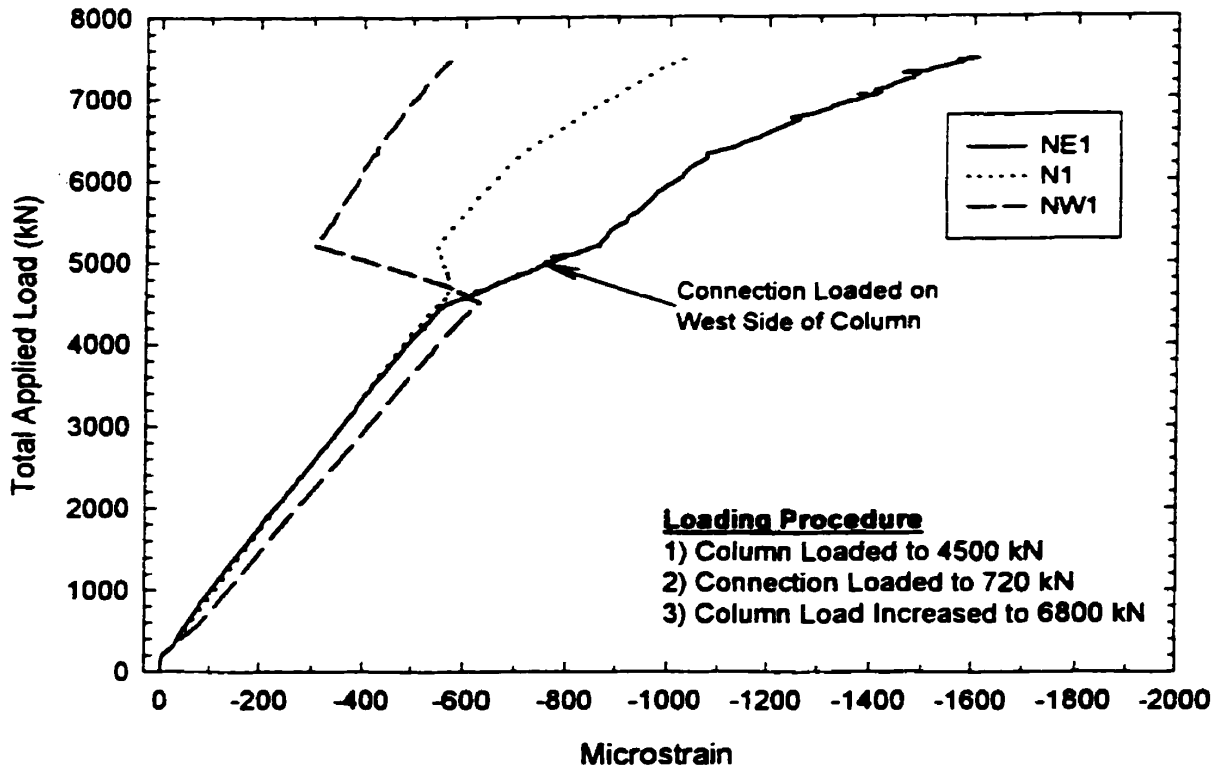
No distortion in column other than connection plate. The separation at the cross plate was minimal compared to other tests. Minimal distortion of the shear tab observed.



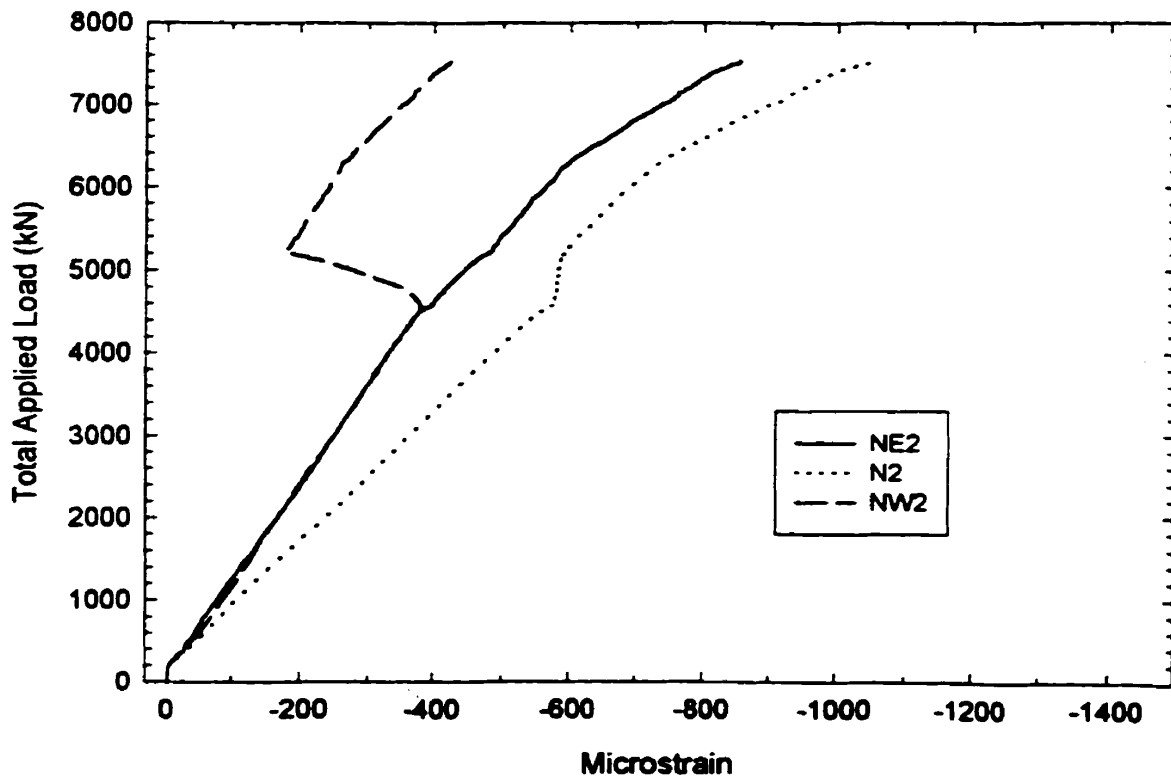
C450-W530-TAB-C: Photographic View of Test Set-up



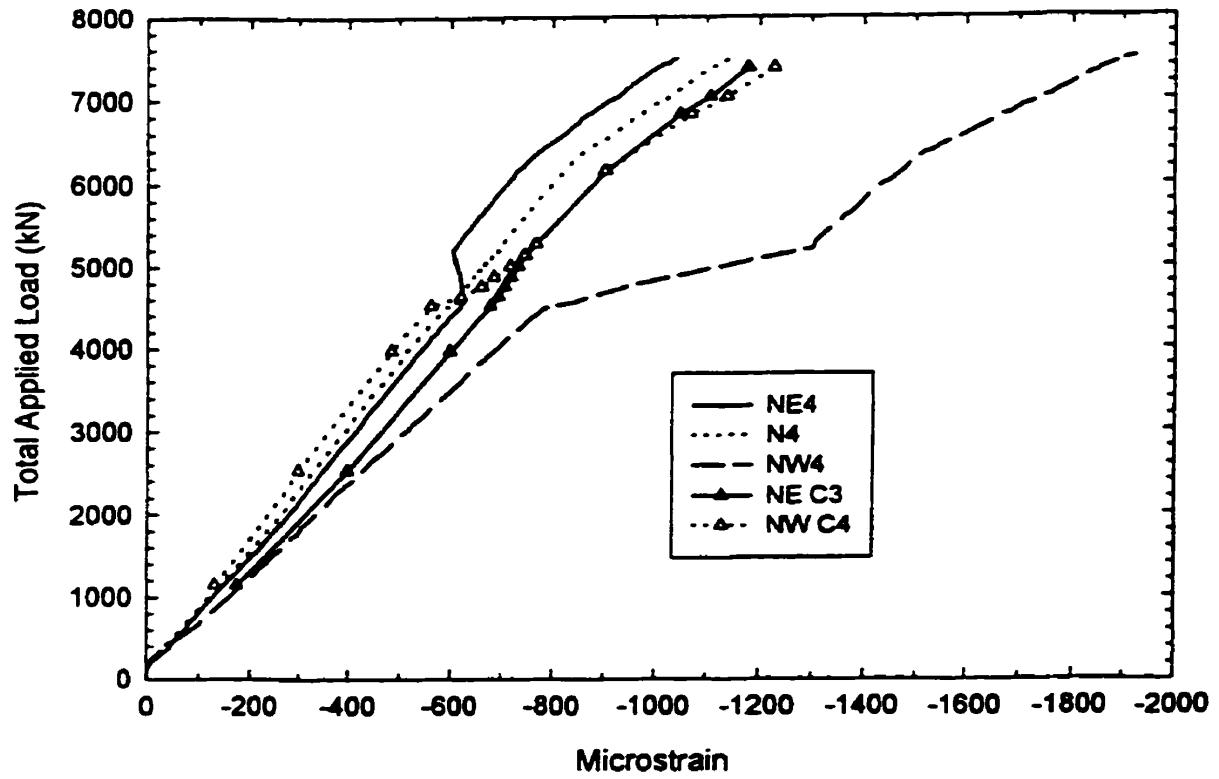
C450-W530-TAB-C: Instrumentation Layout of Test Specimen



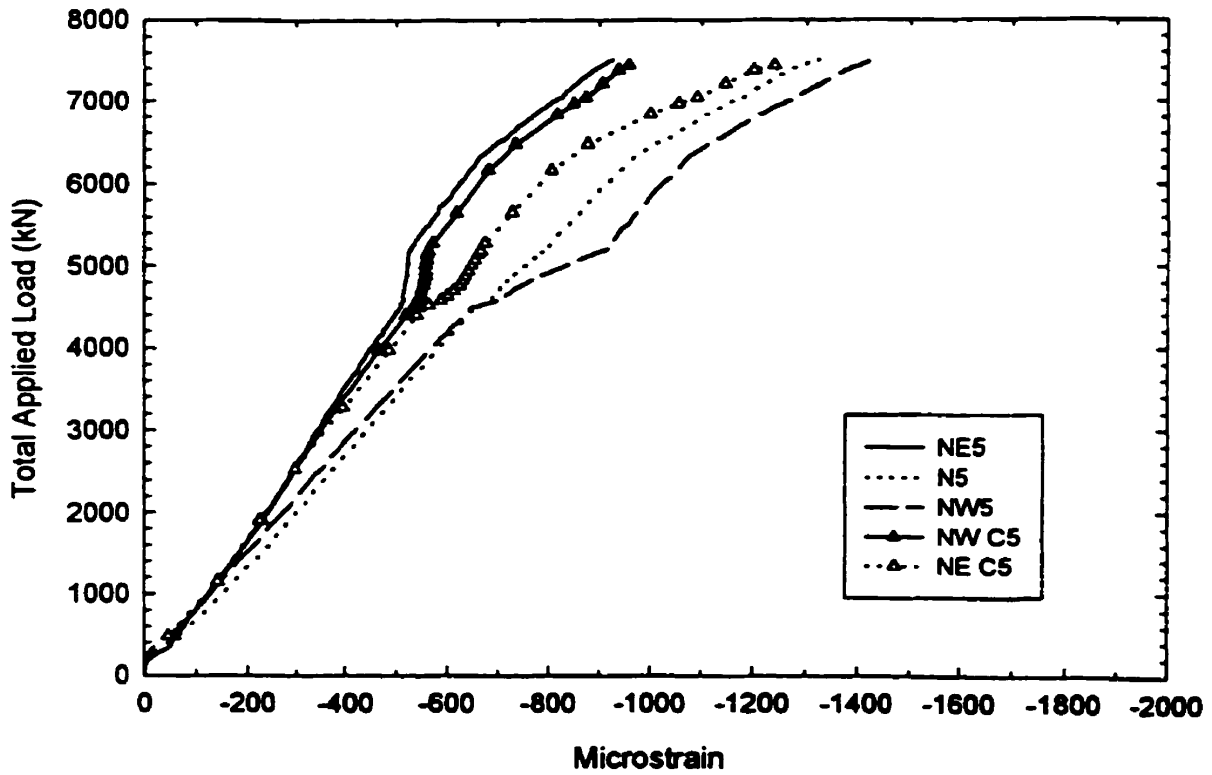
C450-W530-TAB-C: Total Applied Load vs. Strain 225 mm Above Connection Plate (El. 1675)



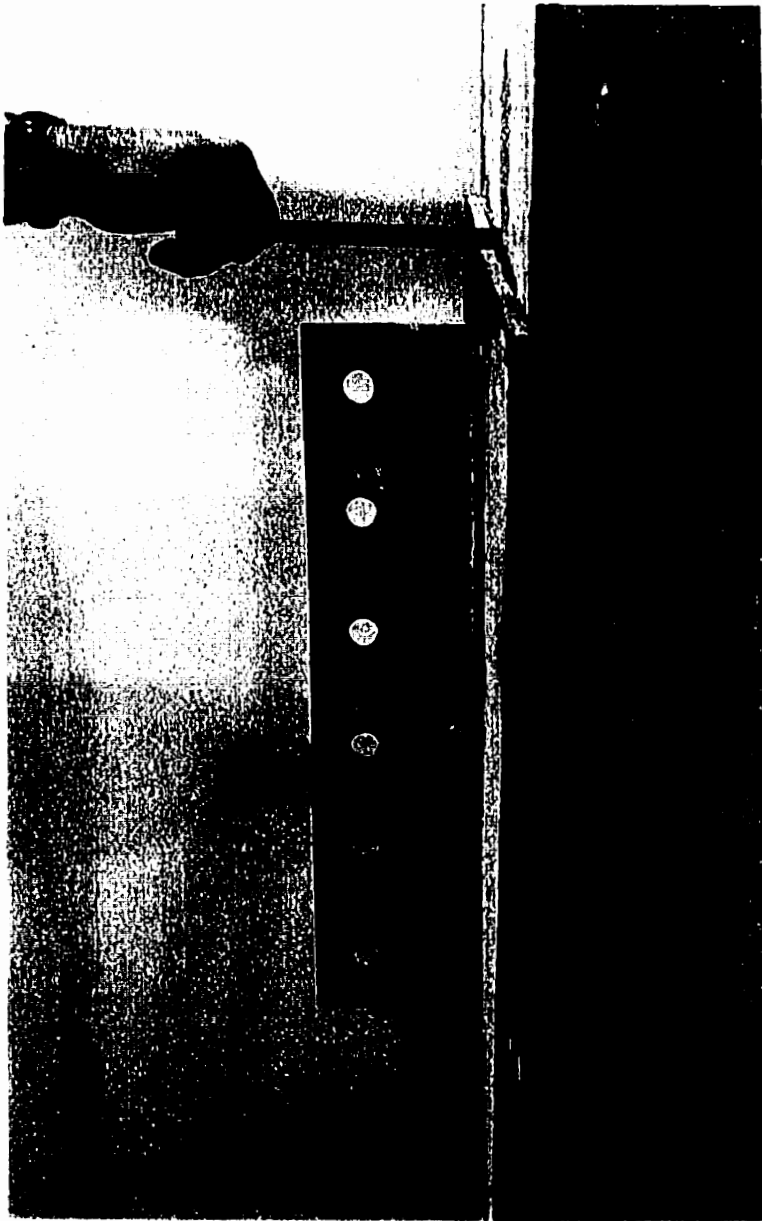
C450-W530-TAB-C: Total Applied Load vs. Strain at Middle of Connection Plate (El. 1180)



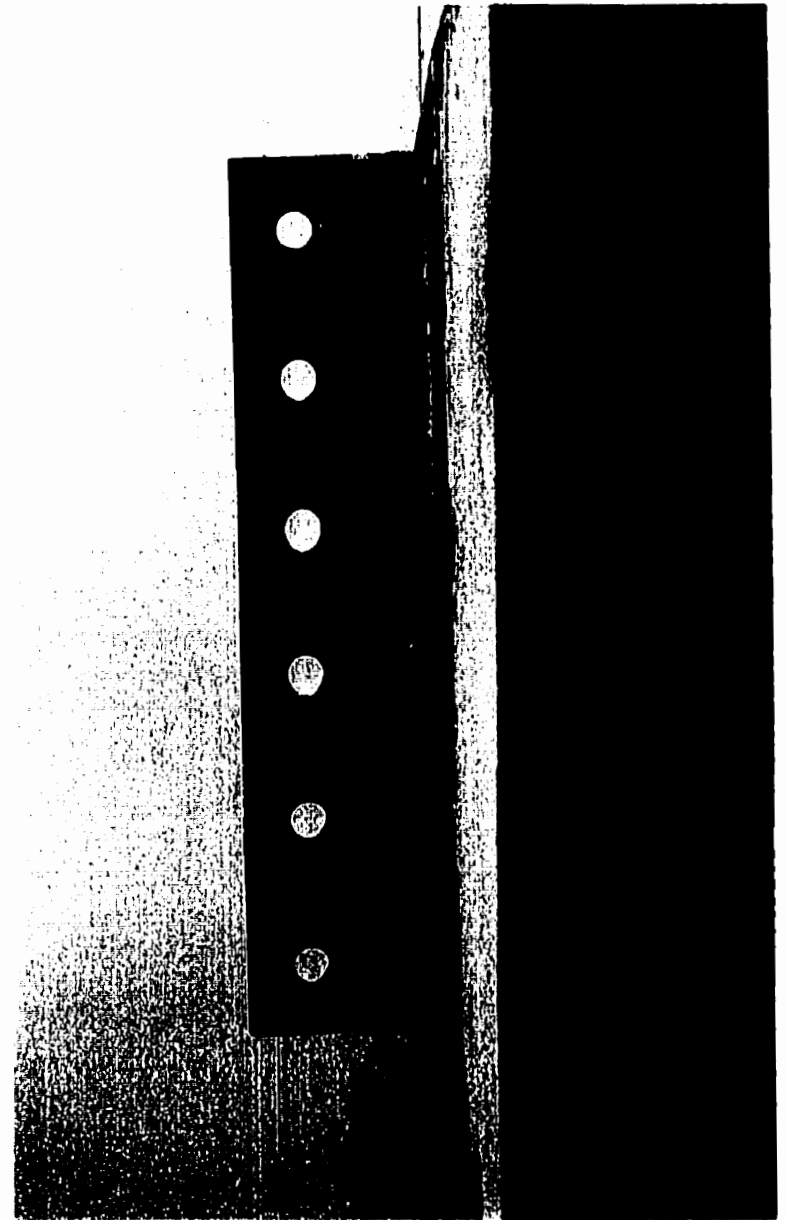
C450-W530-TAB-C: Total Applied Load vs. Strain 50 mm Below Connection Plate (El. 865)



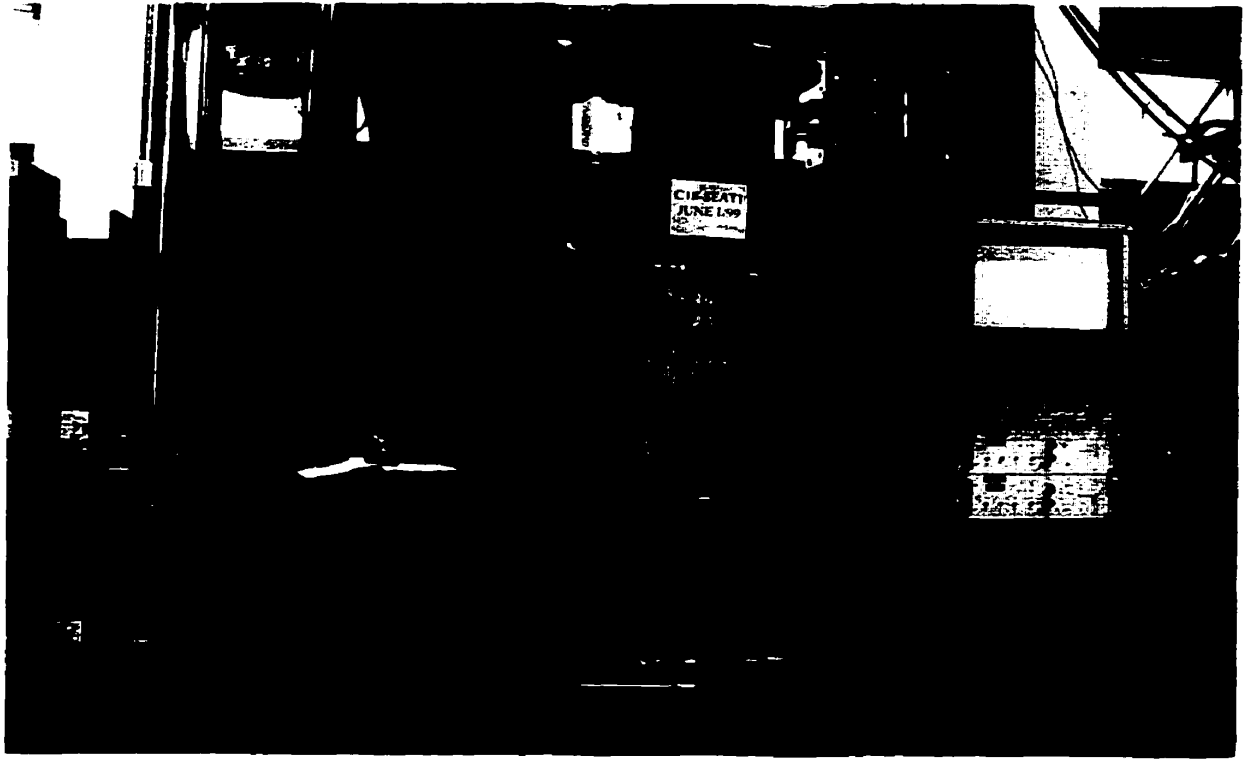
C450-W530-TAB-C: Total Applied Load vs. Strain 370 mm Below Connection Plate (El. 545)



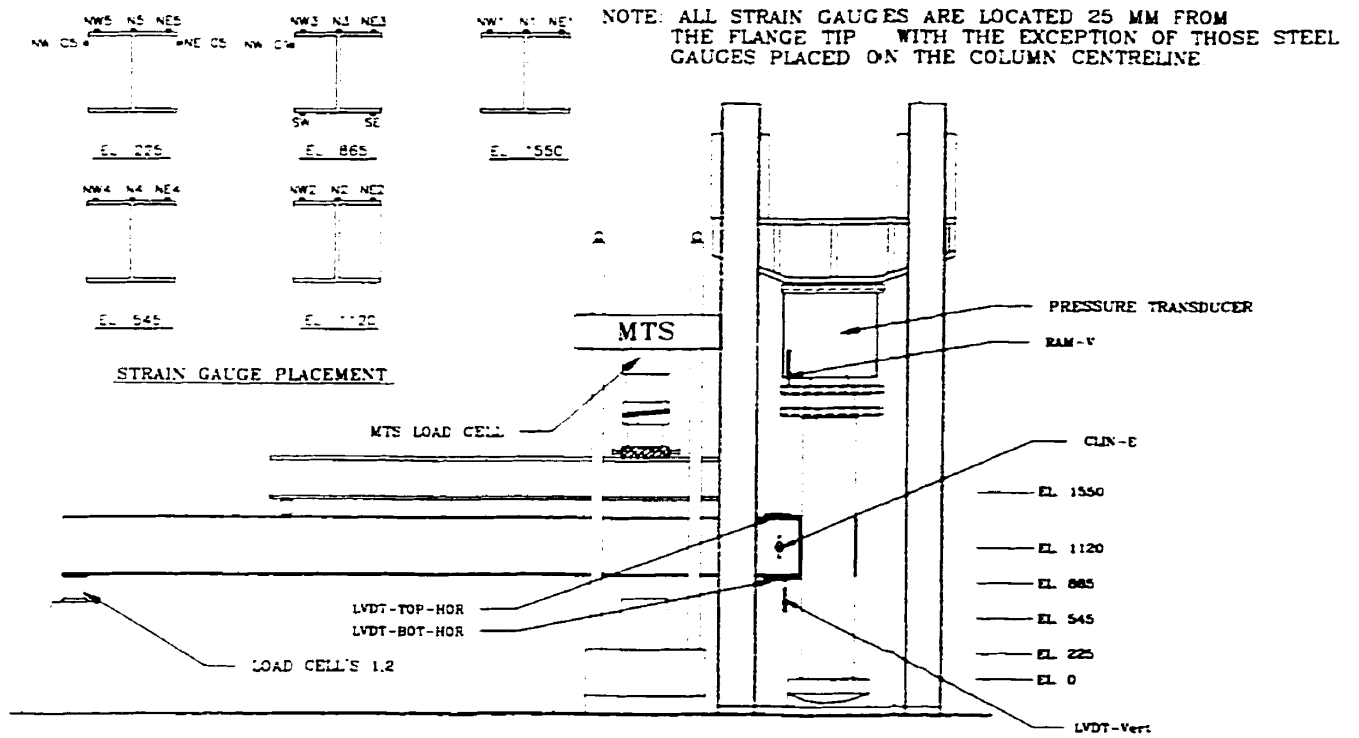
**C450-W530-TAB-C: Oblique View of Tested Specimen
Showing Little Permanent Deformation**



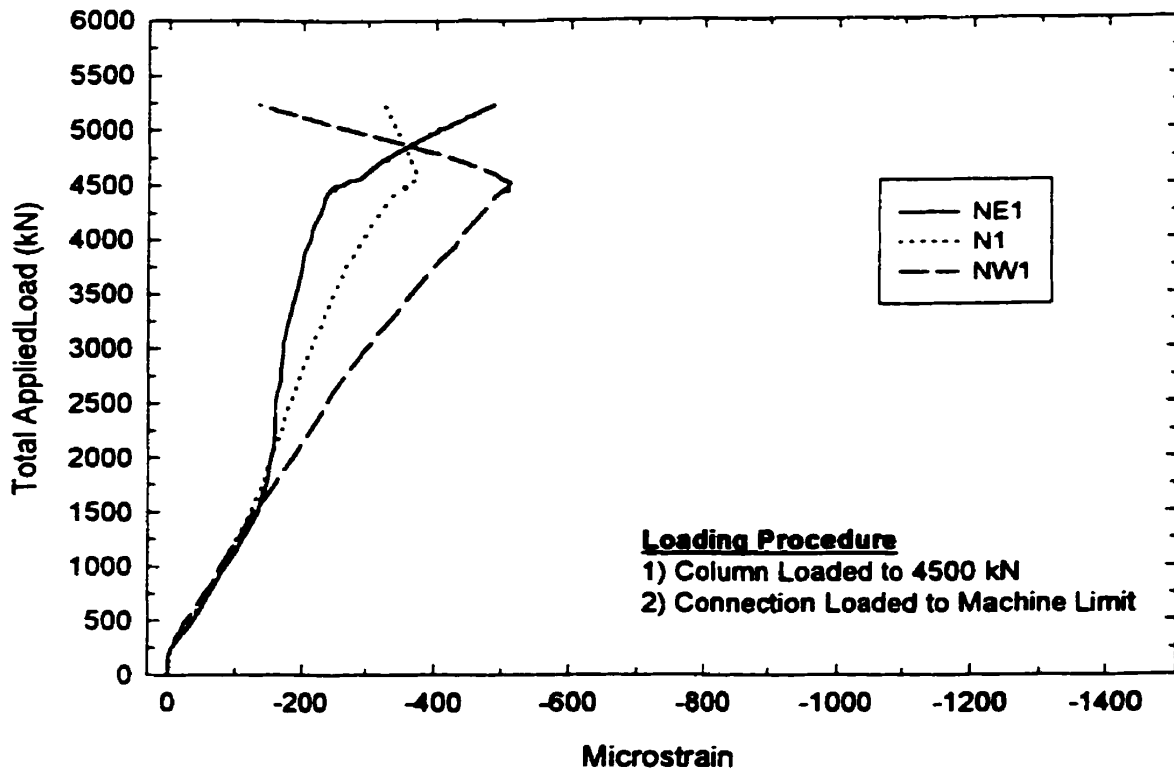
C450-W530-TAB-C: Side View of Tested Connection



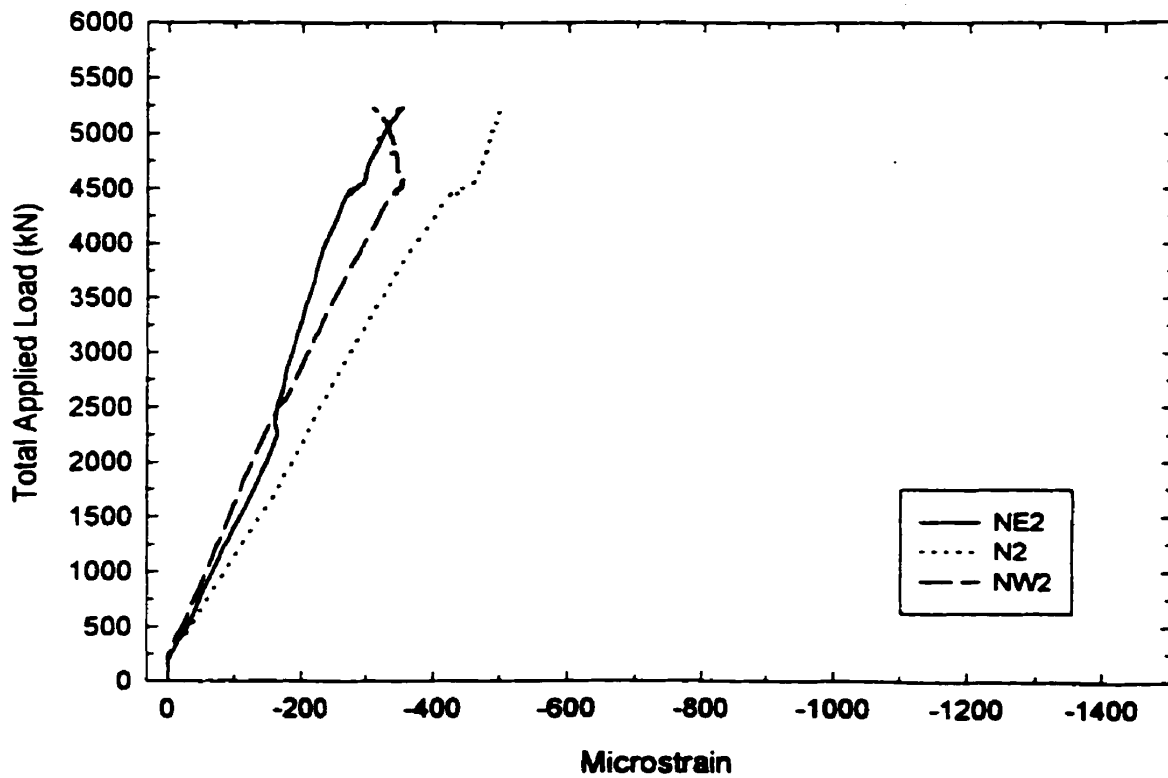
C450-SEAT1-NoANCH: Photographic View of Test Set-up



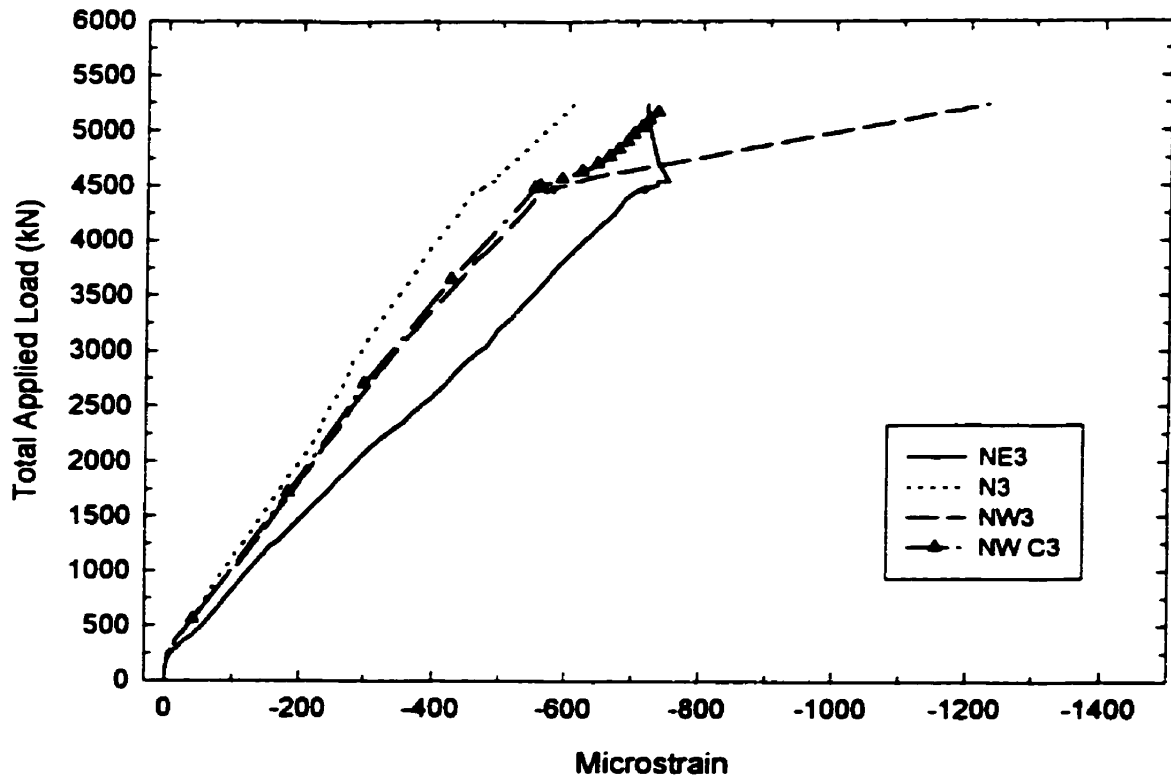
C450-SEAT1-NoANCH: Instrumentation Layout of Test Specimen



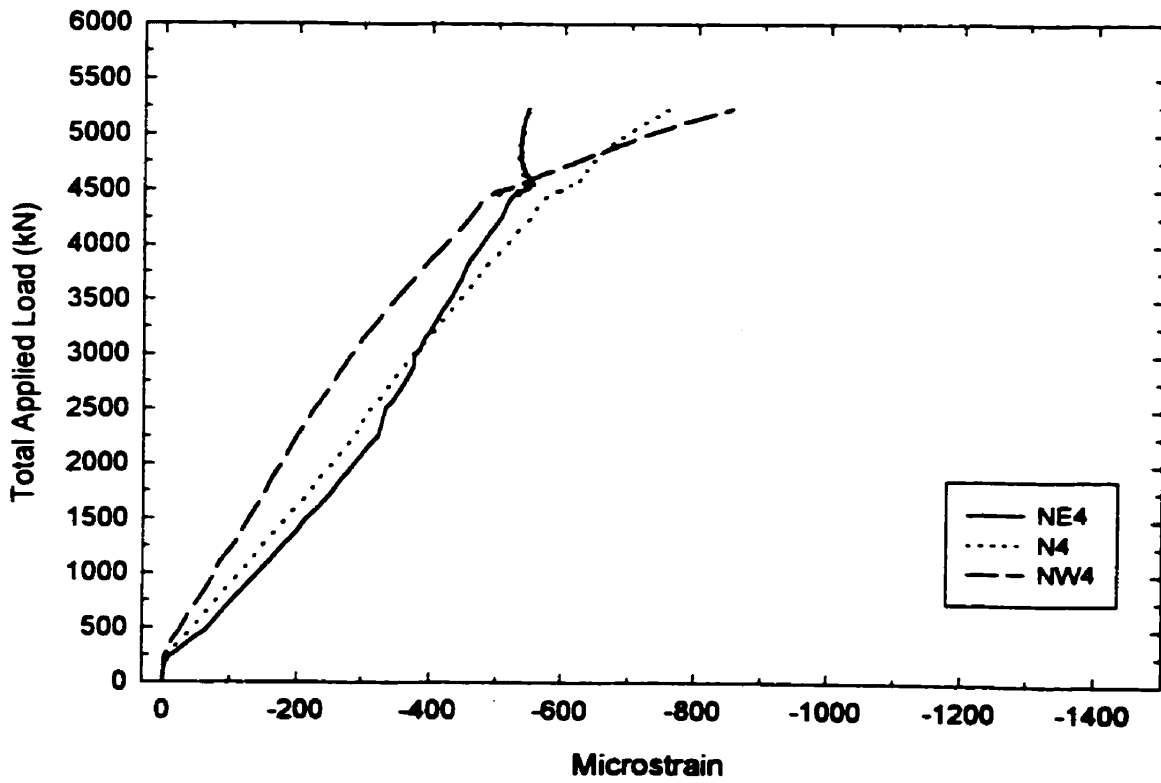
C450-Seat1-NoAnch: Total Applied Load vs. Strain 225 mm Above Connection Plate (El. 1550)



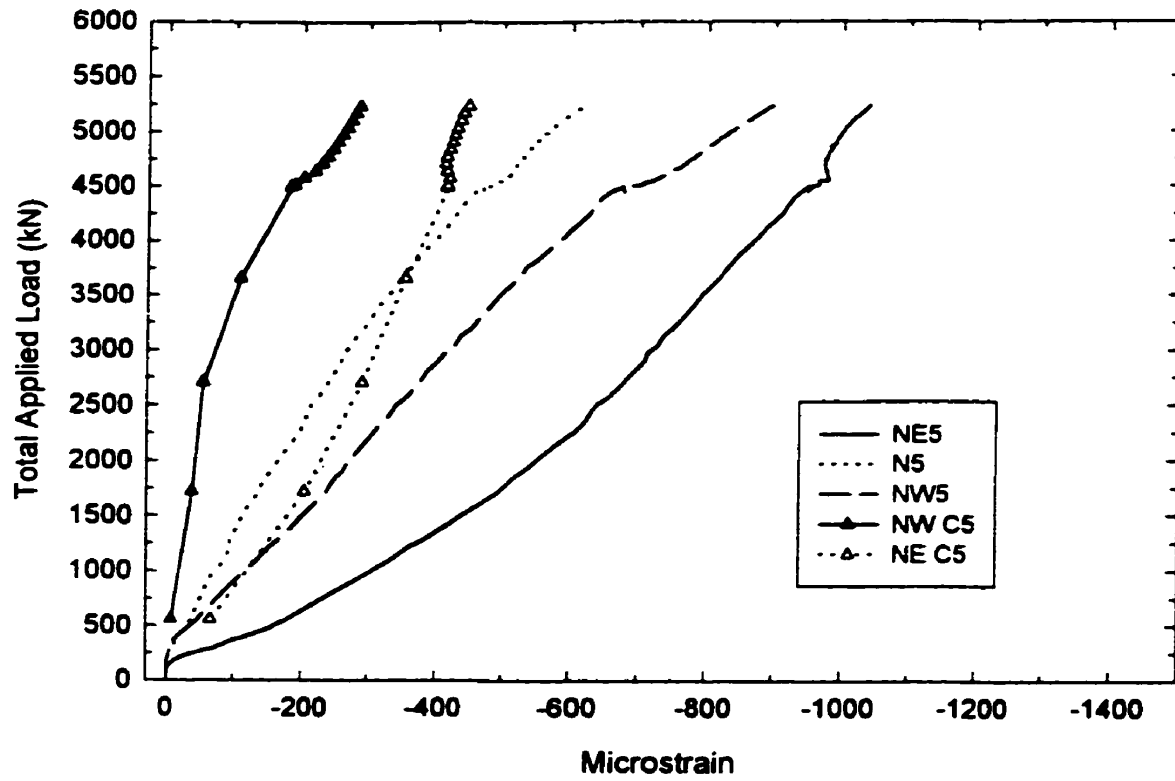
C450-Seat1-NoAnch: Total Applied Load vs. Strain at Middle of Connection Plate (El. 1120)



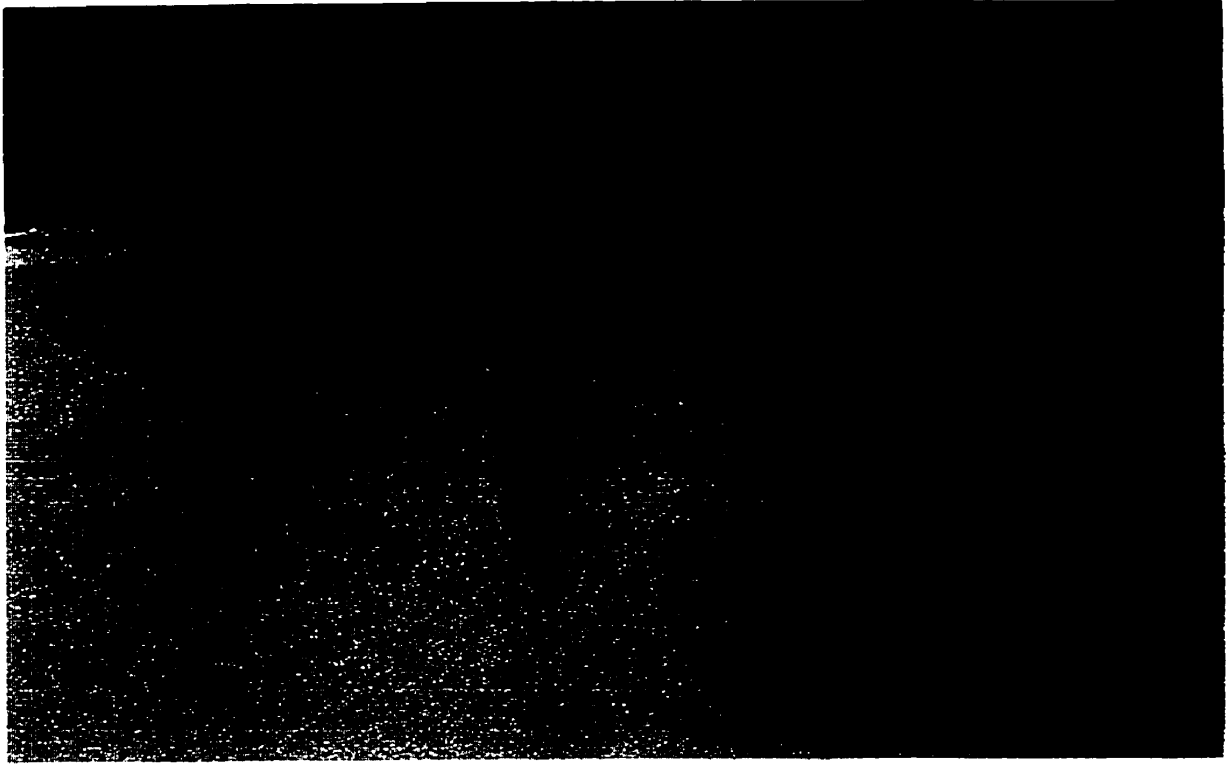
C450-Seat1-NoAnch: Total Load vs. Strain 50 mm Below Connection Plate (El. 865)



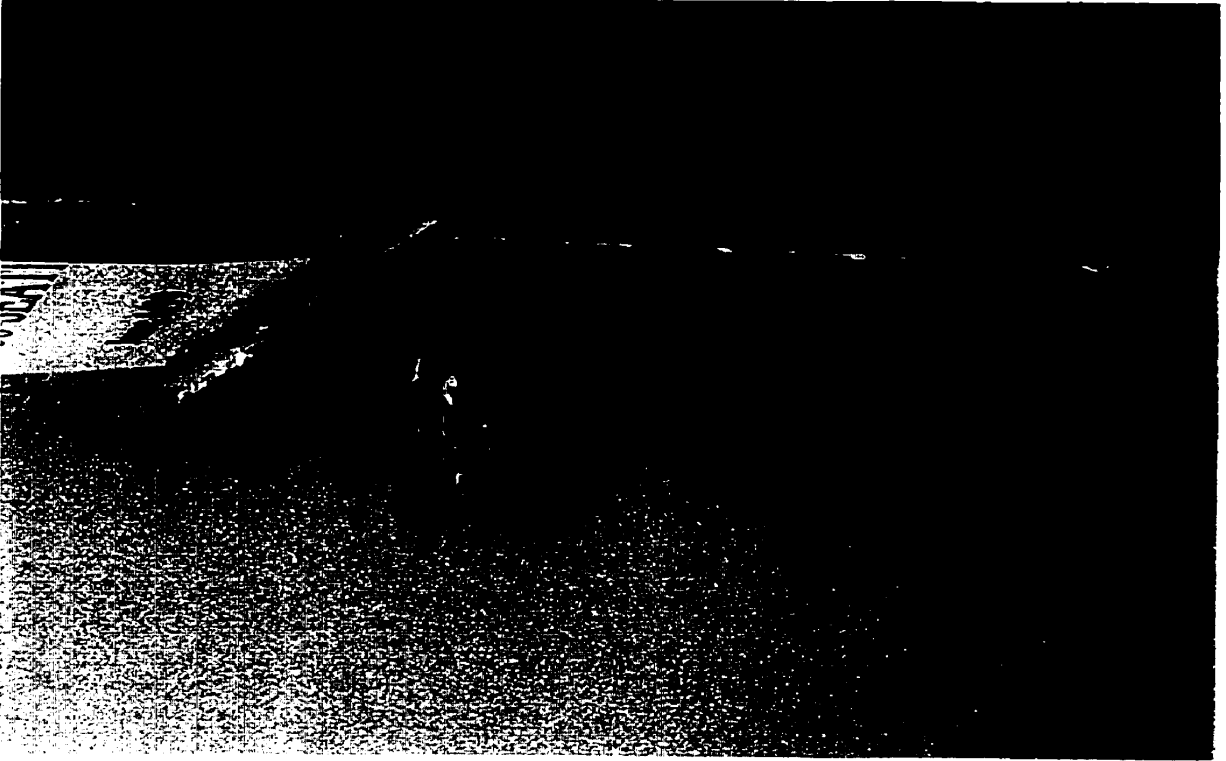
C450-SEAT1-NoAnch: Total Load vs. Strain 370 mm Below Connection Plate (El. 545)



C450-Seat1-NoAnch: Total Applied Load vs. Strain 685 mm Below Connection Plate (El. 225)



C450-Seat1: Side View of Tested Connection



C450-Seat1: Oblique View of Tested Connection

Test No. 12: C450-SEAT2
June 3, 1999

Description: 450 x 450 x 2234 mm Column Seat Connection
W530 x 93 Load Beam 2 - 3/4" A325 Bolts (70% Yield).
Composite State Clipped Angle L203 x 102 x 19
Shear Studs

Testing Procedure:

- 1) Load the column to a nominal load of 4500 kN. This approximately represents 1.0 DL + 0.5 LL.
- 2) Proceed to load the connection unto MTS limits or connection failure.
- 3) If the MTS limit was reached prior to connection failing then drop the connection load to 800 kN and proceed to load the column to either failure of Fox Jack Limits.

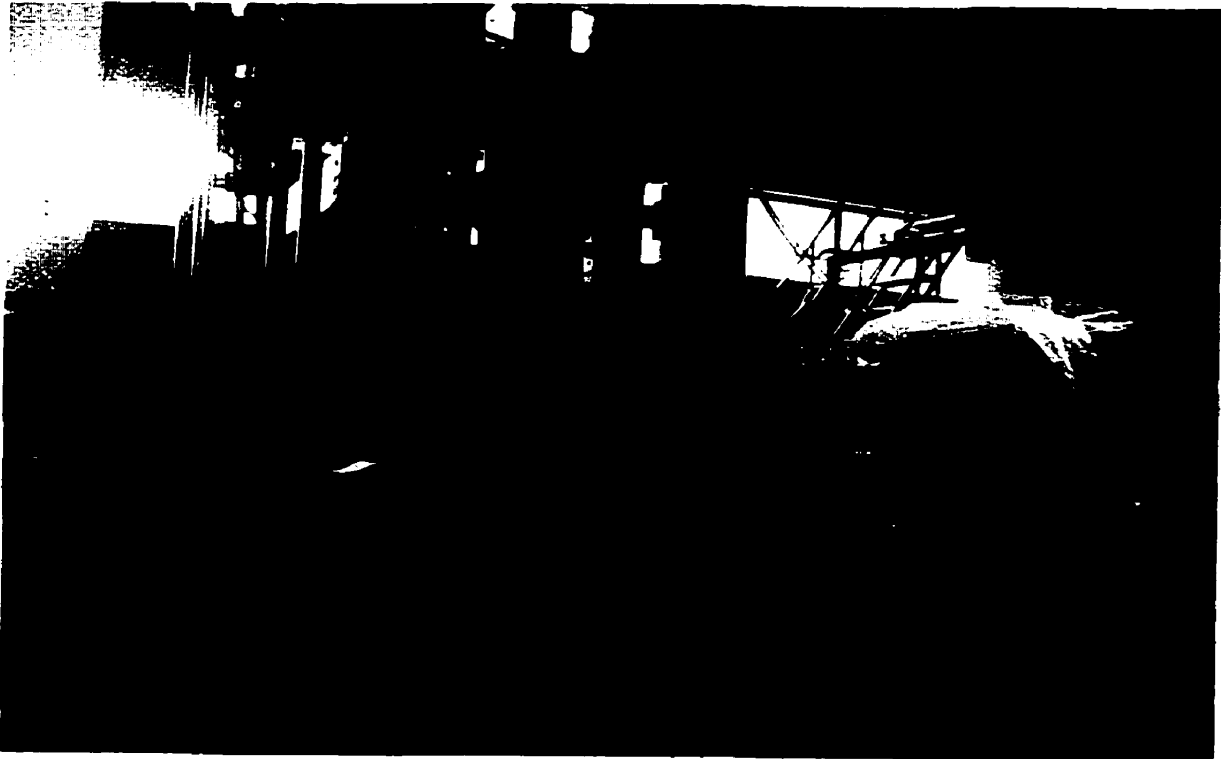
Geometry: $A_1 = 555 \text{ mm}$ $d_{MTS} = 1345 \text{ mm}$
 $A_2 = 4210 \text{ mm}$ $L = 6935 \text{ mm}$

RESULTS:

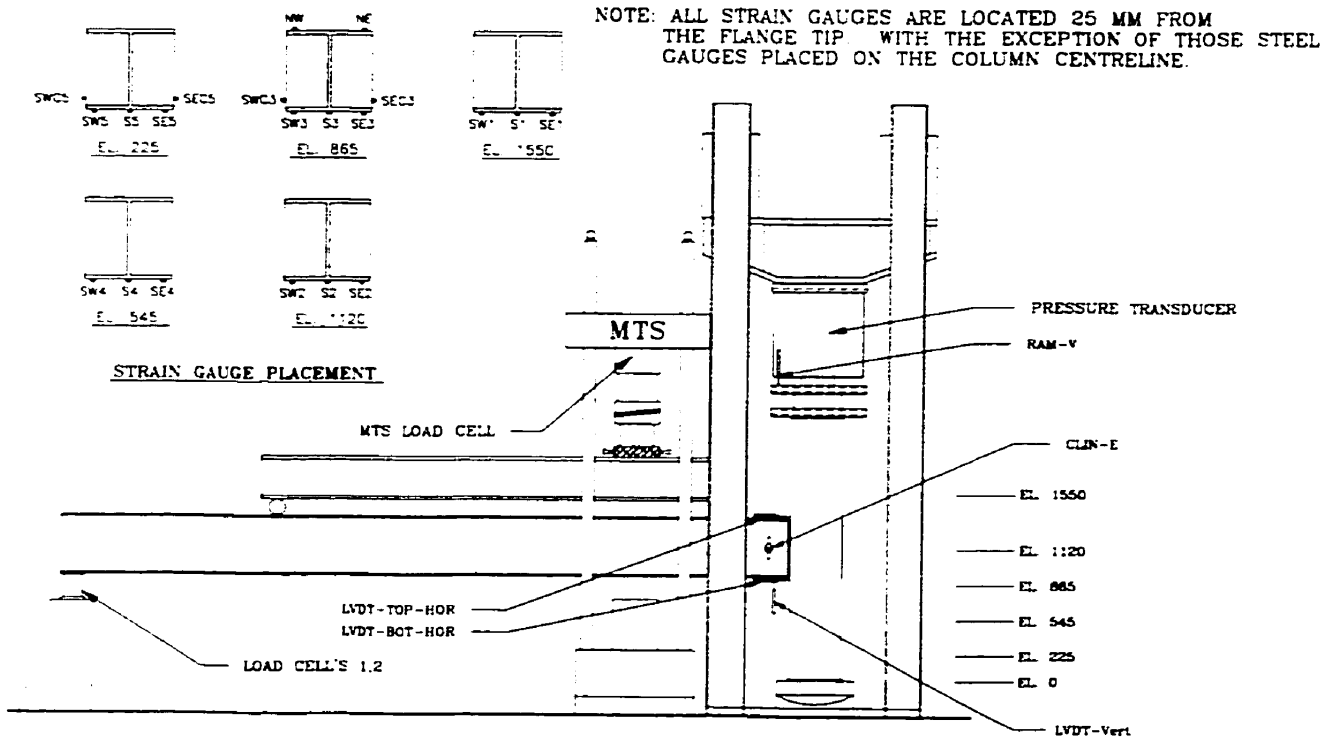
<u>Dataset</u>	<u>Load Stage</u>	<u>Description</u>
57	Column Load = 4500 kN	● Begin loading connection; no abnormal response.
160	Column Load = 4500 kN Connection Load = 754 kN	● Connection loaded to MTS limits, no failure. Begin to increase axial load
197	Column Load = 5518 kN Connection Load = 635 kN	● Column on both sides, above the connection. Sudden failure.

Comments:

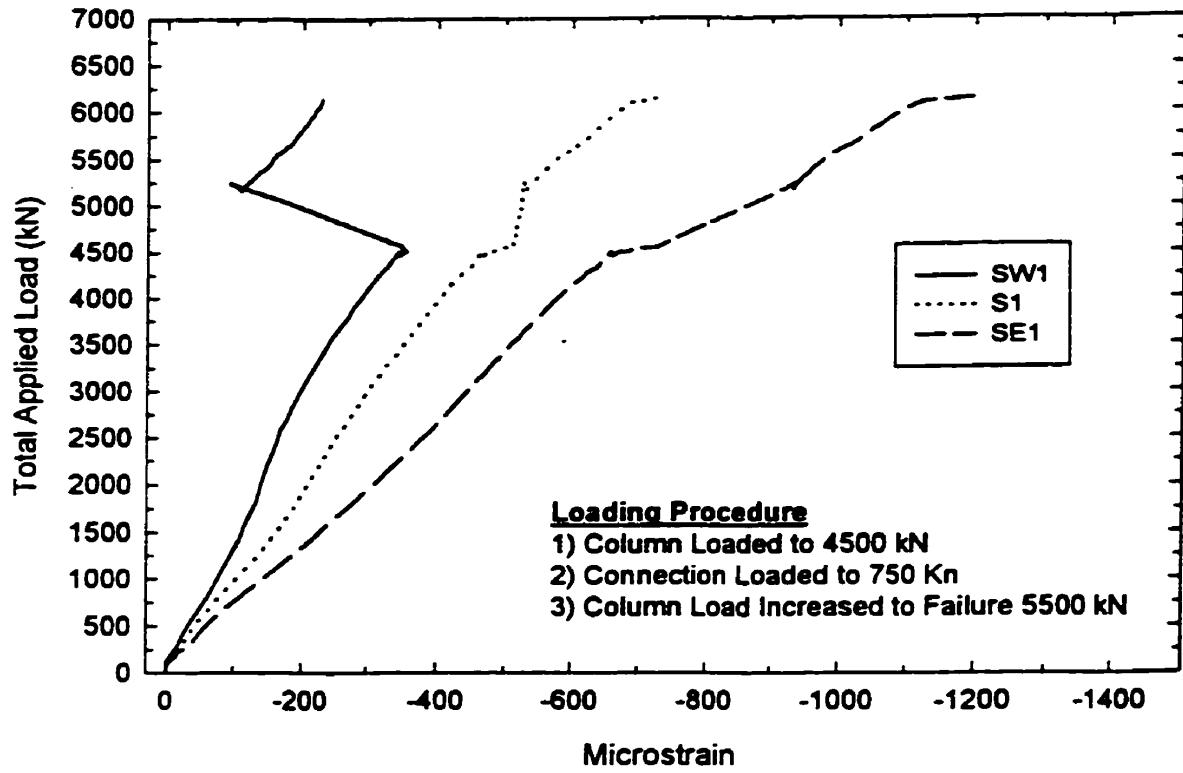
As with the previous seat test there was little permanent deformation observed in either the connection or the connection end plate. Visually the shear studs seems to have little effect on the response. The column failed at relatively low load. This was likely due to the concrete being loaded directly at the top.



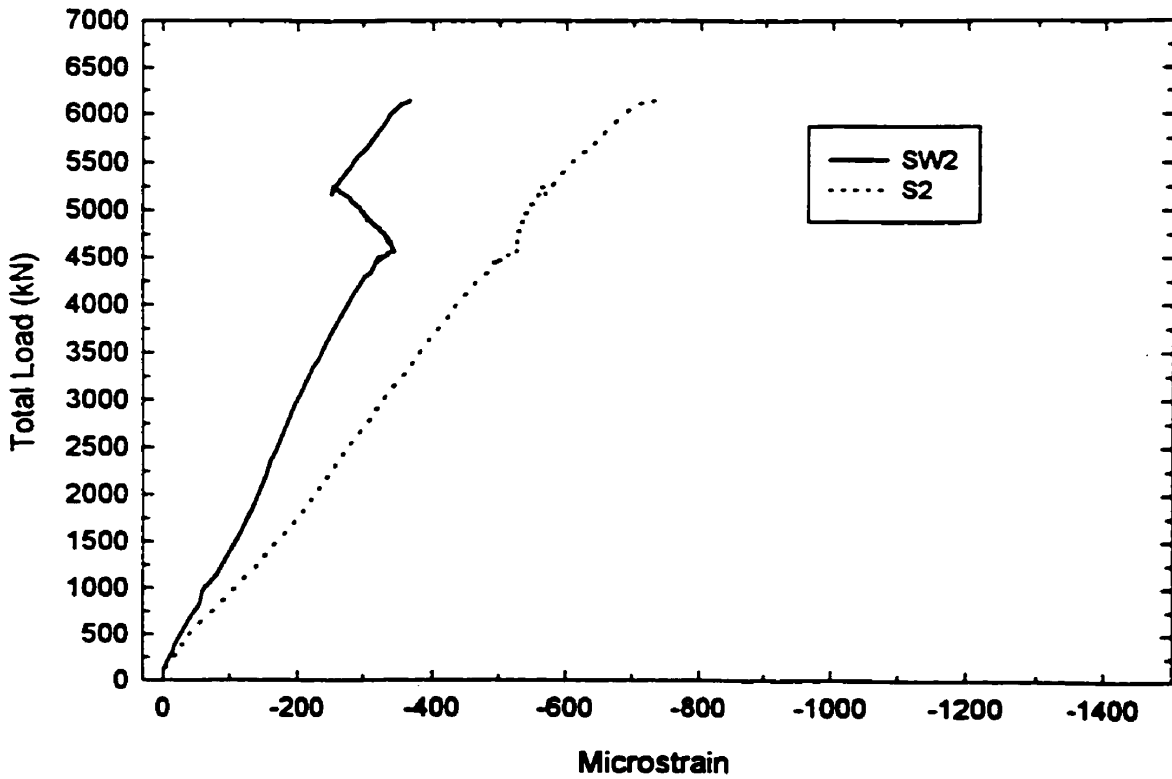
C450-SEAT2-ANCH: Photographic View of Test Specimen



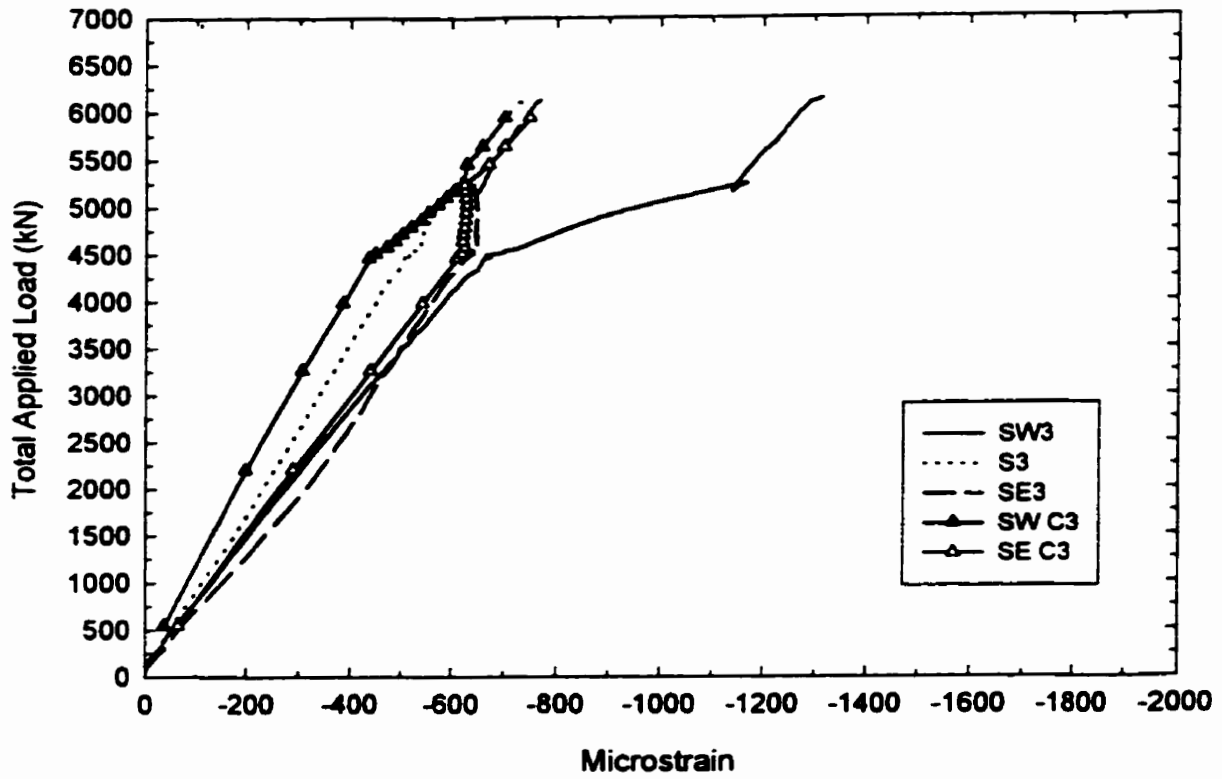
C450-SEAT2-ANCH: Instrumentation Layout of Test Specimen



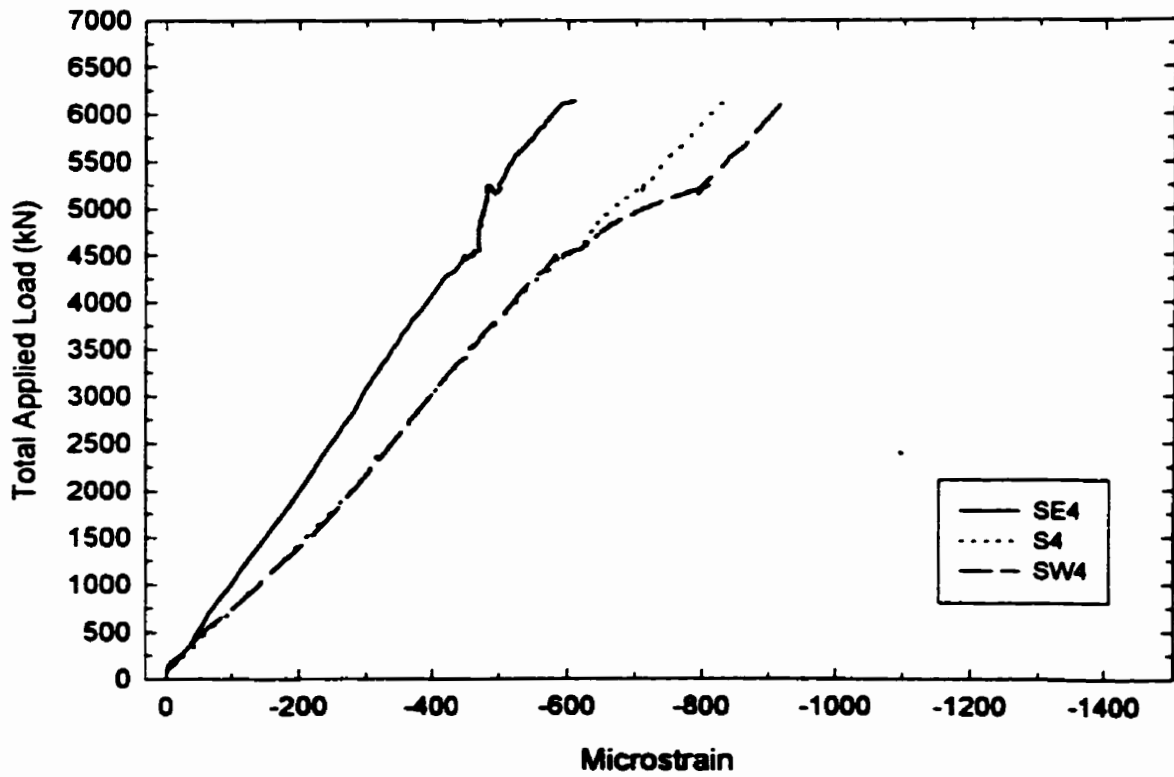
C450-Seat2-Anch: Total Applied Load vs. Strain Above Connection Plate (El. 1550)



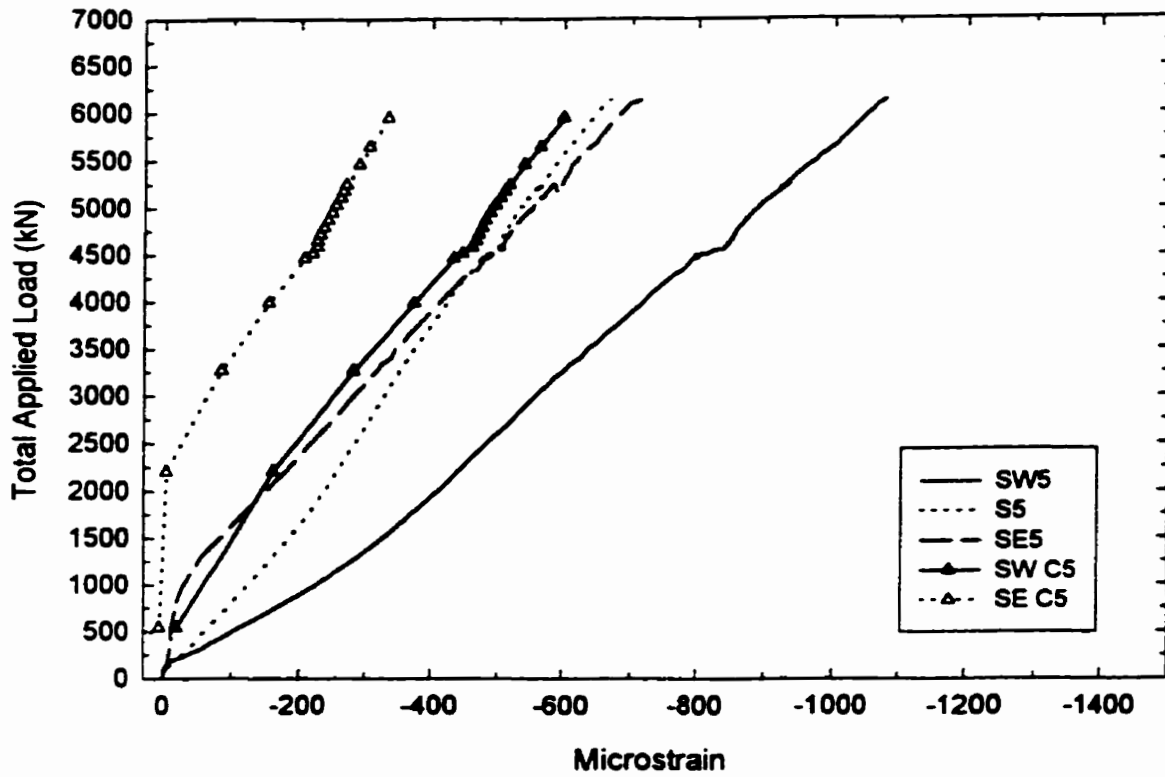
C450-Seat2-Anch: Total Applied Load vs. Strain at Middle of Connection Plate (El. 1120)



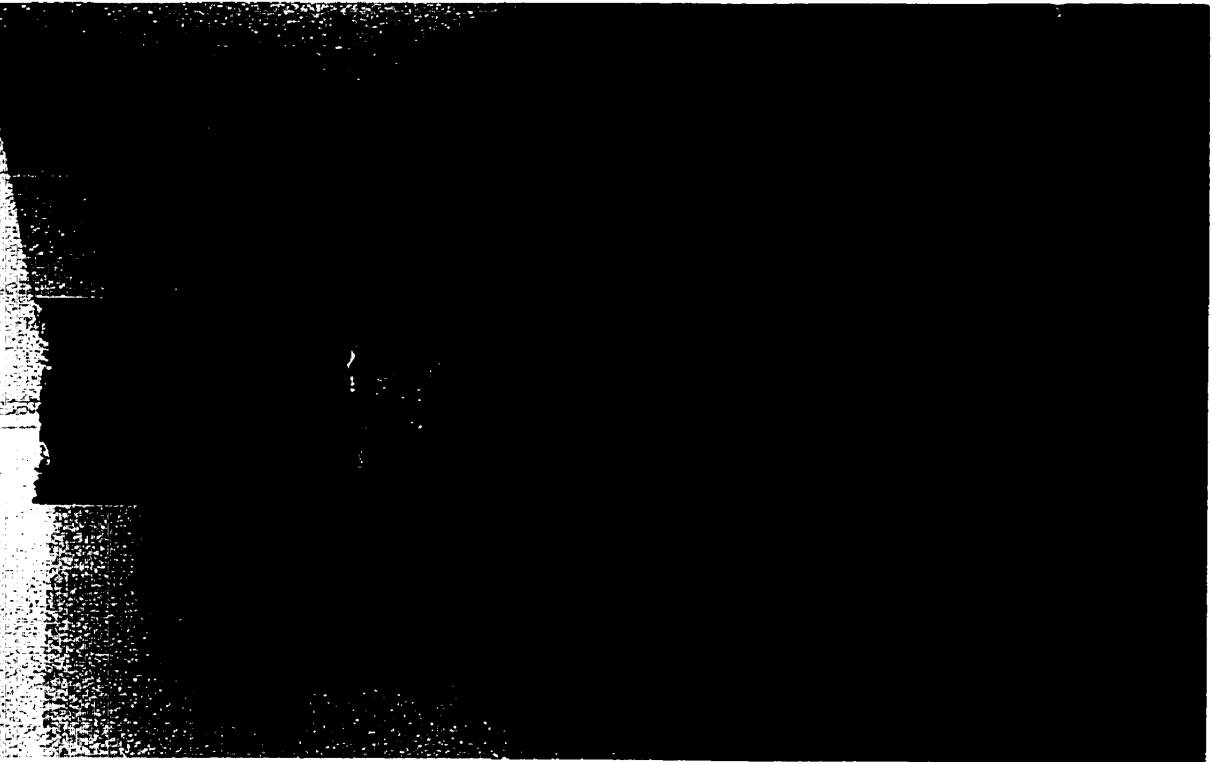
C450-Seat2-Anch: Total Load vs. Strain 50 mm Below Connection Plate (El. 865)



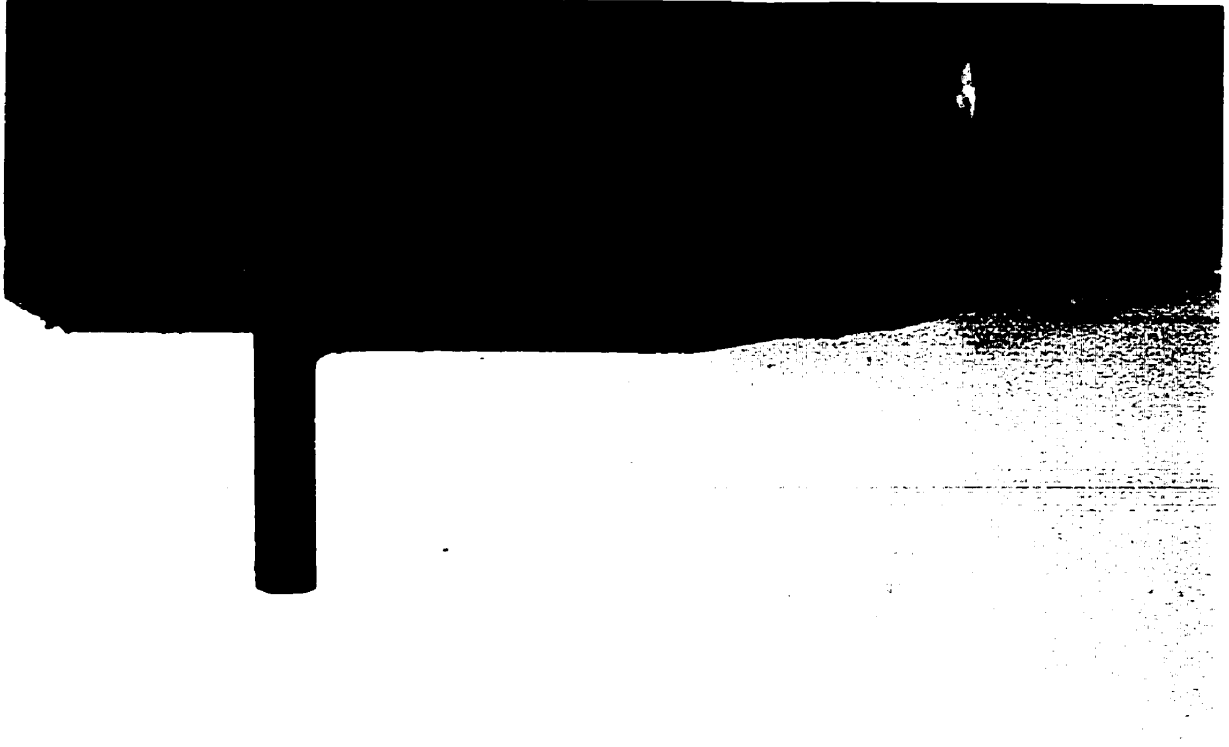
C450-Seat2-Anch: Total Applied Load vs. Strain 370 mm Below Connection Plate (El. 545)



C450-Seat2-Anch: Total Applied Load vs. Strain 685 mm Below Connection Plate (El. 225)



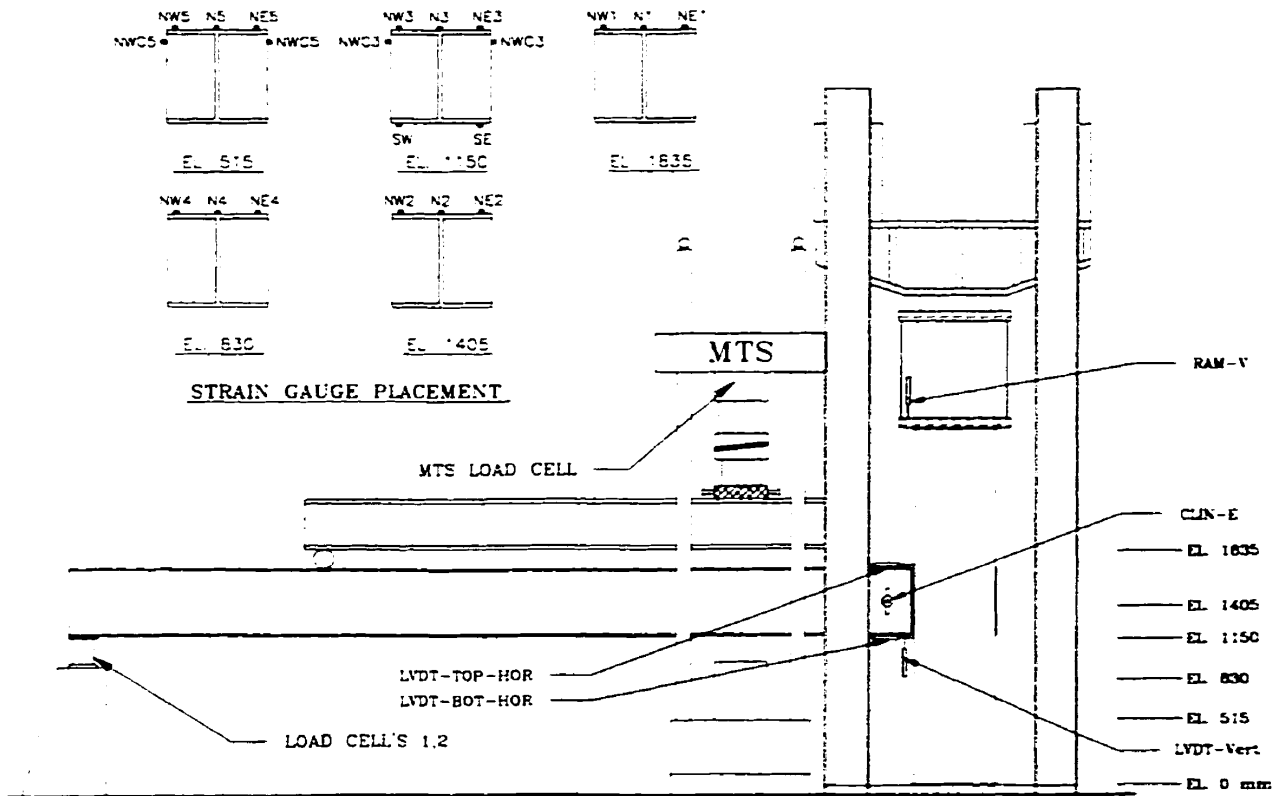
**C450-Seat2: Front View of Tested Connection
Note the Concrete Failure**



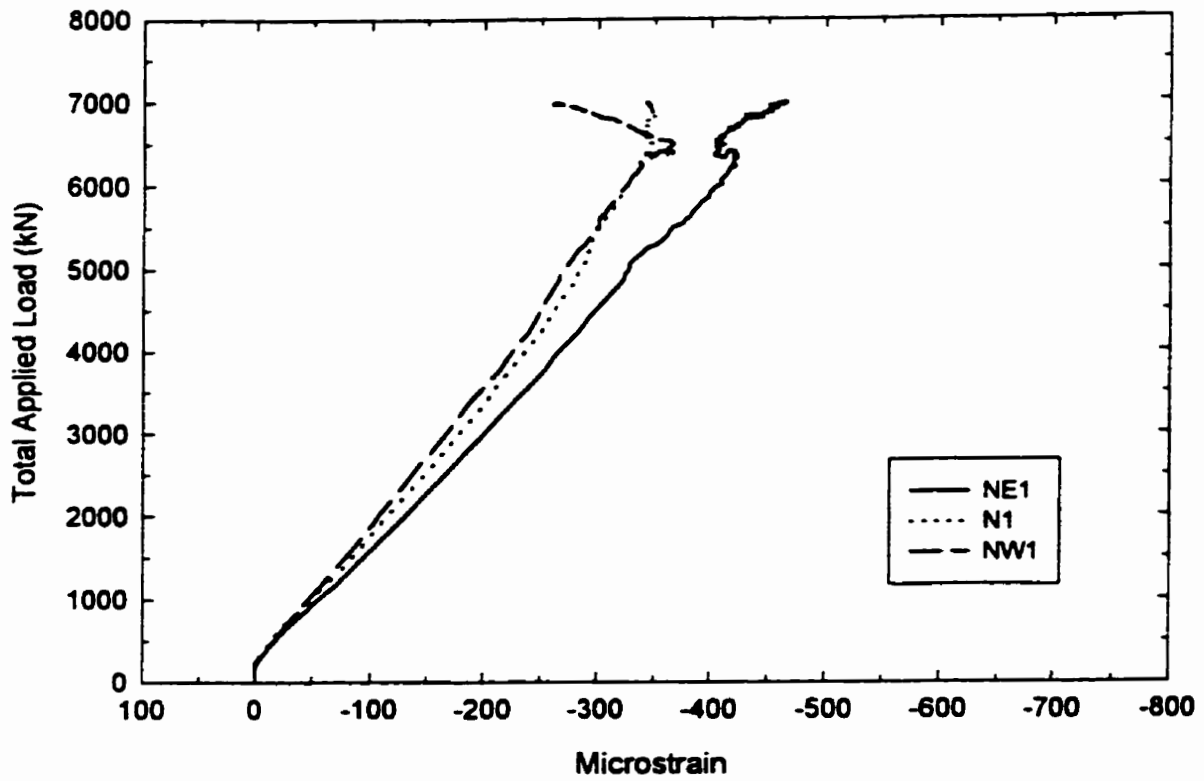
C450-Seat2: Side View of Tested Connection



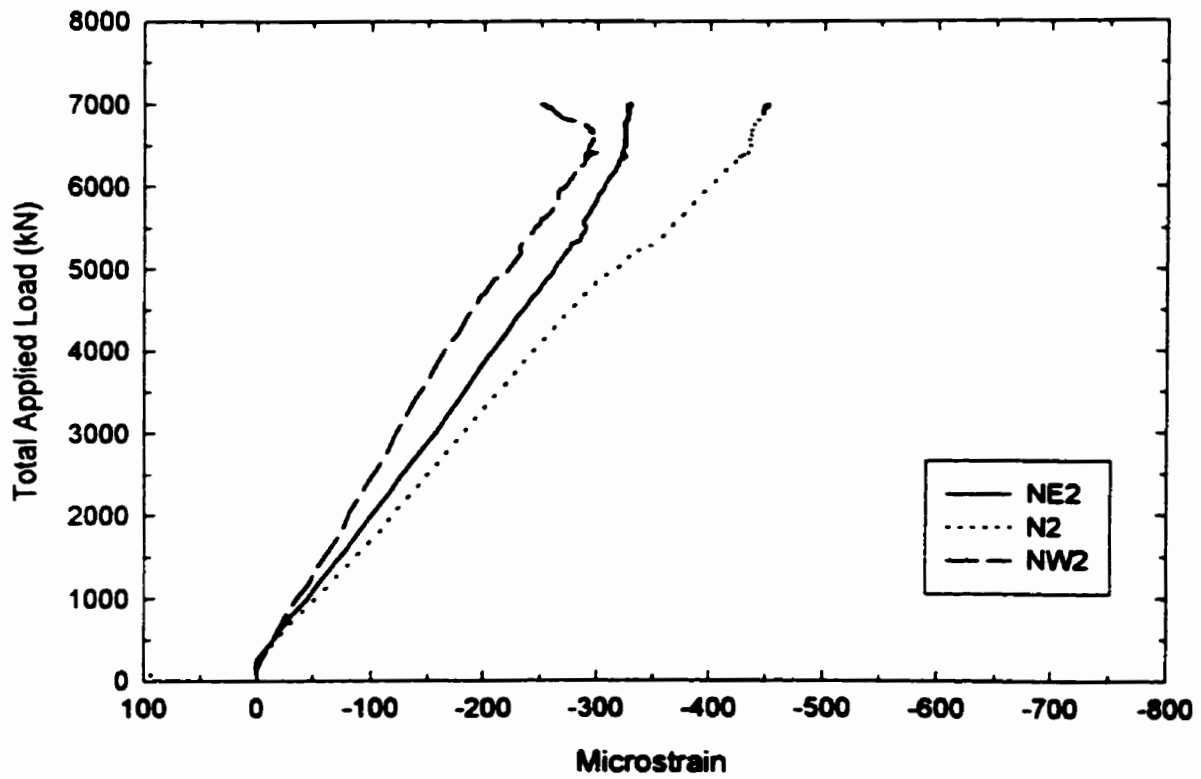
C600-W410-SDA-C: Photographic View of Test Set-up



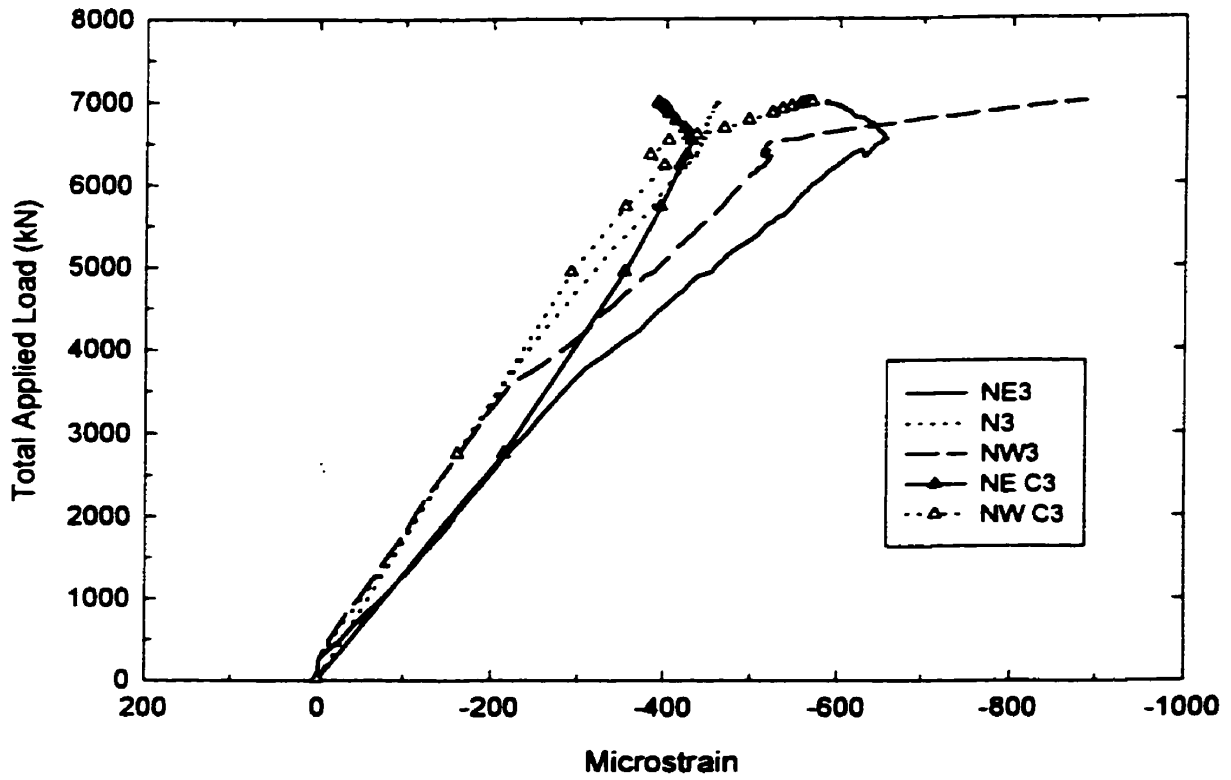
C600-W410-SDA-C: Instrumentation Layout of Test Specimen



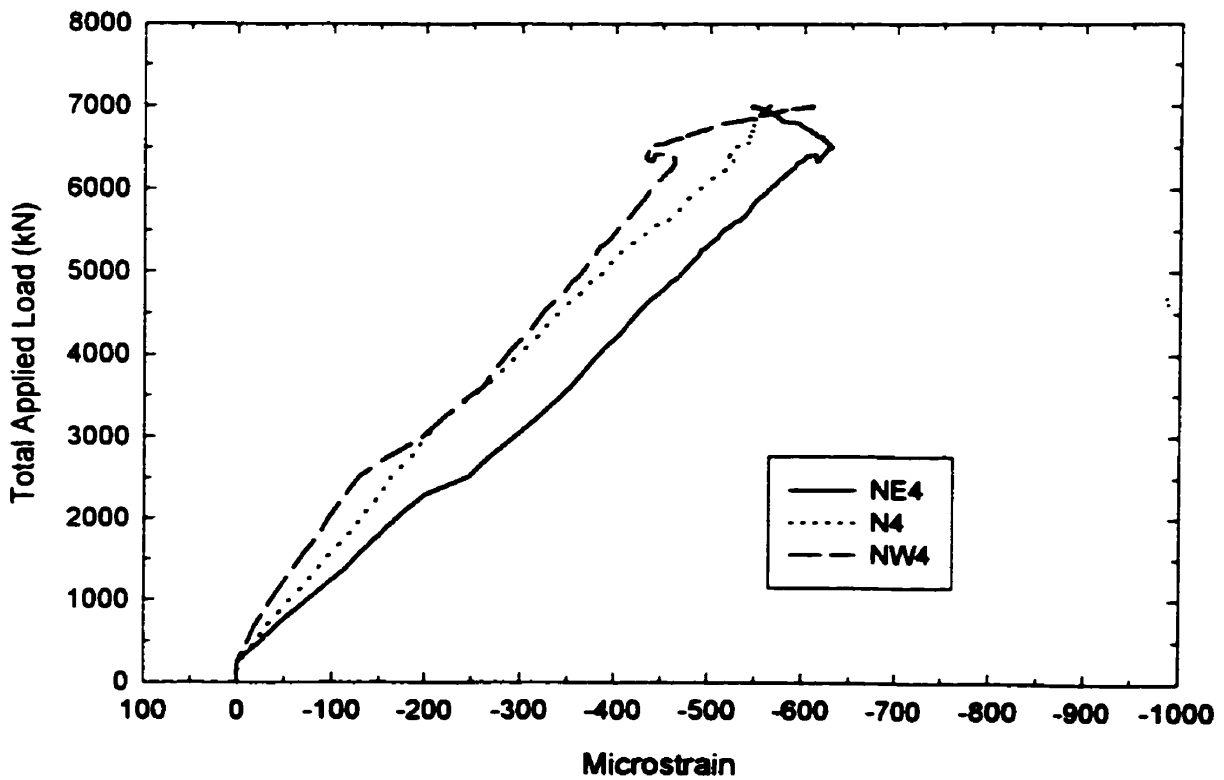
C600-W410-SDA-C: Total Applied Load vs. Strain 225 mm Above Connection Plate (El. 1835)



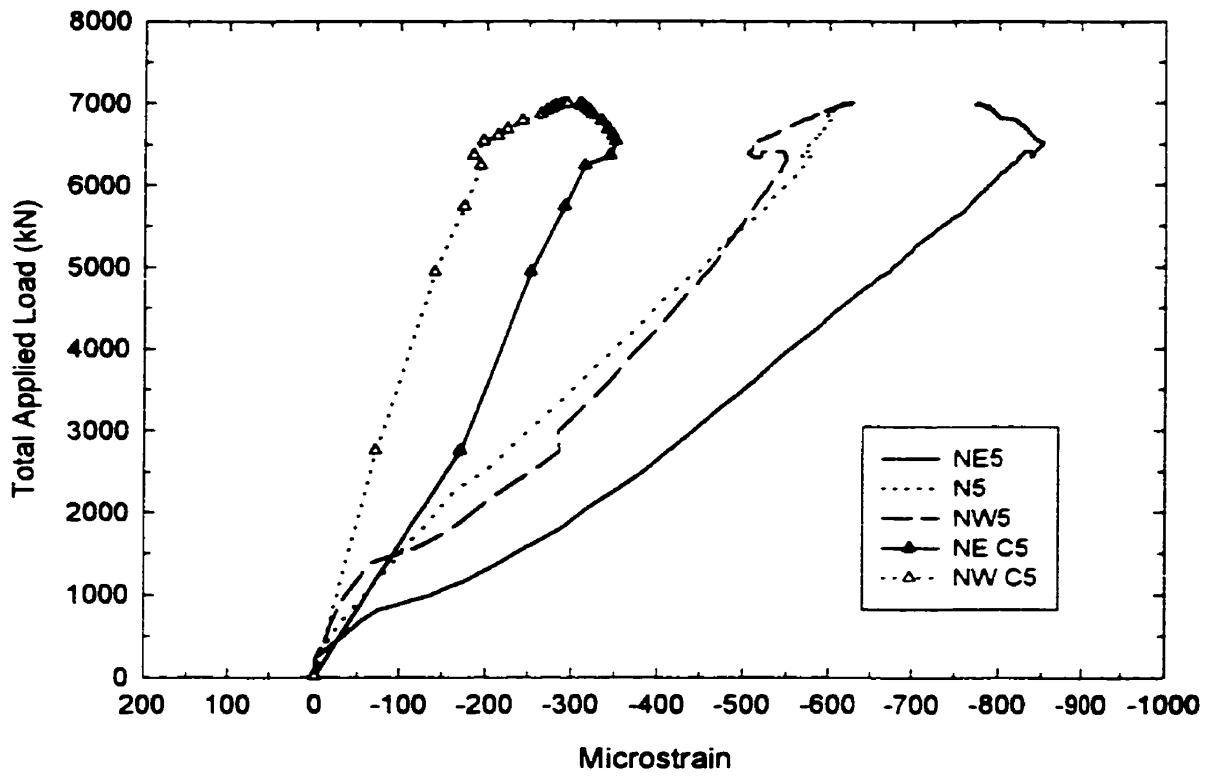
C600-W410-SDA-C: Total Applied Load vs. Strain at Connection Plate Mid-Height (El. 1405)



C600-W410-SDA-C: Total Applied Load vs. Strain 50 mm Below Connection Plate (El. 1150)



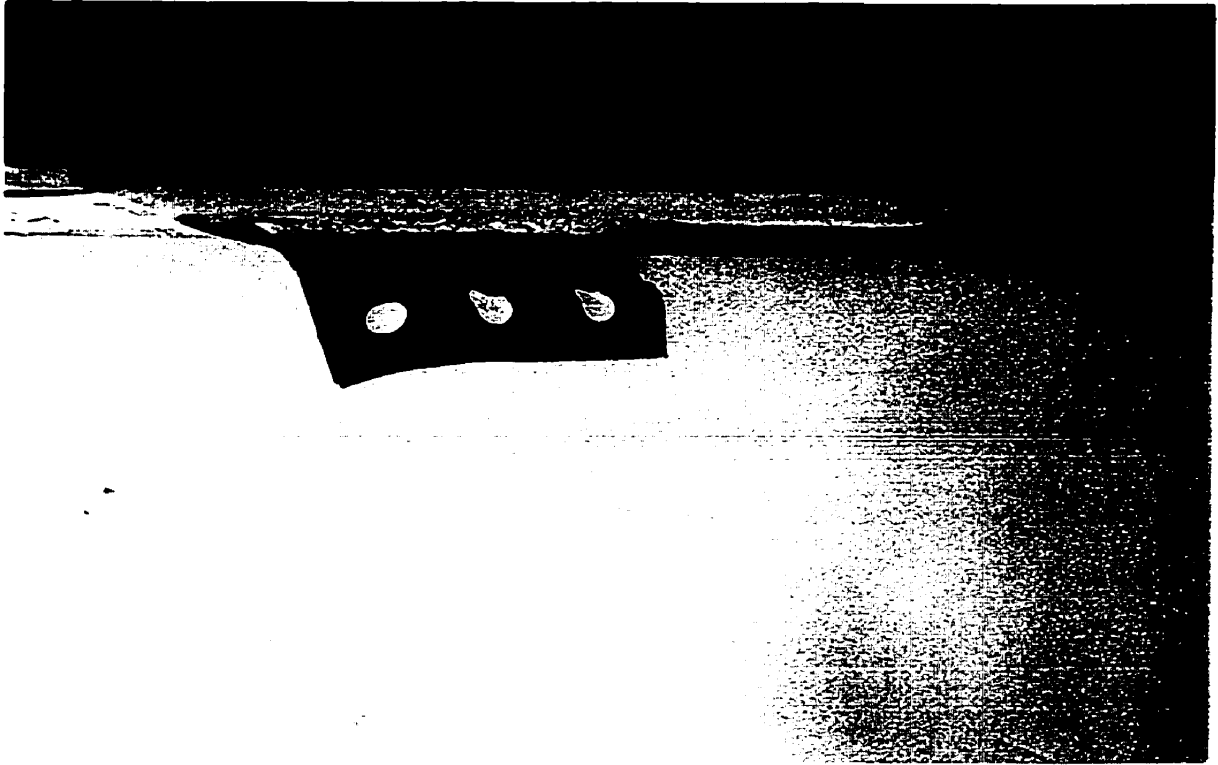
C600-W410-SDA-C: Total Applied Load vs. Strain 370 mm Below Connection (El. 830)



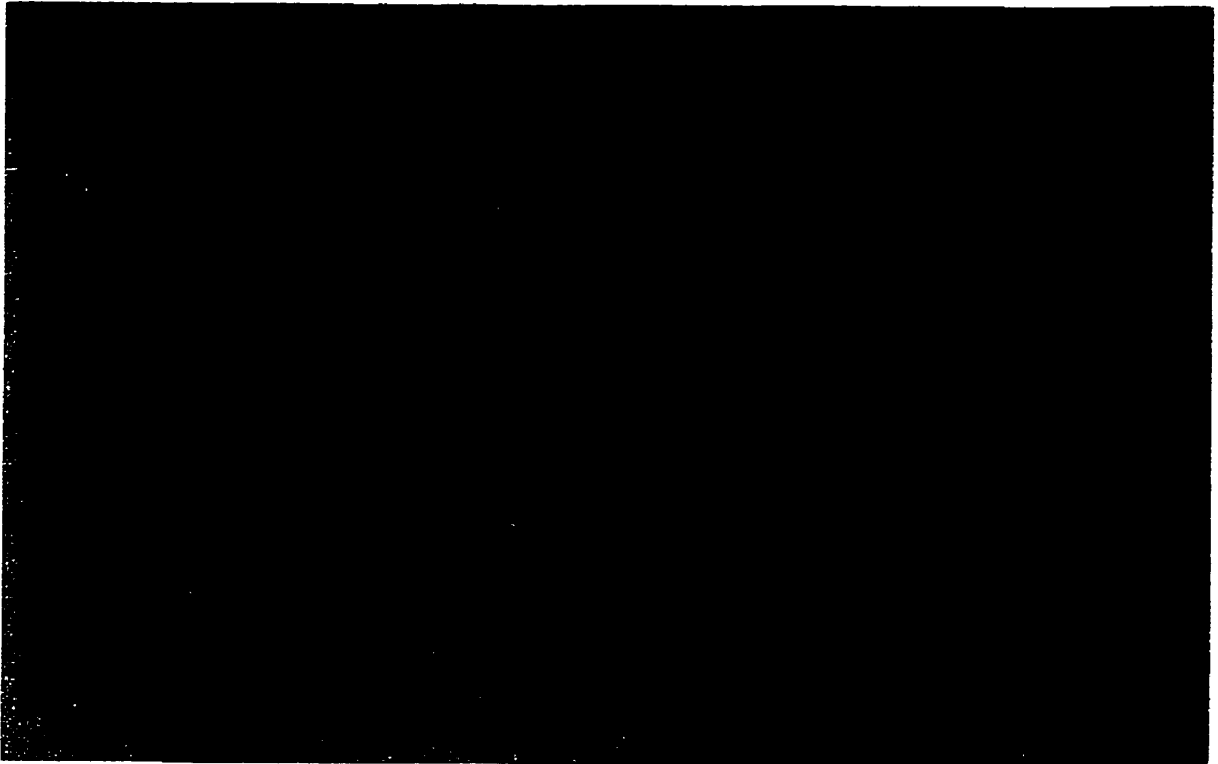
C600-W410-SDA-C: Total Applied Load vs. Strain 690 mm Below Connection Plate (El. 515)



C600-W410-SDA-C: Oblique View of Failed Specimen
Note the Tear Along the Bolt Line



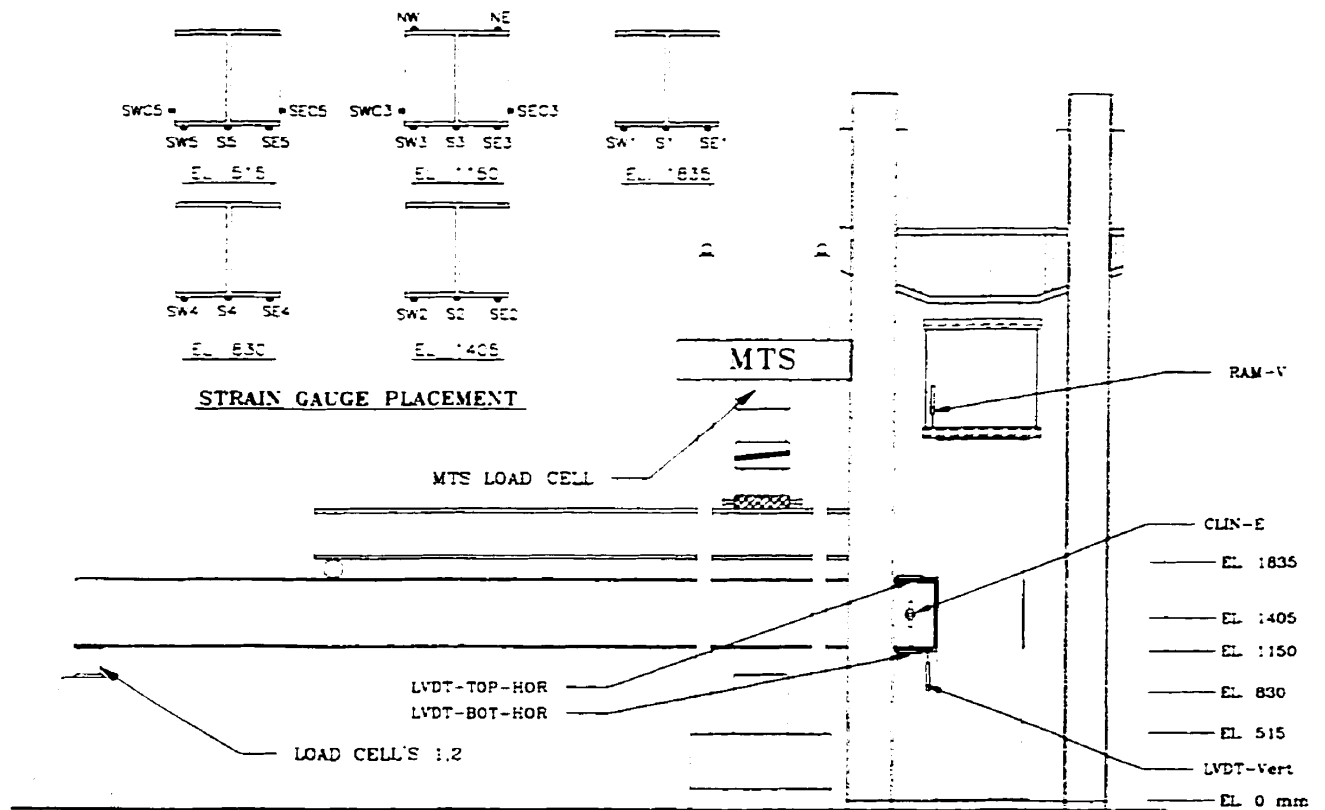
C600-W410-SDA-C: Side View of Connection



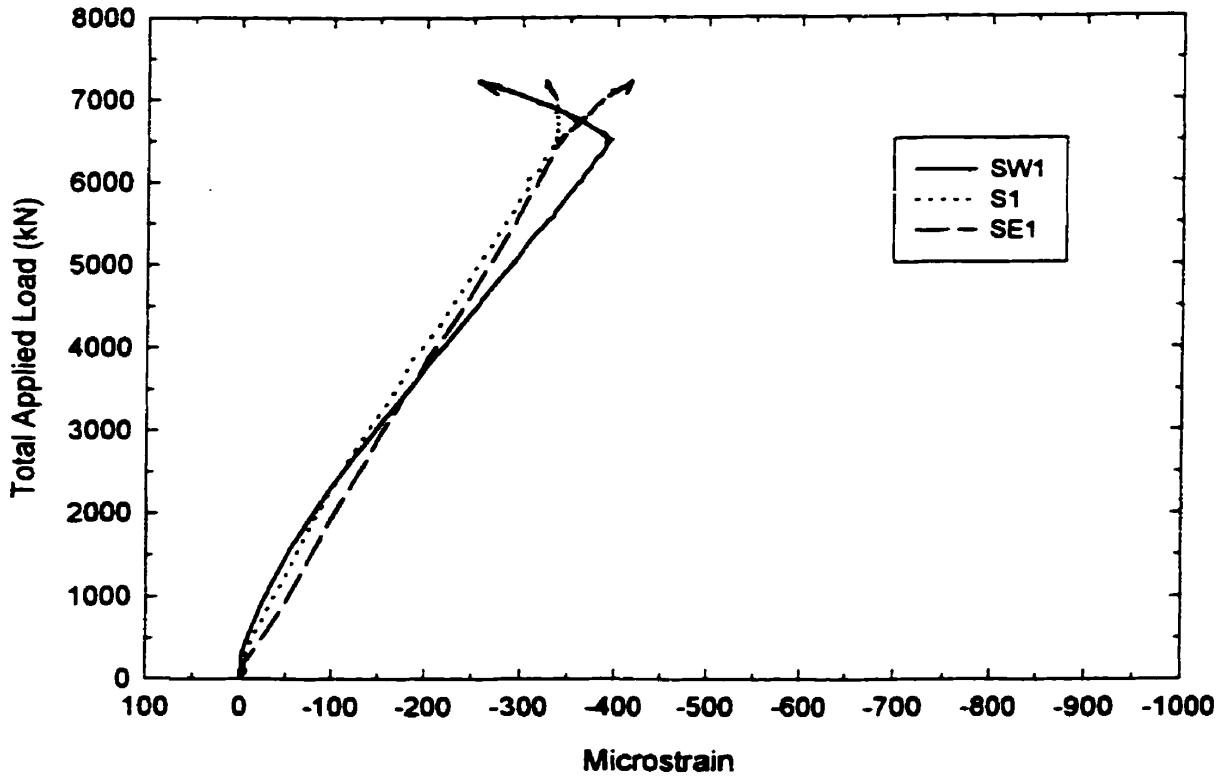
C600-W410-SDA-C: Photo of Beam Web



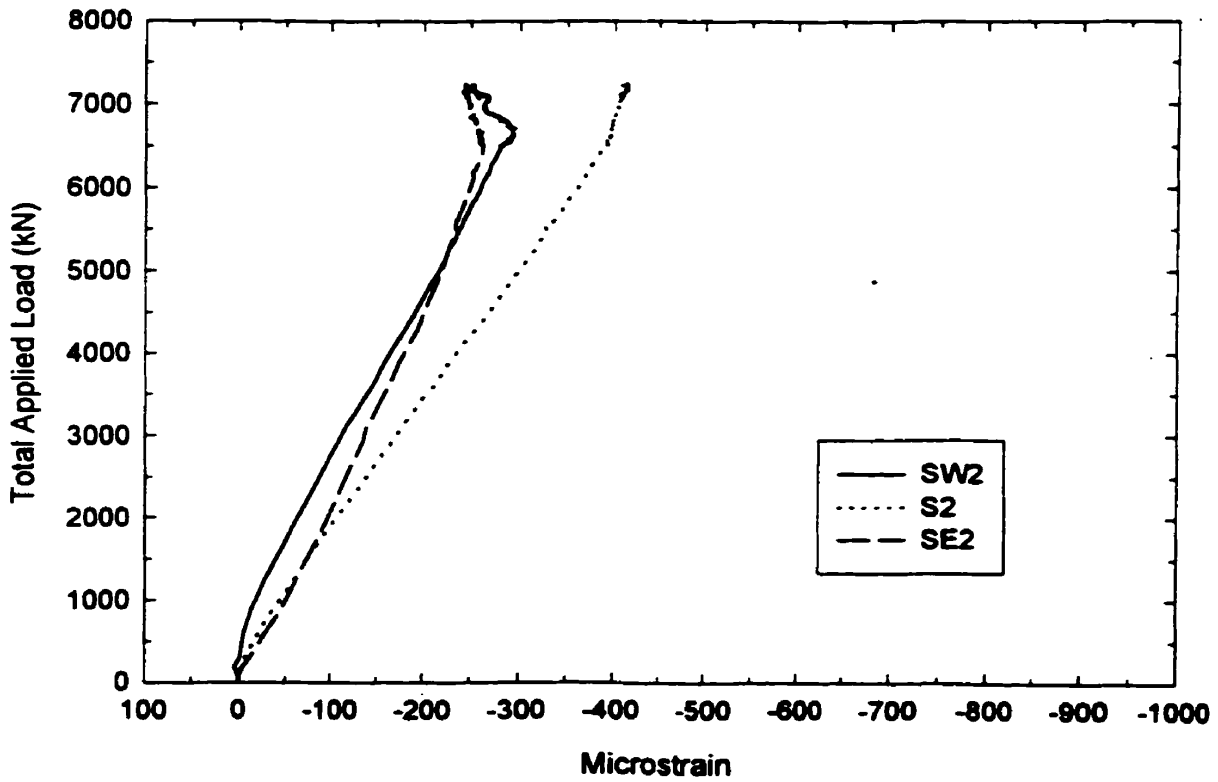
C600-W410-LDA-C: Photographic View of Test Set-up



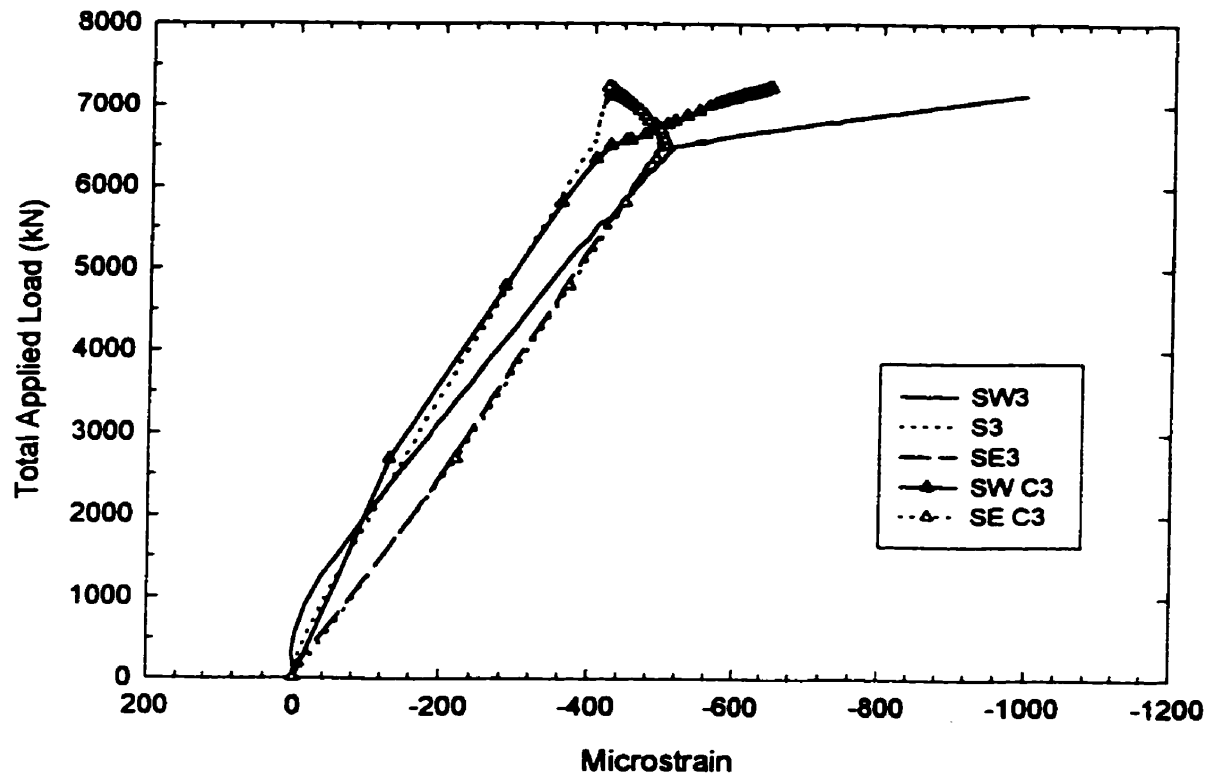
C600-W410-LDA-C: Instrumentation Layout of Test Specimen



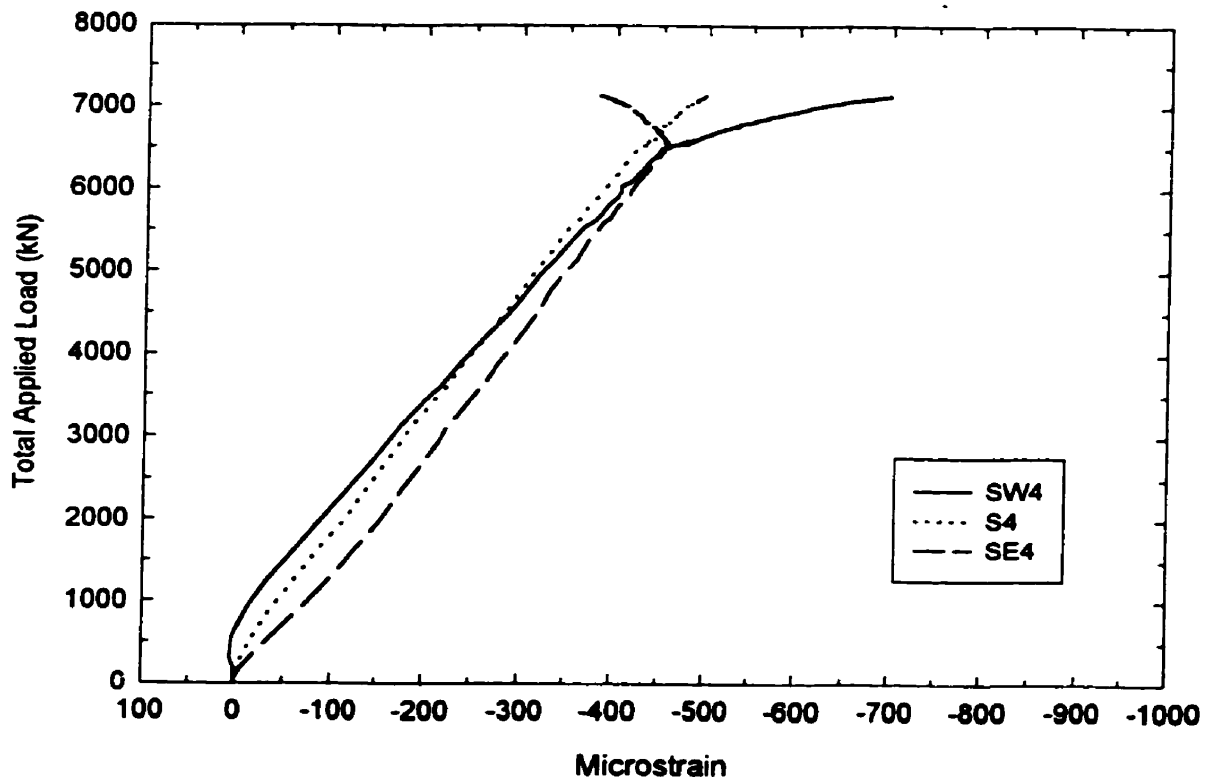
C600-W410-LDA-C: Total Applied Load vs. Strain 225 mm Above Connection Plate (El. 1835)



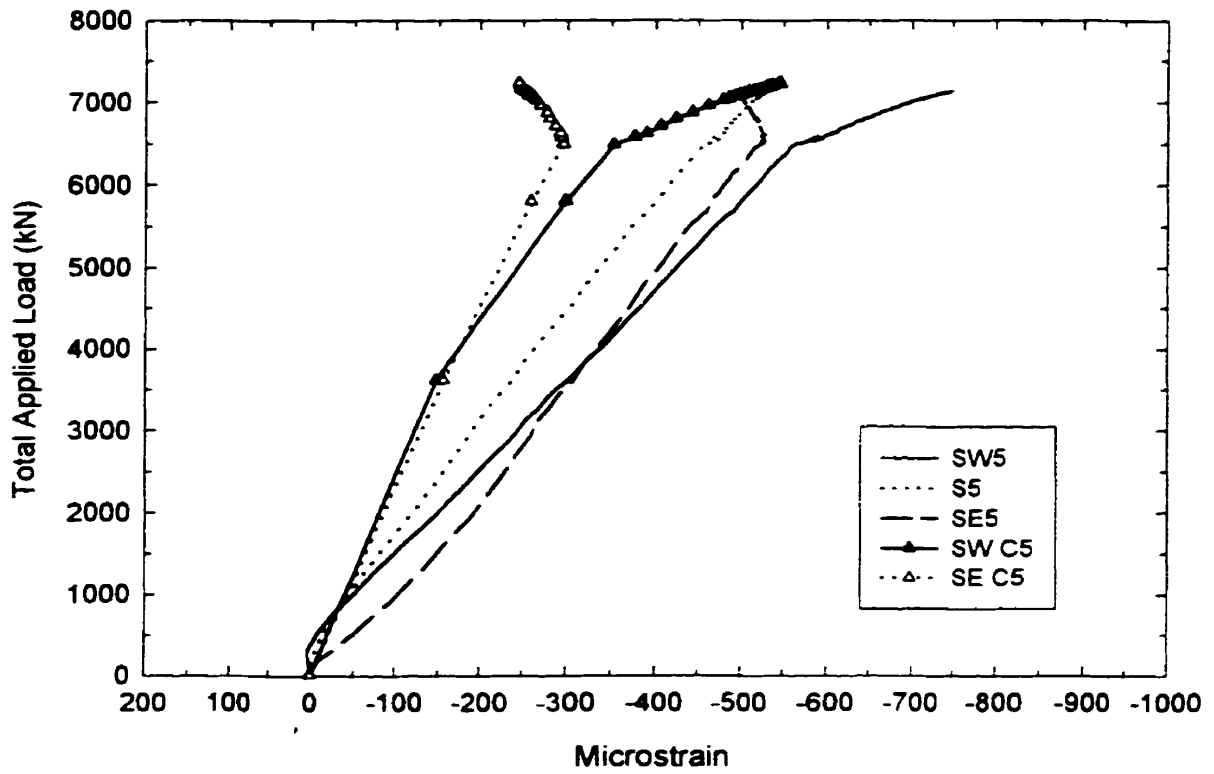
C600-W410-LDA-C: Total Applied Load Vs. Strain at Connection Plate Mid-Height (El. 1405)



C600-W410-LDA-C: Total Applied Load vs. Strain 50 mm Below Connection Plate (El. 1150)



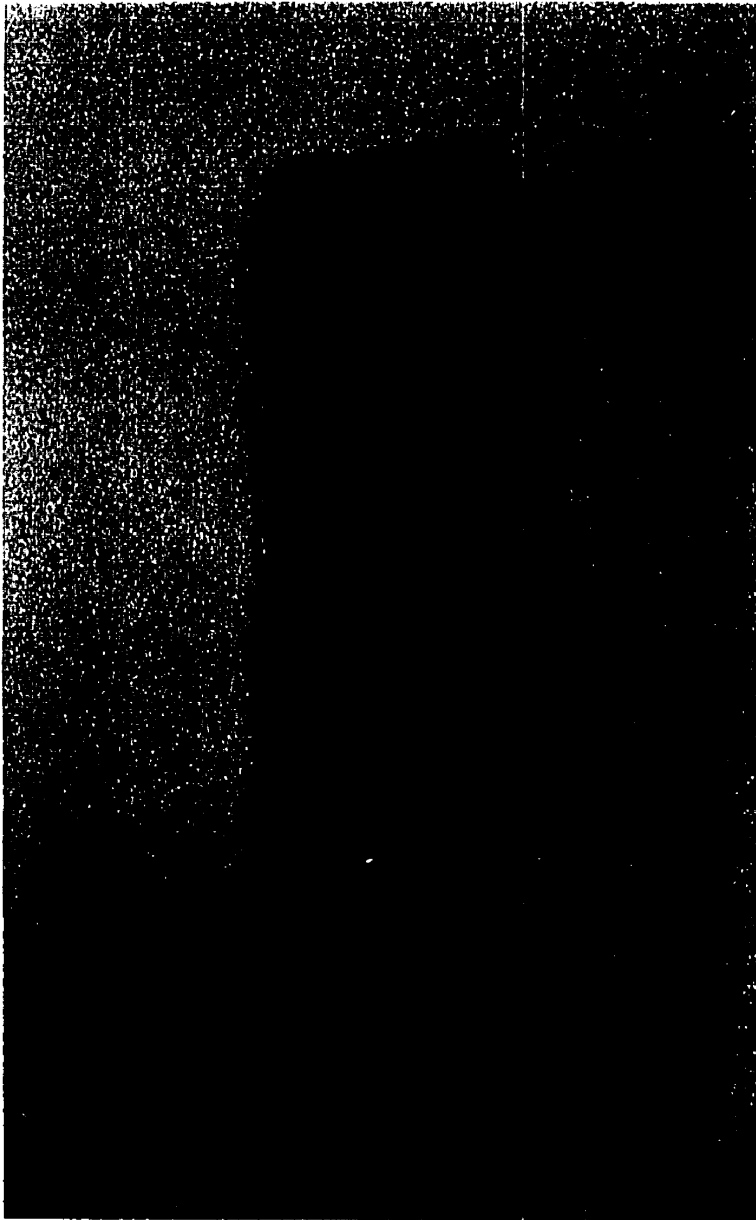
C600-W410-LDA-C: Total Applied Load vs. Strain 370 mm Below Connection (El. 830)



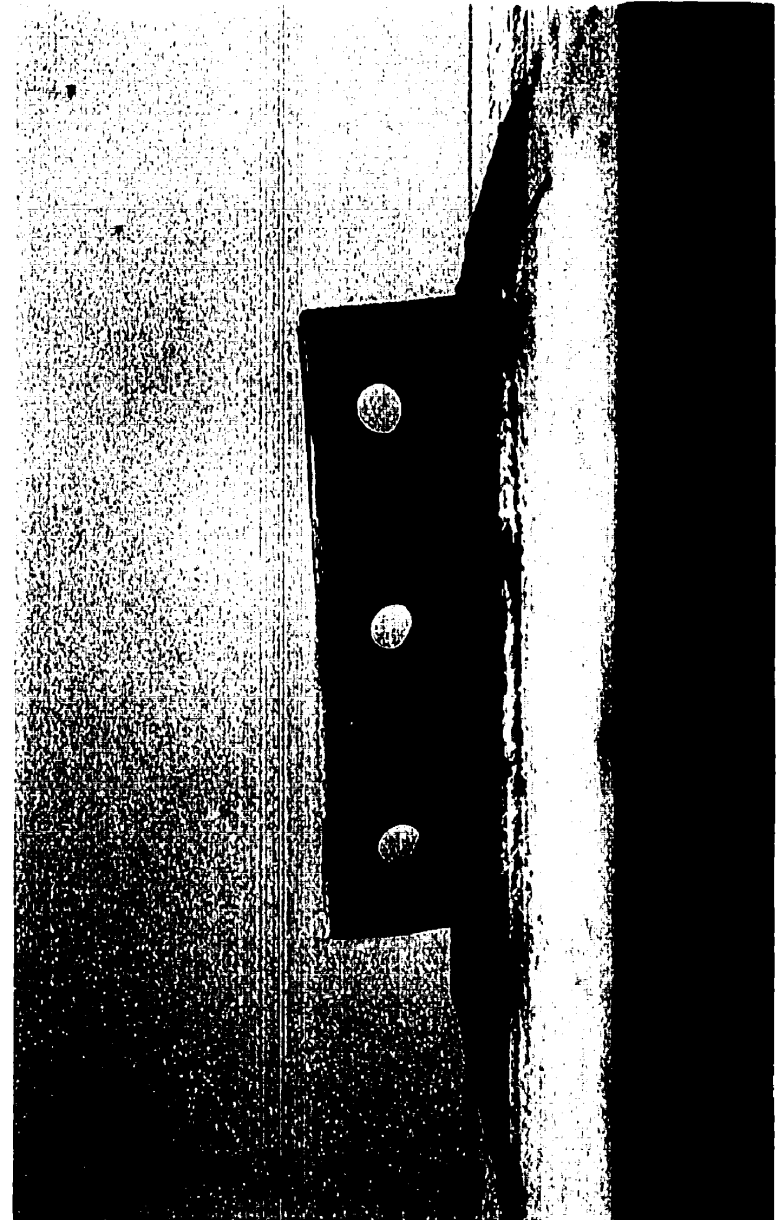
C600-W410-LDA-C: Total Applied Load vs. Strain 690 mm Below Connection Plate (El. 515)



C600-W410-LDA-C: Oblique View of Failed Specimen – Note the Formation of a Tear at the Weld Line



C600-W410-LDA-C: Photo of Beam Web Showing Bolt Hole Deformation



C600-W410-LDA-C: Side View of Tested Connection